National Library of Canada
Acquisitions and Bibliographic Services Branch
395 Wellington Street
Ottawa, Ontario
K1A 0N4

Bibliothèque nationale du Canada
Direction des acquisitions et des services bibliographiques
395, rue Wellington
Ottawa (Ontario)
K1A 0N4

Your file Votre référence

Our file Notre référence

## NOTICE

The quality of this microform is heavily dependent upon the quality of the original thesis submitted for microfilming. Every effort has been made to ensure the highest quality of reproduction possible.

If pages are missing, contact the university which granted the degree.

Some pages may have indistinct print especially if the original pages were typed with a poor typewriter ribbon or if the university sent us an inferior photocopy.



## AVIS

La qualité de cette microforme dépend grandement de la qualité de la thèse soumise au microfilmage. Nous avons tout fait pour assurer une qualité supérieure de reproduction.

S'il manque des pages, veuillez communiquer avec l'université qui a conféré le grade.

La qualité d'impression de certaines pages peut laisser à désirer, surtout si les pages originales ont été dactylographiées à l'aide d'un ruban usé ou si l'université nous a fait parvenir une photocopie de qualité inférieure.



Canada

# Duality of magmatism at Kirkland Lake, Ontario, Canada

by

**Guy Levesque**

A thesis submitted to the School of Graduate Studies and Research in partial fulfillment of the requirements for the degree of M. Sc. in Geology.

**Ottawa-Carleton Geoscience Centre**
**University of Ottawa**

ISBN 0-612-00478-3

Canada

UNIVERSITÉ D'OTTAWA
UNIVERSITY OF OTTAWA

## Abstract

One of the world's most productive gold camps is located along the major east-trending Larder Lake fault (LLF), which extends approximately 250 km from Val d'Or to Kirkland Lake. The western portion of the LLF consists of a 60 km long, narrow (less than 5 km wide) and sinuous deformation zone commonly referred to as the Kirkland Lake-Larder Lake fault zone (KLF). The occurrence of two distinct suites of magmatic rocks, syenitic and granitic, in and around the KLF indicates a magmatic duality. It is possible to identify three distinct magmatic domains defined by mode of emplacement, mineralogy and geochemistry. Mineral chemistry indicates that rocks from both suites evolved under oxidizing conditions in domains 1 and 3. Rare earth element compositions indicate a similar upper mantle source for both magmatic suites. Major element compositions confirm the shoshonitic nature of the syenitic suite, while the granitic suite is comparable to the sanukitoid suite (high-Mg, -K, -LILE andesites). Both the syenitic and granitic suites originate from an upper mantle source that was very probably modified a relatively short time before by fluids and/or melts derived from a subducted slab. The Kirkland Lake area is marked by an early transtensive phase when syenitic and granitic rocks were emplaced in extensional fractures associated to sinistral strike-slip faulting. Uplift of domain 3 and reverse faulting along the Kirkland Lake main break (KLMB) and the LLF are associated with a later transpressive phase; it was during this phase that gold deposits were formed. The structural, mineralogical and geochemical evidence fit in a tectomagmatic model where oblique convergence and accretion dominate.

## Sommaire

Une des régions les plus riches en gîtes aurifères au monde se situe le long de la faille Larder Lake (FLL), qui s'étend sur 250 kilomètres, de Val d'Or à Kirkland Lake. Dans la section ouest de la FLL se retrouve une étroite zone sinueuse et déformée, longue de 60 kilomètres, communément appelée la zone faillée de Kirkland Lake- Larder Lake (ZFKL). Une dualité magmatique est marquée dans la ZFKL par la présence de deux suites magmatiques, une syénitique et l'autre granitique. Trois domaines magmatiques peuvent être identifiés à l'aide de caractéristiques texturelles, minéralogiques et géochimiques des roches. Le chimisme des minéraux indique que les roches situées dans les domaines 1 et 3 ont évolué sous des conditions oxidantes. La chimie des terres rares indique une origine mantellique similaire pour les deux suites. La suite syénitique possède un chimisme à caractère shoshonitique, tandis que la suite granitique s'apparente aux sanukitoïdes (andésites riches en Mg, K et éléments lithophiles à grand rayon). Les deux suites proviennent d'une source du manteau modifiée peu de temps avant leur formation par des fluides émanant d'une croûte altérée lors de sa subduction. L'évolution de la région étudiée se distingue par deux phases: une phase d'extension durant laquelle les roches des deux suites ont envahi les fractures tensionnelles reliées à une faille de décrochement à déplacement sénestre. Une phase tardive de compression explique le soulèvement des roches du domaine 3 et le mouvement de chevauchement le long des failles de Kirkland Lake (KLMB) et de la LLF; la formation des dépôts d'or est associée à cette phase tardive. Les caractéristiques structurales, minéralogiques et géochimiques mènent à un modèle tectonomagmatique où domine les mécanismes de convergence à caractère oblique et d'agglomération.

## Acknowledgements

The author gratefully acknowledges receipt of a Natural Sciences and Engeneering Research Council PostGraduate Scholarship, and of a University of Ottawa Research Scolarship. Further assistance was provided from NSERC grants to Eion Cameron and André Lalonde. Field work was supported by the Geological Survey of Canada.

I would like to thank all of my colleagues at the University of Ottawa for their help and friendship throughout the years. Discussions and reviews of ideas old and new with André Lalonde, Eion Cameron, Keiko Hattori, Marc Legault and Steve Rowins helped form the ideas presented in this dissertation. Technical assistance was provided by Jean-François Tardif, Ron Hartree, John Loop and Edward Hearn at the University of Ottawa, Jean St-Pierre of l'École Polytechnique de l'Université de Montréal, the staff of the Analytical Chemistry Section of the Geological Survey of Canada, the staff of Media Production Services of the University of Ottawa , Glen Poirier of the Microprobe Laboratory at McGill University and the staff of the Ontario Geological Survey Core Library in Swastika.

Many people were instrumental in the completion of this work. Among them, my two supervisors, André Lalonde and Eion Cameron, provided motivation and invaluable guidance for my research. Their expertise and wisdom were invaluable tools in the development of this dissertation. For this I thank them. Finally, I would like to thank my family and especially my wife Kim, for their unending support and encouragement during this memorable journey of my dissertation.

"Si seulement les roches pouvaient parler,
quelles histoires elles pourraient compter ! "

"You don't write something because
you want to say something; you write
because you've got something to say."

F. Scott Fitzgerald

## Table of contents

## List of figures

## List of plates

## List of tables

# 1. Regional geology and tectonic evolution of the Superior Province and Abitibi greenstone belt

## 1.1 Introduction

The Kirkland Lake-Larder Lake fault zone (KLF), located in the southeastern corner of the Abitibi greenstone belt, Superior Province (Fig. 1), was the site of contrasting magmatism in the late Archaean. Igneous activity along the KLF produced two distinct suites of magmatic rocks (Fig. 1). The occurrence of coeval alkaline syenitic (quartz-free, nepheline-normative) and granitic (sensu lato, quartz-bearing or quartz-normative) rocks expresses the duality of magmatism observed along the KLF. The relationship between the granitic and the alkaline igneous rocks of the KLF is the subject of this study.

The shape of the intrusions emplaced along the KLF ranges from large rounded composite plutons, to thin, elongated hypabyssal and extrusive bodies. Three domains are recognized on the basis of the style of magmatic emplacement (Fig. 2). Domain 1 comprises all of the igneous rocks within the KLF. In this domain, discrete granitic bodies occur as thin elongated hypabyssal intrusions, while syenitic rocks are found as both hypabyssal intrusions and extrusive flows. Domain 2 occupies the country north of the KLF (Fig 2). In this domain only granitic rocks emplaced as elongated hypabyssal intrusions are observed. Domain 3 occupies the country south of the KLF (Fig 2). This domain contains large rounded composite intrusions, which are composed of syenitic and granitic phases. Some intrusions, such as the Otto stock and the Murdock Creek intrusion contain both phases, while the Lebel stock appears to be exclusively syenitic and the McElroy stock exclusively granitic.

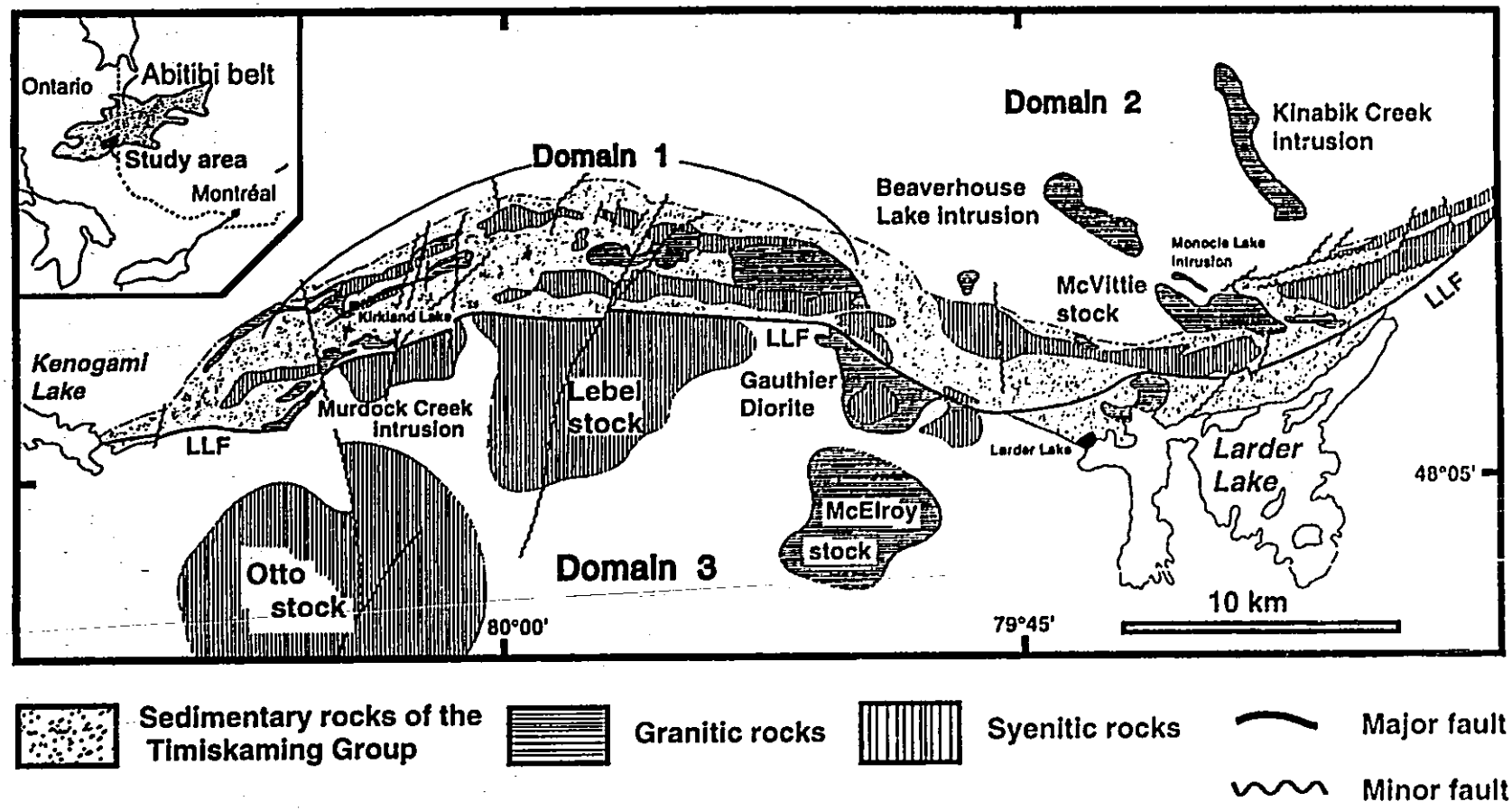


Figure 1 : Main geological features and distribution of syenitic and granitic rocks of the Kirkland Lake - Larder Lake fault zone (KLF). The KLF is bounded to the south by the Larder Lake fault (LLF), and to the north by the basal Timiskaming unconformity (dashed line). The locus of gold mineralization occurs along the Kirkland Lake main break (KLMB).

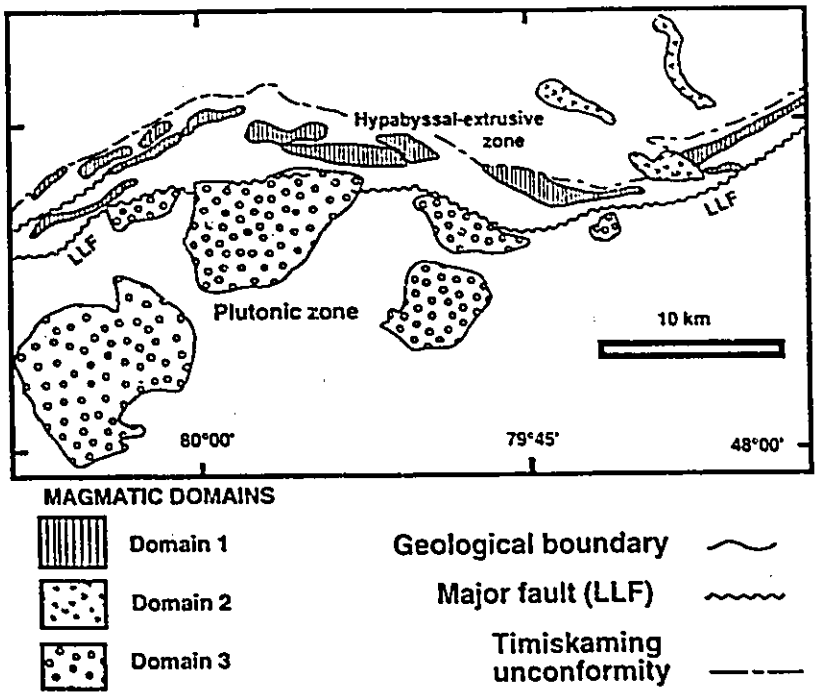


Figure 2 : Magmatic domains and emplacement level of magmatic rocks along the KLF. The LLF separates domain 3 from domain 1, while the northern limit of the KLF (dashed line) marks the boundary between domain 1 and domain 2. The LLF defines the boundary between the plutonic zone (south) and the hypabyssal - extrusive zone (north).

The KLF is host to one of the world's largest gold camps. The Kirkland Lake main break (KLMB), a fault within the KLF, is the locus of the Kirkland Lake gold camp (Fig. 1). A total of seven mines along a 3.5 km stretch of the KLMB have produced over 720 metric tons (25.4 million ounces) of gold since 1913. Today, only the Macassa mine remains in operation.

The syenitic and granitic (i.e., porphyry) intrusions, which host the gold deposists along the KLMB, represent the latest major magmatic event in the development of the KLF. Zircon U-Pb geochronology studies by Corfu et al. (1991) indicate that these rocks were emplaced between 2685 and 2673 Ma.

Among them, the Otto stock yielded a zircon age of 2679 ± 1 Ma (Corfu and Noble, 1992). These late Archaean (circa 2680 Ga) intrusions account for less than 4% of rocks composing the Abitibi belt. However, over 25% of Ontario's Archaean lode gold deposits are found near these intrusions (Colvine et al., 1988). This intimate association between felsic/alkaline magmatism and gold mineralization in the Superior Province has long been a focus of research (Hodgson and MacGeehan, 1982; Ploeger and Crocket, 1982; Cherry, 1983; Colvine et al., 1988; Cameron and Carrigan, 1987; Cameron and Hattori, 1987; Rock and Groves, 1988; Wyman and Kerrich, 1988; Burrows and Spooner, 1989; Fyon et al., 1989; Kerrich, 1989; Levesque and Hattori, 1989; Rock et al., 1989; Wyman and Kerrich, 1989; Edgar et al., 1991). This relationship has also been studied in western Australia (Rock and Groves, 1988; Kerrich, 1989; Rock et al., 1989) and eastern Australia (Perkins et al., 1992), Papua-New Guinea (Davies and Ballantyne, 1987; McInnes, 1992), and in the Cripple Creek gold camp, Colorado (Lindgren et al., 1906; Gott et al., 1969; Mutschler et al., 1986).

The ambiguous nature of this relationship persists. Although a clear spatial association exists between felsic/alkaline magmatism and gold deposits, the temporal association remains enigmatic (Robert, 1990). Recent studies indicate a small time gap between magmatism and mineralization (13 to 15 Ma, Marmont and Corfu, 1989; 20 Ma , Claoué-Long et al., 1990), while others show the mineralization event to be significantly younger than magmatism (more than 250 Ma, Bell et al., 1989; 55 Ma, Jemielita et al., 1990).

At Kirkland Lake, there is a distinct time difference between the emplacement of the thin elongated intrusions and extrusive flows of domain 1

(Fig. 2) and the gold mineralization event. The magmatic bodies of domain 1 were passively emplaced during an extensional phase of tectonism, while gold-bearing fluids were introduced during a later transpressional phase (Cameron, 1990). Therefore, the auriferous fluids could not have been directly derived from the magmas which formed these intrusions and extrusive flows.

Why then does the association of felsic/alkaline magmatism and gold mineralization persist? This question has prompted a series of studies on the nature of alkaline magmatism at Kirkland Lake (Smith and Sutcliffe, 1988; Hattori and Levesque, 1989; Rowins et al., 1989, 1991; Cameron, 1990; Ben Othman et al., 1990; Rowins, 1990; Sutcliffe et al., 1990; Levesque et al., 1991; Rowins et al., 1993).

Two suites of rocks are present along the KLF: alkaline/ syenitic rocks (silica-undersaturated) and granitic rocks (silica-saturated and quartz-bearing). The alkaline magmas have been characterized as intrinsically oxidized (Cameron and Carrigan, 1987; Hattori and Levesque, 1989; Rowins et al., 1989, 1991); this matches the highly oxidized nature of the auriferous fluids of the Kirkland Lake gold camp (Hattori and Cameron, 1986; Cameron and Hattori, 1987 ). One particular characteristic of the KLF is the extensive carbonitization of rocks in domain 1. The important role of $CO_2$ for the generation of alkaline magmas in the upper mantle is now widely accepted (Bailey, 1976; Spera, 1984; Meen, 1987). In domain 1, syenitic rocks are commonly carbonatized, but in places crosscut carbonatized zones (Thomson, 1950). The upper beds of the Timiskaming conglomerate also contain carbonatized clasts (Hewitt, 1963). This indicates a long period of $CO_2$ fluxing, spanning the nascent stages of the KLF to the end of the mineralization event.

The presence of $CO_2$ is a further characteristic of the intimate relationship between alkaline magmatism, oxidized gold-bearing fluids and gold mineralization (Burrows et al., 1986; Cameron and Hattori, 1987; Colvine et al., 1988; Fyon et al., 1989; Hodgson and Hamilton, 1989; Peterson and Newton, 1990).

The main objective of this research is to understand the compositional duality of magmatism present along the KLF in order to better define the relationship between alkaline magmatism and gold mineralization in the Kirkland Lake area. Studies focussing on this relationship have been hampered by the pervasive alteration and, to a lesser degree, deformation of the rocks associated to gold deposits along the KLF. To counter this problem, the author spent over 2 field seasons (1989, 1990, part of 1991) collecting a representative suite of over 300 samples of the intrusive and extrusive rocks along the KLF, between Kenogami Lake to the west and Virginiatown to the east (Fig. 1).

Following detailed petrographic study, where samples were compared and ranked according to intensity of alteration and deformation, approximately 60 specimens were chosen for geochemical analysis. These least-altered specimens were chosen because they contained a predominantly primary mineralogy and lacked alteration assemblages. Geochemical data gathered on these rocks include major, trace and rare-earth element geochemistry; electron microprobe analyses and ferric-ferrous iron ratio determinations were performed on ferromagnesian minerals.

## 1.2 Regional geology

### 1.2.1 Superior Province

The Kirkland Lake-Larder Lake fault zone is located in the southwestern corner of the Abitibi greenstone belt, which is part of the Superior structural province (Fig. 3).

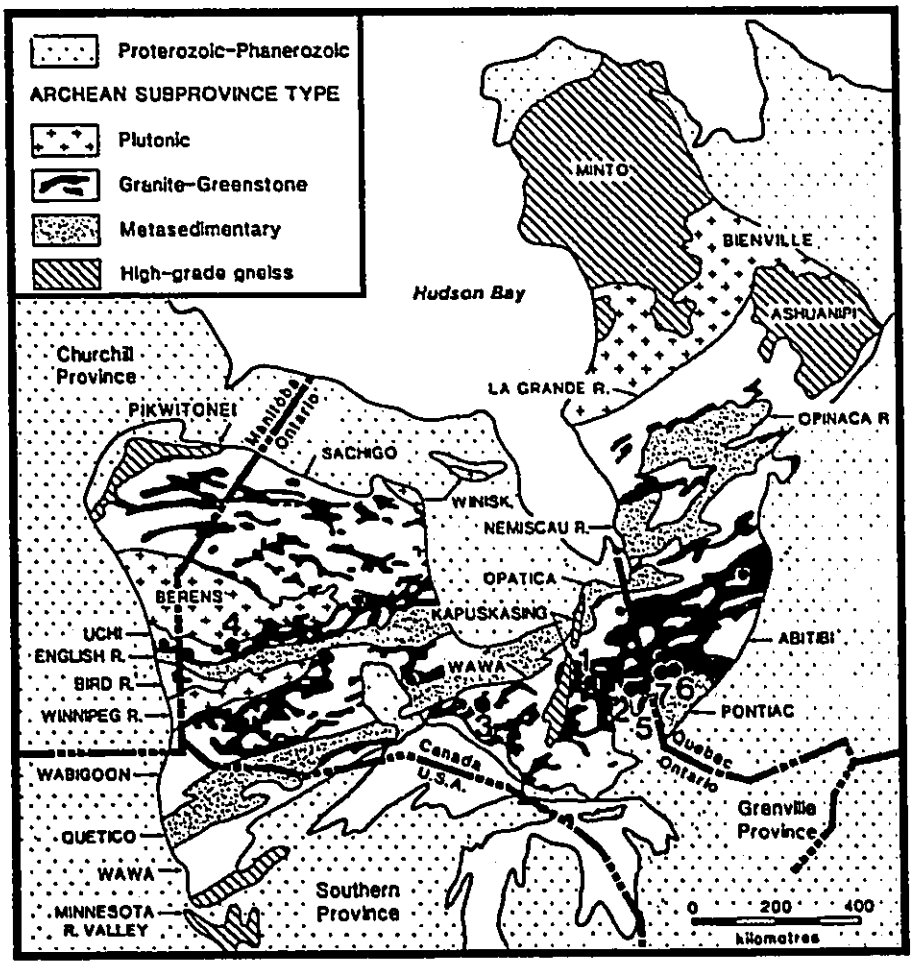


Figure 3 : Subdivisions of the Superior structural province. The Abitibi greenstone belt is located in the south east corner of the the province. The Kirkland Lake and Larder Lake gold camps are represented by numbers 2 and 5 respectively. ( Map reproduced from Colvine et al., 1988)

The Superior Province is by far the largest exposed block of Archaean crust in the world with an area of 1.6 million $km^2$ (Hoffman, 1989). It was assembled between 3.1 and 2.65 Ga as a series of subparallel east-northeast trending belts of contrasting lithologies, ages and metamorphic grade. Card (1990) has classified them into four types of belts: granite-greenstone (volcano-plutonic), metasedimentary, plutonic, and high-grade gneiss belts.

High-grade gneiss belts mark the northern and southern limits of the Superior Province. They are composed mainly of upper amphibolite to granulite facies gneisses of both plutonic and sedimentary origin (Card, 1990). Alternating granite-greenstone terranes (GGT) and metasedimentary subprovinces compose the broad central region of the Superior Province. Metamorphic grade in the GGT and metasedimentary belts is generally low, ranging from sub-greenschist to greenschist facies. Large-scale faulting, metamorphic transition and narrow deformation zones mark the boundaries between the subprovinces of the Superior Province.

### 1.2.2 Abitibi greenstone belt (AGB)

The majority of metallic mineral deposits of the Superior Province lie within granite-greenstone subprovinces. Among these, the Abitibi ranks as the world's most prolific gold-producing greenstone belt (Colvine et al., 1988), having yielded over 3400 metric tons (120 million ounces) of gold. The AGB spans northeastern Ontario and northwestern Québec (Fig. 4). This lozenge-shaped terrane is truncated by the high-grade gneisses of the Kapuskasing structural zone to the west and by the Grenville front tectonic zone to the east (Card, 1990). The Opatica Subprovince para- and orthogneisses mark the

northern boundary of the AGB, while the metasedimentary rocks of the Pontiac Subprovince are in fault contact with the rocks of the AGB to the south.

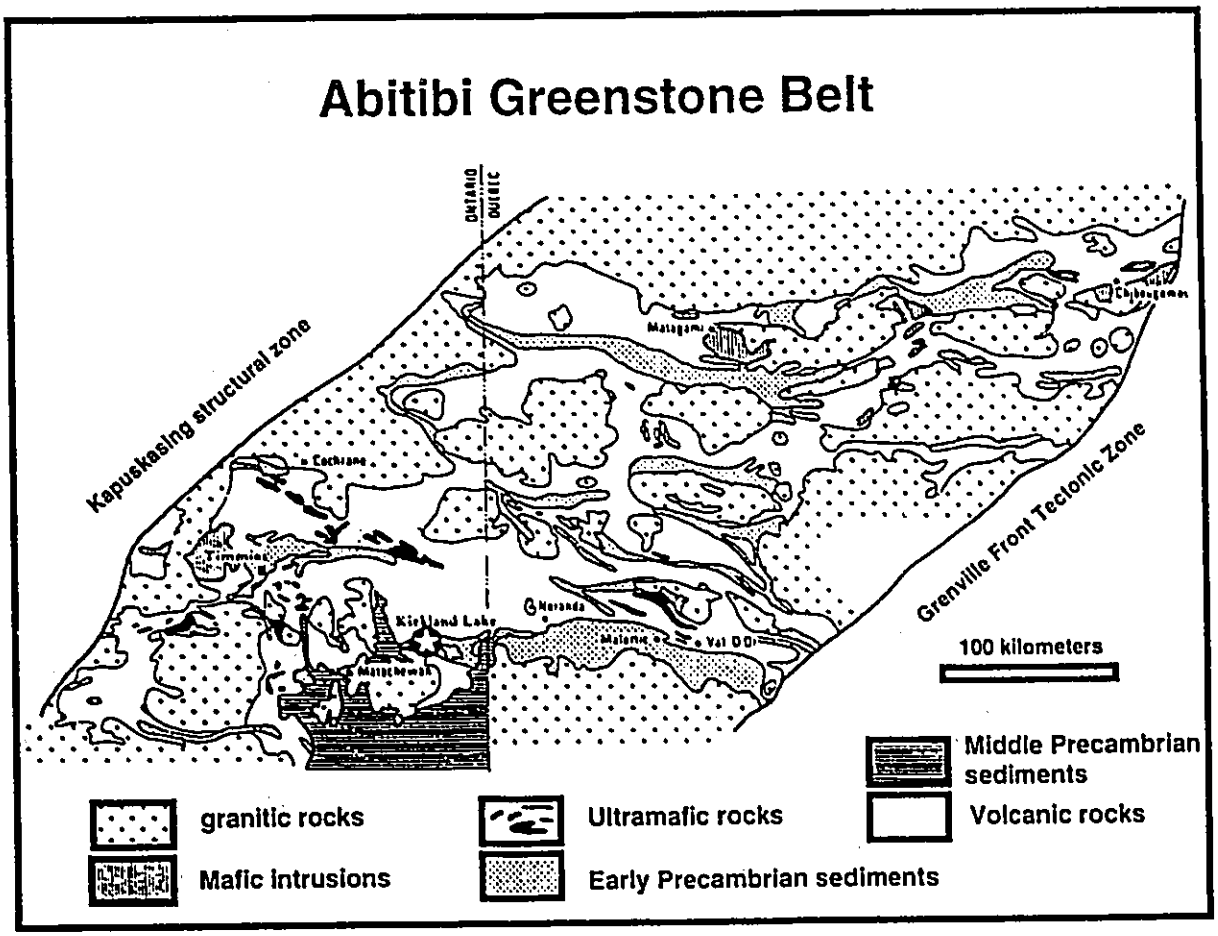


Figure 4 : The Abitibi greenstone belt. The belt is bounded to the east by the Grenville Province and to the west by the Kapuskasing structural zone. The Kirkland Lake area is highlighted by a star. (Map reproduced from Goodwin and Ridler, 1970)

The AGB is the largest greenstone belt in the world, covering an area of over 85 000 $km^2$ (Card, 1990). It is composed of 80% volcanic and plutonic rocks, and 20% metasedimentary rocks. Of the volcanic rocks, 70% are tholeiitic in composition, 25% are calc-alkaline, while komatiitic and alkaline rocks account for the remaining 5% (Card, 1990).

The repeated volcanic sequences of the AGB, composed of vertically-stacked komatiitic, tholeiitic, calc-alkaline, and alkaline rocks, were originally interpreted to be large volcanic cycles representing initial sialic crust formation (Jensen, 1985). However, later U-Pb zircon geochronological studies suggest that the cycles, formed between 2.73 and 2.70 Ga, were tectonically-juxtaposed through major thrusting (Corfu et al., 1989). Recent seismic-reflection profiles of the southern AGB reveal horizontal and shallow-dipping reflectors of regional extent in the upper 15 km of crust; these possibly represent low-angle faults, major thrusts or listric faults (Jackson et al., 1990).

The metasedimentary rocks of the AGB are associated with distinct volcanic types. Iron-formations, chert and mudstones form thin units within the sequences of komatiitic and tholeiitic rocks which are interpreted to represent a submarine lava plain (Card, 1990). Thick turbiditic sequences of siltstone, wacke and conglomerate occur within and adjacent to large tholeiitic to calc-alkalic volcanic centers. These metasedimentary rocks were formed in shallow marine, slope and submarine fan environments (Card, 1990).

Sedimentary rocks associated with alkaline volcanism in the southeastern corner of the AGB belong to the Timiskaming Group. The group

is subdivided into a non-marine series and a re-sedimented series (Hyde, 1980). The non-marine series is composed mostly of pebble-cobble conglomerate and sandstone formed in a braided-river environment. Small amounts of siltstone and argillite were deposited in floodplains. Lacustrine and eolian sandstones are minor constituents of the non-marine series. The re-sedimented series consists of thick (1800 m), interbedded turbidites (sandstone-siltstone-argillite), and conglomerates that were deposited in a submarine fan environment. Timiskaming Group rocks are spatially associated with the two major gold-producing faults in the AGB, the Porcupine-Destor fault (Timmins gold camp) and the Larder Lake fault (Kirkland Lake and Larder Lake gold camps) and its Québec extension, the Cadillac-Malartic break (Val d'Or gold camp).

### 1.2.3 Tectonic evolution of the Superior Province and Abitibi greenstone belt

Recent interpretations suggest that the Superior Province was created by the successive northward accretion of Archaean island arcs and their accompanying sedimentary prisms (Hoffman, 1989; Card, 1990). Subduction-driven, oblique accretion culminating in collision with the foreland to the south is the preferred mechanism for the assemblage of the Superior Province. This mechanism involves north-south compression. Similar interpretations have been made for the AGB (Hodgson and Hamilton, 1989; Hoffman, 1989; Jackson and Fyon, 1991; Jackson, 1992).

However, there is no consensus in the position of the subduction zone(s) during the final assemblage of the AGB. Dimroth et al. (1983b) favor north-dipping orthogonal subduction, while Ludden et al. (1986) favor south-dipping,

sinistral-oblique subduction. Hoffman (1989) suggests north-dipping dextral-oblique subduction. Clearly, the tectonic evolution of the AGB is complex. Hubert et al. (1984) concluded that sinistral strike-slip faulting occurred during oblique subduction early in the development of the Cadillac-Malartic break (CMB) and LLF. Studies along the CMB southeast of Val d'Or indicate that dextral transpression was dominant in the last stages of development of the CMB and LLF, ending in transcurrent shearing (Robert, 1989).

## 1.3. Local Geology

The Kirkland Lake area has a rich mining history. It is also one of the most intensely studied areas in the Canadian shield. Among these studies, the Kirkland Lake area is described in the classic report by Jas. E Thomson (1950). Other early studies include those by Burrows and Hopkins (1923), Todd (1928), Thomson et al. (1950) and Wilson (1956). The research area for this project spans several townships: Teck (Thomson, 1950), Otto (Lovell, 1972), Lebel (MacLean, 1944), Gauthier (Thomson and Griffis, 1941), MacElroy (Abraham, 1950), McVittie (Thomson, 1941) and McGarry (ibid.) . Maps produced from geological investigations of these townships served as the author's primary research tool. It is a tribute to these geologists that their maps are still widely used by geologists today.

### 1.3.1 The Kirkland Lake-Larder Lake fault zone

The prominent feature of the Kirkland Lake-Larder Lake area is a narrow, sinuous belt of deformed and faulted rocks that stretches over 60 km between Kenogami Lake and the Québec-Ontario border (Fig. 1). This belt is

known as the Kirkland Lake-Larder Lake fault zone (KLF). The KLF is the western termination of the major east-trending Larder Lake fault (LLF) and its eastern extension in Québec, the Cadillac-Malartic break (CMB).

The KLF is bound to the south by the Larder Lake fault. Displacement along the LLF has been interpreted as dominantly strike-slip (Hubert et al., 1984) or normal-slip (Dimroth et al., 1983). Subsequent reactivation of the south-dipping LLF occurred as thrusts or reverse faulting with the south side moving upwards (Thomson, 1950: Hodgson, 1986; Sibson et al., 1988; Hodgson et al., 1991). The LLF is a brittle-ductile shear zone, 20 m to 100 m wide, composed mostly of chlorite and chlorite-sericite schists (Hodgson et al., 1991). Carbonitization of the schists within the shear zone is so intense that they were previously viewed as stratiform carbonatites (Stricker, 1978). The LLF acted as the major conduit for the emplacement of felsic magmas, $CO_2$ fluxing and the migration of auriferous fluids along the KLF.

Syenitic and granitic plutons within the KLF (domain 1) intrude the sedimentary and alkaline volcanic rocks of the Timiskaming Group which blanket the KLF (Fig. 1). The basal unconformity between the Timiskaming Group rocks and the metamorphosed greenstone basement, whose youngest member is dated at 2701 ±2 Ma (U-Pb, zircon, Corfu et al., 1989), marks the northern limit of the KLF. Timiskaming sedimentation and volcanism began around 2686 Ma but was most active between 2680 and 2677 Ma (U-Pb, zircon, Corfu et al., 1991). The emplacement of syenitic and granitic rocks in Domain 1 probably occurred in that same time span (Corfu et al., 1991); in domain 3, the Otto stock has been dated at 2679 ± 1 Ma (U-Pb, zircon, Corfu and Noble, 1992). Lamprophyres from the KLF were emplaced over a span of

80 Ma : a dyke from the Larder Lake area was dated at 2755 ± 3 (Corfu et al., 1991) while one dyke from the Kirkland Lake area was dated at 2674 ±2 Ma (Wyman and Kerrich, 1989).

The late Archaean represents a time of many overlapping geologic events in the KLF. Magmatism, deformation, sedimentation, fluid and volatile migration all occurred within a brief time span. One of the keys to understanding the unfolding of these events, as well as the place of gold ore formation, is an understanding of the duality of magmatism of the KLF. The following chapters present a detailed examination of the duality of magmatism observed in the three domains along the KLF. The second chapter presents a detailed description of all the rock types belonging to the two suites found along the KLF. The third chapter focuses on the geochemistry of the rock units, while the fourth chapter discusses the petrogenesis of the two suites of the KLF. Finally, the last chapter will address the duality of magmatism and what it reveals about gold mineralization along the KLF.

## 2. Description and mineralogy of the rock units

Two suites of magmatic rocks, one syenitic, the other granitic, have been recognized along the KLF (Fig. 1). The classification is based on numerous mineralogical and textural differences observed both in the field and under the microscope. Rocks belonging to the syenitic suite are equigranular to porphyritic, contain no quartz, are usually nepheline-normative, have clinopyroxene as their dominant ferromagnesian mineral, and K-feldspar usually dominates over plagioclase. Granitic rocks (sensu lato) are porphyritic, quartz-bearing or quartz-normative, have amphibole as their dominant ferromagnesian mineral, and plagioclase dominates over K-feldspar.

Three magmatic domains have been distinguished along the KLF (Fig. 2). These domains group together intrusions which display similar mineralogy, textures and morphology (reflecting level of emplacement). Both suites are represented by a broad spectrum of rock types within the 3 domains (Fig. 5). All rock types are classified according to IUGS nomenclature (Streckeisen, 1976). Each of these is described in detail in the following sections, grouped by their occurrence within domains 1 to 3.

### 2.1 Domain 1

Domain 1 comprises the Kirkland Lake-Larder Lake fault zone (KLF). It is bound to the south by the Larder Lake fault (LLF) and to the north by the unconformity between the rocks of the Timiskaming Group and the underlying greenstone basement (Fig. 1). The syenitic and granitic rocks of domain 1 were passively intruded into fractures while the KLF was undergoing extension

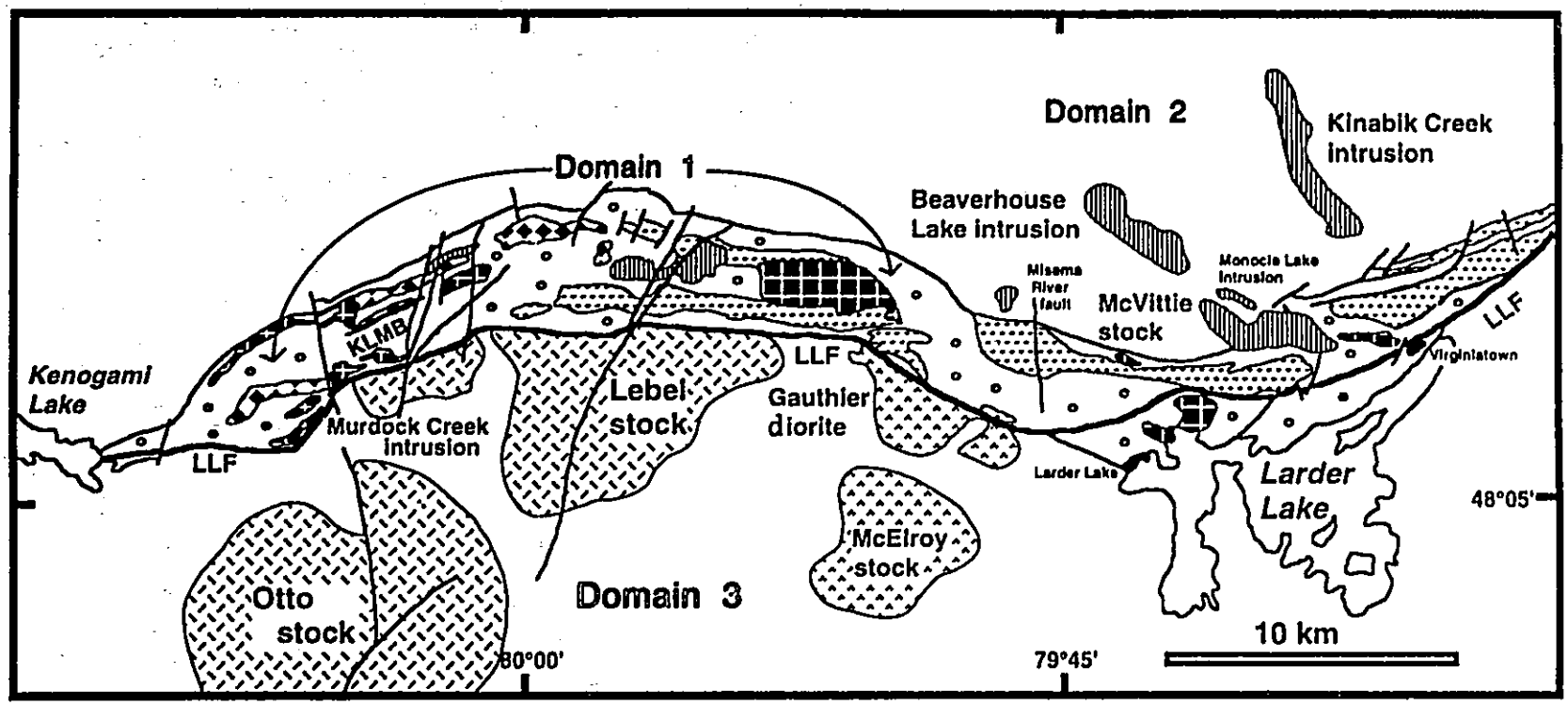


Figure 5: Major rock types found along the KLF. Note the concentration of syenitic rocks in the western portion of the fault zone. The composite syenitic intrusions of domain 3 include lithological units such as clinopyroxenite, hornblendite, alkali-feldspar melasyenite and alkali-feldspar syenite. Granitic rocks are prevalent in the central and eastern portion of the KLF.

(Cameron, 1990). This explains the orientation and morphology of the intrusive and extrusive bodies of domain 1, which are thin and elongated, and are mostly parallel to the general strike of the KLF. This is best exemplified by the elongated syenitic and granitic intrusions into which gold was later deposited along the KLMB (Fig. 6). Domain 1 is characterized by rocks that display extensive cataclastic deformation and fracturing, hematitization, and carbonatization.

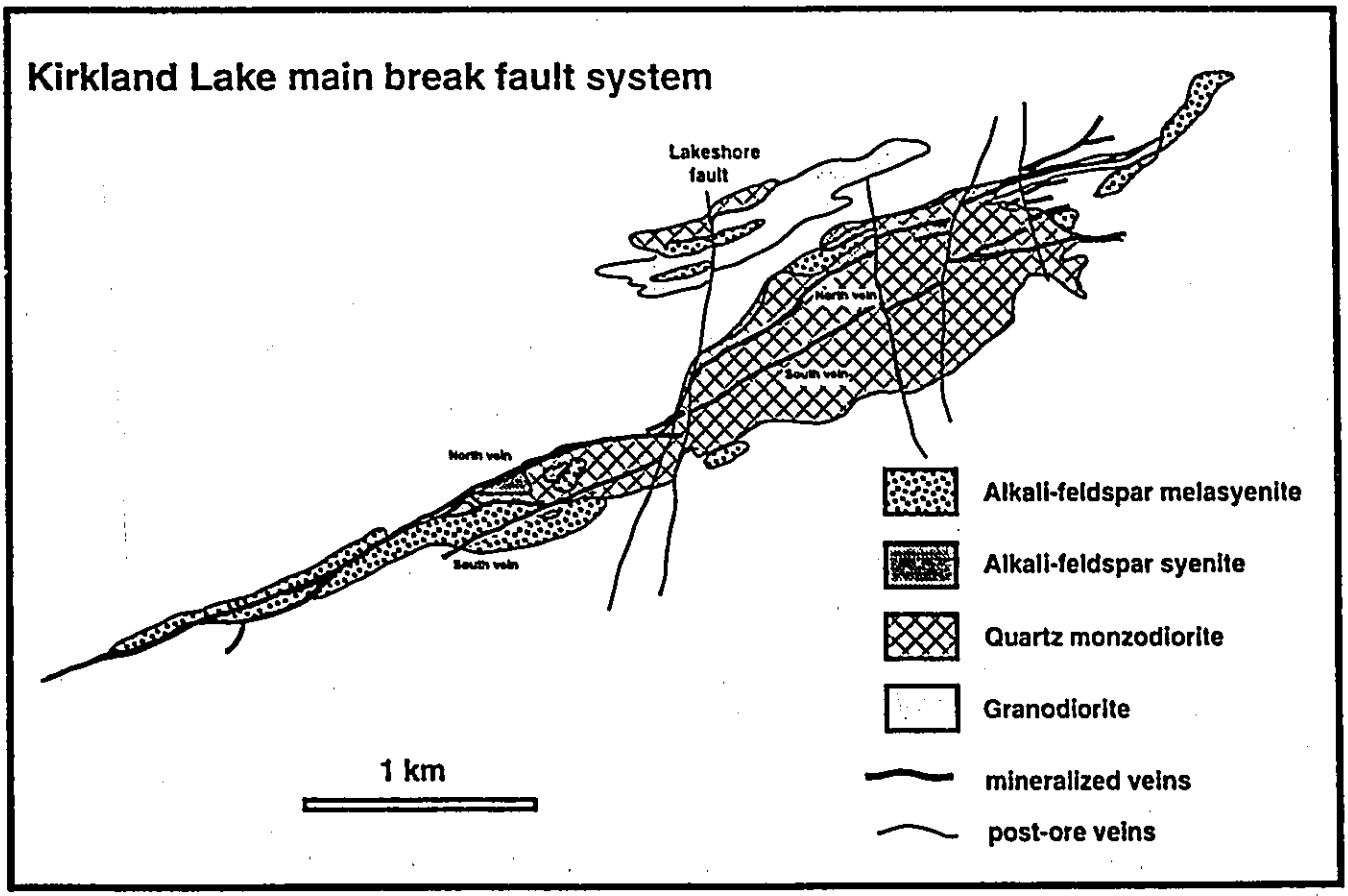


Figure 6: The Kirkland Lake main break. Late gold-bearing fault systems (veins) in the KLF crosscut thin and elongated syenitic and granitic intrusions, which are parallel to the general strike of the KLF basin. The North and South veins are the most prolific gold-producing faults of the Kirkland Lake gold camp.

Within domain 1, both syenitic and granitic rocks outcrop as hypabyssal intrusive bodies, while the extrusive "trachytes" of the Timiskaming Group are predominantly syenitic. Seven different rock types have been identified within domain 1. Alkali-feldspar melasyenite, alkali-feldspar syenite, lamprophyre, and melamonzonite belong to the syenitic suite. Quartz monzodiorite, grading to quartz melamonzodiorite, and granodiorite compose the granitic suite. Trachytes from the Timiskaming Group are mostly syenitic (leucite trachyte and mafic trachyte) ; however, a minor amount of trachyte (some felsic trachyte and andesite) is quartz-normative or quartz-bearing (Cooke and Moorhouse, 1969). The following sections are a compilation of descriptions of both altered and least-altered specimens of each rock type. Both types of specimens were studied to evaluate the effects of alteration in order to select the best samples for geochemical analysis.

## 2.1.1 Syenitic rock units

### 2.1.1.1 Alkali-feldspar melasyenite

This unit is the volumetrically largest intrusive syenitic rock type within domain 1. This rock is commonly referred to as augite syenite (Thomson, 1950); other terms used to describe this unit include mafic syenite (G. Nemscok, pers. communication, 1988), basic syenite (Todd, 1928; Thomson, 1950), and lamprophyre (Todd, 1928). The majority of the alkali-feldspar melasyenite outcrops are found between Kenogami Lake and the eastern limit of the KLMB (Fig. 5). Alkali-feldspar melasyenite is most

commonly observed as dykes (up to 5 m wide) and thin elongate intrusions along the southern and northern margin of domain 1.

Alkali-feldspar melasyenite represents the oldest intrusive unit of domain 1 (Thomson et al., 1950). The unit is texturally slightly heterogeneous, ranging from equigranular to moderately porphyritic. The alteration and leaching of ferromagnesian minerals imparts a pitted surface to the rock on weathered faces in outcrops, giving the unit an apparent "porphyritic" texture. Alkali-feldspar melasyenite, which occurs mainly along the KLMB, is usually altered and fractured, and dark greenish-grey colored due to substantial chloritization.

Least-altered alkali-feldspar melasyenite is dark olive-grey, medium-grained, and hypidiomorphic to idiomorphic. This syenitic rock unit is distinctive by the abundance (30 to 40 vol.%) of large (0.2 to 1.0 cm) euhedral clinopyroxene that commonly display compositional zoning under the microscope. The pyroxene is slightly pleochroic from light greenish-yellow to very light yellow, and contains solid inclusions of magnetite and apatite and abundant pinkish inclusions which probably represent $CO_2$- rich gas. This unit commonly crosscuts carbonatized zones, and is often itself carbonatized (Thomson et al., 1950), indicating that $CO_2$-rich fluids and alkali-feldspar melasyenite were contemperaneous. Clinopyroxene crystals are commonly fractured, the latter filled by hydrothermal biotite and chlorite (Plate 1A) . The assemblage actinolite-chlorite-calcite ± magnetite replaces clinopyroxene in altered alkali-feldspar melasyenite.

**Plate 1**: The intrusive syenitic rocks of domain 1. The field of view for all photographs is 5 mm. (Crossed polars)

**A.** Alkali-feldspar melasyenite, showing fractured euhedral clinopyroxene and altered K-feldspar.

**B.** "Hybrid" syenite, displaying altered feldspar (right) and clinopyroxene (left) phenocrysts. The groundmass is composed of fine-grained interlocking K-feldspar, plagioclase and magnetite.

**C.** Lamprophyre (var. minette) dyke, containing pleochroic zoned biotite. Note the dark brownish green rim of the diagonal biotite crystal.

**D.** Lamprophyre (var. spessartite) dyke, with abundant prismatic amphibole. The groundmass is composed mostly of plagioclase.

**E.** Lamprophyre (var. vogesite) dyke, composed of small equant clinopyroxene (transparent) and the darkly-rimmed pleochroic zoned biotite. Note that the dark rim around the biotite crystal is slightly chloritized.

**F.** Melamonzonite unit of the Teck-Hughes property. The center of the photograph contains a quartz monzodiorite fragment (yellowish-brown amphibole and plagioclase) surrounded by equant rounded white clinopyroxene and a dark hematitized alkali-feldspar matrix.

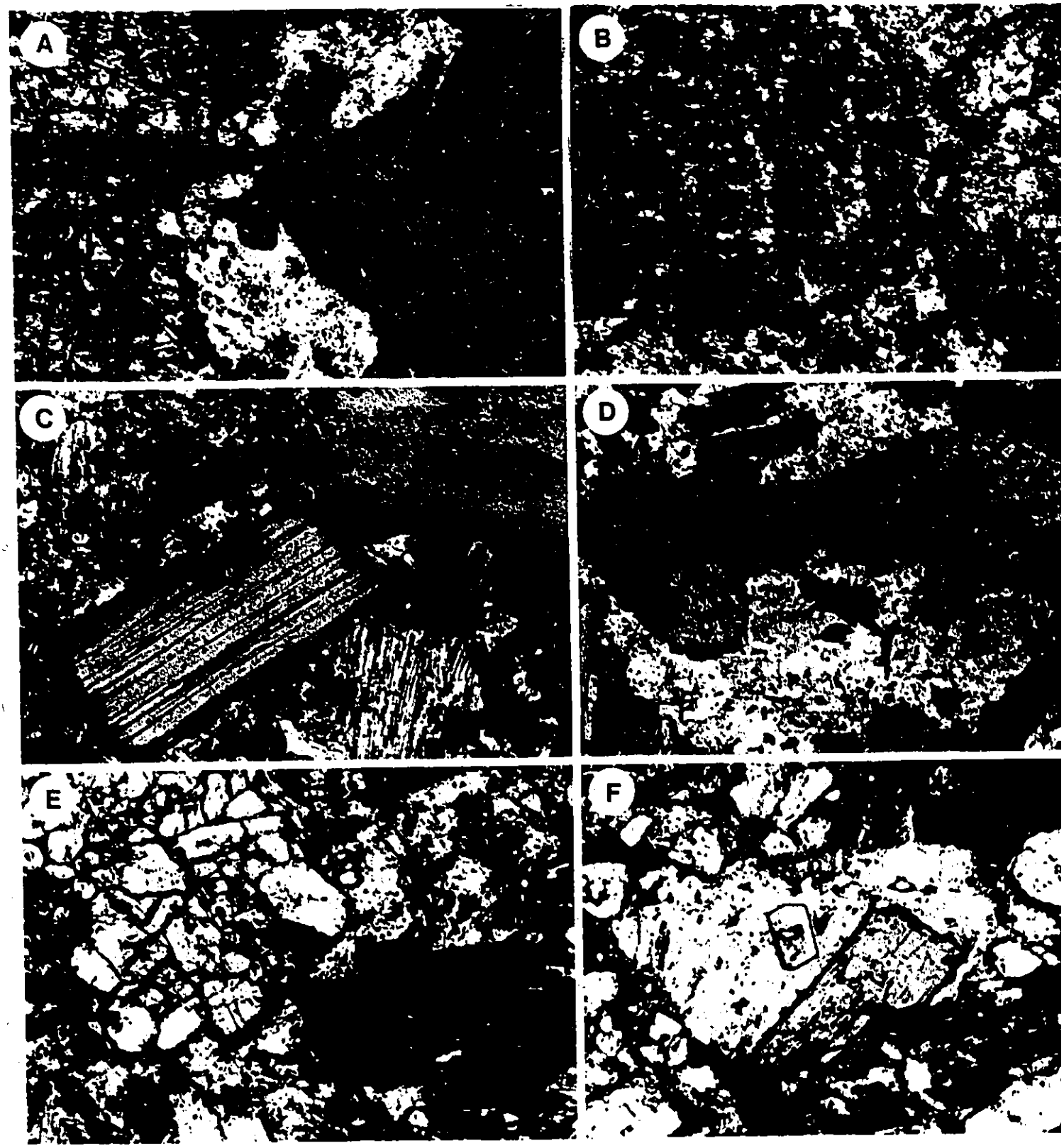
A
B
C
D
E
F

Biotite is the second important ferromagnesian mineral; at least three different types have been identified. Primary biotite (up to 7 vol.%), commonly associated with magnetite, is subhedral and elongate (0.1 to 0.8 cm), pleochroic dark reddish-brown to light tan-brown. Chloritization, accompanied by rutile needles and leucoxene, occurs along the edges and cleavage planes of primary biotite. Hydrothermal biotite (up to 2 vol.%) occurs as aggregates (0.1 to 0.4 cm) and as small single flakes (up to 0.2 cm) and is anhedral to subhedral, pleochroic dark green to light yellow-green. This type of biotite, also observed in the quartz monzodiorite (Hicks, 1990), is frequently observed along fractures in clinopyroxene. Green hydrothermal biotite is commonly mistaken for chlorite; its crystal habit and higher birefringence are distinguishing characteristics. A third type of hydrothermal biotite, occurring as rims around clinopyroxene, is observed in samples collected near mineralized veins, and is typically fine-grained and chocolate-brown.

Magnetite (up to 5 vol.%) is an early crystallizing euhedral phase (up to 0.6 cm), and is commonly enclosed within clinopyroxene crystals. It is intimately associated with primary biotite, crystallizing around or even within biotite crystals. Some magnetite crystals contain exsolved ilmenite lamellae. Minor replacement by hematite along fractures and cleavage planes is common. Magnetite grains associated with biotite are commonly rimmed by titanite and rutile. Apatite (trace to 1 vol.%), like magnetite, is commonly found enclosed in clinopyroxene crystals. It occurs as small (0.2 cm) euhedral prismatic crystals.

Subhedral perthitic feldspar, composed of about 50 to 65 vol.%

K-feldspar and 35 to 50 vol.% Na-feldspar, constitutes between 50 and 60 vol.% of this rock type. The perthite is interlocking and discrete domains range in width from 0.2 to 0.7 mm. Microperthitic textures are clearly visible in least-altered samples although albite exsolution lamellae are generally about 2μm wide. These perthites readily unmix and coarsen during hydrothermal alteration (Martin, 1973; Parsons, 1977); thus most samples do not preserve this primary feature. Reddening of feldspar in less-altered samples is caused by hematitization. Pervasive alteration results in the formation of distinct anhedral patches of albite + calcite ; this assemblage is characteristic of altered alkali-feldspar melasyenite.

#### 2.1.1.2 Alkali-feldspar syenite

This is the least abundant intrusive rock type of domain 1. Syenite (Thomson et al., 1950), acid syenite (Todd, 1928), red syenite (Todd, 1928), and felsic syenite are some of the names used to describe this unit. Alkali-feldspar syenite is spatially associated with alkali-feldspar melasyenite; it differs from the latter only in the amount of mafic minerals present, usually less than 15 vol.%. In outcrop, the unit has a distinct brownish-red color owing to the larger proportion of hematitized alkali-feldspar in the rock. Contact relationships between this rock type and alkali-feldspar melasyenite are varied: in areas, alkali-feldspar syenite grades into alkali-feldspar melasyenite, while in others a sharp intrusive contact is observed. Recent drilling at the Macassa mine intersected a large alkali-feldspar melasyenite unit which grades smoothly into alkali-feldspar syenite (G. Nemscok, pers. communication, 1989); thus both rock types are comagmatic and were emplaced contemporaneously.

Alkali-feldspar syenite is equigranular and predominantly composed (85 to 100 vol.%) of subhedral microperthitic feldspar (0.3 to 0.6 cm). The feldspar is commonly turbid and reddish in color due to the presence of secondary hematite. Some feldspars show minor sericitic alteration; in general, the interlocking perthitic texture is well-preserved. Primary biotite (0.1 to 0.5 cm) is subhedral, pleochroic light yellow-brown to dark brown, and often chloritized along edges and cleavage planes. Altered pseudomorphs of clinopyroxene are composed of green hydrothermal biotite+ carbonate mineral . Small euhedral magnetite crystals (0.05 to 0.2 cm) are partially replaced by hematite in fractures, edges and along octahedral cleavage planes. Some magnetite crystals are rimmed by a thin mantle of leucoxene.

A thin band of syenite outcrops immediately southwest of the KLMB. This rock was named augite porphyrite (Thomson, 1950). The author has used the field term "hybrid" syenite, because mineralogically, it is very similar to the syenitic rock units, while texturally, it resembles the rock units of the granitic suite. On outcrop surfaces, large resistant white feldspar phenocrysts have a slightly raised relief against the groundmass while green clinopyroxene phenocrysts are leached and weather recessively into the face. The groundmass has a medium pinkish-brown color.

Three phenocryst phases (35 vol.%) are present in the "hybrid" syenite: large (0.3 to 0.8 cm) subhedral K-feldspar crystals account for 15 vol.%, large (0.1 to 0.7 cm) euhedral clinopyroxene also account for 15 vol.%, and small (0.1 to 0.3 cm) euhedral plagioclase make up the remaining 5 vol.% of the phenocrysts. The groundmass (65 vol.%) is composed of roughly equal amounts (app. 30 vol.% each) of equigranular alkali-feldspar and plagioclase, and small

euhedral magnetite grains (0.05 to 0.2 cm) disseminated throughout the rock (< 3 vol.%). Anhedral quartz grains and euhedral apatite crystals are trace constituents (< 1 vol.%).

In altered specimens, the large K-feldspar and the smaller plagioclase phenocrysts are sericitized and commonly have secondary albite rims. Clinopyroxene phenocrysts are replaced by an assemblage of actinolite+ chlorite+ epidote± calcite pseudomorphs (Plate 1B). The feldspar groundmass is less altered than the phenocrysts; however, minor replacement of the feldspars by sericite, calcite and epidote can be observed. Finely disseminated secondary hematite imparts to the groundmass a pinkish-brown color.

### 2.1.1.3 Lamprophyre

The mafic nature of alkali-feldspar melasyenite led early workers to name this rock type "lamprophyre" (see Todd, 1928). True lamprophyric dykes were subsequently recognized (Todd, 1928; Thomson, 1950); the name lamprophyre describes small mafic dykes containing large mica phenocrysts. Three types of lamprophyre have been identified in domain 1. The most common type is minette: large biotite phenocrysts are characteristic. Vogesite, the less common lamprophyre, is distinctive by the predominance of commonly zoned clinopyroxene phenocrysts over biotite phenocrysts. One occurrence of spessartite was noted southwest of the KLMB; this rock contains both biotite and amphibole set in a plagioclase matrix. Following IUGS nomenclature, all three belong to the calc-alkaline branch (Streckeisen, 1979); these lamprophyres have also been described as shoshonitic (Rock, 1987).

All three types of lamprophyre occur as small, irregular dykes of varying width (10 cm to 5 m). In the Kirkland Lake gold camp, lamprophyre is the youngest rock type, crosscutting all lithological units; one dyke has been dated at 2674±2 Ma (U-Pb, zircon, Wyman and Kerrich, 1989). However, in the Larder Lake area, one lamprophyre dyke has been dated at 2755 ± 34 Ma (U-Pb, zircon, Corfu et al., 1991), making it one of the oldest intrusive rocks of the KLF. Crosscutting relationships with gold veins in the Kirkland Lake camp remain unclear; some lamprophyres cut gold-bearing and younger barren veins and therefore postdate mineralization (Thomson, 1950), while others are cut by gold veins (McNeil and Kerrich, 1986; Rock and Groves, 1988). Lamprophyre emplacement possibly brackets the gold mineralization event.

Minette dykes are typically dark grey in hand sample. Large (up to 1.5 cm) euhedral biotite phenocrysts (30 to 40 vol.%) are set in a fine-grained (0.01 to 0.1 cm) groundmass (up to 60 vol%) of equigranular K-feldspar and albite. Small (0.05 to 0.1 cm) euhedral magnetite crystals are disseminated throughout the rock (< 5 vol.%). The biotite phenocrysts display pleochroic zoning distinctive of the lamprophyres in the area, with light-colored cores (very light brown to light greenish-brown) and darker-colored rims (olive-green to dark olive-green) (Plate 1C). Carbonate minerals and chlorite are common secondary minerals in more altered specimens. Hematite partially replaces magnetite in more altered samples.

Southwest of the KLMB, a small 2 metre-wide lamprophyre dyke associated with alkali-feldspar melasyenite intrudes the tholeiitic basalts of the Larder Lake Group. This equigranular rock resembles minette described

above, containing abundant (20 vol.%) subhedral to euhedral biotite (0.2 to 0.4 cm) that displays the typical pleochroism of biotite in minettes. However, small prismatic (up to 0.3 cm) subhedral amphibole (30 vol.%) are present, and magnetite is usually absent, distinguishing this rock from typical minette occurrences (Plate 1D). The feldspar matrix (50 vol.%) is composed of anhedral plagioclase grains (0.05 to 0.2 cm) displaying albite twinning. This lamprophyre, which also belongs to the calc-alkaline branch, is most like spessartite (Streckeisen, 1979; Rock, 1987 and 1991).

Vogesite dykes are dark greyish-brown in hand sample. They have two microphenocryst phases: commonly zoned equant subhedral clinopyroxene (30 vol.%) ranges between 0.1 mm to 0.7 cm in size, and euhedral biotite (20 vol.%), up to 0.5 cm in size, which displays pleochroism identical to biotite found in minettes (Plate 1E). The groundmass is composed almost exclusively of subhedral (0.1 to 0.4 cm) lath-shaped and anhedral patchy (usually 0.2 cm) alkali-feldspar (45 vol.%). Fine-grained (0.1 to 1.0 mm) magnetite (< 5 vol.%) is disseminated in the rock. Biotite is commonly chloritized along edges and cleavage planes in altered samples.

#### 2.1.1.4 Melamonzonite

One occurrence of a mafic, clinopyroxene-rich rock type was observed along the KLMB on the old Teck-Hughes mine property. This unit is unlike any of the other syenitic rock types; the unit is a dark olive-green colored, massive, fine-grained equigranular rock. Small (0.05 to 0.2 cm), commonly zoned subhedral clinopyroxene accounts for over 50 vol.% of the rock. The zoned clinopyroxene crystals exhibit very light yellow to light greenish-

yellow pleochroic rims, and colorless cores. Euhedral amphibole (< 1 vol.%) and magnetite (< 2 vol.%) occur as trace constituents. The mafic minerals are set in a fine-grained feldspar matrix, composed of roughly equal amounts of plagioclase and perthitic alkali-feldspar. Subhedral plagioclase laths commonly show primary mineral alignment; alkali-feldspar is anhedral and does not show alignment.

Analysis of thin sections reveals that the melamonzonite contains fragments of both syenitic and granitic rocks set in a syenitic matrix. These fragments are recognized by the varying reddish coloration of their groundmass. The syenitic fragments are most abundant, accounting for more than 50 vol.% of the rock ; these contain the clinopyroxene and fine-grained greyish to reddish perthitic alkali-feldspar. The less common granitic fragments (30 vol.%) contain amphibole phenocrysts surrounded by aligned plagioclase laths in a very-fine grained, reddish and less opaque groundmass (Plate 1F). The dark red rock matrix (20 vol.%) has an identical composition to that of the syenitic fragments. This unit therefore represents an intrusive or hypabyssal breccia. It indicates that syenitic magmatism (excluding lamprophyric magmatism) not only predates (Thomson, 1950), but also postdates granitic magmatism in domain 1.

## 2.1.2 Granitic rock units

### 2.1.2.1 Quartz monzodiorite

Feldspar porphyry is the common name given to the most abundant granitic hypabyssal intrusive rock found within domain 1. The term feldspar

porphyry was used by Hewitt (1963) and Cooke and Moorhouse (1969). It has also been called syenite porphyry (Todd, 1928; Thomson, 1950). According to IUGS nomenclature (Streckeisen, 1976), this unit falls in the quartz monzodiorite field of the QAP diagram (Hicks and Hattori, 1988; Hicks, 1991). Irregularly-shaped elongate bodies of quartz monzodiorite display well-defined intrusive contacts that crosscut both alkali-feldspar melasyenite and alkali-feldspar syenite (Thomson, 1950). Quartz monzodiorite represents the most abundant granitic intrusive rock type of domain 1. Quartz monzodiorite lenses and dykes occur throughout the field area between Kenogami Lake to the west and Virginiatown to the east (Fig. 5), and as elongate intrusions in the eastern half of the KLMB (Fig. 6).

This rock type is generally less altered or deformed than the older syenitic intrusive rocks of domain 1. Outcrops of this unit range from pinkish-red to dark grey in color, are distinctly porphyritic and usually texturally homogeneous; some outcrops display a well-developed flow foliation textures. Both rounded and angular dark-green xenoliths are frequently observed; they were probably stoped from the underlying greenstone basement. Phenocryst phases include plagioclase, alkali-feldspar, amphibole, biotite, and in a rare instance, clinopyroxene. Apatite and magnetite are microphenocrysts. The distribution of small plagioclase and large alkali-feldspar phenocrysts in this rock type produces a rock called bimodal porphyry by Hicks and Hattori (1988). Following their work, four quartz monzodiorite sub-units have been identified on the basis of phenocryst assemblages: plagioclase-biotite quartz monzodiorite, plagioclase-orthoclase-biotite quartz monzodiorite, plagioclase-amphibole-biotite quartz monzodiorite, and quartz-plagioclase-orthoclase-biotite porphyry. The latter is commonly referred to as quartz-feldspar

porphyry (Thomson, 1950) and here is classified as a distinct granodiorite unit. It will be described in the next section. Contacts between all four sub-units of the quartz monzodiorite vary from gradational to sharp; as in the syenitic units, these contact relationships indicate the comagmatic and coeval emplacement of these varieties of monzodiorite. Much of the following information is taken from Hicks and Hattori (1988).

Quartz monzodiorite is typically hypidiomorphic and dark olive-grey, containing abundant, varied phenocrysts set in a fine-grained groundmass (between 35 and 70 vol.%) of varying amounts of plagioclase and K-feldspar, with minor quartz, magnetite, apatite and titanite (Plate 3A). Plagioclase phenocrysts (between 10 and 40 vol.%) are euhedral, small (0.01 to 0.3 cm), commonly display albite twinning, and are less commonly zoned. The plagioclase phenocrysts have compositions that vary between oligoclase and albite. Orthoclase phenocrysts are large (0.1 to 1.5 cm), subhedral, often containing inclusions of plagioclase, and account for up to 10 vol.% of the rock. The feldspars (as phenocrysts and in the matrix) are sericitized and carbonatized in more altered samples. Feldspars are commonly pinkish because of hematite inclusions.

Biotite phenocrysts are small (0.02 to 0.5 cm), euhedral, tabular and elongate, pleochroic dark reddish-brown to greenish-brown, and account for up to 5 vol.% of the rock. Chloritization occurs along edges and cleavage planes. An unusual type of green biotite has been identified in this unit. This hydrothermal biotite has often been mistaken for chlorite; its higher birefringence, bird's eye extinction and crystal form distinguish it from chlorite. This is the same type of green biotite found in alkali-feldspar melasyenite.

Amphibole is usually a minor euhedral, seriate (0.01 to 1.5 cm) phenocryst phase (less than 5 vol.%). However, some outcrops contain over 40 vol.% amphibole, and are therefore quartz melamonzodiorites. In some cases, the amphibole crystals are aligned and define a flow foliation. The latter rock type is not easily distinguished from the andesite phase of the Timiskaming Group extrusive rocks. Amphibole is replaced by actinolite+ chlorite+ carbonate mineral in more altered samples. Only one sample from a suite of over 70 specimens contained clinopyroxene. This clinopyroxene may be xenocrystic.

#### 2.1.2.2 Granodiorite

This unit forms a minor part of the elongated granitic rocks within domain 1. In outcrop and underground exposure, it is practically indistinguishable from quartz monzodiorite. It comes as no surprise that this unit was overlooked in early reports (Todd, 1928). It was recognized as a distinct unit only in 1950 by Thomson, who named this rock type quartz-feldspar porphyry. Both quartz monzodiorite and granodiorite are mineralogically identical; the presence of large rounded quartz phenocrysts is the only distinguishing characteristic of granodiorite. Hicks and Hattori (1988) include this unit as a phase of quartz monzodiorite; it displays both gradational and sharp intrusive contacts with other quartz monzodiorite phases. In outcrops, granodiorite is usually lighter colored (lower mafic phenocryst content), contains less phenocrysts (roughly 30 vol.%), and often contains equant euhedral K-feldspar phenocrysts that are deeply red colored. On the basis of these three features, sharp intrusive contacts can be observed between granodiorite and quartz monzodiorite near the town of Kirkland Lake. Nevertheless, the strong mineralogical and textural similarities between these

two units suggest that they are genetically related, and probably comagmatic in some instances.

Plagioclase (25 vol.%), K-feldspar (5 vol.%) and quartz (< 10 vol.%) are the three principal phenocryst phases of the unit, while amphibole (< 3 vol.%) and titanite (< 1 vol.%) are minor phenocryst phases (Plate 3B). Biotite and magnetite are typically rare or absent in this unit. Plagioclase, K-feldspar and amphibole phenocrysts are identical in appearance to those of the quartz monzodiorite unit. Titanite is small (0.02 to 0.1 cm) and wedge-shaped. Amphibole alters to a mixture of chlorite, carbonate mineral and epidote. Quartz phenocrysts are small (0.02 to 0.5 cm, up to 1.0 cm), stubby, subhedral with roughly hexagonal outlines, and commonly have embayed crystal edges. The crystal morphology of quartz in this unit (stubby hexagonal phenocrysts) is indicative of ß-quartz, the $SiO_2$ polymorph typical of high temperature and low pressure crystallization. The embayed crystal edges of these quartz phenocrysts are characteristic of rapid crystal growth. The fine-grained groundmass is composed of plagioclase, quartz and alkali-feldspar. The groundmass of granodiorite is finer-grained than that of quartz monzodiorite, resembling that of extrusive andesite and leucite trachyte. This implies that granodiorite was emplaced at a higher level than the intrusive syenitic and other granitic rocks of domain 1.

### 2.1.3 Trachyte

Trachyte, in the terminology of Cooke and Moorhouse (1969), represents the volumetrically most important, and only extrusive member of the syenitic suite of domain 1.Unfortunately, these are the least well-preserved rocks

within the KLF. Nonetheless, three distinct trachytic units can be identified on the basis of characteristic relict textures: felsic trachyte, mafic trachyte, and pseudoleucite-bearing trachyte. The elongate trachyte units, part of the Timiskaming Group, are interbedded with sedimentary rocks (conglomerate, greywacke, argillite of the Timiskaming Group) and have great lateral extent. Some units can be followed along strike for 10 km (Fig. 5). The majority of these rocks are strongly cataclastically deformed, and pervasively carbonatized and hematitized.

Cooke and Moorhouse (1969) identified four episodes of volcanism within the KLF. The first episode is characterized by adundant andesite and felsic trachyte flows, with some minor basalt, occurring in the eastern part of domain 1. The following two episodes, occurring in the centre of domain 1, are represented by early mafic trachyte and abundant late leucite-bearing flows and pyroclastic rocks. The fourth episode was dominated by felsic trachyte and mafic trachyte flows. These cyclic episodes, broadly consisting of early mafic and felsic trachyte flows culminating in leucite-bearing flows and pyroclastic rocks, indicate that repeated injection of melts, differentiating in a magma chamber, produced alkaline magmatism (Cooke and Moorhouse, 1969).

Trachyte, according to IUGS nomenclature (Streckeisen, 1979), is the volcanic equivalent to the IUGS syenite field of plutonic rocks (Streckeisen, 1976). The trachyte units of Cooke and Moorhouse (1969) belonging to the syenitic suite include rocks that are feldspathoid-bearing (pseudoleucite), clinopyroxene-bearing (mafic trachyte) and K-feldspar-bearing (felsic trachyte). Trachyte units belonging to the granitic suite are quartz-bearing and have plagioclase as the dominant feldspar type; they include andesite and

some felsic trachyte flows. One common characteristic of all of these rocks is their elongated nature and trachytic texture, defined by primary feldspar alignment. Some confusion remains in the usage of the term trachyte; it refers to both a composition (a volcanic rock where alkali-feldspar is dominant over plagioclase), and to a texture, which is characteristic of the extrusive rocks of domain 1. Thus, in domain 1, almost all rocks have a trachytic texture, but some do not have a trachyte composition. They are described below , in decreasing order of total exposed surface within the KLF.

### 2.1.3.1 Felsic trachyte

Felsic trachyte, the most common of the volcanic rocks of the Timiskaming Group, is the most altered and cataclastically deformed unit of this group. For the most part, it is identifiable only by its association with adjacent mafic and/or leucite-bearing trachyte flows. In outcrop, the rock is typically fine-grained and massive due to extensive recrystallization, displays mottled pink (hematite) and green (chlorite+ carbonate mineral ) patches, and is schistose. A few occurrences of this rock type contain large centimeter-sized K-feldspar phenocrysts surrounded by a fine-grained reddish groundmass.

Two types of felsic trachyte have been identified. The first type, porphyritic felsic trachyte contains large (up to 2.5 cm) euhedral K-feldspar phenocrysts (between 5 and 10 vol.%) set in a fine-grained groundmass of interlocking plagioclase and minor alkali-feldspar (Plate 2C). Calcite and dolomite, hematite (replacing magnetite) and chlorite are common secondary minerals. Apatite is a trace constituent of felsic trachyte. The second type, equigranular felsic trachyte, differs from the first type by the presence of

**Plate 2:** The extrusive rocks of domain 1. The field of view for photographs A, B, C, E, F, G and H is 5 mm (crossed polars). For photograph D, the field is approximately 10 cm.

**A.** Andesite. Note the trachytic texture defined by plagioclase crystals. Amphibole phenocrysts (brown-yellow) are generally parallel to the plagioclase alignment. The cryptocrystalline groundmass is probably composed of plagioclase and quartz.

**B.** Chlorite blebs in a plagioclase phenocryst. These blebs have been interpreted as altered glass by Cooke and Moorhouse (1969)

**C.** Porphyritic felsic trachyte unit containing large euhedral K-feldspar crystals encased in a fine-grained groundmass of plagioclase and alkali-feldspar. The phenocrysts locally define a trachytic texture.

**D.** Clinopyroxene-bearing mafic trachyte. This specimen displays the prominent flow foliation (right to left) defined by aligned clinopyroxene and plagioclase phenocrysts.

**E.** Photomicrograph of specimen above, showing clinopyroxene (beige) and altered plagioclase (hematitized) phenocrysts. Note the small magnetite grains enclosed in the clinopyroxene crystal in the upper left corner.

**F.** Amphibole-bearing mafic trachyte. This unit displays some of the best examples of flow foliation in the extrusive rocks; the foliation is defined by the alkali-feldspar in the groundmass which wraps around the amphibole (black) crystals. Note the euhedral apatite (grey) inclusion in the amphibole crystal in the lower left corner.

**G.** Amphibole-bearing mafic trachyte outcropping southwest of the KLMB. This auto-brecciated rock is composed of red to dark-brown amphibole trachyte fragments bonded in a dark-colored matrix of identical composition. This photograph shows a large fragment containing amphibole phenocrysts (brownish yellow) which are aligned vertically. The surrounding darker matrix contains amphibole crystals that are aligned horizontally.

**H.** Leucite trachyte, displaying the large euhedral pseudoleucite phenocrysts. Note the smaller rounded pseudoleucite crystals occurring in the groundmass between the two larger phenocrysts.

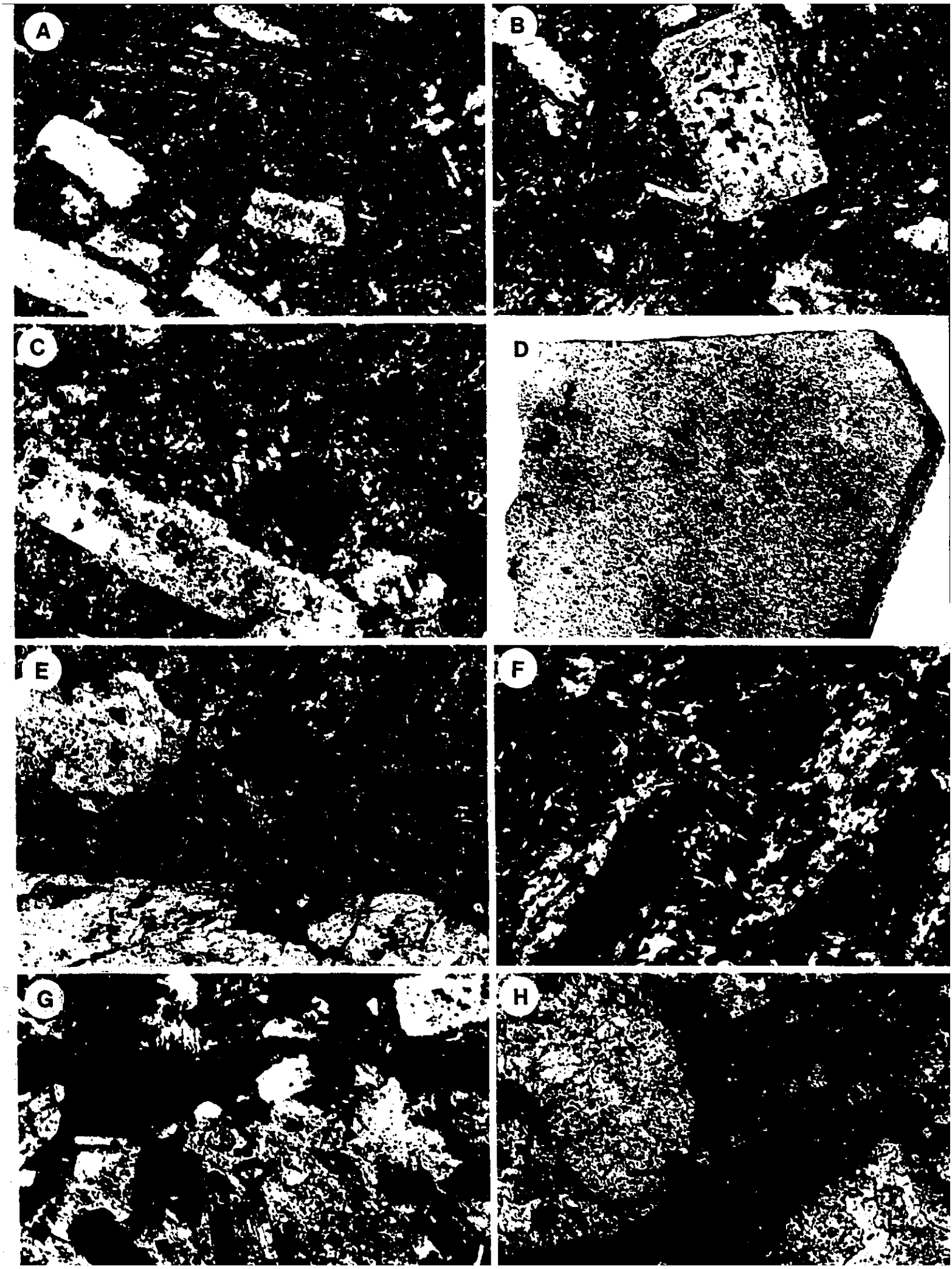
A
B
C
D
E
F
G
H

perthitic alkali-feldspar. The interlocking feldspars range in size from 0.1 to 0.4 cm, with interstitial quartz, which may be secondary, and perthitic alkali-feldspar. Accordingly, the trachytic texture is poorly developed. Sericitization and carbonatization are pervasive.

### 2.1.3.2 Leucite trachyte

One of the most striking volcanic units of domain 1 is the leucite trachyte. This unit is recognized in the field by the presence of conspicuous white, red or green equant patches in a fine-grained light to dark-brown groundmass. The term spotted trachyte and green-spotted trachyte (MacLean, 1956) has been used to describe this rock type. Closer inspection reveals that these colored patches have well-defined faces and are in fact pseudomorphs of leucite which have been replaced by fine-grained aggregates of plagioclase, orthoclase, chlorite, hematite and carbonate minerals. Leucite trachyte is present as the latest phase of volcanism in the second and third volcanic episodes identified by Cooke and Moorhouse (1969). The majority of leucite trachyte is found in the center of domain 1, north of the Lebel stock (Fig. 1). Two types of leucite trachyte occur in domain 1: leucite phonolite (Cooke and Moorhouse, 1969), composed uniquely of pseudoleucite phenocrysts in a fine-grained matrix, and leucite tephrite (ibid.), composed of pseudoleucite, alkali-feldspar and clinopyroxene phenocrysts set in a fine-grained matrix.

Least-altered leucite phonolite contains large (0.2 to 1.5 cm) euhedral pseudoleucite phenocrysts (variable up to 70 vol.%) composed of fine-grained perthitic alkali-feldspar, calcite , sericite, plagioclase and minor chlorite and hematite (Plate 2H). In more intensely altered samples, the pseudoleucite

phenocrysts are replaced by plagioclase, a carbonate mineral, sericite and minor alkali-feldspar. Small (0.01 to 0.05 cm) euhedral apatite accounts for less than 2 vol.%. The fine-grained matrix is composed of equigranular plagioclase and alkali-feldspar, sericite, calcite, hematite and minor chlorite. Anhedral patches of calcite+ quartz are common in more altered specimens. Leucite phenocrysts replaced by alkali-feldspar+ chlorite + sericite± carbonate mineral are green-colored, whereas red-colored phenocrysts contain alkali-feldspar+ carbonate mineral + hematite.

Leucite tephrite is a minor component of the leucite trachyte unit. Following IUGS nomenclature (Streckeisen, 1979), this rock is a mafic leucite phonolite. On weathered surfaces of leucite tephrite, a trachytic texture defined by aligned alkali-feldspar (and clinopyroxene) phenocrysts is clearly visible. The rock is dark greenish-brown, and the resistant pseudoleucite and clinopyroxene phenocrysts have a slightly raised relief against the softer matrix. Leucite tephrite consists of small (0.01 to 0.3 cm) subhedral clinopyroxene (15 vol.%), rounded equant pseudoleucite (20 vol.%) and subhedral alkali-feldspar (up to 25 vol.%) phenocrysts in a fine-grained groundmass of altered feldspar, hematite and carbonate mineral . This is the only rock type where pseudoleucite and alkali-feldspar occur together as phenocryst phases. Clinopyroxene is completely replaced by a mixture of chlorite, hematite and a carbonate mineral. Large apatite crystals (up to 0.1 cm) are a trace constituent.

### 2.1.3.3 Mafic trachyte

Mafic trachyte is present in all four episodes of Timiskaming volcanism (Cooke and Moorhouse, 1969). In outcrop, the rock is usually altered and cataclastically deformed. Mafic minerals are commonly leached out of the rock face, giving a pitted appearance. Mesoscopic features are generally better preserved in this phase compared to all others; flow foliation textures are defined by aligned mafic minerals (Plate 2D) and alteration minerals preserve original textures. Generally, mafic trachyte occurs in the absence of breccias or agglomerates; an amphibole-rich mafic trachyte and trachytic breccia, and accompanying agglomerate outcropping southwest of the KLMB and along the Misema River is a singular exception.

Two types of mafic trachyte have been identified in domain 1: clinopyroxene trachyte, and amphibole trachyte. Clinopyroxene trachyte is the one most commonly encountered in the field: euhedral clinopyroxene, plagioclase, alkali-feldspar and biotite phenocrysts are distinctive of this rock type. All phenocryst phases are aligned to produce a well-defined flow foliation (Plate 2D). Clinopyroxene phenocrysts, accounting for up to 40 vol.% of the rock, are large (0.01 to 0.5 cm), euhedral, pleochroic colorless to light bluish-green and contain magnetite and apatite inclusions, similar to clinopyroxene in the alkali-feldspar melasyenite unit (Plate 2E). Most specimens contain clinopyroxenes that are extensively altered and leached out; alkali-feldspar, actinolite, chlorite and calcite are the most common replacement minerals. Leucoxene rims around altered clinopyroxenes are not uncommon. Plagioclase phenocrysts account for up to 10 vol.% of this trachyte. They usually occur as small (0.01 to 0.2 cm) euhedral crystals and are commonly sericitized and

hematitized. Alkali-feldspar phenocrysts are rare (< 2 vol.%); they occur as equant euhedral crystals which are crudely aligned. All alkali-feldspars are albitized; thus altered samples will not necessarily fall in the trachyte field of Streckeisen (1979). Phenocrysts are set in a recrystallized groundmass of plagioclase, alkali-feldspar, a carbonate mineral , hematite and epidote.

Amphibole trachyte is the less common type of mafic trachyte found in domain 1. It contains amphibole and rare biotite phenocrysts set in a feldspar groundmass. In this rock both the phenocrysts and the groundmass minerals are aligned to produce one of the best examples of trachytic textures in the trachytes of domain 1 (Plate 2F). Subhedral amphibole phenocrysts are elongated (up to 0.4 cm) and account for up to 30 vol.% of the rock. Amphibole is commonly altered to chlorite+ carbonate mineral+ hematite and contain magnetite and apatite inclusions. Biotite phenocrysts are infrequent (< 2 vol.%); they resemble biotite found in the lamprophyre unit. The biotite phenocrysts are subhedral, usually elongate and commonly chloritized. These biotites are probably secondary minerals, since they commonly transect the trachytic texture of the rock. The medium-grained (0.01 to 0.03 cm) groundmass is composed of elongate to acicular alkali-feldspar and plagioclase, and minor hematite; sericitization and carbonatization of the groundmass is common. Apatite is common in the groundmass and is also aligned with the feldspar.

Southwest of the KLMB (Fig. 5) lies a thin band of agglomerates, tuffs and amphibole trachyte outcrops. The amphibole trachyte is clearly extrusive, but has not been described in earlier reports (Thomson, 1950). The amphibole trachyte consists of partially resorbed rounded fragments of different-colored

amphibole trachyte bonded in a grey-colored matrix of amphibole trachyte (Plate 2G). The fragments in the rock were recognized by the degree of hematitization affecting their color, which ranges from dark grey to beige to brownish-orange. The different fragments display trachytic textures of varying orientation. This rock is therefore an extrusive, auto-brecciated flow of restricted lateral extent, since the flow can only be traced out for approximately 30 m.

Pristine euhedral amphibole phenocrysts (40 vol.%) range in size from 0.02 to 0.5 cm, are commonly zoned, and define a flow foliation in the fragments and matrix. Small (0.02 to 0.2 cm), equant to elongate euhedral alkali-feldspar phenocrysts (up to 20 vol.%) also define a trachytic texture in the fragments and matrix. Some of the alkali-feldspar phenocrysts exhibit perthitic exsolution. The groundmass is composed of microcrystalline feldspar and finely disseminated magnetite (< 2 vol.%). Fragments normally have a lower phenocryst content (roughly 25 to 30 vol.%) than the matrix (up to 60 vol%), and amphibole phenocrysts are typically more abundant in the matrix, where the trachytic texture wraps around the fragments. Albitization is pervasive and sericitization is common in the phenocrysts and the groundmass. A similar occurrence has been observed along the west side of the Misema river near Larder Lake. In this area, the rocks are altered and deformed, and only gross textural and mineralogical features are preserved. Angular fragments, composed of varying amounts of amphibole and plagioclase in a fine-grained matrix, ranging in size from 0.05 to 1.5 cm, display trachytic alignment with different orientations. These fragments are surrounded by a matrix with a composition identical to the latter. Again, the proximity of agglomerates indicates the extrusive nature of this rock type. All

of the feldspars in this rock are extensively albitized, carbonatized and hematitized, and amphiboles are replaced by actinolite+ chlorite.

### 2.1.3.4 Andesite

Andesite is the least abundant unit of the volcanic rocks of the Timiskaming Group studied during this project. It is also the only volcanic rock of the Timiskaming Group which displays the characteristic features of the granitic suite. An andesite flow was sampled approximately 3 km north of the town of Larder Lake. In hand sample, this reddish-beige porphyritic rock closely resembles the quartz monzodiorite of domain 1. Three features distinguish andesite from quartz monzodiorite: the andesite flow is surrounded by massive felsic trachyte and small lenses of trachytic agglomerate, the lath-shaped feldspars exhibit a well-defined trachytic texture, usually absent or poorly developped in quartz monzodiorite, and the groundmass is cryptocrystalline. Furthermore, small intrusive quartz monzodiorite bodies crosscut the trachyte flows east of the andesite flow, confirming the extrusive nature of the andesite (Thomson, 1941).

The rock contains abundant (45 to 50 vol.%) lath-shaped plagioclase phenocrysts that are generally 0.05 to 0.2 cm, and small (0.05 to 0.1 cm) euhedral amphibole phenocrysts (< 5 vol.%) that are partially to completely replaced by a carbonate mineral and rimmed by actinolite needles and chlorite. Small (0.01 to 0.05 cm) magnetite crystals, extensively replaced by hematite, account for less than 3 vol.% of the rock. A few K-feldspar phenocrysts (< 1 vol.%) are present. The phenocrysts are imbedded in a cryptocrystalline groundmass probably composed of plagioclase and quartz; quartz can be

recognized at the contact between and on the rims of plagioclase phenocrysts. Sericitization of the plagioclase is pervasive, and some of these display a peculiar feature: small bleb-like inclusions of chlorite in and along faces of the phenocrysts have been interpreted by Cooke and Moorhouse (1969) to be altered glass (Plate 2B). Andesite is remarkably similar to the quartz monzodiorite unit of domain 1. Descriptions in Cooke and Moorhouse (1969) and Thomson (1941) indicate the close correspondence between both rock types. These were the earliest flows of the Timiskaming Group (episode 1, Cooke and Moorhouse, 1969), implying that volcanism was initially calc-alkaline, and evolved to alkaline compositions. The andesite flows have been interpreted as being transitional between the preceding tholeiitic (Kinojevis Group) and calc-alkaline (Blake River Group) volcanism,and the subsequent alkaline volcanism of the Timiskaming Group (Cooke and Moorhouse, 1969).

## 2.2 Domain 2

The country immediately north of the KLF represents domain 2 (Fig. 1). The unconformity between the Timiskaming Group rocks and the underlying greenstone basement marks its southern limit. Domain 2 is largely covered by tholeiitic basalts and diorites of the Kinojevis Group and the calc-alkaline basalts, andesites and rhyolites of the Blake River Group (Jensen, 1985). Elongate hypabyssal intrusions crosscut the greenstone basement in the area of McVittie township, intersecting the KLF at an oblique angle (Fig. 5). These are the McVittie stock, which transects the southern limit of domain 2, the Kinabik Creek intrusion, the Beaverhouse Lake intrusion and the Monocle Lake intrusion. Field relationships suggest that three of these intrusions may be connected at depth. The Beaverhouse Lake intrusion (quartz phenocrysts),

Monocle Lake intrusions (quartz microphenocrysts and quartz in groundmass) and the McVittie stock (quartz in groundmass) form a discontinous line of granodiorite outcrops (Map 50b, Thomson, 1941). The mode of occurrence of quartz in the intrusions marks the only mineralogical or textural difference between them.

Rocks of domain 2 are exclusively granitic. They share many textural and mineralogical similarities with the granitic rocks of domain 1. Texturally, these thin, elongate porphyritic intrusions are identical to the quartz monzodiorites and granodiorites of domain 1. Mineralogically, the rocks of domain 2 are nearly identical to those of domain 1, differing only by an overall higher quartz content in the groundmass phase. Accordingly, these rocks fall in the granodiorite field of Streckeisen (1976), in some cases approaching a quartz diorite or quartz monzodiorite composition. Some of these intrusions were originally classified as quartz monzodiorite (feldspar porphyry) and diorites because quartz was not recognized as an important constituent of the groundmass (Thomson, 1941). The following descriptions are of least-altered specimens of each intrusion.

## 2.2.1 Intrusions

### 2.2.1.1 McVittie stock

The McVittie stock, also known as the Bear Lake stock (Thomson, 1941), is the losenge-shaped intrusion truncated by the northern limit of the KLF (Fig. 5). Because of intense shearing and pyritization along its perimeter, the intrusion was the target of mineral exploration for over 40 years. Most of

the McVittie stock is altered and deformed; a small area in the western section of the core is relatively unaltered and undeformed. The McVittie stock is a homogeneous porphyritic granodiorite intrusion that is generally greyish-brown colored. The typical red coloration of the granitic rocks of domain 1 is absent. The rock is composed of plagioclase, amphibole and K-feldspar phenocrysts set in a fine-grained matrix. In some areas, amphibole phenocrysts accentuate a flow foliation.

Small (0.05 to 0.3 cm), euhedral plagioclase (roughly 25 vol.%, up to 40 vol.%) and small (0.05 to 0.2 cm) euhedral amphibole (20 vol.%) are the two major phenocryst phases of the McVittie stock. Plagioclase phenocrysts are sometimes zoned. Large (up to 0.7 cm), subhedral K-feldspar phenocrysts and glomerocrysts can account for up to 10 vol.% of the rock. Both types of feldspar are commonly sericitized and hematitized along edges, but retain pristine cores (Plate 3C). Albitization of the original feldspars is pervasive. Amphibole is commonly replaced by chlorite+ epidote in more altered samples. Miarolitic cavities are a common feature of the McVittie stock. They are usually small (0.05 to 0.2 cm) and are lined by quartz and chlorite and filled with epidote. Cavities are less commonly lined with quartz and filled with calcite; these are usually larger (up to 0.5 cm). Magnetite, apatite, zircon, titanite and rare biotite are trace constituents of this intrusion. The fine-grained (average of 0.03 mm) groundmass is composed of interlocking anhedral plagioclase, quartz and alkali-feldspar. Sericite and calcite are common secondary minerals in the groundmass.

**Plate 3:** The granitic rocks of domains 1 and 2. The field of view in all photographs is 5 mm. (Crossed polars)

**A.** Quartz monzodiorite unit of Domain 1. The rock is composed of large subhedral plagioclase and euhedral amphibole (dark green to black) phenocrysts. The amphibole crystals are located in the upper right corner.

**B.** Granodiorite unit of domain 1. Large hexagonal-shaped and commonly embayed quartz phenocrysts are characteristic of this unit. Subhedral plagioclase phenocrysts are common while large euhedral K-feldspar phenocrysts (lower left corner) are rare.

**C.** Granodiorite of the McVittie stock. Plagioclase phenocrysts are commonly hematitized along their edges but display pristine cores; amphibole is dark brown and usually subhedral. The groundmass contains a significant proportion of quartz (white areas not affected by hematitization).

**D.** Granodiorite of the Monocle Lake intrusion. Plagioclase phenocrysts are more altered than in the McVittie stock. Amphibole phenocrysts are commonly wedge-shaped or prismatic and dark green (center of photograph). Quartz in the groundmass is subhedral and coarser than in other intrusions of domain 2.

**E.** Granodiorite of the Beaverhouse Lake intrusion. Quartz (black) phenocrysts are subhedral, and the groundmass is highly carbonatized, sericitized and partly recrystallized.

**F.** Granodiorite of the Kinabik Creek intrusion. This is the least-altered intrusion encountered in the Kirkland Lake area. Large subhedral to euhedral zoned plagioclase phenocrysts (black, white) are pristine; quartz phenocrysts (yellow, grey) are subhedral. Amphibole crystals (dark brown or black) are usually subhedral and prismatic. The groundmass consists of rounded equant plagioclase and quartz.

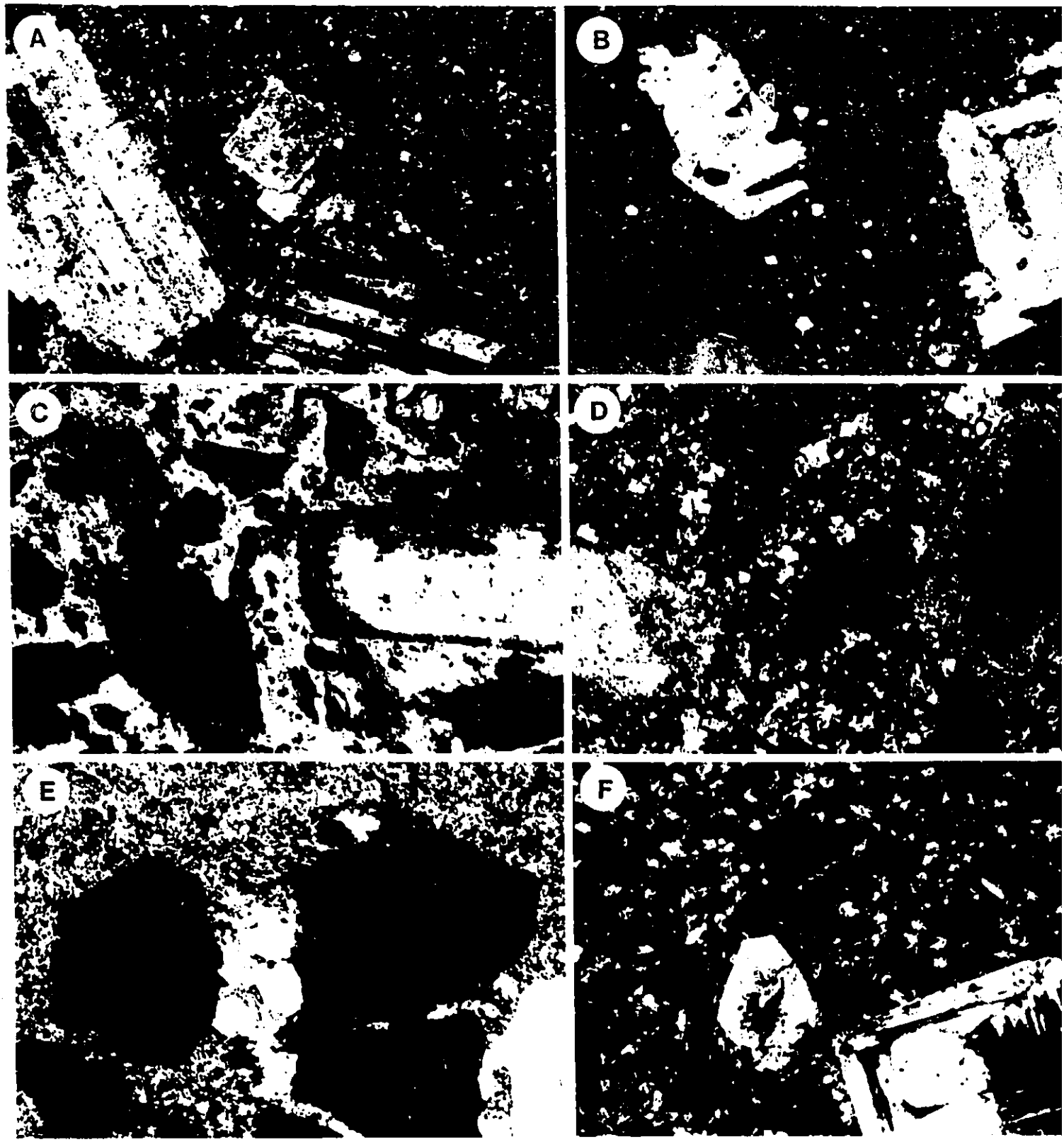
A
B
C
D
E
F

### 2.2.1.2 Monocle Lake intrusion

The Monocle Lake intrusion is the thin southeast-trending elongate body immediately north of the McVittie stock (Fig. 5). It is relatively unaltered and undeformed and is composed of two units, one porphyritic and the other glomeroporphyritic. The latter contains large plagioclase glomerocrysts (up to 2.5 cm) encased in a very-fine grained dark-grey matrix. The porphyritic unit contains smaller plagioclase phenocrysts (less than 0.8 cm) and the groundmass is usually reddish-grey and coarser-grained.

Small (0.1 to 0.5 cm) euhedral plagioclase (10 vol.%) and small (0.05 to 0.2 cm) euhedral prismatic amphibole (up to 30 vol.%) are the two important phenocrysts of the porphyritic unit. Large (up to 0.8 cm) subhedral K-feldspar is a minor phenocryst (< 3 vol.%). In the porphyritic unit, plagioclase glomerocrysts are uncommon (< 2 vol.%). The groundmass of the porphyritic unit is composed of interlocking plagioclase and quartz, with minor alkali-feldspar. Quartz is usually the largest mineral in the groundmass, and will rarely occur as small (0.05 cm) euhedral microphenocrysts identical to the quartz phenocrysts of the granodiorite of domain 1 (Plate 3D). Miarolitic cavities identical to those found in the McVittie stock are common. The plagioclase phenocrysts occasionally exhibit oscillatory zoning. Sericitization and albitization are pervasive in the porphyritic unit (Plate 3D). Apatite, magnetite and zircon are accessory phases. The amphibole is sometimes replaced by chlorite+ epidote.

The glomeroporphyritic unit is characterized by the presence of plagioclase glomerocrysts accounting for up to 20 vol.% of the rock. The

glomerocrysts are composed of interlocking subhedral plagioclase crystals. Amphibole is completely replaced by chlorite, which form small slip planes indicative of deformation. The glomerocrysts are pervasively albitized, slightly sericitized, and are commonly pinkish in color from hematite inclusions. K-feldspar (< 2 vol.%) is completely replaced by albite. The cryptocrystalline groundmass is composed of plagioclase and quartz, which can be observed in some coarser-grained patches. Apatite and magnetite are accessory phases.

### 2.2.1.3 Beaverhouse Lake intrusion

The Beaverhouse Lake intrusion is the most altered of the intrusions of domain 2. It has been mapped as a composite quartz monzodiorite (feldspar porphyry) intrusion containing varying amounts of amphibole and feldspar phenocrysts (Thomson, 1941). The more-altered rocks occur in the eastern end of the intrusion and are greyish colored; this rock type is composed of plagioclase and euhedral to subhedral quartz phenocrysts in a very-fined grained carbonatized groundmass composed of equal amounts of rounded anhedral quartz and plagioclase.

True quartz monzodiorite occurs in the western portion of the intrusion; here plagioclase and amphibole, with minor K-feldspar, are the phenocrysts present. The groundmass is composed of plagioclase, quartz and alkali-feldspar. Apatite and magnetite are the common accessory phases. Granodiorite occurs in the eastern part of the intrusion; however, unlike other granodiorite units of domain 1, plagioclase phenocrysts are less common, accounting for less than 15 vol.%. They are completely replaced by sericite and calcite and form anhedral patches that often appear to be part of the

groundmass; only by the absence of quartz and the abundance of sericite in these patches can they be recognized. Chlorite aggregates probably represent original amphibole. Only quartz phenocrysts remain unaffected; they are euhedral to subhedral, with resorbed crystal surfaces, range in size from 0.02 to 0.3 cm, and account for 5 to 10 vol.% of the rock (Plate 3E). Apatite, magnetite and titanite are trace constituents.

#### 2.2.1.4 Kinabik Creek intrusion

The Kinabik Creek intrusion outcrops at the northernmost limit of the field area. It outcrops almost perpendicularly to the KLF; the other intrusions of domain 2 are subparallel to the strike of the KLF west of Larder Lake. The rock is unaltered and undeformed. It is dark-grey and unfractured in hand sample. These features suggest that the intrusion was probably emplaced very late in the evolution of the KLF. The abundant feldspar and amphibole phenocrysts define a flow foliation observed throughout the intrusion. In outcrops, the rock is massive and lacks the typical reddish tinge from hematitization ; the absence of fractures hindered sampling.
The intrusion is mineralogically homogeneous and falls in the granodiorite field of Streckeisen (1976). Small rounded green xenoliths are commonly observed; they most probably come from the surrounding greenstone. Miarolitic cavities are also common. Three important phenocrysts are readily recognized: plagioclase, amphibole and quartz (Plate 3F). Biotite phenocrysts are infrequent, and K-feldspar is uncommon.

Plagioclase phenocrysts are euhedral, range in size from 0.05 to 0.8 cm, are commonly zoned and twinned, and exhibit partially resorbed crystal faces.

The plagioclase phenocrysts, which account for up to 35 vol.% of the rock, are typically aligned to define a trachytic texture. Amphibole phenocrysts are small (0.02 to 0.2 cm, rarely to 0.5 cm), subhedral to euhedral, make up roughly 10 vol.%. Some amphiboles are zoned. Quartz (approximately 10 vol.%) phenocrysts are subhedral, usually rounded and equant (0.02 to 0.3 cm), and like plagioclase, have partially resorbed faces. Biotite phenocrysts (<2 vol.%) are rounded (resorbed) and usually partially replaced by a mixture of chlorite, epidote, and a carbonate mineral and have a fuzzy appearance. Magnetite crystals (< 1 vol.%) are small (0.01 to 0.05 cm) and euhedral and contain ilmenite lamellae. Apatite and metamict zircon are accessory phases. The groundmass is composed of interlocking, rounded, anhedral plagioclase and quartz. The groundmass minerals commonly encroach phenocryst faces. Minor secondary minerals include sericite for plagioclase, chlorite and epidote for amphibole and biotite.

## 2.3 Domain 3

Domain 3 occupies the country south of the KLF (Fig. 2). The Larder Lake fault (LLF) defines the boundary between it and domain 1 (to the north). Tholeiitic basalts, komatiites, and some conglomerate, greywacke and iron formation of the Larder Lake Group are the main lithological units of domain 3 (Jensen, 1985). The rocks of the Larder Lake Group are truncated by large intrusions. These are the Otto stock, the Murdock Creek intrusion, the Lebel stock, the Gauthier diorite and the McElroy stock (Fig. 5). These intrusions are usually rounded, although those in fault contact with the LLF are truncated and appear more elliptical.

The plutons of domain 3 constitute the least-altered and least-deformed rocks of the study area. Alteration and deformation are restricted to faulted areas; they are most intense along the LLF, where carbonatization, shearing and cataclasis are prevalent. Alteration and deformation are also related to the late cross-faults that cut the Otto and Lebel stocks, and the Murdock Creek intrusion (Fig. 5). Otherwise, these intrusions are unaffected by the hydrothermal events of domain 1. Pluton margins are commonly intermingled with surrounding basalts and sharp intrusive contacts are not well-defined. In many cases, the intrusions produce small thermal aureoles indicated by the presence of metamorphic amphibole in the adjacent country rock.

The intrusions of domain 3 are composite in nature. All of the plutons have a mafic margin. However, these mafic margins account for a very small proportion of the total volume of the intrusion at the present level of erosion. The predominant units of the intrusions are leucocratic in nature. Unlike the rocks of domain 1, where syenitic and granitic rocks occur as discrete bodies, one intrusion in domain 3 contains both syenitic and granitic units. This is the case for the syenitic Otto stock, which contains a quartz syenite unit, and a porphyritic syenite unit (Smith and Sutcliffe, 1988) that is remarkably similar to the quartz monzodiorite unit of domain 1. The McElroy stock is the only predominantly granitic intrusion of domain 3. The duality of composition is therefore not restricted to domain 1.

The study of the intrusions of domain 3 was undertaken because of their strong similarities to the gold-hosting intrusions of domain 1. Petrological studies of the magmatic bodies which host gold along the KLF have been hampered because of the extensive alteration by hydrothermal fluids and

brittle-ductile deformation suffered by the intrusions of domain 1. The plutons of domain 3 present an opportunity to examine relatively unaltered and undeformed equivalents of domain 1 rocks. The evolution from a single feldspar (perthitic alkali-feldspar) rock to a two feldspar (plagioclase+ K-feldspar) rock, the predominance of clinopyroxene and biotite in syenitic units and of amphibole in granitic units, the occurrence of primary titanite, apatite and magnetite in most units, and gradational contacts between units are all characteristics shared by the rocks of domains 1 and 3. The following descriptions of individual intrusions represent a combination of a literature review of previous work and of original work carried out by the author.

## 2.3.1 Syenitic intrusions

### 2.3.1.1 Otto stock:

The Otto stock is the largest intrusion of domain 3. It covers an area of approximately 90 $km^2$. The Otto stock has previously been studied by Lovell (1972), Smith and Sutcliffe (1988), Othman et al. (1990) and Sutcliffe et al. (1990). The intrusion is cut and displaced by a late north-south fault named the Blanche River fault (Fig. 5). Smith and Sutcliffe (1988) divide the Otto stock into five lithological units, with their corresponding IUGS classification in parentheses: syenite (alkali-feldspar syenite), porphyritic syenite (granite), quartz syenite (granite), hornblendite- diorite (hornblendite), and mafic syenite (alkali-feldspar melasyenite). For the mafic syenite unit, the author distinguishes two sub-units: biotite clinopyroxenite and alkali-feldspar melasyenite. The first two units, syenite and porphyritic syenite, account for over 80% of the total volume of the pluton (Smith and Sutcliffe, 1988). A

nepheline syenite phase was mapped by Lovell (1972) but was not encountered in the field. The mafic units occur along the northeastern margin (alkali-feldspar melasyenite) and in the core of the pluton (hornblendite-diorite). The rocks are relatively unaltered and undeformed, except in areas near the faults. In places where the syenite is fractured, a lining of blue alkali-amphiboles and epidote is formed on fractured surfaces. Otherwise, the rocks are pristine. The intrusion is medium to coarse-grained, equigranular to porphyritic, hypidiomorphic, and is usually massive.

The mafic margin is composed mainly of faintly pleochroic light yellowish-green to light green clinopyroxene, with minor amounts of highly pleochroic light tan brown to dark brownish-green biotite, K-feldspar, magnetite, titanite and apatite. This coarse-grained and hypidiomorphic rock corresponds to the mafic syenite unit of Smith and Sutcliffe (1988). Large, faintly zoned subhedral clinopyroxene (0.01 to 1.0 cm) accounts for over 90 vol% of the unit. Inclusions of apatite, biotite and magnetite are common in clinopyroxene (Plate 4A). All other minerals are interstitial between interlocking clinopyroxene crystals. Subhedral to anhedral biotite accounts for roughly 7 vol.% of the rock, while anhedral K-feldspar represents approximately 1 vol.%. Ki-feldspar contains abundant pinkish oval to rounded inclusions, which resemble the pink inclusions observed in the clinopyroxene crystals of the alkali-feldspar melasyenite unit of domain 1. Magnetite, apatite and titanite are accessory phases totalling about 2 vol.%. Accordingly, this rock is classified as an ultramafic biotite clinopyroxenite.

**Plate 4:** The composite intrusions of domain 3. The field of view in all photographs is 5 mm. (Crossed polars)

**A.** Biotite clinopyroxenite of the Otto stock. This rock is composed of large clinopyroxene with interstitial biotite and K-feldspar (< 1 vol. %). Note the inclusions of apatite (white) and magnetite (black) in the light yellow clinopyroxene.

**B.** Alkali-feldspar melasyenite of the Otto stock, composed of clinopyroxene, biotite and perthitic alkali-feldspar (40 vol. %).Mafic minerals commonly occur in bands or aggregates, commonly imparting to the rock a streaky appearance.

**C.** Alkali granite of the Otto stock, containing the uncommon alkali amphibole (greyish blue high positive relief mineral on the left). Clinopyroxene (black) crystals are commonly uralitized.

**D.** Granite (porhyritic syenite) of the Otto stock, which presents textural similarities to the granitic rocks of domains 1 and 2. The rock contains large K-feldspar and smaller plagioclase phenocrysts; the presence of clinopyroxene (red-yellow) crystals (lower right corner) distinguishes this rock from those of domains 1 and 2. The fine-grained groundmass is composed mostly of quartz.

**E.** Alkali-feldspar melasyenite of the Lebel stock, composed of large perthitic alkali-feldspar crystals, brown biotite (lower right corner) and clinopyroxene (green and black). Note the yellow-red coloration of the perthite crystal (left half) due to hematitization. The alignment of perthite and mafic minerals defines a banding in the rock.

**F.** Meladiorite of the Gauthier diorite intrusion. The rock is composed of large prismatic clinopyroxene (pink) crystals with interstitial plagioclase. Edges of clinopyroxene crystals are commonly rimmed by secondary amphibole.

**G.** Quartz diorite of the Gauthier diorite intrusion. This rock is the felsic equivalent of meladiorite. Micrographic and granophyric intergrowths are common throughout the unit (center of photograph). In this rock, clinopyroxene is completely replaced by a mixture of amphibole + epidote + chlorite (black crystal in upper left corner).

**H.** Quartz monzonite of the McElroy stock, composed of interlocking alkali-feldspar, plagioclase, quartz and interstitial amphibole (greyish-green). Myrmekitic intergrowths are commonly observed at the boundary between quartz and plagioclase (center of photograph).

**I.** Quartz monzonite of the McElroy stock, containing an amphibole (orange-brown) crystal with a dark granular center. This feature is common to most amphibole crystals of the quartz monzonite unit. These granular centers generally contain a mixture of clinopyroxene and epidote. This indicates that clinopyroxene was the first ferromagnesian mineral to crystallize in this rock, but was subsequently replaced by late-crystallizing interstitial amphibole.

**J.** Hornblendite unit on the eastern margin of the Murdock Creek intrusion containing large subhedral to euhedral amphibole (orange, red and grey) phenocrysts. Biotite, clinopyroxene, plagioclase and K-feldspar occur as interstitial phases.

A
B
C
D
E
F
G
H
I
J

Biotite clinopyroxenite grades smoothly into a less mafic syenite, as alkali-feldspar content increases and clinopyroxene decreases. This rock is part of the mafic syenite unit of Smith and Sutcliffe (1988). Following IUGS nomenclature, this unit is named alkali-feldspar melasyenite. It contains the same minerals as the clinopyroxenite but in different modal abundances (Plate 4B). Alkali-feldspar (over 40 vol.%) is anhedral, inequigranular, and commonly exhibits perthitic exsolution. Clinopyroxene (50 vol.%) and biotite (5 vol.%) accordingly decrease in abundance. Magnetite, apatite, titanite and epidote are the accessory phases. Alkali-feldspar melasyenite is gradational into alkali-feldspar syenite; this is the syenite unit of Smith and Sutcliffe (1988).

Alkali-feldspar syenite is the largest unit of the Otto stock. It is inequigranular, hypidiomorphic and characterized by large (0.2 to 3 cm) equant subhedral perthitic alkali-feldspar (85 vol.%). Small (0.02 to 0.9 cm) subhedral faintly to non-pleochroic clinopyroxene (10 vol.%) and pleochroic light tan brown to dark greenish-brown biotite (3 vol.%) are interstitial between interlocking K-feldspar crystals. Apatite and magnetite are the common accessory minerals. Apatite, magnetite and biotite are common inclusions in clinopyroxene, while biotite inclusions in K-feldspar are commonly observed. Titanite is less common in this rock unit. In more altered samples, K-feldspar is slightly hematitized and carbonatized; clinopyroxene crystals are more fractured and partly uralitized.

The quartz syenite unit of Smith and Sutcliffe (1988) outcrops in the core of the intrusion. It is composed of interlocking, anhedral to subhedral a K-feldspar, plagioclase and quartz. Clinopyroxene, titanite, and blue alkali-amphibole are the only mafic minerals present, and account for less than 3

vol.% of the rock (Plate 4C). K-feldspar (60 vol.%) is usually subhedral, large (0.3 to 1.5 cm) and displays perthitic exsolution (60% alkali-feldspar, 40% plagioclase). Plagioclase is small (0.02 to 0.3 cm), anhedral, commonly twinned and accounts for 15 vol.% of the rock. Quartz is anhedral, ranges in size from 0.02 to 0.3 cm, and makes up approximately 20 vol.% of the rock. Clinopyroxene is subhedral to euhedral, is pleochroic light yellow to light green, and commonly fractured. Alkali-amphibole is subhedral, pleochroic very light purple to light purplish-blue and typically occurs adjacent to clinopyroxene. Titanite is wedge-shaped, and usually rims both clinopyroxene and amphibole. According to IUGS nomenclature, this rock type is a granite sensu stricto; this is in accordance with Sutcliffe et al. (1990), who identified this rock as an alkali granite.

The porphyritic syenite unit of Smith and Sutcliffe (1988) forms the western rim of the Otto stock and also outcrops in the central part of the southern half of the intrusion. In outcrop, the rock exhibits a moderately developed flow foliation defined by aligned feldspar phenocrysts, contains large alkali-feldspar, small plagioclase and clinopyroxene phenocrysts set in a very fine-grained pinkish groundmass (Plate 4D). Texturally, this rock is similar to the quartz monzodiorite unit of domain 1; the presence and abundance of clinopyroxene phenocrysts and visible quartz in the groundmass are the only distinguishing features of this unit, although clinopyroxene has been identified once in the quartz monzodiorite unit of domain 1.

Large (up to 0.7 cm) euhedral perthitic alkali-feldspar, commonly containing plagioclase inclusions, account for 30 vol.% of the rock, while small (0.1 to 0.3 cm) euhedral to subhedral plagioclase accounts for 20 vol.%.

Clinopyroxene (< 3 vol.%) is subhedral, faintly pleochroic, and commonly uralitized; thin, prismatic, fibrous and acicular amphibole (< 5 vol.%) occurs throughout the rock and defines a flow foliation in the groundmass. Larger equant subhedral amphibole crystals are infrequent (< 1 vol.%). Magnetite, apatite and titanite are accessory phases. The groundmass is inequigranular with patches of larger-grained anhedral quartz (30 vol.%), and very fine-grained plagioclase (15 vol.%). Small anhedral quartz grains commonly occur along feldspar phenocryst edges. According to IUGS nomenclature, this rock type falls within the granite field near the granodiorite boundary.

The hornblendite-diorite unit occurs as an oval body near the core of, and as isolated pods and lenses throughout the intrusion (Smith and Sutcliffe, 1988). This is the only unit of the Otto stock that the author did not encounter in the field. It is nevertheless very similar or identical (in description) to the hornblendite lenses found within the Murdock Creek intrusion, and the plug found adjacent to its eastern margin. The rock consists primarily of cumulate-textured large euhedral amphibole (over 70 vol.%) with minor interstitial green biotite, clinopyroxene, plagioclase and alkali-feldspar. It is considered to be a late intrusive unit, displaying chilled contacts and regular decrease in grain size towards the margins (Smith and Sutcliffe, 1988), which are also observed in the hornblendite body east of the the Murdock Creek intrusion.

### 2.3.1.2 Murdock Creek intrusion

The Murdock Creek intrusion has been the subject of recent studies by Rowins (Rowins, 1990; Rowins et al., 1989, 1991). The author had access to the samples used in these studies. Much of the following description is taken

from these papers. The Murdock Creek intrusion is an elliptical composite pluton of syenitic composition. The northern margin of the intrusion is in fault contact with the LLF (Fig. 5), while the southern margin is interpreted to be in fault contact with the surrounding country rock (Rowins, 1990). The pluton is cut by late north-south cross faults, including the Lakeshore fault, which intersects the KLMB (Fig. 5). The western half of the intrusion is the least-altered and least-deformed portion; five of the six units of the Murdock Creek intrusion classified by Rowins (1990) outcrop in this area. The sixth unit, hornblendite, occurs along the eastern margin of the pluton. The six units composing the Murdock Creek intrusion are (IUGS classification): biotite clinopyroxenite, meladiorite, hornblendite, melamonzodiorite, melasyenite, and alkali-feldspar syenite. Contacts between the units are usually gradational; sharp intrusive contacts observed in the field are interpreted to be produced by injection of magma into earlier solidified rock (Rowins, 1990).

Biotite clinopyroxenite is massive, homogeneous and medium-grained. In outcrop, the rock is dark greenish-grey to brownish-grey when altered. This unit forms a thin mafic margin on the western rim of the intrusion. The cumulate-textured unit is composed mainly (around 60 vol.%) of small (0.03 to 0.4 cm) faintly pleochroic pale green euhedral clinopyroxene, and subhedral brown biotite (up to 25 vol.%) interstitial to clinopyroxene. Magnetite is a common accessory phase (<5 vol.%), and the content of altered interstitial subhedral plagioclase is variable between 5 and 10 vol.%. Apatite, magnetite and titanite inclusions are commonly observed in clinopyroxene. Other accessory phases include zircon and pyrite. Clinopyroxene is partly uralitized and plagioclase is sericitized in more altered specimens. Biotite clinopyroxenite grades smoothly into a less mafic equivalent, meladiorite, which differs from

clinopyroxenite only by the content of plagioclase which accounts for up to 30 vol.% of the rock. Plagioclase are lath-shaped (0.1 to 0.8 cm), and are sometimes aligned to produce a flow foliation which wraps around clinopyroxene. Clinopyroxene (35 vol.%), biotite (20 vol.%) and magnetite (<3 vol.%) contents accordingly decrease.

One of the most striking rock types to occur in the study area is hornblendite. The knobby surface of outcrops is produced by uneven weathering of the soft matrix and resistant amphibole phenocrysts. This unit outcrops as a small plug adjacent to the east margin, and sporadically in the mafic margin of the Murdock Creek intrusion (and in the core of the Otto stock). The rock is heterogeneous, showing considerable variation in grain-size and texture, from equigranular to porphyritic and from cumulate-textured to interlocking. The rock is composed of large (up to 1.5 cm) interlocking, pleochroic light yellowish-green to light greenish-brown, euhedral amphibole (70 vol.%), with interstitial (when cumulate-textured) clinopyroxene, biotite, plagioclase and alkali-feldspar. Clinopyroxene, apatite, biotite and magnetite inclusions are commonly observed in amphibole. Titanite and rutile are the other accessory phases present in the rock. The euhedral amphibole is usually partly replaced by fibrous amphibole along crystal edges.

Melamonzodiorite is a small transitional unit between the more mafic meladiorite and melasyenite. This rock is quite heterogeneous, containing patches of variable grain size that are either syenitic or clinopyroxenitic in composition. This rock is the first unit containing perthitic alkali-feldspar. The rock is composed of subhedral lath-shaped plagioclase (40 vol.%), perthitic alkali-feldspar (10 vol.%), with equal amounts of clinopyroxene (20 vol.%) and

biotite (20 vol.%), that are identical to those of the more mafic phases. Apatite, magnetite and titanite are the usual accessory minerals.

Melasyenite is a small transitional unit which becomes more leucocratic towards the core of the intrusion. Melasyenite outcrops sporadically throughout the pluton. In outcrop, the rock is massive to trachytic, medium- to coarse-grained to slightly porphyritic with large pinkish-orange interlocking K-feldspar and subordinate plagioclase crystals in a dark green matrix composed of clinopyroxene and biotite. The large (up to 1.0 cm) subhedral K-feldspar crystals, which display bleb and vein perthitic exsolution, account for 55 vol.% of the rock; small (up to 0.5 cm) plagioclase crystals are less common (rougly 5 vol.%). The mafic minerals tend to occur in mafic clots interstitial between large K-feldspar crystals: the typical pale green clinopyroxene (20 vol.%) and brown biotite (10 vol.%) found in the more mafic phases, magnetite (< 2 vol.%), apatite (tr.) and titanite (tr.) are found in these clots.

Alkali-feldspar syenite is volumetrically the largest unit of the Murdock Creek intrusion, covering over 80% of the surface area of the pluton. The rock is pinkish colored in outcrop, medium- to coarse-grained, and massive to foliated (trachytic). The dominant feature of the rock is the abundance (between 70 and 85 vol.%) of large perthitic lath-shaped K-feldspar crystals. Albitic rims around the K-feldspar crystals are frequently observed. Normally, plagioclase occurs as small aggregates (< 1 vol.%) interstitial to K-feldspar. Clinopyroxene (up to 25 vol.%) is equant, subhedral to euhedral, pleochroic light green to light yellowish-green, and commonly zoned. Biotite is less common,

accounting for approximately 5 vol.%. Magnetite, apatite and titanite are the accessory phases.

### 2.3.1.3 Lebel stock

The Lebel stock is the second largest intrusion of domain 3. As for the Otto stock and Murdock Creek intrusion, the Lebel stock is cut by north-south late cross faults (Fig. 5). The intrusion is a composite syenitic pluton, with a thin mafic margin and an extensive leucocratic syenite core. Exposure of the Lebel stock is poor; most of the core lies under marshes. The majority of outcrops are found along the western and northern margins of the pluton; the rocks of the northern margin are in fault contact with the LLF and are heavily carbonatized. All of the specimens from the Lebel stock were sampled from the western margin. Three units compose the stock: a thin marginal biotite clinopyroxenite unit, a foliated (trachytic) alkali-feldspar melasyenite, and the leucocratic alkali-feldspar syenite core. The margin of the intrusion is a narrow (30 m) zone of intermingled amphibolitized basalts and biotite clinopyroxenite; only a few outcrops show an abrupt change (within 30 cm) from country rock to biotite clinopyroxenite.

The biotite clinopyroxenite mafic marginal unit is hypidiomorphic, medium- to coarse-grained, equigranular and contains less than 2 vol.% K-feldspar. This ultramafic rock is identical to the biotite clinopyroxenite of the Otto stock; both of these differ from that of the Murdock Creek intrusion only by the presence of K-feldspar instead of plagioclase. Large (0.05 to 0.8 cm) subhedral interlocking clinopyroxene is commonly optically zoned, pleochroic light greenish-yellow to light emerald green, and accounts for 90 vol.% of the

rock. Interstitial anhedral biotite is pleochroic light tan-brown to dark greenish-brown, and accounts for less than 10 vol.%. Apatite, titanite and magnetite (total <2 vol.%) are also interstitial to clinopyroxene and biotite and commonly occur as inclusions within both minerals. Perthitic alkali-feldspar is the latest crystallizing phase and is interstitial to all other minerals. It is commonly hematitized. Rare plagioclase, recognized by albite twins and the lack of hematitization, occurs as a replacement mineral usually rimming K-feldspar.

Biotite clinopyroxenite grades smoothly into alkali-feldspar melasyenite; no sharp intrusive contacts were observed in outcrop. This unit displays a well-developed trachytic texture defined by aligned lath-shaped K-feldspar crystals. This alignment produces a banded appearance in the rock, composed of alternating felsic (K-feldspar) and mafic (clinopyroxene, biotite, magnetite and apatite) bands (Plate 4E). The foliation disappears towards the core of the intrusion as the rock becomes leucocratic. Alkali-feldspar melasyenite is composed of large (up to 1.5 cm) perthitic K-feldspar crystals (variable, up to 60 vol.%), and smaller rounded anhedral K-feldspar occurring exclusively in the mafic bands. Clinopyroxene is equant to prismatic, subhedral, has non-pleochroic cores and pleochroic rims light greyish-yellow to light yellowish-green and commonly zoned. It accounts for up to 40 vol.% of the rock. Biotite (8 vol.%) is subhedral, both non-pleochroic dark greenish-brown and pleochroic light tan-brown to dark brownish-green and is commonly interstitial to clinopyroxene. Biotite, apatite and magnetite inclusions are common in clinopyroxene. The only alteration minerals observed are chlorite which rarely partially replaces biotite along edges and cleavage planes.

Alkali-feldspar syenite is the most extensive unit of the Lebel stock. It differs from the foliated alkali-feldspar melasyenite only in the abundance of clinopyroxene and biotite. The rock is essentially composed of large interlocking lath-shaped, subhedral, perthitic alkali-feldspar. Unfortunaltely most of the exposures of this phase are located in the northwestern corner and along the northern margin of the intrusion, where alteration is pervasive. All primary clinopyroxene is altered to amphibole + chlorite + carbonate mineral and biotite is completely chloritized. Titanite is an important primary constituent, accounting for up to 3 vol.% of the rock. Small anhedral quartz grains occur as aggregates surrounding the large alkali-feldspar crystals. In some specimens, secondary amphibole is euhedral, with well-developed cleavage and resembles primary amphibole; nonetheless, it is secondary after clinopyroxene.

#### 2.3.1.4 Lamprophyre

Lamprophyres crosscut all of the intrusions of domain 3. They are most commonly found around the Otto stock, but also cut the Gauthier diorite intrusion and the Lebel stock. Lamprophyres were not encountered in the McElroy stock, but have been reported to transect it (Abraham, 1950). No lamprophyre dykes cut the Murdock Creek intrusion (Rowins, 1990). The typical lamprophyre is porphyritic, biotite-rich, dark greyish-green in outcrop, commonly contains rounded xenoliths, and occurs as thin tabular and irregularly-shaped intrusive bodies.

All lamprophyres of domain 3 are minettes: large biotite phenocrysts are encased in a finer-grained groudmass of alkali-feldspar. Biotite (up to 30 vol.%) is large (up to 1.5 cm), subhedral, pleochroic light beige to medium

brownish-green, and locally defines a flow foliation. The pleochroic zoning observed in the biotite from lamprophyres of domain 1 is not common in these biotites. Smaller (up to 0.3 cm) prismatic, subhedral, pleochroic very light yellow to light green amphibole accounts for 25 vol.% of the rock. The mafic minerals are set in a groundmass of interlocking subhedral microcline (30 vol.%) and plagioclase (10 vol.%). Magnetite, titanite and apatite are the accessory phases. The groundmass is slightly carbonatized.

#### 2.3.1.5 Hornblendite

Hornblendite occurs as a minor unit of the Otto and McElroy stocks, the Murdock Creek intrusion, and outcrops as a small rounded plug adjacent to the eastern margin of the Murdock Creek intrusion (Plate 4J). A complete description of hornblendite can be found in the sections of the Otto stock and Murdock Creek intrusion.

### 2.3.2 Granitic intrusions

#### 2.3.2.1 Gauthier diorite intrusion

The Gauthier diorite intrusion is a small irregularly-shaped composite pluton that is poorly exposed because of thick overlying glacial deposits. In areas where the intrusion outcrops, notably along the LLF and in the northeast corner, two types of rocks are recognized: meladiorite and quartz diorite. A third rock type, described as syenite (Thomson and Griffis, 1941) was not encountered during field work. Nevertheless, this syenite is intrusive into

the other two units and is a comparatively small part of the Gauthier diorite intrusion. Samples collected along the LLF are usually altered and deformed; however, much of the primary textures and mineralogy is conserved. The intrusion is medium-grained, heterogeneous and inequigranular; subhedral plagioclase are interstitial to interlocking prismatic clinopyroxene in the more mafic phase. The association of this rock type with quartz diorite, which commonly exhibits micrographic and granophyric textures, is reminiscent of differentiated diabase sills.

Meladiorite is the most mafic unit of the Gauthier diorite intrusion. It invariably grades into quartz diorite; no sharp contacts between these two units are observed. Meladiorite makes up roughly 60% of the exposed rocks of the intrusion. Large (0.2 to 0.6 cm) interlocking prismatic clinopyroxene crystals are non-pleochroic, partly to extensively replaced by pleochroic light yellow to medium green amphibole and account for 65 to 75 vol.% of the rock. The remainder of the rock consists of pristine subhedral lath-shaped plagioclase crystals filling the interstices between clinopyroxene (Plate 4F). Titanite and magnetite are also interstitial; apatite is rare or absent. In some samples, clinopyroxene is completely replaced or mantled by amphibole; the rock then resembles hornblendite.

Quartz diorite is the more felsic unit of the Gauthier Diorite intrusion; clinopyroxene is replaced by a mixture of amphibole, epidote and chlorite (20 vol.%). The rock is essentially composed of large (up to 0.8 cm) euhedral lath-shaped interlocking plagioclase crystals, accounting for approximately 40 vol.%. Anhedral plagioclase (25 vol.%) and alkali-feldspar (5 vol.%) are interstitial to plagioclase laths. Micrographic and granophyric intergrowths are

very common in the interstices (Plate 4G). Quartz is another interstitial phase, but also occurs as intergrowths within the large plagioclase crystals, accounting for 10 vol.% of the rock. The feldspars are commonly sericitized. Apatite, titanite and magnetite are rare or absent; magnetite grains with titanite rims have been recognized.

#### 2.3.2.2 McElroy stock

The McElroy stock is a small composite granitic intrusion emplaced south of the Gauthier diorite intrusion (Fig. 5). Thick glacial deposits in the form of eskers cover much of the intrusion; outcrop exposure is limited to the northeastern margin and sporadically along the southern rim. Most of the exposed outcrops along the northeastern margin were mapped as a hornblende syenite (Abraham, 1950). The majority of outcrops in the southern half of the intrusion are either diorite or hornblendite. Hornblendite was not encountered during field work. In outcrop, the hornblende syenite is unaltered and undeformed, whitish-grey in color with contrasting dark green clots of amphibole. The diorite is a grey-green rock composed of equal amounts of whitish-grey feldspar and dark green amphibole. Quartz is visible in the hornblende syenite; in the IUGS classification, this rock falls in the quartz monzonite field. Description of the hornblendite unit in Abraham (1950) is identical to the hornblendite units of the Otto stock and Murdock Creek intrusion. The relationship between the Gauthier diorite intrusion and the McElroy stock is unclear.

The southern half of the intrusion is composed mostly of diorite, with subordinate amounts of hornblendite. Hornblendite is described (Abraham,

1950) as "heavy, black, massive... composed of hornblende, augite, biotite, magnetite and very small amounts of interstitial feldspar...small pyroxene and magnetite crystals included in large anhedral crystals of hornblende." These features are common to the all of the hornblendite rocks of domain 3.

The diorite is composed of large (0.2 to 0.5 cm) subhedral pleochroic light greenish-yellow to medium green amphibole (50 vol.%). Magnetite, apatite and biotite inclusions are common in amphibole; titanite often occurs between adjacent amphibole crystals. Biotite is pleochroic light tan brown to dark olive green and commonly replaced by chlorite +epidote. Plagioclase (50 vol%) is subhedral, interlocking and extensively sericitized, so that primary textures are difficult to recognize. Epidote inclusions in amphibole are common; some of these are partially or completely replacing biotite. Other epidote inclusions are fine-grained rounded patches; these may be replacing primary clinopyroxene. Similar textures are observed in the quartz monzonite phase, where primary clinopyroxene occurs in the center of large pristine amphibole crystals like those of the diorite unit.

Quartz monzonite is homogeneous, equigranular, hypidiomorphic and massive. It is the predominant unit of the northern half of the McElroy stock. It is composed of subhedral interlocking K-feldspar, plagioclase, quartz and amphibole (Plate 4H). Two types of alkali-feldspar occur in the rock: anhedral microcline (less than 10 vol.%), displaying typical tartan twinning and perthitic K-feldspar (50 vol.%), composed of equal amounts of alkali-feldspar and plagioclase. Microcline is usally small (0.01 to 0.1 cm) and occurs as an interstitial mineral between larger perthitic orthoclase and plagioclase crystals. Subhedral to anhedral plagioclase (20 vol.%), displaying albite

twinning, usually occurs near fine-grained rounded quartz aggregates. In these areas, myrmekitic and micrographic textures are frequently observed (Plate 4H). Quartz makes up 10 vol.% of the rock and is mostly interstitial to feldspar. Amphibole is the common mafic mineral. Its crystal outlines are defined by feldspar crystal faces; it is interstitial to the feldspars. Amphibole (10 vol.%), which represent the latest crystallizing phase of the intrusion, is small (up to 0.3 cm), euhedral, and contains inclusions of apatite, epidote, magnetite and will rarely poikilitically enclose plagioclase crystals. Titanite is an interstitial accessory phase.

Plagioclase is commonly intensely hematitized; this feature distinguishes it from K-feldspar. Rarely, K-feldspar crystals will display albitic rims. Amphiboles commonly contain granular centers that are either epidote or clinopyroxene fragments (Plate 4I). Primary clinopyroxene is uncommon, but when observed, is always rimmed by amphibole. This texture indicates that clinopyroxene was the first mafic mineral phase to crystallize, but was replaced by amphibole (interstitial, accompanied by quartz) late in the crystallization of quartz monzonite.

# 3. Geochemistry of the syenitic and granitic rocks

Gold mineralization is one outstanding feature of the KLF; the duality of magmatism is another. In order to gain insight on the gold mineralization-felsic/alkaline magmatism relationship, the nature and origin of the gold-hosting rocks must be well constrained. This will be accomplished by examining whole rock, trace and rare earth element data of the granitic and syenitic suites and, by studying the mineral chemistry of the rocks of the Kirkland Lake area. This chapter will focus on outlining the geochemical trends, characteristics and particularities of the syenitic and granitic suites of the Kirkland Lake area. Interpretations based upon geochemical features will be briefly discussed in this chapter. Detailed interpretations are reserved for the following chapter.

## 3.1 Analytical rationale

Mineral analyses were performed on 30 least-altered (hydrothermally) samples. Electron microprobe work focused on three ferromagnesian minerals: clinopyroxene, amphibole and biotite. These minerals were selected because they allow comparisons between rocks of the three domains; clinopyroxene and biotite occur in domains 1 and 3, while amphibole occurs in domains 1, 2 and 3. Minerals analyzed were chosen on the basis of the absence of alteration rims and fractures in the minerals, the presence of primary textures (chemical zoning, gas inclusions,...) and the absence of characteristic secondary hematite and carbonate minerals in the host rock. Whole rock analyses of least-altered samples cover all rock types encountered in the three domains of the study

area. Rare earth element analyses were performed on samples usually containing less than 1.0 wt.% $CO_2$, chosen as an arbitrary upper limit for least-altered specimens of the KLF, except in the case of some syenitic extrusive rocks (up to 2.5 wt.%), and lamprophyres (up to 2.9 wt.%) which normally have higher primary $CO_2$ contents (Rock, 1991).

## 3.2 Analytical methods

All electron microprobe mineral analyses were carried out by wavelength-dispersive X-ray spectroscopy on the Camebax electron microprobe at McGill University using the ONQUANT software package and a series of natural and synthetic standards. The instrument parameters were as follows: acceleration potential was 15 kV, beam current was 8 nA, beam size ranged from 5 to 8 μm, counting times were 25s for major elements and varied between 25 and 100 s for F and Cl.

Clinopyroxene, amphibole and biotite separates from 12 representative samples were obtained by a combination of magnetic and heavy liquid separation techniques. Amphibole and clinopyroxene were then analyzed for ferrous iron by the modified Wilson cold acid method, after Wilson (1960). Samples were prepared by room-temperature HF digestion for 12 to 16 hours, during which ferrous iron is released and oxidized with an aliquot of ammonium metavanadate. An aliquot of excess $Fe^{2+}$ (blank sample) is added to react with all the unreacted vanadate and $Fe^{2+}$ is then determined by titration with potassium dichromate. The difference in the titration volumes between the sample and the excess $Fe^{2+}$ (blank) sample is equivalent to the concentration of ferrous iron in the

sample. The common problems associated with this analytical method (incomplete digestion of iron-bearing minerals such as tourmaline, pyrite and chromite and the presence of organic matter or $MnO_2$ which hinder redox reactions) were not encountered since all of the analyzed samples were mineral separates which dissolved completely in HF. Biotite separates were analyzed for ferric iron by Mössbauer spectroscopy following the methods of Rancourt et al. (1992).

Measured ferric and ferrous iron are an important line of evidence in the documentation of magmatic oxidation. By obtaining $Fe^{3+}/(Fe^{3+}+Fe^{2+})$ molar ratios for ferromagnesian minerals of 12 representative rocks of the Kirkland Lake area, these ratios can be used to calculate FeO and $Fe_2O_3$ of ferromagnesian minerals in similar rock units, providing a better estimate than simple charge balancing in mineral formula calculations. However, some electron microprobe analyses report iron as FeOt where no suitable ferric/ferrous ratios could be applied or inferred. Mineral analyses were recalculated using the MINFILE public domain software package. Clinopyroxene analyses were calculated on the basis of 4 cations, the preferred method when dealing with electron microprobe analyses where iron is reported as FeO total (Morimoto, 1989). Amphibole and biotite analyses were recalculated on the basis of 22 oxygens + 2 (OH, F, Cl).

Whole rock analyses of glass disks (fusion with a mixture of lithium metaborate and lithium carbonate) by wavelength dispersive X-ray fluorescence spectroscopy were performed at the Geological Survey of Canada and at the University of Ottawa. The results were calibrated

against standard rock samples; the following are the estimates of accuracy of the results :

Major elements :

| | |
|---|---|
| $SiO_2$, $Al_2O_3$ : | ± 0.4 % + 1% of concentration |
| $TiO_2$ $P_2O_5$ : | ± 0.02 % + 1% of concentration |
| $Fe_2O_3$(t) , MgO, CaO: | ± 0.1 % + 1% of concentration |
| MnO : | ± 0.01 % + 2% of concentration |
| $Na_2O$ : | ± 0.5 % + 1% of concentration |
| $K_2O$ : | ± 0.05 % + 1% of concentration |
| FeO : | ± 0.2 % + 5% of concentration |
| $H_2O$(t) : | ± 0.1 % + 5% of concentration |
| $CO_2$ : | ± 0.1 % + 3% of concentration |
| S(t) : | ± 0.04 % + 5% of concentration |

Minor elements :

| | |
|---|---|
| Ba, Pb, Sr, Zr : | ± 20 ppm+ 10% of concentration |
| Be, Sc, Yb : | ± 0.5 ppm+ 5% of concentration |
| Co, V, Y, Zn : | ± 5 ppm+ 5% of concentration |
| Cr, Cu, La, Ni : | ± 10 ppm+ 5% of concentration |
| Nb : | ± 30 ppm+ 10% of concentration |
| Rb : | ± 20 ppm+ 2% of concentration |

All samples analyzed contained Nb values lower than the detection limit and are reported as zero. FeO was determined by iron titration following the method of Wilson (1960). $Fe_2O_3$ was calculated using measured FeO values. $H_2O$(t) was determined by the furnace method, $CO_2$ was determined by combustion and infrared detection, while S(t) was determined by ion chromatography.

Samples submitted for neutron activation analyses were carefully prepared: approximately 120 g of each sample was crushed and sieved over nylon mesh to the 200 mesh fraction to ensure homogeneity, and 15 to 25 g of each sample was submitted for analysis. Weathered rinds of samples chosen for both whole rock and rare earth analyses were removed before

crushing in a tungsten carbide shatterbox. Before each crushing run, the crushers and shatterbox were thoroughly cleaned to prevent contamination. Rare earth and selected trace elements were analyzed by instrumental neutron activation (INAA) at l'École Polytechnique in Montréal. All reported values are precise to within ± 5 % of reported concentrations of the following elements : Sc, Co, La, Ce, Nd, Sm, Eu, Tb, Dy, Ho, Yb, Lu, Hf, Ta, Th, U.

## 3.3 Mineral chemistry

### 3.3.1 Clinopyroxene

Clinopyroxene is the dominant ferromagnesian mineral of the syenitic suite of the study area. It is present in all of the intrusions of domain 3, and is present in the following units of domain 1: alkali-feldspar melasyenite, alkali-feldspar syenite, mafic trachyte, leucite tephrite, melamonzonite and lamprophyre. The data gathered from the clinopyroxene of the mafic trachyte will not be treated in this chapter; petrographic observation and electron microprobe analyses indicate that it is extensively replaced by actinolite. Clinopyroxene was also identified in one sample of quartz monzodiorite; its origin is unclear. A total of 94 mineral analyses from this study and from others were used in the examination of clinopyroxene from the Kirkland Lake area.

Clinopyroxene is classified according to the International Mineralogical Association nomenclature of Morimoto (1989). Thirty-one

representative clinopyroxene analyses were used for classification purposes. The Q-J diagram is a useful graph on which the four main chemical groups of pyroxenes can be classified : the **QUAD**rilateral pyroxenes (Ca-Mg-Fe), the **Na-Ca** pyroxenes, the **Na** pyroxenes and **OTHERS** (Morimoto, 1989). The 'y' value (Q) is the sum of Ca + Mg + $Fe^{2+}$ cations and the 'x' value (J) is equal to 2 times the sum of Na cations. Clinopyroxene of the Kirkland Lake area fall in the Quad and Ca-Na fields (Fig. 7). The Quad pyroxene plots onto the familiar pyroxene quadrilateral (Fig. 8A), while Ca-Na pyroxene falls in the Jadeite-Aegirine-Quad ternary diagram (Fig. 8B).

Analyses of clinopyroxene in the quadrilateral cluster into two groups: most fall in the diopside field or straddle the diopside-augite boundary, while a small group falls significantly nearer the augite-pigeonite boundary (Fig. 8A). All of the composite syenitic intrusions, as well as the alkali-feldspar melasyenite unit of domain 1, display an Mg-enrichment trend: mafic units contain diopside that evolves towards pure diopside and/or Mg-rich augite in the more felsic units. Clinopyroxene of the Gauthier diorite intrusion, melamonzonite and vogesite are nearest to the diopside corner. The small group of clinopyroxene which falls near the augite-pigeonite boundary is from the hypabyssal quartz monzodiorite unit (1 analysis) and the mafic trachyte unit (4 analyses). The clinopyroxene from the quartz monzodiorite unit is a Ca-poor augite (nearly subcalcic augite), which is characteristic of rapidly-cooled rocks (Deer et al., 1978).

Q-J Diagram

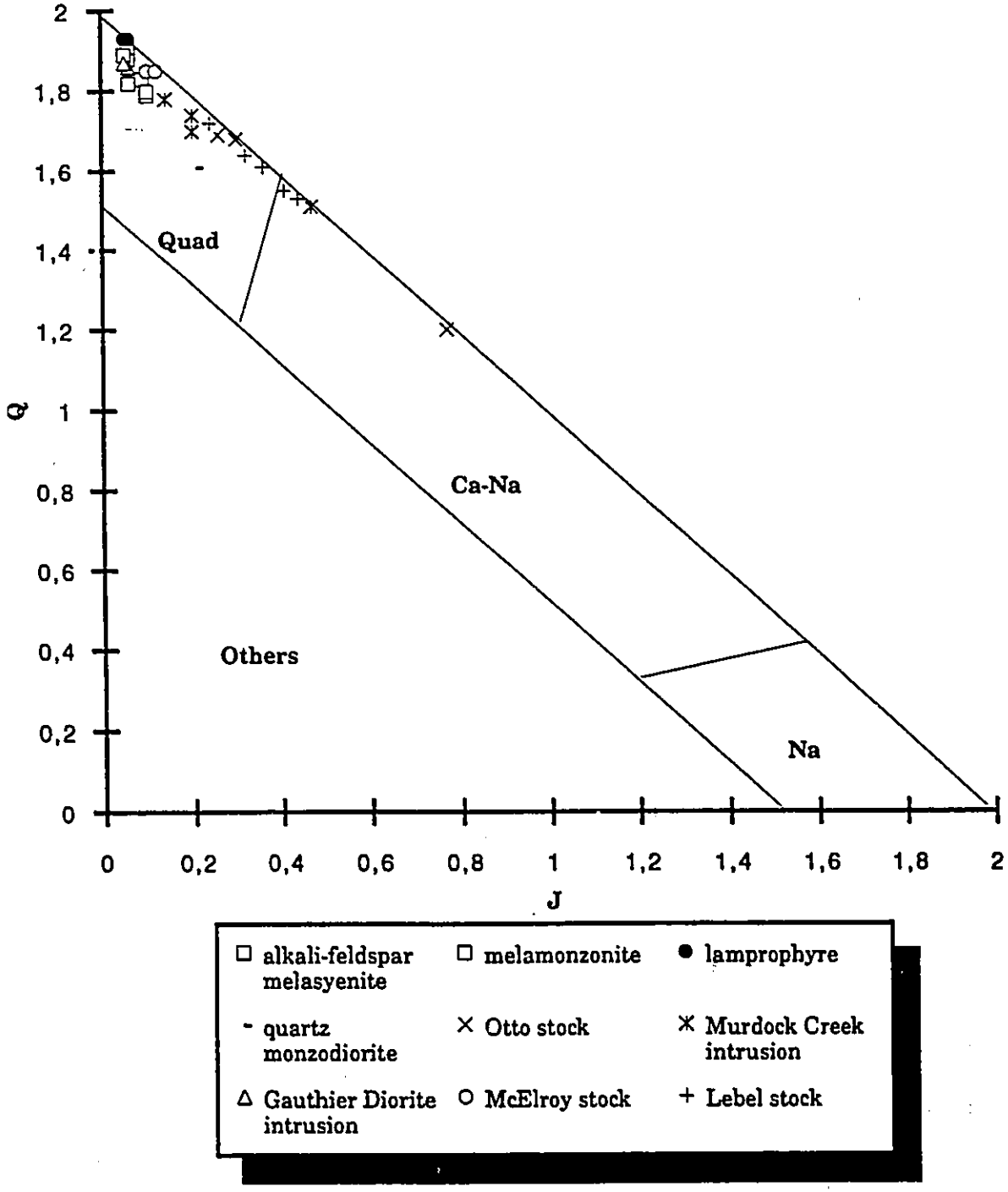


Figure 7 : The Q-J diagram of Morimoto (1989). This diagram classifies pyroxenes into four chemical groups, based on their relative abundances of Ca, Fe $^{2+}$, Mg (Q) and Na (J) cations. The clinopyroxenes of the Kirkland Lake area fall mainly in the Quad field (Ca, Mg, Fe $^{2+}$) ; some belong to the Ca-Na group.

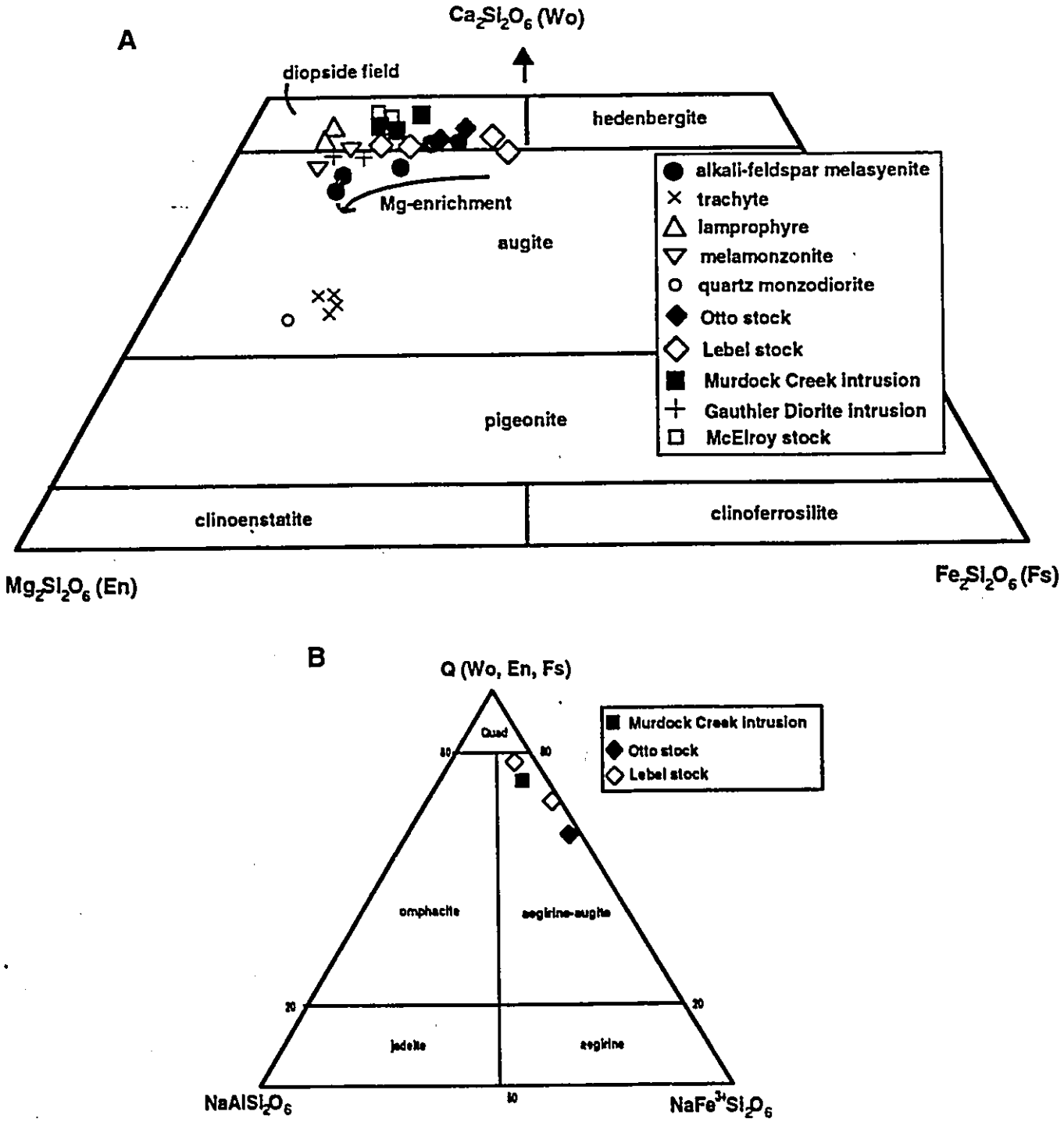


Figure 8 : A) Pyroxene quadrilateral and B) Jadeite-Aegirine-Quadrilateral ternary diagram. A) Most clinopyroxene compositions fall within the diopside field or straddle the diopside-augite boundary. Those belonging to the extrusive syenitic rocks of domain 1 are altered and fall near the augite-pigeonite boundary. Clinopyroxene compositions define an unusual Mg-enrichment trend. B) Clinopyroxene consistently falls in the aegirine-augite field. These belong to the syenitic composite intrusions of domain 3. Aegirine-augite occurs as rims around diopside crystals.

Mineral formula calculations (Appendix A) reveal that the clinopyroxene of the mafic trachyte unit has $Si^{4+}$ T-site occupancy greater than 2.00 (varying between 2.08 and 2.12) and has Al content lower than 0.05 and Ca content near 0.50. These values are indicative of extensive replacement of clinopyroxene by actinolite (Deer et al., 1978).

Iron enrichment is the normal trend observed for the liquid compositions of differentiating basic magmas (Hall, 1987). Iron-bearing minerals usually have lower liquidus temperatures than their magnesian counterparts, so that the residual magma becomes enriched in iron. For syenitic rocks containing clinopyroxene, this mineral will generally evolve towards hedenbergite compositions. This classic differentiation trend is observed in many alkaline intrusions and volcanic rocks, including the Shonkin Sag laccolith (Nash and Wilkinson, 1970), the Klokken gabbro-syenite complex (Parsons, 1979) and Tristan de Cunha islands (Baker et al., 1964). The clinopyroxene of the Kirkland Lake area departs from this "normal" trend; instead, it becomes progessively enriched in magnesium with differentiation. Mg-enrichment trends have been documented in other syenitic and granitic rocks, including the Finnmarka complex (Czamanske and Wones, 1973), the Baie-des-Moutons complex (Lalonde and Martin, 1983), and the Murdock Creek intrusion, Kirkland Lake area (Rowins et al., 1991). Highly oxidizing conditions during magmatic differentiation have been invoked by these authors as the mechanism responsible for this trend. Under these conditions, ferrous iron in the magma ($Fe^{2+}$) is oxidized to ferric iron ($Fe^{3+}$) and is preferentially incorporated into magnetite, resulting in a deficiency in ferrous iron in the magma. Consequently, $Mg^{2+}$ substitutes for $Fe^{2+}$ in the crystallizing clinopyroxene.

Clinopyroxene analyses that fall in the Ca-Na pyroxene field of the Q-J diagram are presented in Figure 8B. All of the clinopyroxene analyses fall in the aegirine-augite field. This clinopyroxene occurs exclusively in the composite syenitic intrusions of domain 3, the Lebel and Otto stocks and the Murdock Creek intrusion. Aegirine-augite invariably rims clinopyroxene with diopsidic cores, giving the mineral an irregular patchy zonation. Aegirine-augite rimming diopside is typical of alkaline igneous complexes such as the Shonkin Sag (Nash and Wilkinson, 1970) and the Seabrook Lake complex (Mitchell, 1972). Aegirine-augite is probably a late deuteric product associated with the Na-rich fluid which was responsible for the formation of alkali-amphibole along fractures in the three intrusions of domain 3 (Lovell, 1972).

Two types of zoning are present in clinopyroxene of the alkali-feldspar melasyenite unit of domain 1: concentric zoning, and less commonly, oscillatory zoning. The concentrically-zoned clinopyroxene displays three distinct bands: a core, a mantle and a rim (Plates 5A and 5B). The boundaries between the concentric bands are sharp and usually subparallel to crystal outlines. The core and rim are optically continuous and microprobe analyses confirm that both are chemically identical (Fig. 9). Calcium is the only major element that remains nearly constant throughout the zoned mineral, averaging between 21.8 (core and rim) and 22.2 (mantle) wt.% CaO. The mantle is compositionally distinct from the core and rim; in this band, the major variations are noticed in increasing $SiO_2$ (from 51 wt.% in the core to 54 wt.% in the mantle) and MgO (from 14 wt.% in the core to 17 wt.%), and decreasing FeO(t) and $Al_2O_3$ (Fig. 9).

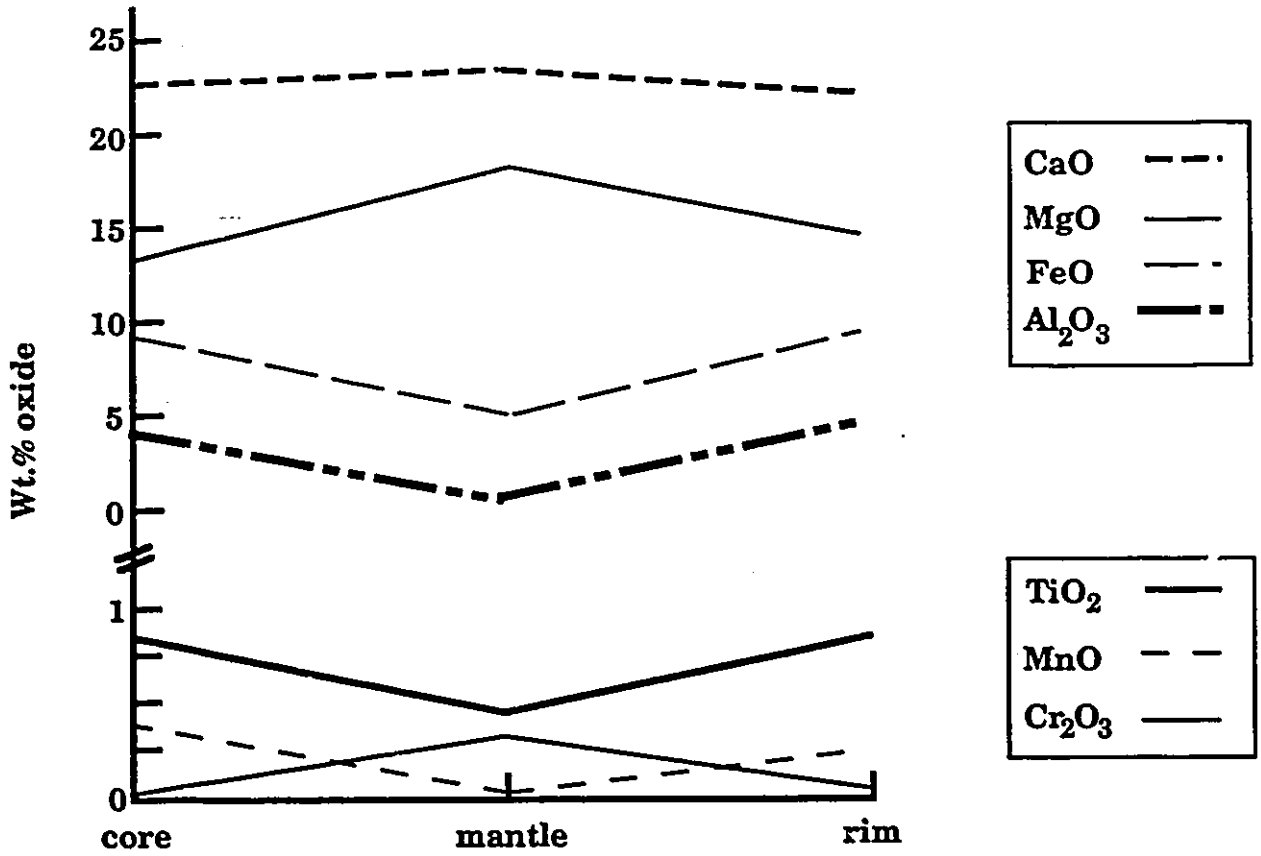


Figure 9 : Compositional trends in concentrically-zoned clinopyroxene of domain 1. The clinopyroxene crystals have three zones: the core, the mantle and the rim. While the core and rim are compositionally identical, the mantle is chemically distinct. It is characterized by higher MgO and $Cr_2O_3$ content, and a lower FeO(t), $Al_2O_3$, $TiO_2$ and MnO content relative to the core and rim.

Zoning is also shown by decreasing $TiO_2$ and MnO and increasing $Cr_2O_3$ in the mantle relative to the core. The general Mg-enrichment trend displayed by the clinopyroxene in the rocks of the study area is also observed within these concentrically-zoned crystals. In this case, Mg-enrichment occurs from the core to the mantle, but returns to the initial clinopyroxene composition in the rim.

**Plate 5 :** Mineralogical features of the ferromagnesian minerals of the Kirkland Lake area. Field of view for all photographs is 5 mm.

**A** and **B**. Concentric zoning in clinopyroxene of the alkali-feldspar melasyenite unit of domain 1. Clinopyroxene displays three zones: the core, the mantle and the rim. Note that the core and rim, which are chemically identical, are optically continuous. The mantle is chemically different from the two other zones. (Crossed polars)

**C.** Intimate association of primary brown biotite and secondary hydrothermal green biotite in domain 1. Green biotite is commonly observed in alteration assemblages replacing clinopyroxene and biotite in the rocks of domain 1. This hydrothermal biotite has often been mistaken for chlorite. (Plane polarized light)

**D.** Pleochroic zoning in green micas of the quartz monzodiorite unit of domain 1. The light-colored core is mantled by a dark green and brown rim enriched in iron and titanium. The end of magnetite crystallization could explain the unusual Fe-enrichment trend exhibited by this biotite. (Plane polarized light)

**E.** Amphibole from the McElroy stock. These amphibole crystals commonly display dark rounded centers containing clinopyroxene fragments. They also commonly poikilitically enclose plagioclase crystals. This amphibole is interstitial to plagioclase and represents the latest crystallizing phase of the McElroy stock, produced by late-magmatic fluid alteration of primary clinopyroxene. (Crossed polars)

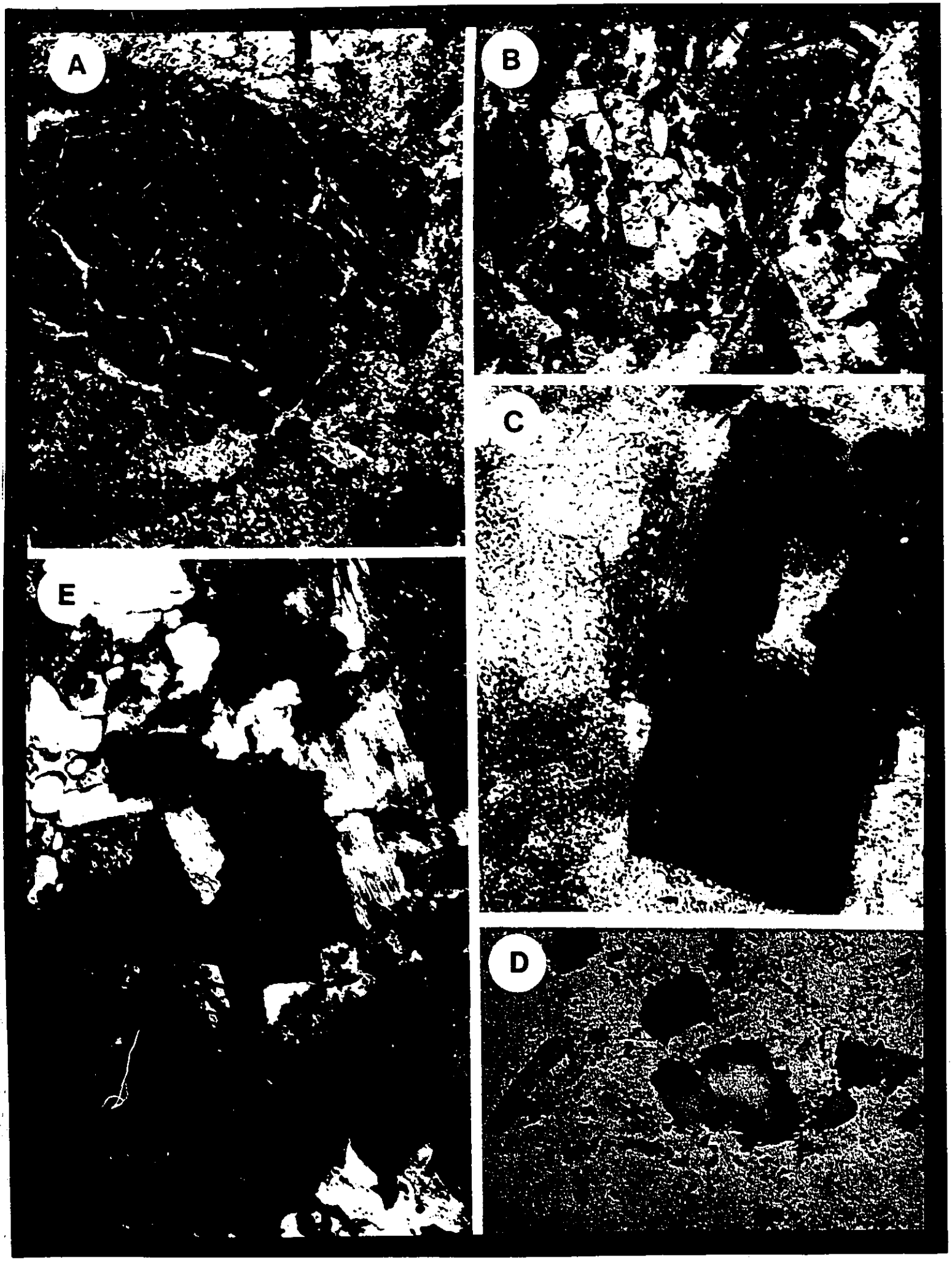
A
B
C
D
E

Fe/(Fe+Mg) atomic ratios (Fe expressed as $Fe^{2+}$+ $Fe^{3+}$) for clinopyroxene in the rock units of domain 1 vary between 0.11 (in melamonzonite) to 0.28 (in alkali-feldspar melasyenite), with a mean Fe/(Fe+Mg) ratio of 0.22 (Fig. 10A). These are typical values for diospide (Robinson, 1980); they are comparable to those of diopside found in alkaline rocks form Italy (Aurissichio et al., 1988) and Papua New Guinea (Richards, 1990). For clinopyroxene found in the lamprophyre and melamonzonite units, the ratios are consistent; this can be observed in the restricted range of the ratios displayed on Fig 10A. Ratios for clinopyroxene in the alkali-feldspar melasyenite depart slightly from this trend: most clinopyroxene analyses have a ratio averaging 0.25, but with increasing silica, this ratio progressively drops to 0.12 (in the mantle of the concentrically-zoned crystals). This feature, illustrated in Figure 10A, reflects the Mg-enrichment trend observed in the clinopyroxene of domain 1.

Fe/(Fe+Mg) ratios of clinopyroxene in the plutons of domain 3 range from 0.15 for the Gauthier diorite intrusion to 0.43 for the Lebel stock with a mean ratio of 0.3, slightly higher than that of domain 1. Ratios in the clinopyroxene from domain 3 exhibit characteristics similar to those of clinopyroxene ratios of domain 1, in that individual plutons (e.g., McElroy stock, Gauthier diorite intrusion) possess ratios with restricted ranges (Figure 10B); clinopyroxene in the Lebel and Otto stocks and the Murdock Creek intrusion display the same Mg-enrichment trend observed for the clinopyroxene in the alkali-feldspar melasyenite unit of domain 1.

Figure 10. Fe/(Fe+Mg) versus Si cation plots for clinopyroxene. A) Clinopyroxene in the units of domain 1 has ratios that range from 0.11 in melamonzonite to 0.28 in alkali-feldspar melasyenite. The ratio decreases (arrow) with increasing Si , indicating an Mg-enrichment trend; this trend is best defined by the clinopyroxene of the alkali-feldspar melasyenite unit. B) Clinopyroxene of the composite intrusions of domain 3 has ratios that vary between 0.15 in the Gauthier diorite intrusion to 0.43 in the Lebel stock. The Mg-enrichment trend is best defined by the clinopyroxene of the Lebel stock and Murdock Creek intrusion.

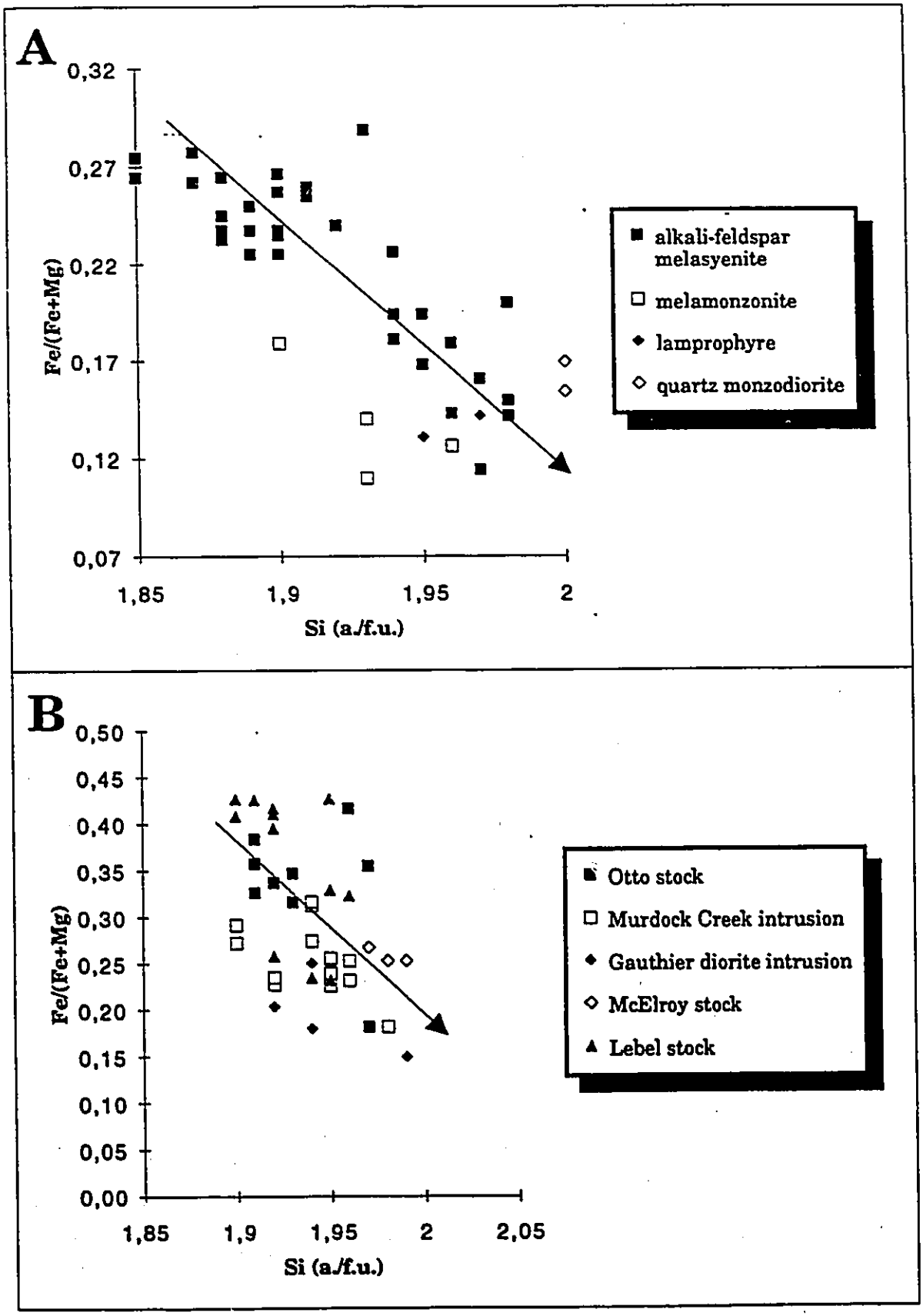
A
0,32
0,27
0,22
0,17
0,12
0,07
Fe/(Fe+Mg)
1,85
1,9
1,95
2
Si (a./f.u.)
alkali-feldspar melasyenite
melamonzonite
lamprophyre
quartz monzodiorite
B
0,50
0,45
0,40
0,35
0,30
0,25
0,20
0,15
0,10
0,05
0,00
Fe/(Fe+Mg)
1,85
1,9
1,95
2
2,05
Si (a./f.u.)
Otto stock
Murdock Creek intrusion
Gauthier diorite intrusion
McElroy stock
Lebel stock

Mg-enrichment in the clinopyroxene of the Kirkland Lake area is more explicitely illustrated in Figure 11. Two trends can be distinguished: the solid arrow joins the compositions of clinopyroxene and shows increasing whole-rock $SiO_2$ in domain 1 while the dashed arrow joins the compositions of clinopyroxene in domain 3 and shows increasing whole-rock $SiO_2$. In domain 1, Mg in clinopyroxene varies from 0.74 (in alkali-feldspar melasyenite) to 1.1 (in quartz monzodiorite) over a range of 49 to 58 wt.% whole-rock $SiO_2$ (whole-rock MgO = 13.2 to 20.2 wt.%), while in domain 3, Mg content in clinopyroxene varies from 0.54 (in alkali-feldspar melasyenite of the Lebel stock and Murdock Creek intrusion) to 0.91 (in meladiorite of the Gauthier diorite intrusion) over a much smaller range of 50 to 54 wt.% whole-rock $SiO_2$ (whole-rock MgO = 7.2 to 16.6 wt.%).

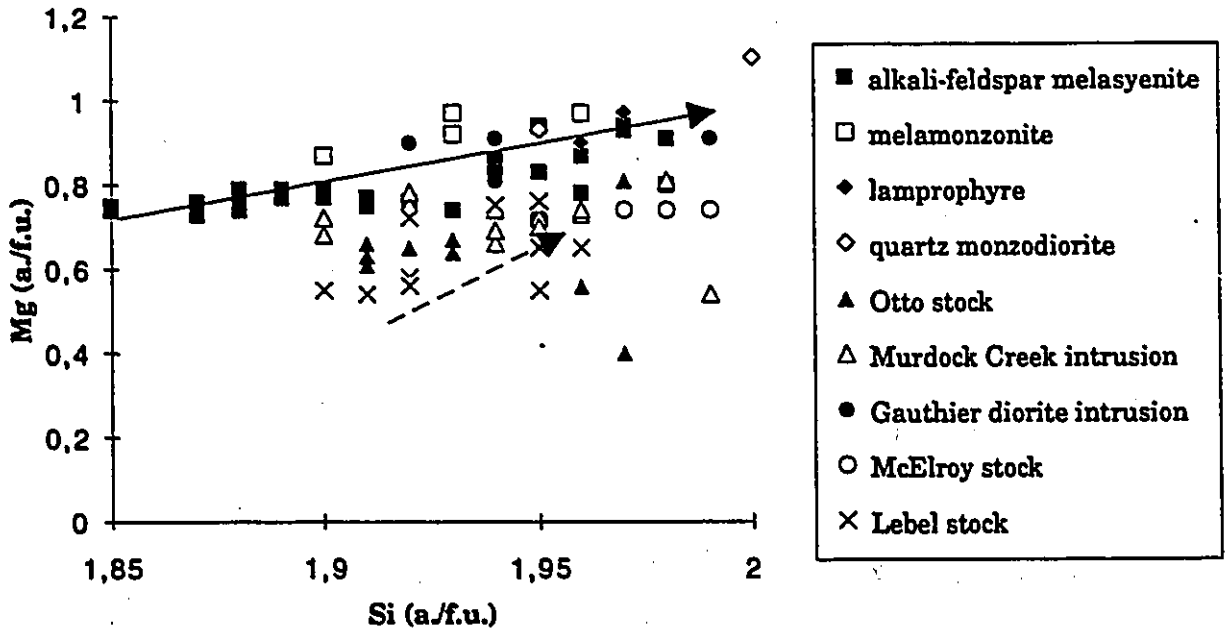


Figure 11. Mg versus Si cation plot for clinopyroxene of domains 1 and 3. Two Mg-enrichment trends in clinopyroxene can be observed: the solid arrow, showing increasing whole-rock $SiO_2$, is for the clinopyroxene in domain 1, the dashed arrow, also showing increasing whole-rock $SiO_2$, is for clinopyroxene in domain 3.

As observed in the concentrically-zoned clinopyroxene of domain 1 (Fig. 9), Ca content is remarkably constant in the clinopyroxene compositions of the Kirkland Lake area (Fig. 12). Two exceptions exist: aegirine-augite in the alkali granite from the Otto stock, and Ca-poor augite from the quartz monzodiorite unit. Ca content (average= 0.85) shows little or no variation with increasing Si (Fig. 12A). Ca increases slightly with increasing Mg (Fig. 12B); this graph illustrates the tendency for the clinopyroxene to evolve towards pure diopside.

The common occurrence of aegirine-augite in the Lebel and Otto stocks and the Murdock Creek intrusion, usually rimming diopside, accounts for the high Na content in the clinopyroxene of domain 3 compared to that of domain 1. The clinopyroxene found in the Gauthier diorite intrusion and McElroy stock share the low Na content observed in the clinopyroxene of domain 1, since neither contain clinopyroxene rimmed by aegirine-augite. However, the lone Ca-poor clinopyroxene from the quartz monzodiorite unit has elevated Na contents. Mn content does not show any systematic variation in clinopyroxene, although clinopyroxene from domain 3 does a have slightly higher Mn content than clinopyroxene in domain 1. The most titaniferous clinopyroxene (up to 0.97 wt.%) is found in the alkali-feldspar melasyenite unit of domain 1 (Fig. 13); this unit shows that Ti is negatively correlated to Si for clinopyroxene. This feature is readily explained by the $Ti^{4+}$-$Al^{3+}$ coupled substitution for $Si^{4+}$-$Mg^{2+}$ or $Si^{4+}$-$Fe^{2+}$ (Morimoto, 1989). Accordingly, Al content is positively correlated to Ti (Fig. 14).

Figure 12. (A) Ca versus Si and (B) Ca versus Mg cation plots for clinopyroxene of domains 1 and 3. Ca content in clinopyroxene of domains 1 and 3 is remarkably constant, even with increasing Si or Mg. B) Clinopyroxene compositions tend to evolve towards pure diopside.

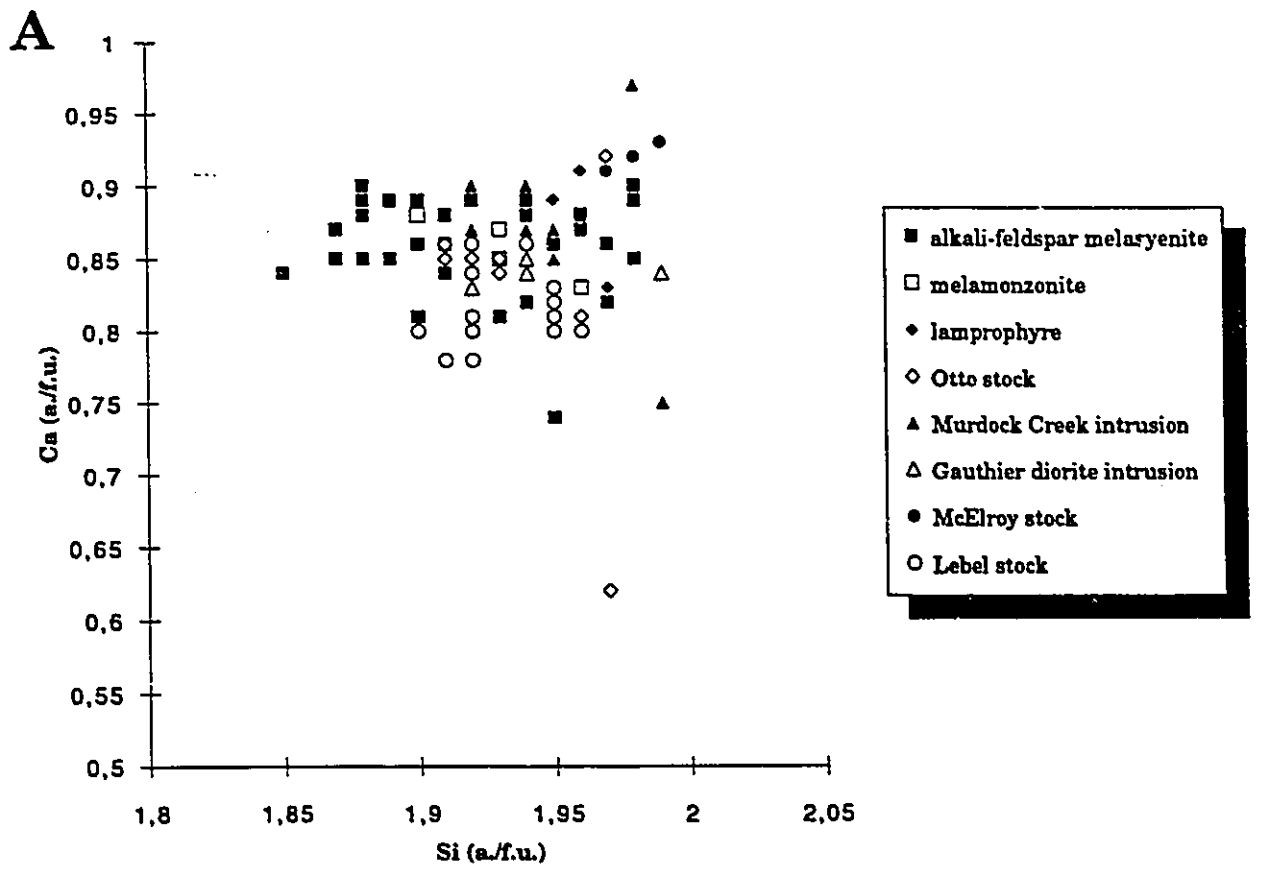
A
1
0,95
0,9
0,85
0,8
0,75
0,7
0,65
0,6
0,55
0,5
Ca (a./f.u.)
1,8
1,85
1,9
1,95
2
2,05
Si (a./f.u.)
alkali-feldspar melasyenite
melamonzonite
lamprophyre
Otto stock
Murdock Creek intrusion
Gauthier diorite intrusion
McElroy stock
Lebel stock

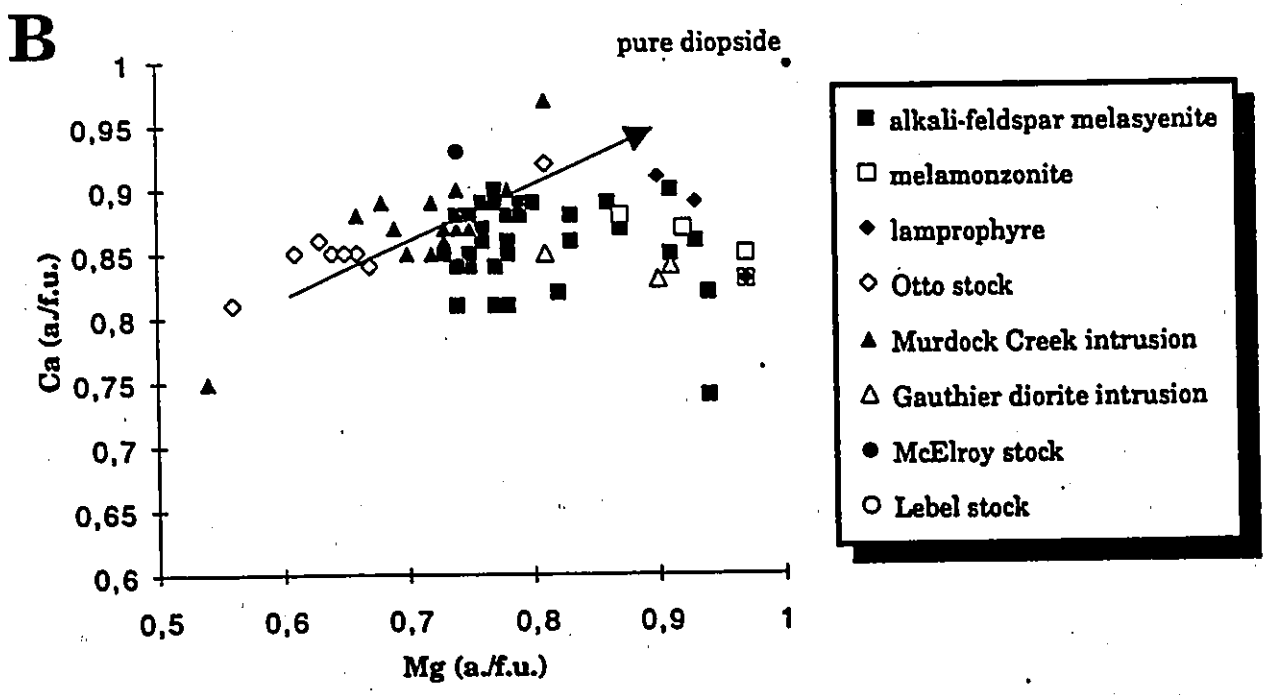
B
pure diopside
1
0,95
0,9
0,85
0,8
0,75
0,7
0,65
0,6
Ca (a./f.u.)
0,5
0,6
0,7
0,8
0,9
1
Mg (a./f.u.)
alkali-feldspar melasyenite
melamonzonite
lamprophyre
Otto stock
Murdock Creek intrusion
Gauthier diorite intrusion
McElroy stock
Lebel stock

Figure 13. Negative correlation between $TiO_2$ and $SiO_2$ in the clinopyroxene of domains 1 and 3. Clinopyroxene compositions from the alkali-feldspar melasyenite unit of domain 1 are the most titaniferous. In domain 1, titanium content sharply decreases with differentiation (arrow). Clinopyroxene compositions from domain 3 are usually less Ti-rich.

Figure 14. Positive correlation between $TiO_2$ and $Al_2O_3$ in clinopyroxene of domains 1 and 3. Following the coupled substitution of $Ti^{4+}$-$Al^{3+}$ for $Si^{4+}$-$Mg^{2+}$ or $Si^{4+}$-$Fe^{2+}$, the most titaniferous clinopyroxene (in domain 1) also contains the highest amount of $Al^{3+}$ .

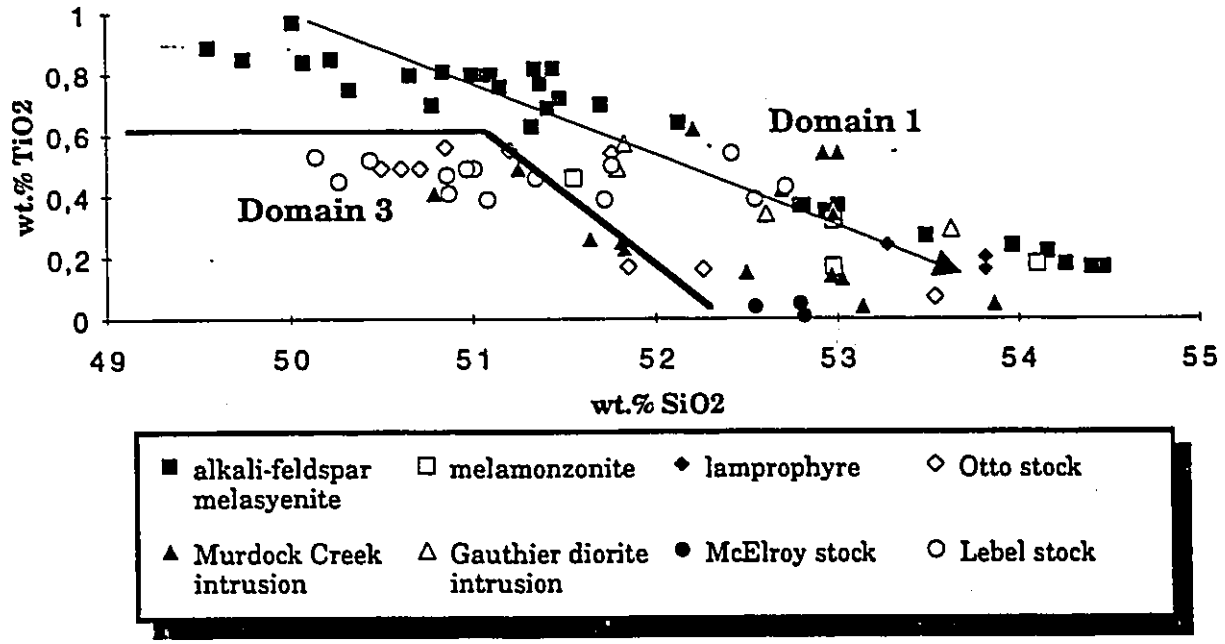
wt.% TiO2
1
0,8
0,6
0,4
0,2
0
Domain 1
Domain 3
49
50
51
52
53
54
55
wt.% SiO2
alkali-feldspar melasyenite
melamonzonite
lamprophyre
Otto stock
Murdock Creek intrusion
Gauthier diorite intrusion
McElroy stock
Lebel stock

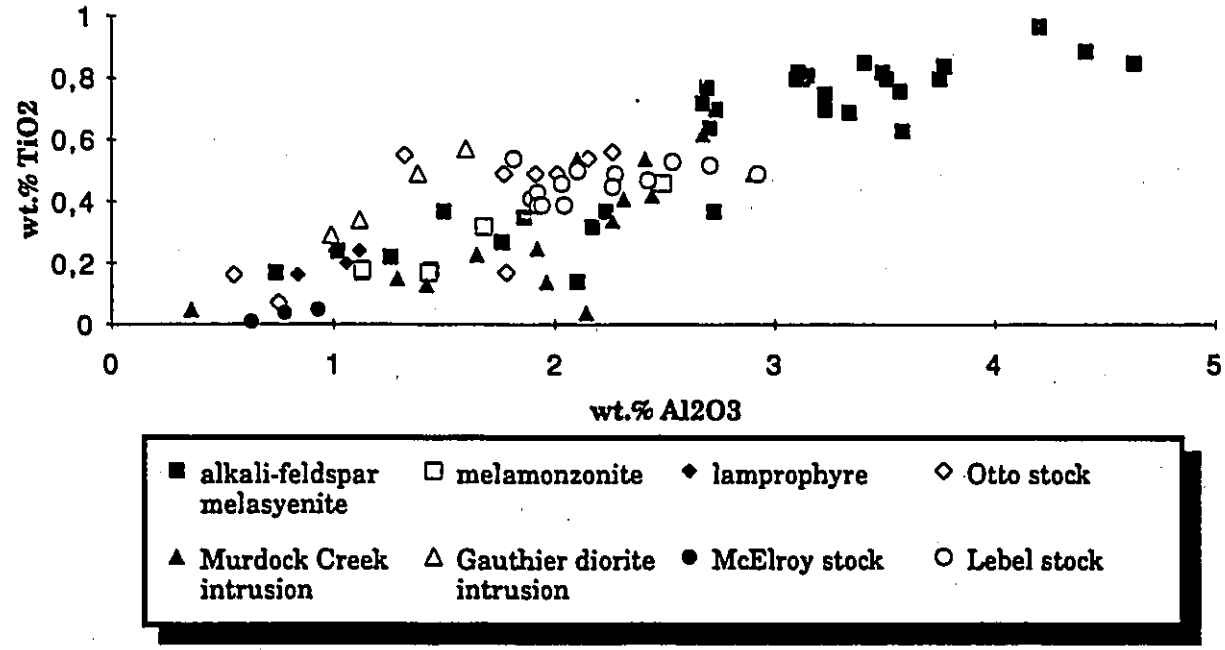
wt.% TiO2
1
0,8
0,6
0,4
0,2
0
0
1
2
3
4
5
wt.% Al2O3
alkali-feldspar melasyenite
melamonzonite
lamprophyre
Otto stock
Murdock Creek intrusion
Gauthier diorite intrusion
McElroy stock
Lebel stock

### 3.3.2 Biotite

Biotite is an important constituent of the composite syenitic plutons of domain 3, the alkali-feldspar melasyenite and quartz monzodiorite units of domain 1, and the three types of lamprophyre. Biotite also occurs as a minor or trace constituent in mafic trachyte, the Kinabik Creek intrusion and the McVittie stock. Two distinct type of biotite have been identified in the rocks of the Kirkland Lake area (Plate 5C): dark reddish-brown primary biotite and yellowish-green biotite. This green biotite is often observed replacing clinopyroxene and brown biotite (Thomson et al., 1950) and is believed to be of hydrothermal origin. The green biotite is prevalent in the rocks of domain 1, but are also found in some rock units of domain 3. A total of 82 biotite analyses from this study and others were used in the examination of biotites from the KLF.

Twenty-nine representative biotite analyses were classified using the annite-siderophyllite-eastonite-phlogopite diagram of Deer et al. (1966) (Fig. 15). Three outstanding features are recognized: 1) the majority of biotite analyses have a relatively low and very uniform Fe/(Fe+Mg) atomic ratio (avg. 0.40), 2) the vogesite and minette lamprophyres of domain 1 contain magmatic phlogopite (ratio avg. = 0.17), and 3) some hydrothermal green biotites of domain 1 straddle the biotite-phlogopite boundary and fall outside the diagram with tetrahedral Al ($Al^{iv}$=1.91) lower than 2.00. Similar hydrothermal green micas have been identified in peralkaline granites of Nigeria (Deer et al., 1972).

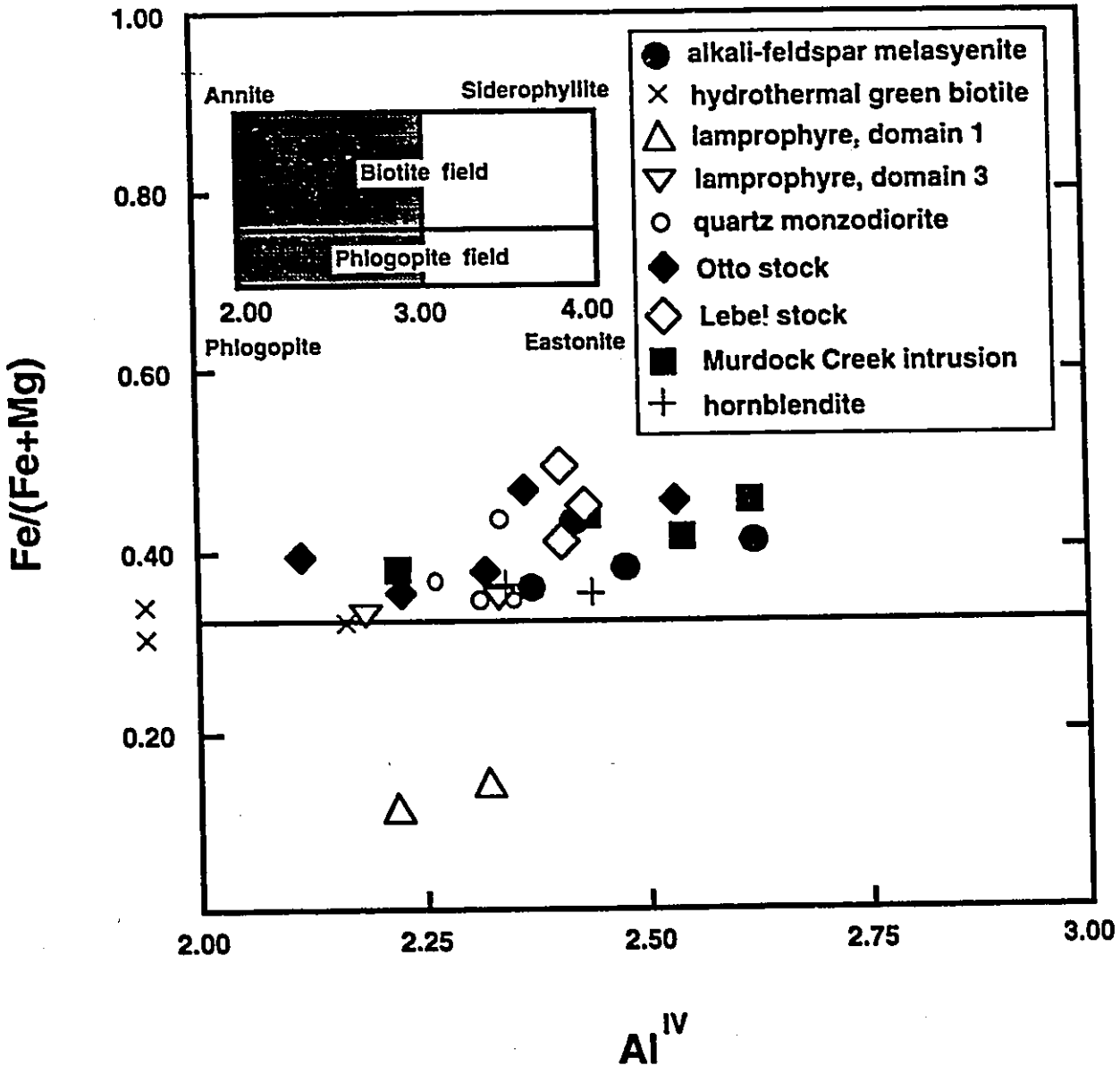


Figure 15. The annite-siderophyllite-eastonite-phlogopite diagram. Note the uniform low Fe/(Fe+Mg) ratios (avg. 0.40) for biotite of domains 1 and 3. Lamprophyres of domain 1 contain primary phlogopite; this mica is also green in color. The hydrothermal green biotite actually falls outside the boundaries of the diagram, having Al $^{iv}$ site occupancies below 2.00.

Fe/(Fe+Mg) atomic ratios of biotite from the Kirkland Lake area are lower than ratios for average biotite from syenitic and granitic rocks (Speer, 1984). The ratios for biotite of domains 1 and 3, which remain low and uniform at approximately 0.40 (Figure 16), are quite different from those found in the Sierra Nevada batholith (Dodge and Moore, 1968) and the Shonkin Sag laccolith (Nash and Wilkinson, 1970), in which the ratio increases through normal iron enrichment with differentiation (Speer, 1984). Low and uniform Fe/(Fe+Mg) atomic ratios can be achieved through magmatic oxidation (Rowins et al., 1991) or by re-equilibration with a late- or postmagmatic fluid (Dodge and Moore, 1968). Postmagmatic alteration resulting in the formation of green micas (Plate 5C) obviously occurred in the Kirkland Lake fault zone (domain 1). However, the majority of biotite analyses were performed on undeformed rocks containing little or no evidence of hydrothermal alteration (domain 3), or in rocks where both primary and hydrothermal biotite is present (domain 1). Since the composition of primary biotite from domain 1 mimics that of domain 3 (see Figs. 15 to 18), we can rule out any major effects from late- or postmagmatic re-equilibration.

The green mica in the Kirkland Lake area has two distinct modes of occurrence: as primary phlogopite in lamprophyre and as secondary hydrothermal biotite replacing ferromagnesian minerals in the rocks of domain 1. These modes can be distinguished on Figure 15. Primary green mica compositions have $Al^{iv}$ values of approximately 2.25, while green hydrothermal biotite compositions have values near 1.90. Values lower than 2.00 for $Al^{iv}$ in biotite can reflect the unavailability of Si and Al during the crystallization of biotite; this feature is observed in plutons which

Figure 16. Fe/(Fe+Mg) versus Si cation plot for mica. Ratios remain low and uniform for all analyses of biotite of the Kirkland Lake area, averaging less than 0.40. This trend is indicative of magmatic oxidation (Rowins et al., 1991). The lowest ratios are for primary phlogopite from lamprophyres and hydrothermal phlogopite from quartz monzodiorite units of domain 1.

Figure 17. Mg versus Fe cation plot for mica. This diagram illustrates the difference between mica types of the Kirkland Lake area. The dividing line between biotite and phlogopite (solid) is after Deer et al., 1966, while the line dividing field 1 from fields 2 and 3 is at Mg = 3.30. Most mica analyses represent primary brown biotite (field 1) or primary brown and hydrothermal green biotite (field 2). Primary and hydrothermal green phlogopite (field 3) occur exclusively in domain 1.

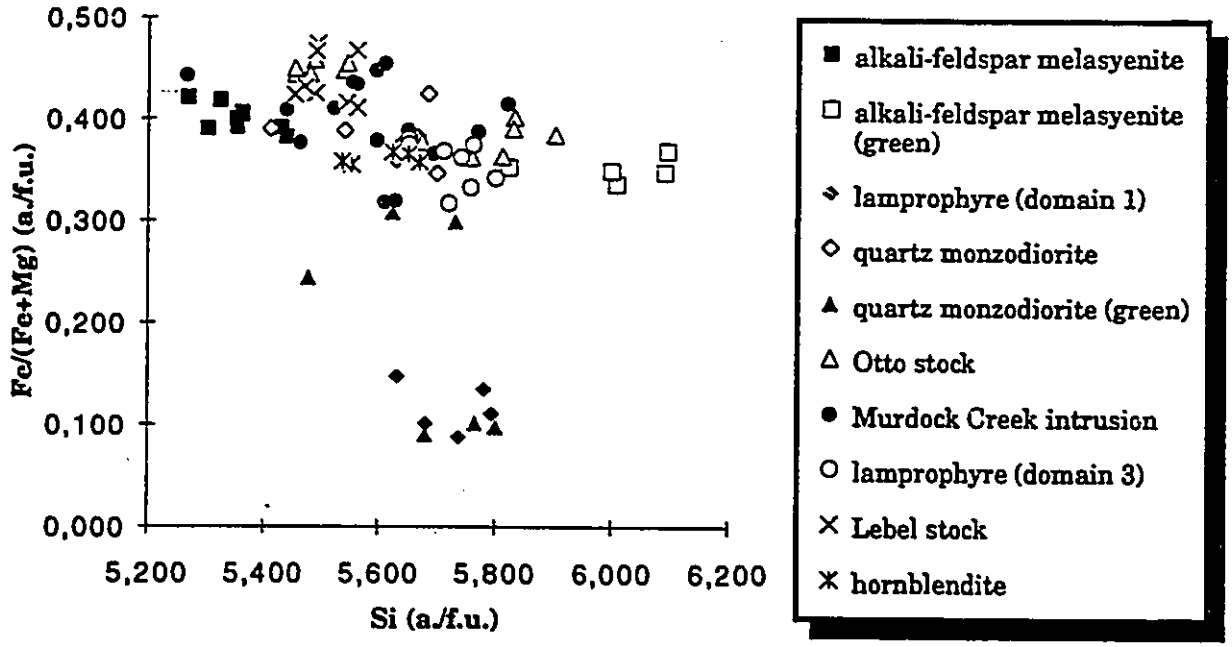
0,500
0,400
0,300
0,200
0,100
0,000
Fe/(Fe+Mg) (a./f.u.)
5,200
5,400
5,600
5,800
6,000
6,200
Si (a./f.u.)
alkali-feldspar melasyenite
alkali-feldspar melasyenite (green)
lamprophyre (domain 1)
quartz monzodiorite
quartz monzodiorite (green)
Otto stock
Murdock Creek intrusion
lamprophyre (domain 3)
Lebel stock
hornblendite

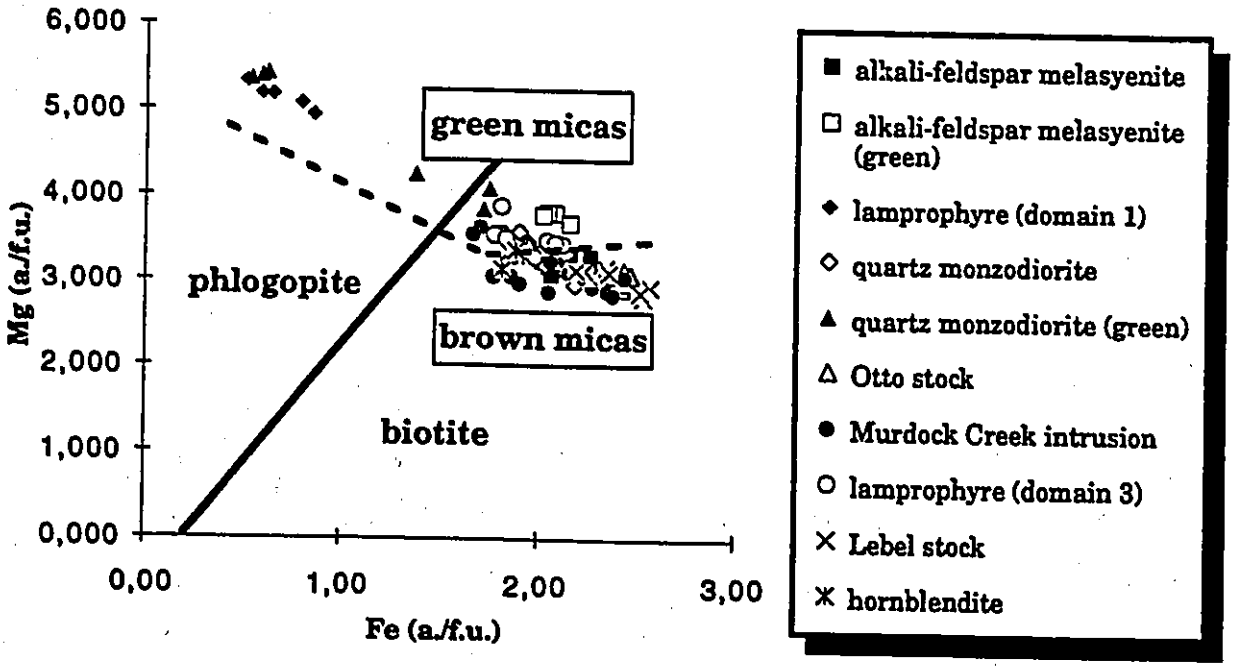
6,000
5,000
4,000
3,000
2,000
1,000
0,000
Mg (a./f.u.)
green micas
phlogopite
brown micas
biotite
0,00
1,00
2,00
3,00
Fe (a./f.u.)
alkali-feldspar melasyenite
alkali-feldspar melasyenite (green)
lamprophyre (domain 1)
quartz monzodiorite
quartz monzodiorite (green)
Otto stock
Murdock Creek intrusion
lamprophyre (domain 3)
Lebel stock
hornblendite

evolved under oxidized conditions: Baie-des-Moutons, (Lalonde and Martin, 1983), Finnmarka, (Czamanske and Wones, 1973). Another mechanism which may explain this feature is a substitution involving $Fe^{3+}$ for $Al^{3+}$ (Hazen and Wones, 1972). This is in accordance with evidence that the green mica contains elevated amounts of $Fe^{3+}$ (Lalonde, 1992). Since this type of green mica is secondary, this implies that the hydrothermal fluids responsible for alteration were also strongly oxidized.

Figure 17 illustrates the three groups of mica compositions occurring in the rocks of the KLF. The dividing line is after Deer et al. (1966), where the Mg:Fe ratio of 2:1 separates the phlogopite and biotite fields and the dashed line (Mg a./f.u. = 3.30) defines the boundary between green mica and brown mica. A large tight cluster of analyses fall in field 1 (primary brown biotite) and in field 2 (green biotite) which can be either primary (lamprophyre unit of domain 3) or secondary (alkali-feldspar melasyenite unit of domain 1). Mica analyses that fall in field 3 are primary phlogopite from the lamprophyres and hydrothermal phlogopite from the quartz monzodiorite unit of domain 1. This suggests at least two different generations of green mica: a hydrothermal and a magmatic phase.

Brown and green micas from the Kirkland Lake area are characterized by uniform Mg content (Fig. 18A). Brown biotite usually contain less Si (5.20 to 5.60) than green biotite (5.60 to 6.10), which is to be expected since green micas have phlogopite or near-phlogopite compositions (Deer et al., 1972). Accordingly, brown biotite has a higher

$Al^{iv}$ and lower Si content than green mica. $Al^{iv}$ decreases with increasing Si; this trend is defined by a negative slope approximately equal to -1, following the compositional line of the biotite ($Si_5Al_3$) to phlogopite ($Si_6Al_2$) transition (Deer et al., 1972) (Fig. 18B). The most titaniferous (up to 0.72 a./f.u.) biotite occurs in the alkali-feldspar melasyenite unit of domain 1 (Fig. 18C). This feature was also observed in the clinopyroxene of this unit. Ti progressively decreases with increasing Si, with green mica containing the lowest amount of Ti (below 0.15).

Cr content in biotite is present in appreciable quantity (up to 0.25 a./f.u.) in only two rock units: lamprophyres (vogesite and minette) in domains 1 and 3 and the hydrothermal green mica in the quartz monzodiorite of domain 1. The latter finding was initially explained as alteration of the the quartz monzodiorite unit by lamprophyric fluids which crystallized this Cr-bearing biotite (Hattori and Levesque, 1989). It is now believed that lamprophyres may be parent magmas to quartz monzodiorites (syenite porphyries) (Barnes et al., 1986; Rock et al., 1987; Nemec, 1988). Fluorine content in the micas of the Kirkland Lake area is variable; the green mica of lamprophyre and the quartz monzodiorite units of domain 1 contain up to 1.03 a./f.u., while biotite from other units generally contain less than 0.2 a./f.u.

The green mica present in the lamprophyre and quartz monzodiorite units of domain 1 exhibit pleochroic zoning, with light-colored cores and darker-colored rims. The green phlogopite of the quartz monzodiorite exhibits this texture (Plate 5D). Microprobe analyses indicate that compositional zoning is responsible for these color changes. The dark rims

Figure 18. Mg, Ti and Al versus Si cation plots for mica. A) Brown biotite usually contain less Si than the green mica, which have a phlogopite or near-phlogopite composition. Note the uniform Mg content (avg 1.90). B) $Al^{iv}$ content is negatively correlated to Si content; the trend follows the compostional line of the biotite to phlogopite transition. C) Ti decreases progressively with increasing Si. Green mica has the lowest Ti content, with less than 0.15 a./f..u.

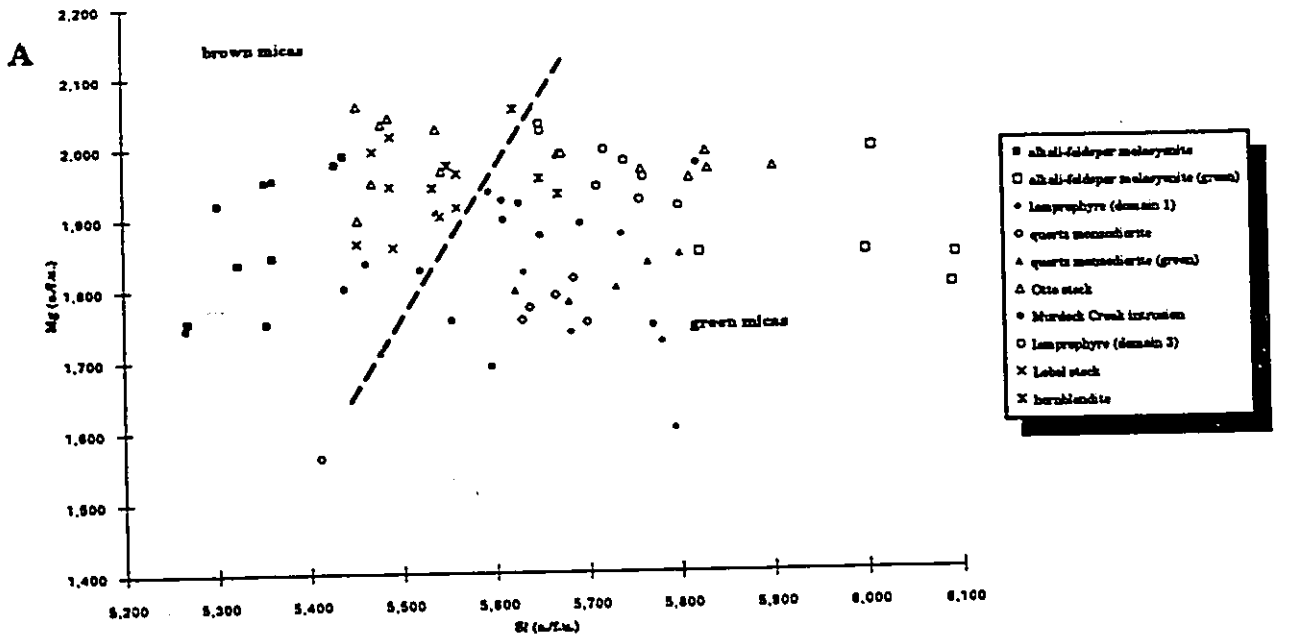
A
brown micas
green micas
Mg (a.f.u.)
Si (a.f.u.)
2,200
2,100
2,000
1,900
1,800
1,700
1,600
1,500
1,400
5,200
5,300
5,400
5,500
5,600
5,700
5,800
5,900
6,000
6,100
alkali-feldspar malaeyenite
alkali-feldspar malaeyenite (green)
lamprophyre (domain 1)
quartz monzodiorite
quartz monzodiorite (green)
Otto stock
Murdoch Creek intrusion
lamprophyre (domain 3)
Lebel stock
hornblendite

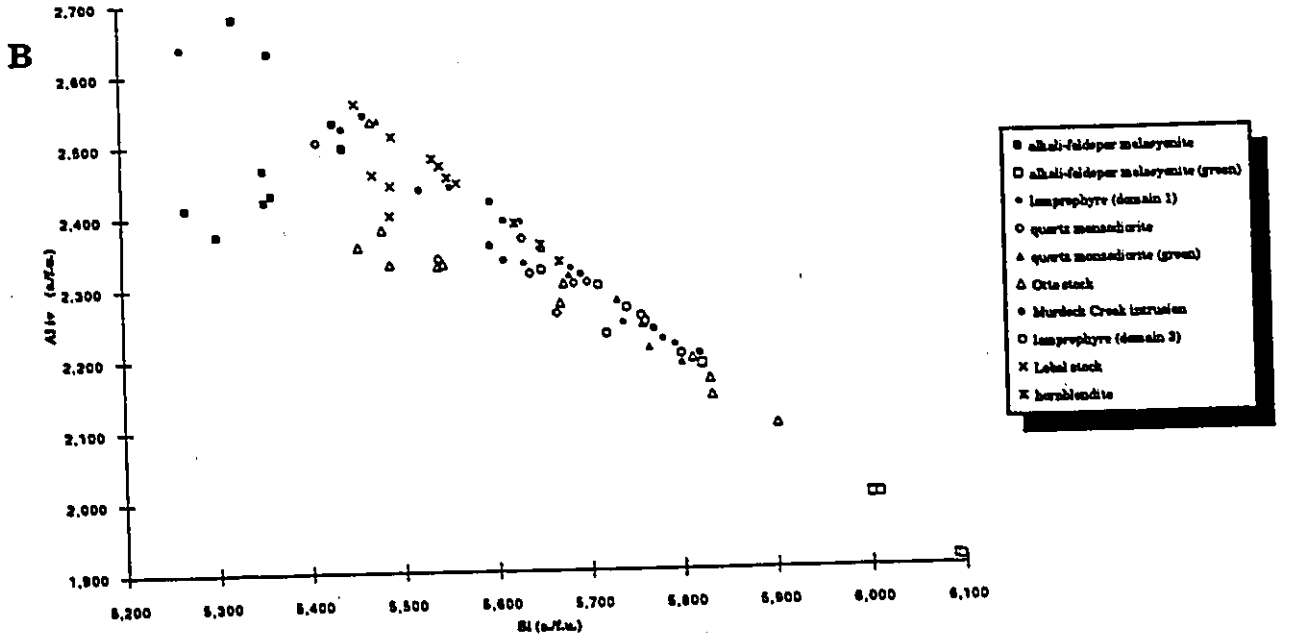
B
Al iv (a.f.u.)
Si (a.f.u.)
2,700
2,600
2,500
2,400
2,300
2,200
2,100
2,000
1,900
5,200
5,300
5,400
5,500
5,600
5,700
5,800
5,900
6,000
6,100
alkali-feldspar malaeyenite
alkali-feldspar malaeyenite (green)
lamprophyre (domain 1)
quartz monzodiorite
quartz monzodiorite (green)
Otto stock
Murdoch Creek intrusion
lamprophyre (domain 3)
Lebel stock
hornblendite

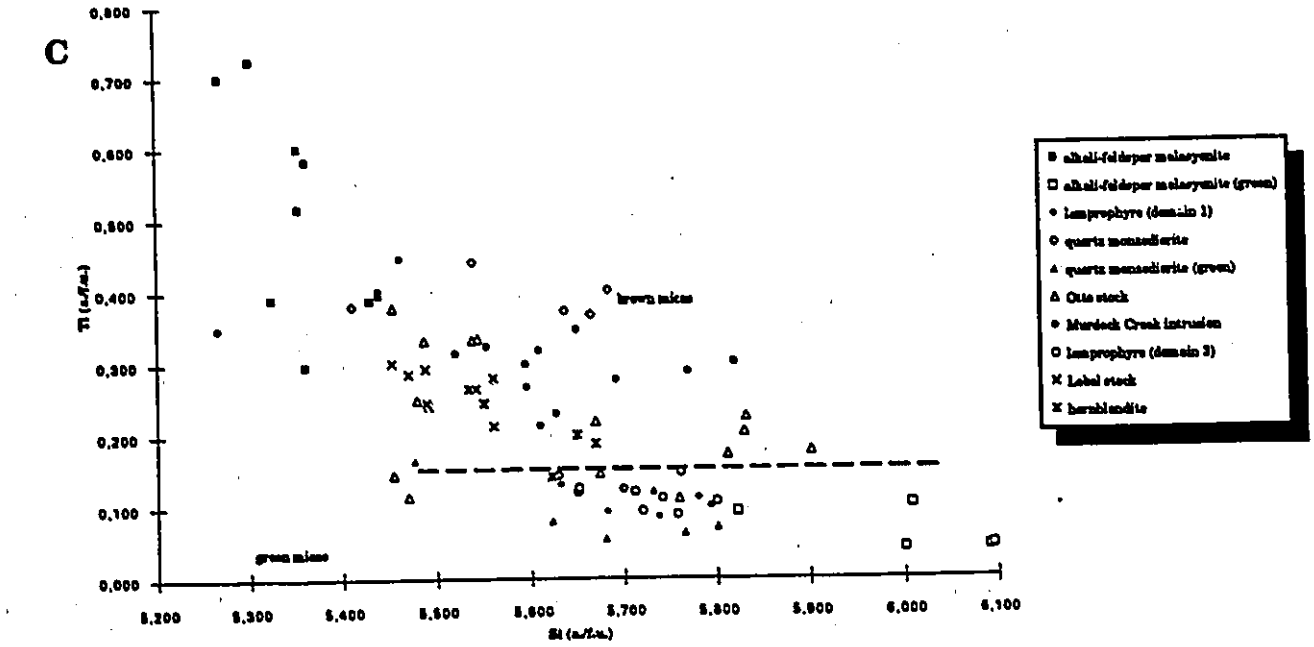
C
Ti (a.f.u.)
Si (a.f.u.)
brown micas
green micas
0,800
0,700
0,600
0,500
0,400
0,300
0,200
0,100
0,000
5,200
5,300
5,400
5,500
5,600
5,700
5,800
5,900
6,000
6,100
alkali-feldspar malaeyenite
alkali-feldspar malaeyenite (green)
lamprophyre (domain 1)
quartz monzodiorite
quartz monzodiorite (green)
Otto stock
Murdoch Creek intrusion
lamprophyre (domain 3)
Lebel stock
hornblendite

have higher Fe, Ti and lower Si, Mg and Cr contents than the light-colored cores, which have similar compositions to the green mica from other units. The reasons why this zoned green mica exhibits a Fe-enrichment trend contrary to the typical Mg-enrichment trend seen in clinopyroxene and other mica of the Kirkland Lake area are not clear.

### 3.3.3 Amphibole

Amphibole is the most abundant ferromagnesian mineral of the granitic rock types of the Kirkland Lake area. It is present in quartz monzodiorite, granodiorite, andesite and mafic trachyte units of domain 1 and all of the intrusions of domain 2. It is the main constituent of the mafic hornblendite unit of domain 3, as well as a minor phase of the alkali granite unit of the Otto stock, and also occurs in minette and spessartite lamprophyres. Amphibole occasionally replaces primary clinopyroxene, like in the McElroy stock, where large, pristine euhedral amphibole completely encloses small, rounded clinopyroxene fragments and commonly poikilitically enclose plagioclase crystals (Plate 5E). In these cases, it is difficult to distinguish primary amphibole from secondary amphibole. A total of seventy analyses from this study and others were used in the study of amphibole of the Kirkland Lake area. All amphibole analyses are classified according to International Mineralogical Association nomenclature (Leake, 1978). Twenty-nine representative analyses were used for classification purposes.

All of the amphiboles encountered in the Kirkland Lake area are from the calcic amphibole group. However, an alkali amphibole has been

identified in domain 3, where it infrequently occurs as fracture-coating hydrothermal minerals or possibly as primary amphibole in the quartz syenite unit of the Otto stock. Zoning in amphibole is an inconspicuous but widespread feature; the systematic variation in optical properties that accompanies zoning is rare. Where present, phenocrysts usually display slightly pleochroic light green or yellow cores and correspondingly darker, more strongly pleochroic rims. This texture can be seen in the amphibole of the intrusions of domain 2 and of the quartz monzodiorite and granodiorite units of domain 1.

The classification diagrams for calcic amphiboles (Fig. 19) display the compositional variation exhibited by amphibole of the Kirkland Lake area. Amphibole from the intrusions of domain 2 spans a wide range of compositions from pargasitic hornblende to edenite (and edenitic hornblende) to magnesio-hornblende. Amphibole in the quartz monzodiorite unit of domain 1 has a pargasite to edenite composition, while that in granodiorite is edenite and magnesio-hornblende. In the extrusive units of domain 1, amphibole of the mafic trachyte ranges from magnesian hastingsite to magnesio-hastingsitic hornblende; in the melamonzonite unit, amphibole ranges from magnesio-hastingsite to magnesian hastingsitic hornblende. It is interesting to note that all amphibole compositions that fall in diagram C ($Fe^{3+} > Al^{iv}$) are from rocks of domains 1 and 3. Although the classification diagrams give the impression that amphibole has a wide-ranging compositional spectrum, it consistently falls in the upper right portion of the diagrams, differing only in higher $Fe^{3+}$ content (diagram C) or in lower $(Na+K)_A$ content (diagram A) .

Figure 19. Classification of the calcic amphiboles. Two types of zoning are observed in the amphibole: in domain 2, amphibole displays light cores and dark rims enriched in Si and Fe, while those of domain 1 have light cores and dark rims enriched in both Si and Mg. Diagram A is for amphibole having $(Na+K)_A < 0.50$ and $Ti < 0.50$. Diagram B represents amphibole with $(Na+K)_A \geq 0.50$, $Ti < 0.50$ and $Fe^{3+} \leq Al^{vi}$. Diagram C is for amphibole with $(Na+K)_A \geq 0.50$, $Ti < 0.50$ and $Fe^{3+} > Al^{vi}$. Note that all amphibole compositions falling in diagram C are from rocks of domain 1 and 3. Abbreviations of the different compositional fields are : ac=actinolite, mho= magnesio-hornblende, ed=edenite, eh=edenitic hornblende, ph=pargasitic hornblende, p=pargasite, fph=ferroan pargasitic hornblende, mhh= magnesio-hastingsitic hornblende, moh= magnesio-hastingsite, mah=magnesian hastingsite.

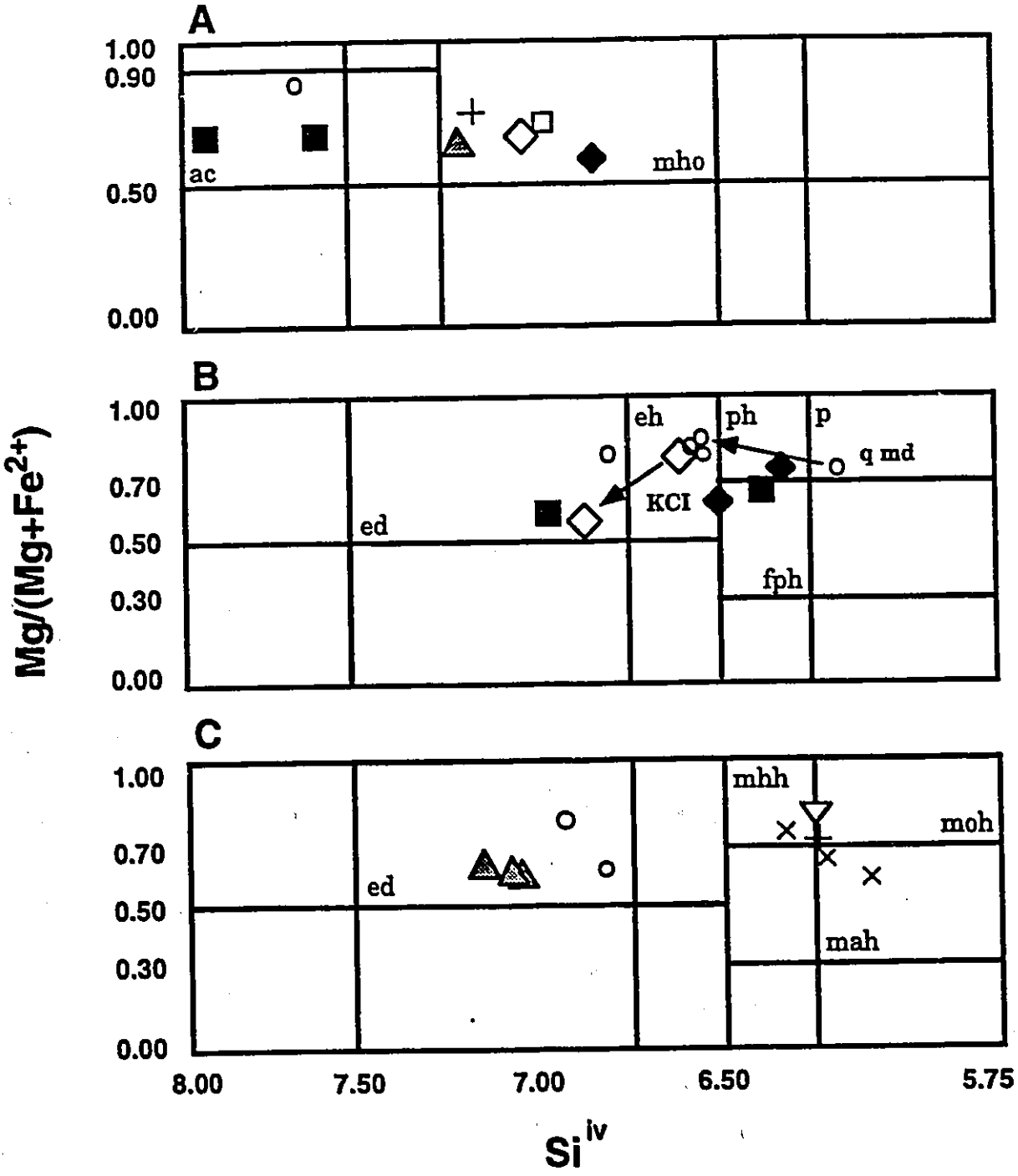


| | | |
|---|---|---|
| × trachyte | ○ quartz monzodiorite | ■ Monocle Lake intrusion |
| ▲ granodiorite | ◆ McVittie stock | + hornblendite |
| ▽ melamonzonite | ◇ Kinabik Creek intrusion | □ McElroy stock |

Zoning trends in individual amphibole crystals are variable (Fig. 19): in the Kinabik Creek intrusion (KCI, domain 2), a large phenocryst has a light-colored edenitic hornblende core and a darker-colored edenite/magnesio-hornblende rim, corresponding, from core to rim, to an increase in Si and Fe and a decrease in Mg and Al. This type of zoning has been observed in amphibole of the volcanic rocks of southwestern British Columbia (Green, 1982). In a zoned amphibole of quartz monzodiorite (q md, domain 1), the light core has a pargasite composition that evolves to a dark-green edenitic hornblende rim, indicating a decrease, from core to rim, in Al and Fe, and an increase in Si and Mg. Interestingly, the zoned amphibole crystals evolved in very different directions: in domain 1, the amphibole evolved towards edenite (increase in Mg), with a slightly increasing $Mg/(Mg+Fe^{2+})$ratio, while amphibole in domain 2 evolved towards edenite/magnesio-hornblende (increase in Fe), with the corresponding decrease in the $Mg/(Mg+Fe^{2+})$ ratio. These zoning trends define Fe-enrichment in domain 2, and Mg-enrichment in domain 1.

Fe/(Fe+Mg) atomic ratios in amphibole exhibit more variation than those of clinopyroxene and biotite, averaging 0.35 ±0.15. These ratios are low compared to similar syenitic and granitic (calc-alkaline) rocks (Baie-des-Moutons syenite, Lalonde and Martin, 1983; Red Lake and Eagle Peek plutons, Noyes et al., 1983; Wones and Gilbert, 1982). Fe/(Fe+Mg) atomic ratios for amphibole in domains 1 and 3 define a trend identical to that of Mg-enrichment observed in the zoned crystals of the quartz monzodiorite unit of domain 1 (solid line, Fig. 20A); the ratio decreases with increasing Si content (Fig. 20A). This trend, best exhibited in the granodiorite unit, is consistent with the overall Mg-enrichment observed in the other

Figure 20. Fe/(Fe+Mg) versus Si cation plots for amphibole. A) In domains 1 and 3, the ratio decreases with increasing Si content, defining a Mg-enrichment trend, consistent with the compositional features of clinopyroxene and mica. This trend is best observed in the granodiorite unit (solid arrow). This conforms with the Mg-enrichment trend observed in zoned amphibole crystals (solid line). B) In domain 2, amphibole displays ratios that increase with increasing Si content, defining an Fe-enrichment trend (solid arrow), identical to the trend observed in zoned crystals (solid line). Fields: 1 = magnesio hastingsite and pargasitic hornblende, 2 = edenitic hornblende, 3 = edenite and magnesio-hornblende, 4 = actinolite, 5 = silicic edenite from the alkali granite unit of the Otto stock.

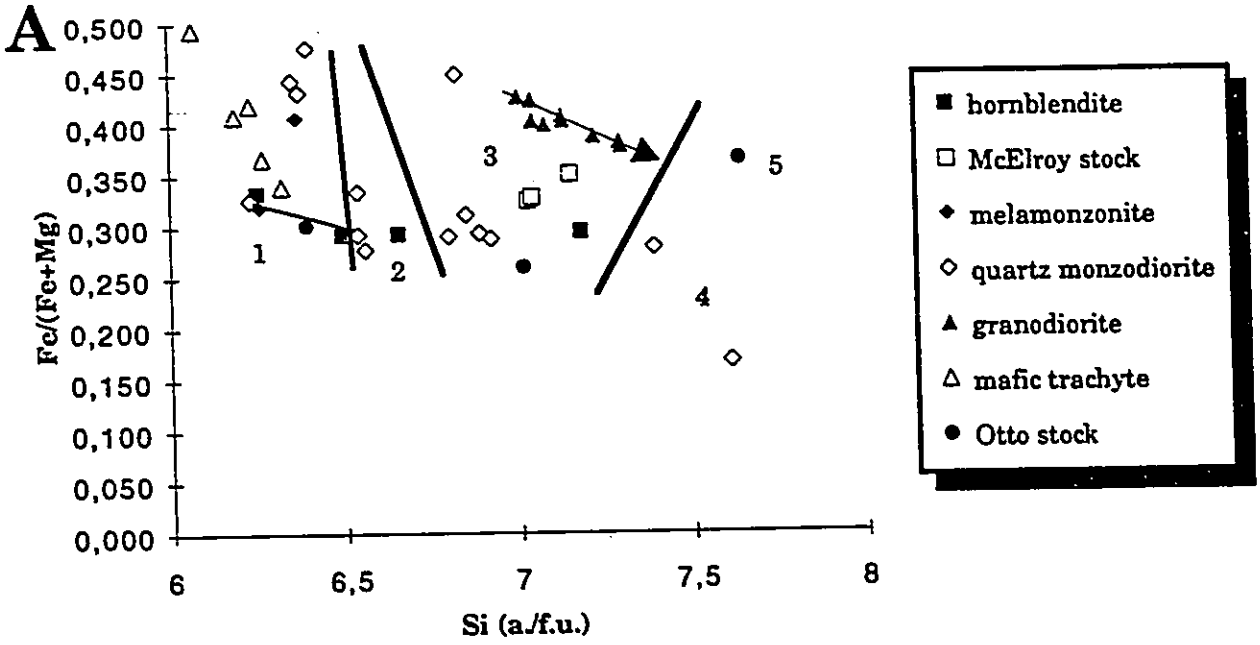
A
0,500
0,450
0,400
0,350
0,300
0,250
0,200
0,150
0,100
0,050
0,000
Fe/(Fe+Mg)
6
6,5
7
7,5
8
Si (a./f.u.)
1
2
3
4
5
hornblendite
McElroy stock
melamonzonite
quartz monzodiorite
granodiorite
mafic trachyte
Otto stock

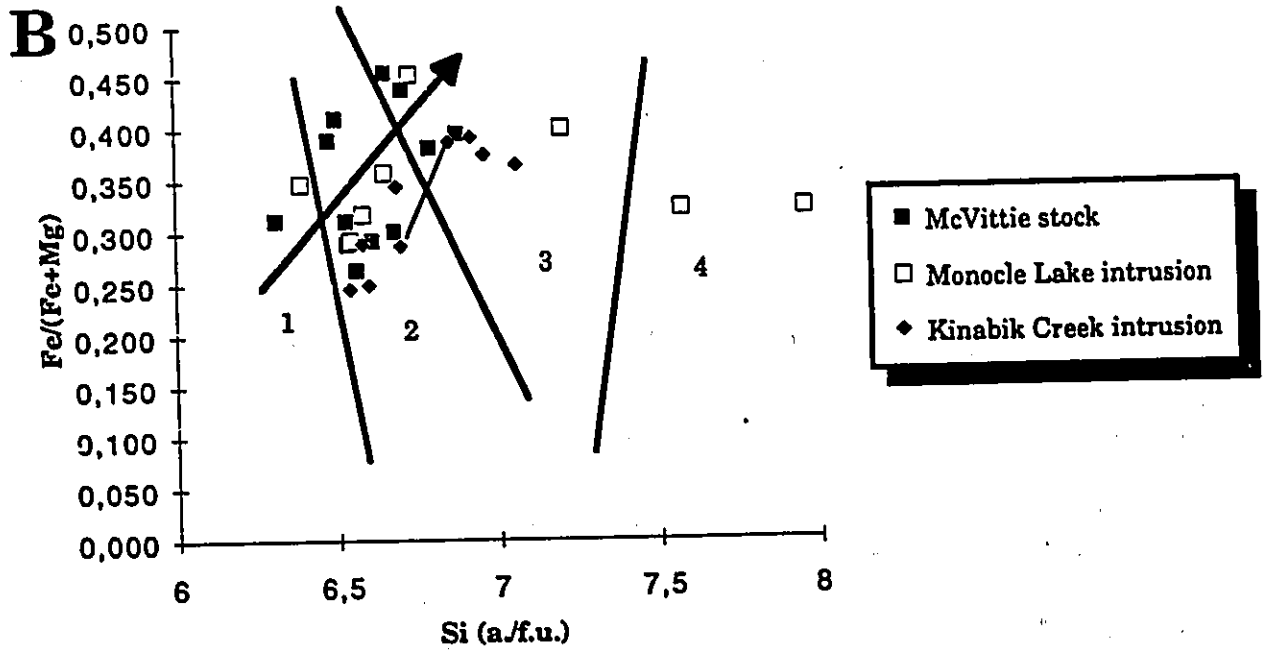
B
0,500
0,450
0,400
0,350
0,300
0,250
0,200
0,150
0,100
0,050
0,000
Fe/(Fe+Mg)
6
6,5
7
7,5
8
Si (a./f.u.)
1
2
3
4
McVittie stock
Monocle Lake intrusion
Kinabik Creek intrusion

ferromagnesian minerals of domains 1 and 3. This trend has been observed in the amphibole of the alkaline rocks of Papua New Guinea (Mason and MacDonald, 1978; Richards, 1990) and the Finnmarka complex (Czamanske and Wones, 1973). However, amphibole in the rocks of domain 2 display the opposite trend: the Fe/(Fe+Mg) atomic ratio increases with Si content (Fig. 20B). This represents an Fe-enrichment trend, also defined by zoned amphibole crystals of this domain (solid line of Fig. 20B). It is interesting to note that the amphibole of domain 1 (Mg-enrichment) and domain 2 (Fe-enrichment) have similar compositions (pargasite to edenite and magnesio-hornblende crystallization trend) but display contrasting enrichment trends. This clearly indicates that although the initial composition of the crystallizing amphibole was similar in both domains, they subsequently evolved under different crystallization conditions.

Ca content of amphibole of the Kirkland Lake area remains constant throughout crystallization, at approximately 1.75 ±0.15 a./f.u. (Fig. 21A). As demonstrated by Cawthorn (1976), virtually all hornblende compositions contain 1.7 to 1.9 a./f.u. Ca regardless of magma composition. Na content slightly decreases with increasing Si; this is best observed in the granodiorite unit of domain 1 (Fig. 21B). The compositional variation in amphibole is largely dependent on $Al^{iv}$ content. $Al^{iv}$ is strongly negatively correlated with Si, with an approximate slope of -0.9 (Fig. 22A), reflecting the pargasite ($Si_6Al_2$) to edenite ($Si_7Al$) crystallization trend (Deer et al., 1972) in amphibole of the Kirkland Lake area. Ti content, which is highest in the melamonzonite unit of domain 1 (up to 0.23 a./f.u.), also decreases with increasing Si (Figs. 22B). Potassium behaves as Ti, with values highest in mafic trachyte (K= 0.59 a./f.u.) and lowest in

Figure 21. Ca and Na versus Si cation plots for amphibole. A) Ca content in amphibole is constant throughout the Kirkland Lake area. B) Na content in amphibole show a slight decrease at Si = 7.00, especially in the amphibole of the granodiorite unit. The solid line in both diagrams divides the large cluster of primary amphibole compositions from secondary actinolite and silicic edenite of the Otto stock.

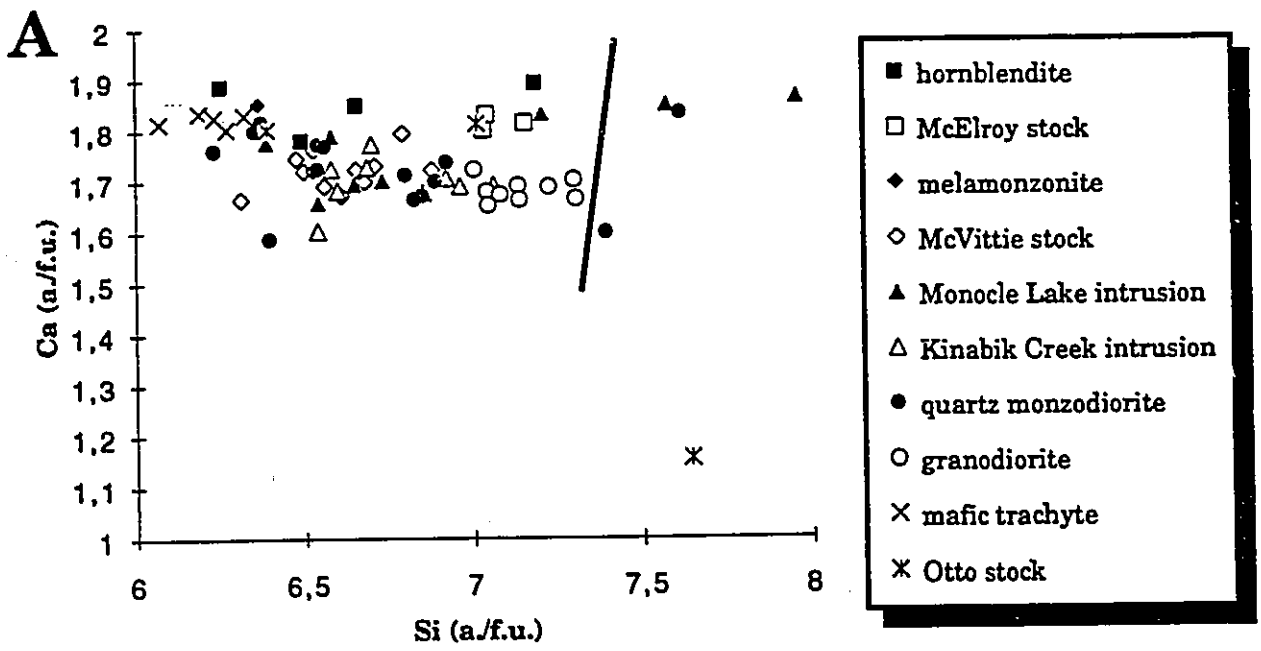
A
Ca (a./f.u.)
2
1,9
1,8
1,7
1,6
1,5
1,4
1,3
1,2
1,1
1
6
6,5
7
7,5
8
Si (a./f.u.)
hornblendite
McElroy stock
melamonzonite
McVittie stock
Monocle Lake intrusion
Kinabik Creek intrusion
quartz monzodiorite
granodiorite
mafic trachyte
Otto stock

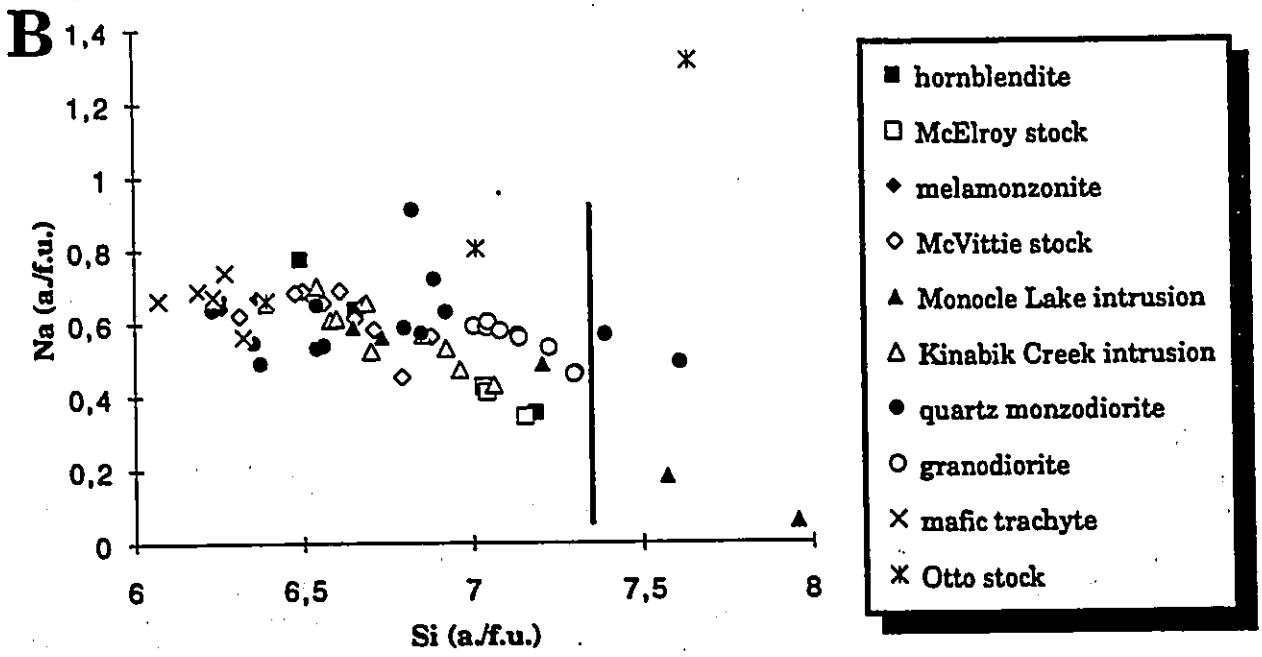
B
Na (a./f.u.)
1,4
1,2
1
0,8
0,6
0,4
0,2
0
6
6,5
7
7,5
8
Si (a./f.u.)
hornblendite
McElroy stock
melamonzonite
McVittie stock
Monocle Lake intrusion
Kinabik Creek intrusion
quartz monzodiorite
granodiorite
mafic trachyte
Otto stock

Figure 22. Al $^{iv}$ and Ti versus Si cation plots for amphibole. A) Al $^{iv}$ is negatively correlated to Si, reflecting the pargasite ($Si_6Al_2$) to edenite ($Si_7Al$) crystallization trend. B) Ti decreases as Si increases. The most titaniferous amphibole is found in the melamonzonite unit of domain 1, the least are from the granodiorite unit of domain 1. The solid line divides primary amphibole from secondary actinolite and silicic edenite from the Otto stock.

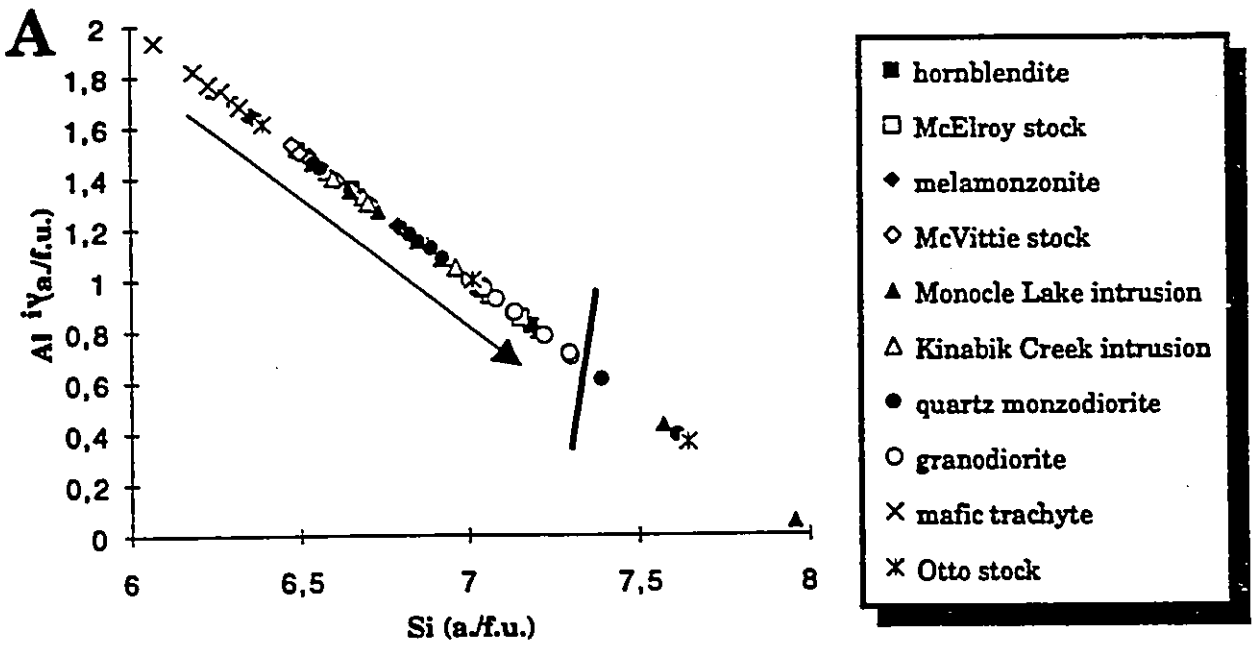
A
2
1,8
1,6
1,4
1,2
1
0,8
0,6
0,4
0,2
0
Al iv (a./f.u.)
6
6,5
7
7,5
8
Si (a./f.u.)
hornblendite
McElroy stock
melamonzonite
McVittie stock
Monocle Lake intrusion
Kinabik Creek intrusion
quartz monzodiorite
granodiorite
mafic trachyte
Otto stock

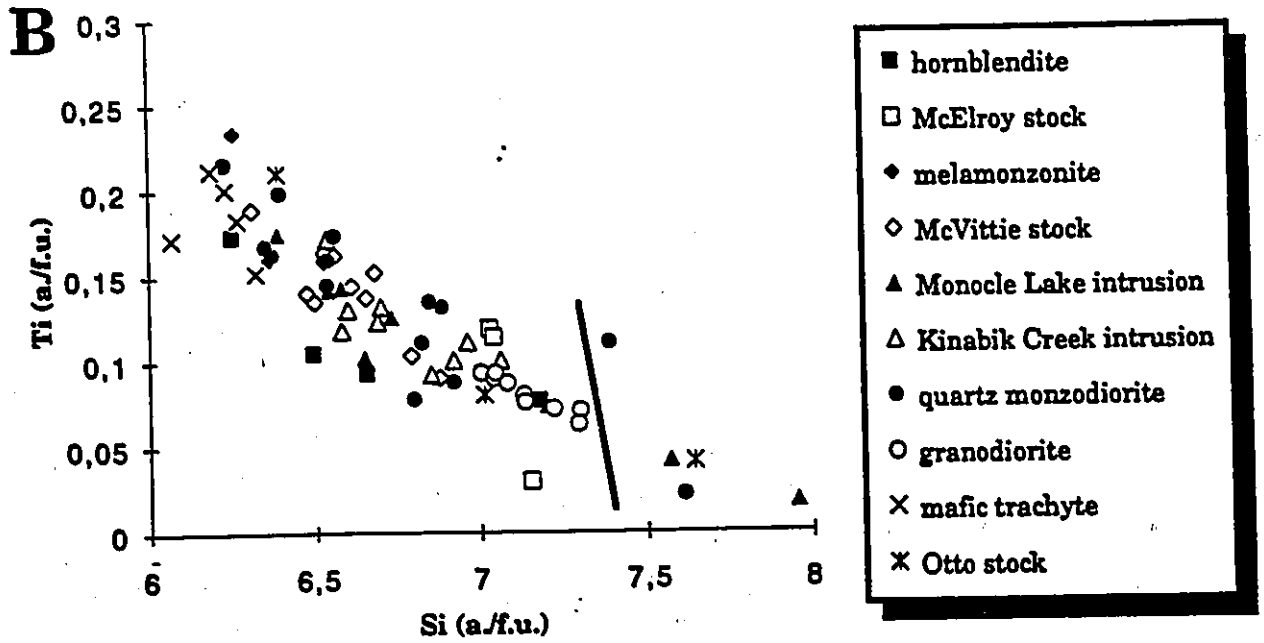
B
0,3
0,25
0,2
0,15
0,1
0,05
0
Ti (a./f.u.)
6
6,5
7
7,5
8
Si (a./f.u.)
hornblendite
McElroy stock
melamonzonite
McVittie stock
Monocle Lake intrusion
Kinabik Creek intrusion
quartz monzodiorite
granodiorite
mafic trachyte
Otto stock

granodiorite (0.04 a./f.u.). Mn is most abundant in amphibole from the McElroy stock, which mimics the high Mn content of the clinopyroxene it replaces.

Amphibole compositions from the Kirkland Lake area fail to follow either of the two major amphibole compositional trends of Mitchell (1990). The primary magmatic trend is characterized by increasing Si, Na and decreasing Ca, Al and Mg number ($Mg/(Mg+Fe^{2+})$). The primary miaskitic magmatic trend is characterized by a decreasing Mg number at constant Si, Ca and Al content. The amphibole of both of these trends display decreasing Mg numbers, which is a consequence of Fe-enrichment. Amphibole from The Baie-des-Moutons syenite complex also fails to follow either of these trends; coincidently, this complex evolved under highly oxidizing conditions (Lalonde and Martin, 1983), as have the rocks of domains 1 and 3. The amphibole of domain 1 and 3 is remarkably similar to those found in the Finnmarka complex, in that they are both characterized by constant Ca and decreasing $Al^{iv}$, Fe, Ti, Na, K and Fe/(Fe+Mg) ratios (Czamanske and Wones, 1973). The Finnmarka complex also evolved under highly oxidizing conditions. The amphibole of domain 2 also shares these features except for increasing Fe/(Fe+Mg) ratios.

### 3.3.4 Ferric-ferrous iron ratios of mineral separates

A total of twelve mineral separates were obtained to analyze for $Fe^{2+}$ and $Fe^{3+}$ data, either by wet chemical methods (clinopyroxene and amphibole) or by Mössbauer spectroscopy (biotite). Although these minerals were separated from only a small portion of the rock types from

the Kirkland Lake area, they present a good overview of the oxidation trends observed in the ferromagnesian minerals of this and other studies in the Kirkland Lake area (Cameron and Carrigan, 1987; Hattori and Levesque, 1989; Rowins et al., 1991).

Ferric-ferrous iron ratios for the ferromagnesian minerals studied (clinopyroxene, biotite, amphibole) differ for the three minerals and for the three domains. In clinopyroxene, the ratio increases gradually with host rock silica, while biotite ratios are uniform and those of amphibole steadily decrease (Fig. 23A). Care was taken in selecting clinopyroxene that contained the least amount of magnetite inclusions which could enhance the ferric-ferrous iron ratio. All biotite separates were obtained from samples of domain 3, and have very similar ratios averaging $0.30 \pm 0.07$. Mg-enrichment trends, interpreted to reflect increasing magmatic oxidation in rocks, are best defined by decreasing Fe/(Fe+Mg) ratios in clinopyroxene (Fig. 10) and constant Fe/(Fe+Mg) ratios in biotite (Fig. 16). This is reflected in the close correspondence to the ferric-ferrous iron ratios observed for these minerals (Fig. 23A). The amphibole trend is based on data obtained on two samples from domain 1 and one sample from domain 2 (Kinabik Creek intrusion). The amphibole trend in Figure 23A does not reflect the Mg-enrichment trend (magmatic oxidation) exhibited by the amphibole of domain 1; it does however concord with the Fe-enrichment trend observed in the amphibole of domain 2. The limited data presented here does not permit to make a strong case for decreasing or increasing ferric-ferrous iron ratios for the amphibole of the Kirkland Lake area. They can however demonstrate that ratios seem higher in domain 1 compared to

domain 2, and thus indicate that the amphibole of domain 1 may be more oxidized that in domain 2.

Ferric-ferrous iron ratios are usually higher in domain 3 than in domain 1, and lowest in domain 2 (Fig. 23B). Magmatic oxidation appears to be strongest in domain 3, strong in domain 1 and weak in domain 2. Clinopyroxene in domain 3 has a ratio exceeding 0.40, much higher than that for typical diopside (0.25 to 0.30) (Deer et al., 1972). This explains, among other features, the presence of aegirine-augite in the units of the syenitic composite intrusions of domain 3. Clinopyroxene in domain 1 has a smaller proportion of $Fe^{3+}$, falling within the typical range of diopside. Biotite in domain 3 has elevated ratios compared to typical micas in syenitic and granitic rocks (Fig. 1, Speer, 1984). The hydrothermal green mica of domain 1 does not appear on Figure 23B because of the difficulty in separating them for chemical determination; their green color is indicative of elevated $Fe^{3+}$ content (Lalonde, 1992) and it probably has ratios that exceed those for biotite in domain 3.

The average ferric-ferrous iron ratios of calcic amphibole in syenites and granites is approximately 0.20 (Wones and Gilbert, 1982). The ratios of amphibole from domain 1 are in general agreement with this value; however, ratios in domain 2 approach 0.10, which is somewhat lower than the typical value described above. Amphibole from the hornblendite unit of the Otto stock has ratios that range from 0.10 to 0.30 (Sutcliffe et al., 1990). Ratios for clinopyroxene and biotite from the Kirkland Lake area clearly indicate that domain 3 rocks evolved under highly oxidizing conditions and domain 1 rocks under slightly less oxidizing conditions. Amphibole ratios

Figure 23. Ferric-ferrous iron molar ratios of the ferromagnesian minerals. A. Ratios for the three minerals studied (clinopyroxene, biotite and amphibole) exhibit distinctive features: clinopyroxene ratios increase with host rock silica, while biotite ratios are uniform and amphibole ratios decrease. Note that clinopyroxene may contain magnetite inclusions which could enhance this ratio; this effect is probably responsible for the clinopyroxene in the upper left corner of the diagram. The decreasing amphibole trend is based on limited data (see text for explanation). B. Ferric-ferrous iron ratios for the different minerals are usually highest in domain 3 and lowest in domain 2. Clinopyroxene and biotite have ratios that generally exceed typical values for these minerals. Amphibole ratios suggest that domain 2 rocks evolved under unoxidized or reduced conditions in comparison to domain 1.

**A** Ferric-ferrous molar ratio trends of mafic silicate minerals

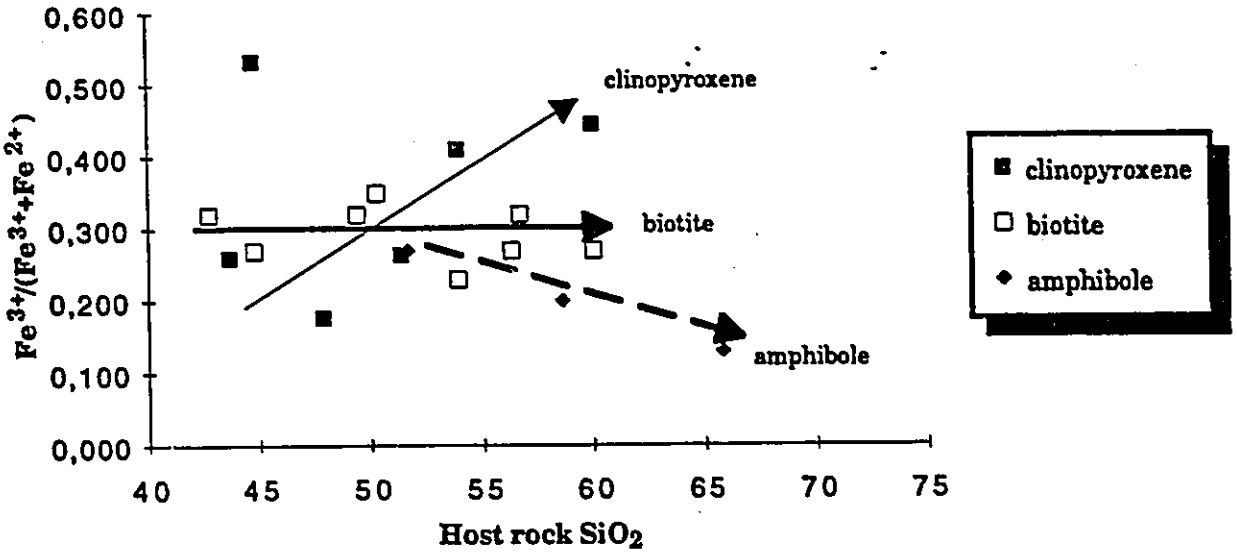


**Comparison of ferric-ferrous molar ratios of mafic silicate minerals**

**B**

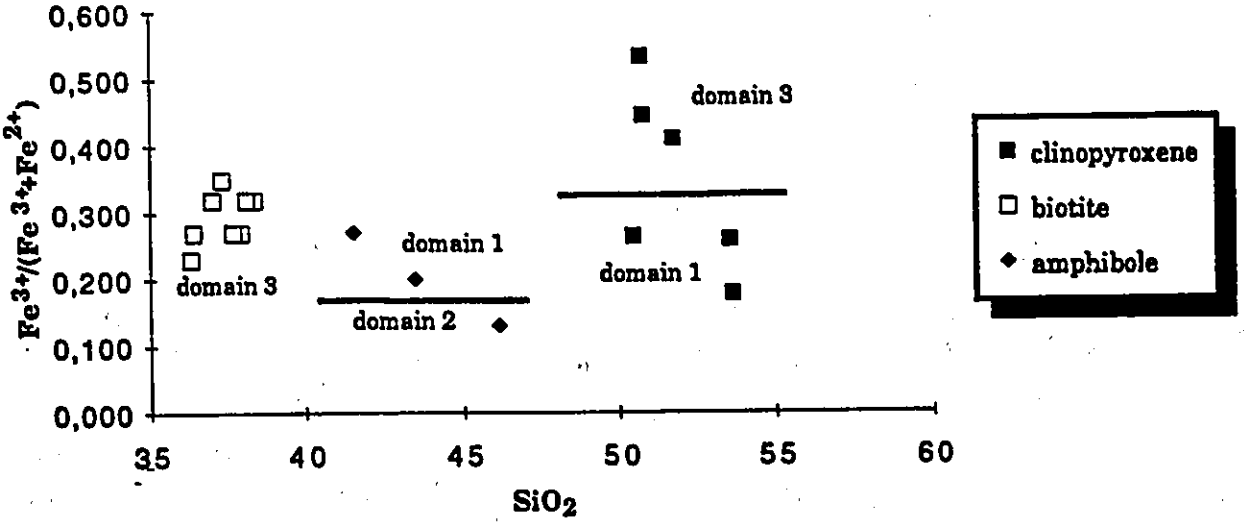

suggest that domain 2 rocks evolved under unoxidized or reduced conditions. Evidence for this statement must be interpreted with caution for the following reasons: 1) the limited data available on amphibole ferric ferrous iron ratio determinations of the Kirkland Lake area, and 2) amphibole and biotite, occurring in the absence of clinopyroxene, crystallize from magmas containing up to 5 vol.% water (Noyes et al., 1983), making these rocks susceptible to late and/or postmagmatic alteration and oxidation.

## 3.4 Rare-earth elements

A total of forty-three representative samples of rock types of the Kirkland Lake area were used in the study of rare earth elements (REE), including 20 analyses from samples collected by the author. The samples were analyzed for the following REE: La, Ce, Nd, Sm, Eu, Tb, Dy, Ho, Yb and Lu. All data were normalized to the chondrite values of Anders and Grevesse (1989). The following sections will examine the REE patterns for the following four groups: syenitic rocks from domain 1, composite intrusions of domain 3, extrusive rocks from domain 1, and granitic rocks of domains 1 and 2. The last section will examine the duality of magmatism of the Kirkland Lake area based on REE patterns.

### 3.4.1 Syenitic rocks of domain 1

The syenitic rocks and lamprophyres of domain 1 present strikingly similar fractionated REE patterns (Fig. 24A). The patterns show light rare

earth element (LREE) enrichment (La) of 150 to 400X chondrite, and heavy rare earth element (HREE) enrichment (Yb, Lu) of 8 to 12X chondrite, with lamprophyres being the most LREE enriched rocks of domain 1. The presence of a positive Eu-anomaly ($(Eu/Sm)_{ch}$ = 0.64-0.75, in the sense of Cullers and Graf, 1984) is a consistent feature of the syenitic rocks of domain 1. Thus, Eu/Sm ratios for these rocks are elevated (0.64 to 0.75) with regards to the range of 0.24 to 0.47 for mafic to felsic alkaline rocks (Cullers and Graf, 1984a).

Calc-alkaline lamprophyres of domain 1 also display a positive Ho-anomaly, common to calc-alkaline lamprophyres (Figure 5.6c, Rock, 1990). Yb and Lu are the least-enriched REE of these rocks ($(La/Lu)_{ch}$ ratio= 11 to 47; $(Sm/Yb)_{ch}$ ratio= 3.6 to 19), especially in lamprophyre ($(La/Lu)_{ch}$ ratio= 33 to 47; $(Sm/Yb)_{ch}$ = 9 to 19); these ratios suggest the presence of garnet in the source region where the lamprophyric melts were formed. Garnet is a mineral phase commonly present in upper mantle rocks (i.e. garnet peridotite, garnet lherzolite) (Hess, 1989). Its crystal structure readily accomodates HREE but virtually excludes LREE; when small degrees of partial melting of garnet-bearing rocks occurs in the upper mantle, the liquid formed will be LREE-rich, while the garnet remains in the source as a residual or refractory mineral. Consequently, HREE will remain in the source region where these LREE-rich liquids are generated (Cullers and Graf, 1984b; Hess, 1989). This produces fractionated, LREE-enriched patterns such as those found on Fig. 24. The Ho-anomaly is present in many syenitic to granitic rock suites, such as the Tuolumne Intrusive Series (Frey et al., 1978) and the Sunda Arc volcanic rocks (Wheller et al.,

Figure 24. Rare earth element patterns for intrusive syenitic and volcanic rocks of domain 1. A) The intrusive syenitic rocks of domain 1 share strikingly similar fractionated patterns. The patterns are characterized by high $\Sigma$REE = 156 to 457 ppm, $(La/Lu)_{ch}$ = 11 to 47 , $(Sm/Yb)_{ch}$ = 3.6 to 19 and the lack of a Eu-anomaly ($(Eu/Sm)_{ch}$ = 0.64 to 0.75). Of significant interest is the positive Ho-anomaly, a feature commonly observed in calc-alkaline lamprophyres and some syenitic and granitic rocks. B) The Timiskaming Group volcanic rocks of domain 1 also share nearly identical fractionated REE patterns. They are characterized by high $\Sigma$REE = 149 to 544 ppm, $(La/Lu)_{ch}$ = 11.2 to 13.9 , $(Sm/Yb)_{ch}$ = 3.3 to 3.9, and a small positive Eu-anomaly ($(Eu/Sm)_{ch}$ = 0.60 to 0.75). The trough shape of the HREE, along with low La/Lu and Sm/Yb ratios suggest that amphibole was present in the source region of parental magmas.

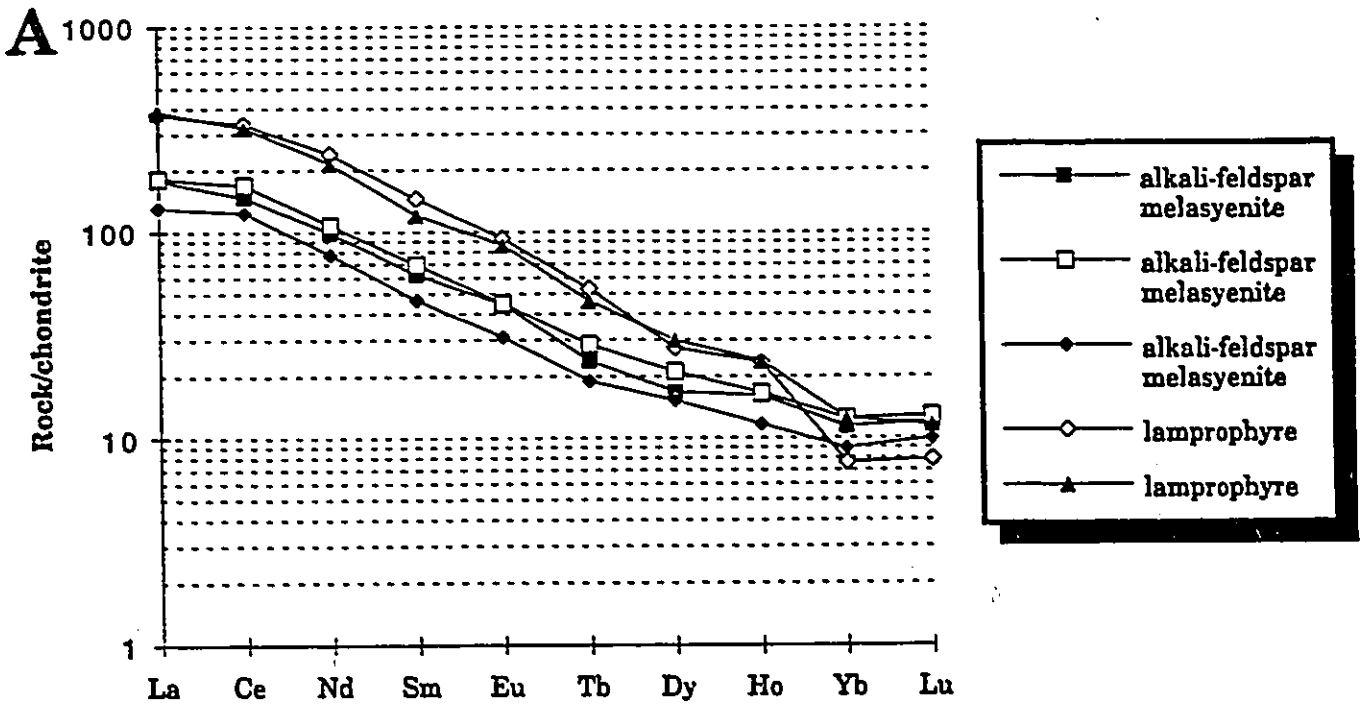
A
1000
100
10
1
Rock/chondrite
La
Ce
Nd
Sm
Eu
Tb
Dy
Ho
Yb
Lu
alkali-feldspar melasyenite
alkali-feldspar melasyenite
alkali-feldspar melasyenite
lamprophyre
lamprophyre

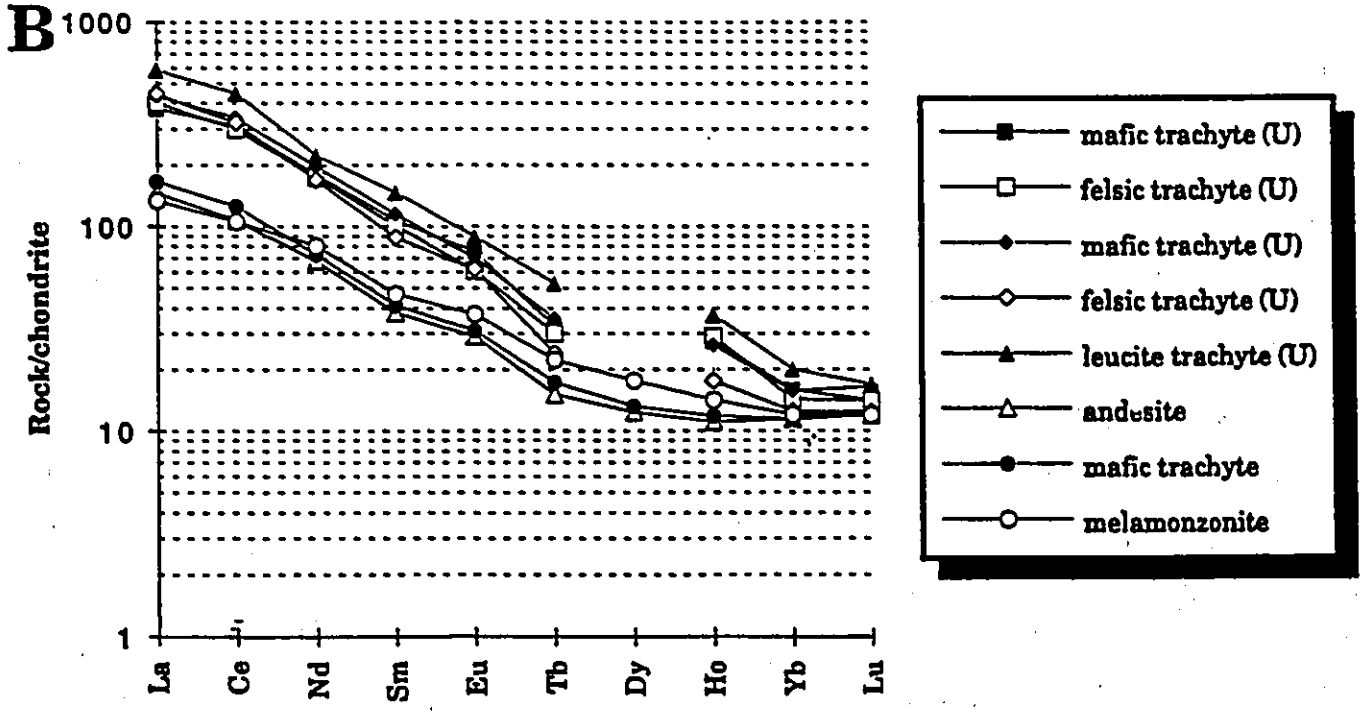
B
1000
100
10
1
Rock/chondrite
La
Ce
Nd
Sm
Eu
Tb
Dy
Ho
Yb
Lu
mafic trachyte (U)
felsic trachyte (U)
mafic trachyte (U)
felsic trachyte (U)
leucite trachyte (U)
andesite
mafic trachyte
melamonzonite

1987); the question as to whether this anomaly is due to analytical error (overestimation) or represents a primary magmatic feature remains.

### 3.4.2 Volcanic rocks of the Timiskaming Group

Figure 24B presents REE patterns for the volcanic rocks of the Timiskaming Group found in domain 1. It includes, for comparative purposes, partial analyses of mafic, felsic and leucite trachyte from Ujike (1985). However, the latter are from highly altered samples where primary mineralogy is extensively carbonatized and textures are extensively or completely obliterated, so that caution must be used in their interpretation. The three analyses from this study show nearly identical patterns, even though they range from andesitic to trachytic compositions, with $\Sigma$REE = 143-544 ppm, LREE enrichment (La) of 160X chondrite and HREE enrichment (Yb, Lu) of 12X chondrite, while those of Ujike are considerably more LREE enriched (400 to 600X chondrite), typical for K-rich (eg. leucite-bearing) rocks (Cullers and Graf, 1984a). A small positive Eu-anomaly ($(Eu/Sm)_{ch}$= 0.60 to 0.75) is present in the three volcanic rocks of domain 1 analyzed for this study; it can also be seen in some analyses from Ujike (1985). Another feature of the REE patterns is the concave-upward shape for HREE, which are not observed for the analyses of Ujike. This shape is indicative of a residual amphibole phase in the region where the primary magmas were formed (Cullers and Graf, 1984b; Wilson, 1989); the low $(La/Lu)_{ch}$ = 11.2 to 13.9 and $(Sm/Yb)_{ch}$ = 3.3 to 3.9 ratios (compared to lamprophyres) also suggest that amphibole, rather than garnet, was the refractory mineral phase present. The amphibole crystal structure

accomodates the intermediate REE (Nd to Ho) better than the HREE to produce the trough-shaped pattern of Fig. 24B (Hess, 1989)

### 3.4.3 Composite intrusions of domain 3

In domain 3, the intrusions have units that range from clinopyroxenite (Gauthier diorite intrusion) to alkali granite (Otto stock). The predominant units of the Lebel and Otto stocks and Murdock Creek intrusion are alkali-feldspar melasyenite and alkali-feldspar syenite. This wide range of rock types is reflected in the broad spectrum of REE patterns (Fig. 25A). The most LREE enriched samples (500 to 600X chondrite) are from the alkali-feldspar melasyenite and syenite units of the Otto and Lebel stocks and Murdock Creek intrusion (270 to 400X, not shown); the least LREE enriched unit is clinopyroxenite from the Gauthier diorite intrusion (20X chondrite). Hornblendite and the quartz monzonite unit of the McElroy stock fall between the two extremes (LREE 150X chondrite). Small positive Eu anomalies are observed in all but hornblendite and Murdock Creek intrusion; in fact, small negative Eu anomalies are reported for this intrusion (Rowins, 1990). The REE patterns of the Lebel and McElroy stocks best display the concave-up shape observed in the extrusive rocks of domain 1 (Fig. 24B), and have high $(La/Lu)_{ch}$ = 16.5 to 28 and $(Sm/Yb)_{ch}$ = 4.8 to 7.7 ratios; this favors the presence of garnet in the source region (Cullers and Graf, 1984b; Hess, 1989). Similarly, REE patterns of the Otto stock, Murdock Creek intrusion and hornblendite show marked decreases in Yb and Lu, also observed in lamprophyres. The high $(La/Lu)_{ch}$= 16.5 to 44.7 and $(Sm/Yb)_{ch}$ = 8.46 to 13.3 ratios are very similar to those in lamprophyres.

Figure 25. Rare earth element patterns for A) the composite intrusions of domain 3 and B) the granitic rocks of domains 1 and 2. A) The composite intrusions of domain 3 contain a wide range of rock units, from clinopyroxenite to alkali granite; this diversity is reflected in the wide ranging fractionated REE patterns. The most fractionated patterns are from the syenite and melasyenite units of the Otto and Lebel stocks. The Gauthier diorite intrusion has a flat, tholeiitic pattern. B) REE patterns for the granitic rocks of domains 1 and 2 are very similar to the syenitic rocks of domain 1, although they are less fractionated ($(La/Lu)_{ch}$ = 5.5 to 22.4 compared to 11 to 47 for domain 1). Granodiorite patterns exhibit the positive Ho-anomaly seen in some domain 1 syenitic rock patterns. Low La/Lu and Sm/Yb ratios and pattern shapes for HREE suggest that amphibole was present in the source region.

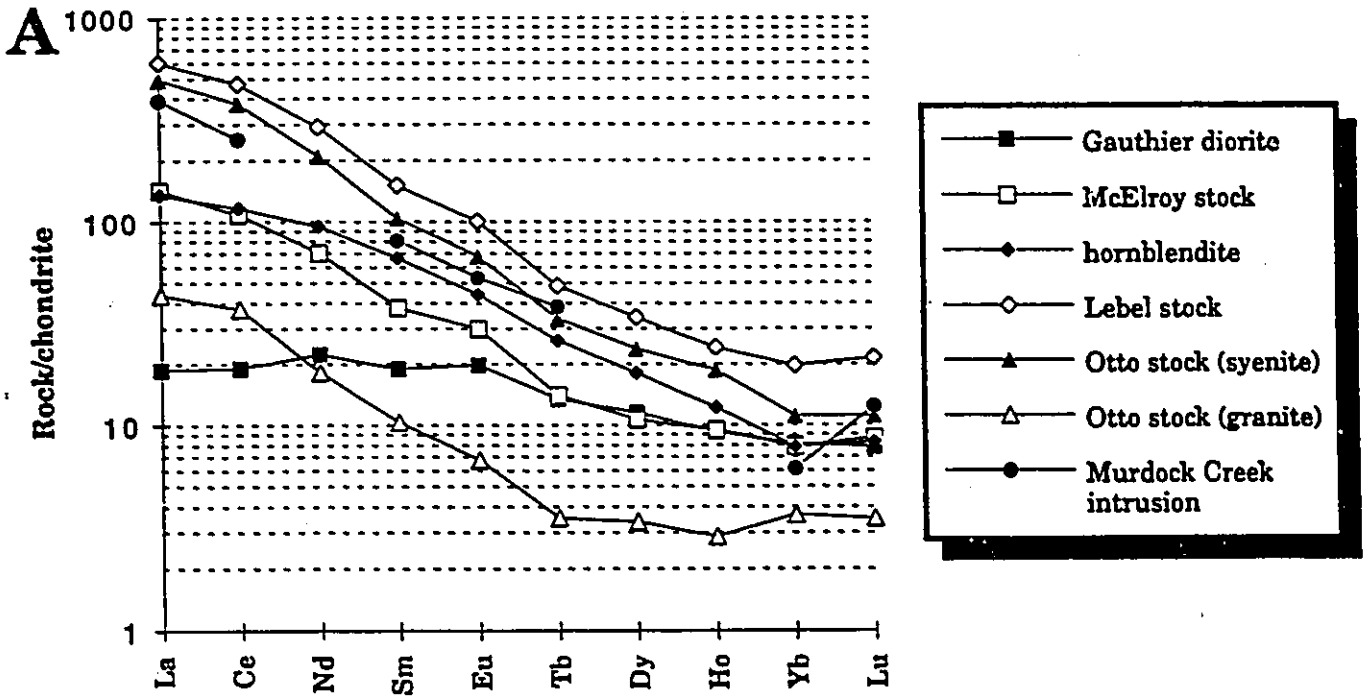
A
1000
100
10
1
Rock/chondrite
La
Ce
Nd
Sm
Eu
Tb
Dy
Ho
Yb
Lu
Gauthier diorite
McElroy stock
hornblendite
Lebel stock
Otto stock (syenite)
Otto stock (granite)
Murdock Creek intrusion

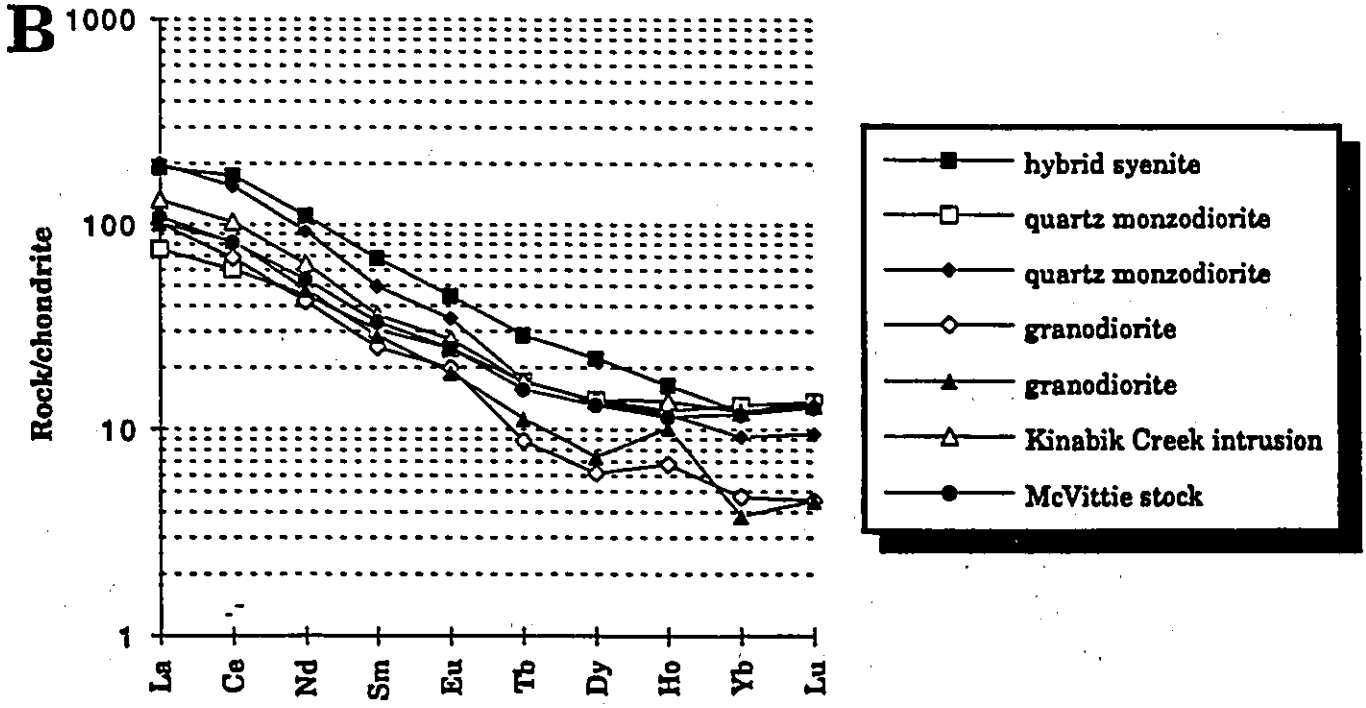
B
1000
100
10
1
Rock/chondrite
La
Ce
Nd
Sm
Eu
Tb
Dy
Ho
Yb
Lu
hybrid syenite
quartz monzodiorite
quartz monzodiorite
granodiorite
granodiorite
Kinabik Creek intrusion
McVittie stock

The Otto stock is the only intrusion in domain 3 containing both syenitic and granitic units. Thus, it also exhibits the widest ranges for LREE enrichment (15 to 800X chondrite), HREE enrichment (2 to 15X chondrite), with syenitic rocks at the upper limit and granitic rocks at the lower limit (Sutcliffe et al., 1990). Syenite REE patterns resemble those of lamprophyres, while granitic REE patterns flatten out between Tb to Lu (Fig. 25A); this trend is indicative of the presence of amphibole in the source region for primary magmas. Lower $(La/Lu)_{ch}$ = 12.5 to 13.8 and $(Sm/Yb)_{ch}$ = 2.8 to 5.6 ratios for the granitic units of the Otto stock also support the presence of amphibole.

The pattern for the Gauthier diorite intrusion is the flattest observed for the rocks of the KLF, and approximates a tholeiitic pattern (Cullers and Graf, 1984a). Furthermore, low $\Sigma REE_{ch}$ (149.5), $(La/Lu)_{ch}$ = 2.4 and $(Sm/Yb)_{ch}$ = 2.3 are all characteristic of tholeiitic basalts and their intrusive equivalents (diabase). The presence of quartz diorite displaying abundant micrographic textures confirms the tholeiitic nature of the Gauthier diorite intrusion. Its relationship to the syenitic and granitic rocks of the Kirkland Lake area remains unclear.

### 3.4.4 Granitic rocks of domains 1 and 2

The granitic rocks of domains 1 and 2 exhibit REE patterns defined by $\Sigma REE$ = 87-197 ppm, LREE enrichment (75 to 110X chondrite) and HREE enrichment (3 to 14X chondrite) (Fig. 25B). These are very similar to the patterns of the syenitic and extrusive rocks of domain 1 (Fig. 25), differing only by their overall lower values and smaller $(La/Lu)_{ch}$ = 5 to 22.4 ratios.

$(Sm/Yb)_{ch}$ = 2.3 to 7.5 ratios are comparable to those of the extrusive rocks of domain 1 and the granitic rocks of domain 3. This explains the intermediate position of the hybrid syenite pattern, between the higher syenitic (Fig. 25) and lower granitic REE patterns; hybrid syenite is the only rock type in domain 1 exhibiting characteristics of both syenitic (clinopyroxene phenocrysts) and granitic (plagioclase phenocrysts) suites. The small positive Eu-anomaly common in the syenitic rocks is present in all the granitic rocks of domains 1 and 2 ($(Eu/Sm)_{ch}$= 0.66 to 0.81) but the hybrid syenite ($(Eu/Sm)_{ch}$= 0.65). Granodiorites from domain 1 and from the Kinabik Creek intrusion exhibit a positive Ho-anomaly commonly observed in the lamprophyres of the KLF. There is a very close correspondence between the REE pattern of andesite (Fig. 24B) and all of the granitic rocks of domain 1. The concave-up shape of HREE for many of the REE patterns, coupled with low ratios ($(La/Lu)_{ch}$= 5.5 to 22.4 in domain 1, 8.5 to 10 in domain 2) and ($(Sm/Yb)_{ch}$= 2.3 to 7.5 in domain 1, 2.8 to 3 in domain 2) , indicate the presence of amphibole as a refractory phase in the source region (Cullers and Graf, 1984b). This evidence seems conflicting, since quartz monzodiorite can contain up to 40 vol.% amphibole.

### 3.4.5 Rare earth elements and the duality of magmatism

REE patterns for all rock types from the Kirkland Lake area share strong similarities even though they span a wide range of silica saturation, from undersaturated nepheline-normative lamprophyres (46 wt.% $SiO_2$) to saturated quartz-phenocryst-bearing hypabyssal granodiorites (68.8 wt.%). Yet, all REE patterns are coherent (Fig. 26). The lone exception is the tholeiitic Gauthier diorite intrusion (Fig. 25A). The following table

summarizes the major similarities and differences between the syenitic and granitic suites, and domains of the Kirkland Lake area.

| rock type | ΣREE$_{ch}$ | (La/Lu)$_{ch}$ | (Eu/Sm)$_{ch}$ | (Sm/Yb)$_{ch}$ |
|---|---|---|---|---|
| **syenitic** | 475-1765 | 11.2-47.6 | 0.64-0.8 | 3.6-19.1 |
| **granitic** | 149.5-593 | 5.6-22.4 | 0.66-1.04 | 2.32-7.5 |
| **Domain 1** | 289-1308 | 5.6-47.6 | 0.64-0.81 | 2.32-19.1 |
| **Domain 2** | 368-433 | 8.5-10 | 0.75-0.76 | 2.8-2.96 |
| **Domain 3** | 149.5-1765 | 2.4-44.7 | 0.65-1.04 | 2.34-16.2 |
| **Range** | 149.5-1765 | 2.4-47.6 | 0.64-1.04 | 2.32-19.1 |

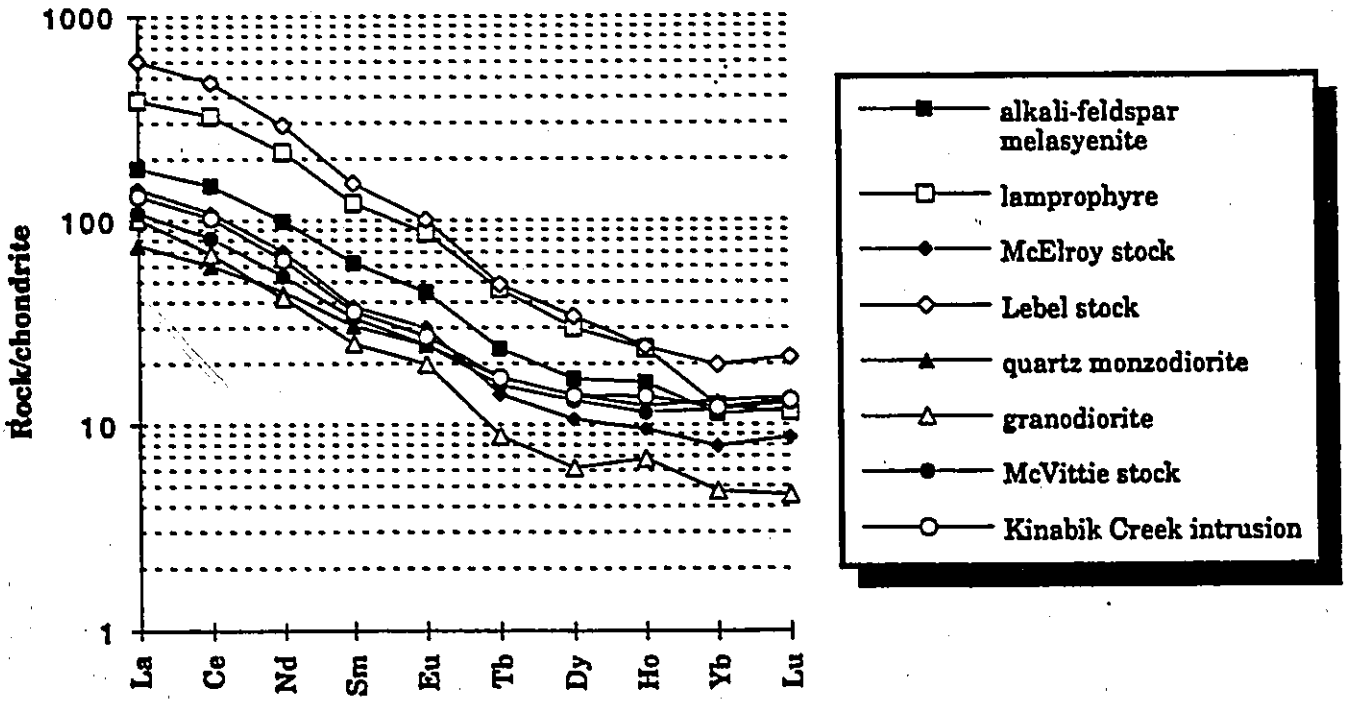


Figure 26. Comparison of REE patterns for syenitic and granitic rocks. All REE patterns are coherent, with syenitic rocks occupying the upper part of the spectrum and granitic rocks, the lower part. The more fractionated granodiorite pattern (relative to quartz monzodiorite) probably occurred as a result of amphibole fractionation.

Syenitic rocks have the highest $\Sigma REE_{ch}$ , $(Sm/Yb)_{ch}$ and $(La/Lu)_{ch}$ ratios, indicating that they are the products of highly fractionated, enriched magmas (Cullers and Graf, 1984a). Granitic rocks have lower total $REE_{ch}$ , $(Sm/Yb)_{ch}$ and $(La/Lu)_{ch}$ ratios which suggest that were produced by less enriched and less fractionated magmas. However, $(Eu/Sm)_{ch}$ ratios are consistently high for both suites (ie. no to slightly positive Eu anomaly). The absence of Eu-anomalies in the rocks of the Kirkland Lake area can be explained by 1) the absence of plagioclase in the source region where the syenitic and granitic magmas were produced, 2) hornblende accumulation in the source region of parental magmas, especially in Precambrian granitic rocks (Cullers and Graf, 1984b) or 3) high oxygen fugacity in the source region. Eu commonly substitutes for Sr and Ca in the plagioclase crystal structure (Hess, 1989). Magmas produced by low degrees of partial melting in the upper mantle where plagioclase is a residual mineral will have negative Eu anomalies (Cullers and Graf, 1984b; Hess, 1989). This would suggest that plagioclase was not present in the source region where the syenitic and granitic magmas of the KLF were generated. Similarly, Eu is preferentially incorporated in the magmas relative to residual amphibole accumulated in the source region (Cullers and Graf, 1984b). This concords with the trough-shaped HREE patterns observed in some of the rocks of the Kirkland Lake area. Thirdly, $Eu^{2+}$ can be converted to $Eu^{3+}$ under highly oxydizing conditions (Hanson, 1980). Under these circumstances, $Eu^{3+}$ cannot substitute for Ca in plagioclase (Hess, 1989). The best explanation for the absence of Eu-anomalies in the rocks of the Kirkland Lake area probably combines all of the three mechanisms described above.

$(Sm/Yb)_{ch}$ ratios are highest in the syenitic rocks of domains 1 and 3, signifying the presence of garnet as a refractory phase in the source region (Hanson, 1980), while lower ratios in granitic rocks of domains 1, 2 and 3 indicate that garnet and amphibole were residual minerals in the source region where these granitic rocks were generated (Martin, 1986). Alternatively, progessive removal of amphibole from the crystallizing magmas can account for the fractionated REE patterns in the granitic rocks (Frey et al., 1978). This interpretation is consistent with the observed HREE depletions in granodiorite (< 5 vol% amphibole) relative to quartz monzodiorite (5 to 40 vol% amphibole) (Fig. 26). The positive Ho-anomaly present in both lamprophyres and granodiorite rocks is significant if it is not produced as a result of analytical error. Ho-anomalies have not been discussed in the literature; they are however present in many REE patterns of syenitic and granitic rocks, including calc-alkaline lamprophyres (Fig 5.6, Rock, 1990). The similarity of REE patterns exhibited by the syenitic and granitic rocks of the Kirkland Lake area confirms the inherent cogenetic nature of the duality of magmatism.

## 3.5 Whole-rock geochemistry

More than twenty different rock types have been identified in the three domains of the Kirkland Lake area. All of these belong to either a syenitic or a granitic suite. This is referred to as the duality of magmatism. These rock types span the spectrum of silica saturation, from undersaturated, one feldspar nepheline-normative syenites and clinopyroxenites, to saturated, two feldspar quartz-normative granodiorites and granites. The clinopyroxenite and quartz diorite units of the Gauthier

diorite intrusion are tholeiitic in nature and do not necessarily belong to either suite. A total of one hundred and thirty-four analyses from this study (seventy-two) and others were used in the characterization of the whole rock geochemistry of the duality of magmatism.

Table 1 contains CIPW normative mineral calculations for twenty-five representative samples of the Kirkland Lake area. In domain 1, the syenitic units (alkali-feldspar melasyenite, alkali-feldspar syenite, lamprophyre) are all nepheline- and olivine-normative, while the hybrid syenite is neither nepheline- nor quartz-normative; these rocks are subaluminous to metaluminous, which accounts for the predominance of clinopyroxene. All granitic units (quartz monzdiorite and granodiorite) are quartz-normative. The granitic rocks of domain 1 are metaluminous to peraluminous, which explains the predominance of amphibole and biotite over clinopyroxene in these rocks. The Timiskaming Group volcanic rocks range from nepheline-normative (leucite trachyte and felsic trachyte) to neither nepheline- nor quartz-normative (mafic amphibole trachyte and andesite), to quartz-normative (felsic and mafic clinopyroxene trachyte). Accordingly, these volcanic rocks are usually metaluminous to slightly peraluminous.

In domain 2, as expected, all samples from the McVittie stock and the Beaverhouse Lake, Monocle Lake and Kinabik Creek intrusions (quartz monzodiorite and granodiorite) are quartz-normative. The McVittie stock also contains corundum in the norm, indicating excess alumina over that required for the feldspars; this excess may appear as mica (sericite) in the rock. As in domain 1, these rocks are metaluminous to peraluminous.

Table 1. CIPW normative mineralogy of representative rock types. Syenitic rocks are predominantly nepheline and olivine normative; one sample contains leucite (Lc) in the norm. Granitic rocks are quartz normative; one sample contains corundum (C) in the norm. Abbreviations for the units are as follows: AFMS = alkali-feldspar melasyenite, AFS = alkali-feldpar syenite, HS = hybrid syenite, LAMP = lamprophyre (D1 = domain 1, D3 = domain 3), FTRACH = felsic trachyte, MTRACH= mafic trachyte, MELAMONZ= melamonzonite, AMPHTRACH = amphibole trachyte, QMD = quartz monzodiorite, GRD = granodiorite, MLI = Monocle Lake intrusion, KCI = Kinabik Creek intrusion, McVS = McVittie stock, OS = Otto stock, LS = Lebel stock, McES =McElroy stock, HBLITE = hornblendite,

| sample # | LC-1 | GL8857 | GL8858 | GL90016 | GL89020 | GL90141 | GL90091 | GL90099 | GL90202 | GL90038 | GL89037 | GL90192 | GL90165 |
|---|---|---|---|---|---|---|---|---|---|---|---|---|---|
| description | ARMS | AFS | HS | LAMP D1 | LAMP D3 | ANDESITE | FTRACH | MTRACH | MELAMONZ | AMPHTRACH | CMD | CMD | CPD |
| SiO2 | 48,31 | 50,61 | 50,62 | 45,88 | 46,79 | 53,35 | 57,68 | 47,47 | 49,67 | 49,52 | 54,94 | 59,00 | 63,64 |
| TiO2 | 0,59 | 0,48 | 0,66 | 0,58 | 0,60 | 0,40 | 0,34 | 0,60 | 0,55 | 0,61 | 0,56 | 0,29 | 0,14 |
| Al2O3 | 14,32 | 16,22 | 17,65 | 12,53 | 13,10 | 17,73 | 17,13 | 17,98 | 10,32 | 16,71 | 16,69 | 16,05 | 17,07 |
| Fe2O3 | 2,27 | 1,82 | 2,50 | 2,45 | 1,80 | 1,67 | 1,85 | 2,70 | 2,03 | 3,17 | 1,69 | 0,78 | 0,49 |
| FeO | 4,17 | 2,42 | 4,28 | 3,93 | 5,17 | 3,24 | 1,97 | 3,42 | 4,03 | 3,68 | 3,76 | 2,04 | 0,85 |
| MnO | 0,11 | 0,08 | 0,12 | 0,11 | 0,16 | 0,09 | 0,07 | 0,12 | 0,15 | 0,14 | 0,10 | 0,06 | 0,02 |
| MgO | 10,78 | 4,67 | 6,39 | 15,99 | 13,84 | 5,34 | 4,80 | 5,72 | 11,95 | 8,16 | 6,61 | 4,26 | 1,58 |
| CaO | 7,58 | 5,47 | 4,49 | 10,06 | 8,11 | 3,26 | 3,83 | 7,46 | 12,79 | 6,56 | 6,66 | 3,28 | 1,73 |
| Na2O | 5,30 | 6,62 | 7,54 | 2,97 | 7,69 | 12,88 | 7,81 | 6,31 | 5,04 | 5,76 | 7,27 | 9,65 | 10,91 |
| K2O | 6,12 | 7,15 | 5,33 | 4,91 | 2,45 | 1,77 | 4,50 | 5,75 | 3,10 | 5,38 | 1,47 | 4,36 | 3,49 |
| P2O5 | 0,45 | 0,29 | 0,42 | 0,59 | 0,47 | 0,25 | 0,24 | 0,46 | 0,29 | 0,29 | 0,21 | 0,23 | 0,09 |
| Ap | 1,25 | 0,77 | 1,14 | 1,61 | 1,28 | 0,70 | 0,64 | 1,21 | 0,77 | 0,79 | 0,59 | 0,64 | 0,24 |
| Il | 1,58 | 1,22 | 1,77 | 1,52 | 1,58 | 1,09 | 0,88 | 1,52 | 1,45 | 1,62 | 1,52 | 0,76 | 0,36 |
| Mt | 4,65 | 3,63 | 5,09 | 4,94 | 3,20 | 3,49 | 3,63 | 5,23 | 4,07 | 6,39 | 3,49 | 1,60 | 1,02 |
| Or | 30,06 | 34,26 | 26,06 | 23,74 | 11,75 | 8,86 | 21,21 | 28,70 | 15,29 | 25,99 | 7,27 | 21,51 | 17,55 |
| Ab | 16,31 | 22,01 | 34,70 | 9,78 | 25,13 | 60,92 | 34,70 | 15,85 | 19,98 | 26,23 | 33,85 | 44,86 | 51,62 |
| An | 7,15 | 5,88 | 11,69 | 11,23 | 7,10 | 7,73 | 11,38 | 9,10 | 5,06 | 13,47 | 19,62 | 5,02 | 6,89 |
| Di | 21,16 | 14,51 | 5,58 | 25,90 | 22,51 | 5,40 | 3,06 | 17,66 | 43,33 | 12,68 | 9,42 | 7,48 | 1,03 |
| Hy | | | 2,64 | | | 2,38 | 6,44 | | | 2,62 | 12,97 | 7,26 | 3,53 |
| Ol | 10,80 | 2,68 | 8,50 | 14,83 | 15,92 | 7,04 | | 3,34 | 4,34 | 6,70 | | | |
| Ne | 4,45 | 9,15 | | 2,03 | 5,17 | | | 11,12 | 1,55 | | 9,99 | 7,84 | 16,76 |
| C | | | | | | | 9,70 | | | | | | |
| Q | | | | | | | | | | | | | |

| sample # | GL90211 | GL90215 | GL89006 | GL89017 | GL89XX | GL89025 | GL89029 | GL89030 | SMR07 | SMR24 | GL8854 | GL90089 |
|---|---|---|---|---|---|---|---|---|---|---|---|---|
| description | MLI | KCI | McVS | OS CPXITE | OS SYENITE | OS GRANITE | LS AFMS | LS AFS | McES DIORITE | McES GM | HBLITE | Gauthier cpxt |
| SiO2 | 61,24 | 61,24 | 62,67 | 41,71 | 52,24 | 60,21 | 42,54 | 51,12 | 46,05 | 55,47 | 46,29 | 49,30 |
| TiO2 | 0,28 | 0,27 | 0,27 | 0,90 | 0,47 | 0,30 | 1,09 | 0,58 | 0,68 | 0,36 | 0,58 | 0,74 |
| Al2O3 | 17,09 | 16,69 | 17,21 | 6,17 | 15,97 | 15,85 | 8,17 | 14,20 | 17,36 | 16,89 | 11,85 | 6,74 |
| Fe2O3 | 1,19 | 0,14 | 1,19 | 4,38 | 2,67 | 0,56 | 4,64 | 2,64 | 3,25 | 1,85 | 2,00 | 1,75 |
| FeO | 1,63 | 2,57 | 1,24 | 6,25 | 2,50 | 2,09 | 6,19 | 3,01 | 4,31 | 1,75 | 4,60 | 7,76 |
| MnO | 0,06 | 0,06 | 0,04 | 0,23 | 0,09 | 0,06 | 0,27 | 0,15 | 0,14 | 0,08 | 0,11 | 0,16 |
| MgO | 3,13 | 3,77 | 2,43 | 16,34 | 5,70 | 3,40 | 14,72 | 7,06 | 10,19 | 3,38 | 16,55 | 17,18 |
| CaO | 2,83 | 3,51 | 1,66 | 16,94 | 5,41 | 3,04 | 13,53 | 8,04 | 9,35 | 4,57 | 10,16 | 12,67 |
| Na2O | 5,83 | 10,47 | 10,82 | 2,26 | 7,25 | 9,69 | 4,05 | 6,44 | 6,55 | 9,89 | 4,05 | 3,19 |
| K2O | 3,57 | 0,94 | 2,34 | 3,19 | 7,22 | 4,38 | 3,68 | 6,15 | 1,78 | 3,59 | 3,35 | 0,23 |
| P2O5 | 0,16 | 0,15 | 0,13 | 1,63 | 0,48 | 0,20 | 1,10 | 0,62 | 0,34 | 0,18 | 0,45 | 0,05 |
| Ap | 0,44 | 0,42 | 0,37 | 4,36 | 1,34 | 0,57 | 3,01 | 1,69 | 0,95 | 0,51 | 1,23 | 0,13 |
| Il | 0,76 | 0,72 | 0,74 | 2,38 | 1,28 | 0,82 | 2,89 | 1,54 | 1,85 | 0,99 | 1,56 | 1,94 |
| Mt | 2,47 | 0,29 | 2,47 | 6,73 | 5,52 | 1,16 | 9,45 | 5,38 | 6,68 | 3,92 | 4,07 | 3,49 |
| Or | 17,78 | 4,67 | 11,64 | 8,03 | 35,81 | 21,66 | 17,96 | 30,01 | 8,80 | 16,26 | 16,35 | 1,12 |
| Ab | 41,47 | 49,08 | 50,77 | | 29,89 | 46,55 | 2,07 | 25,70 | 29,23 | 47,39 | 16,36 | 14,37 |
| An | 11,68 | 13,65 | 7,17 | 1,73 | 3,71 | 3,95 | 1,06 | 3,94 | 22,27 | 13,76 | 10,86 | 7,90 |
| Di | 0,89 | 2,11 | | 52,97 | 15,17 | 7,76 | 44,76 | 24,15 | 16,83 | 6,33 | 27,99 | 43,11 |
| Hy | 7,11 | 11,12 | 5,33 | | | 6,07 | | | | 4,52 | | 23,09 |
| Ol | | | | 7,64 | 3,49 | | 8,40 | 2,81 | 10,68 | | 16,55 | |
| Ne | | | | 5,50 | 2,15 | | 8,96 | 2,12 | 0,66 | | 1,21 | |
| C | | | 1,07 | | | | | | | 4,53 | | 1,11 |
| Q | 16,37 | 16,10 | 16,83 | | | 9,63 | | | | | | |
| Lc | | | | 5,66 | | | | | | | | |

The intrusions of domain 3 can be categorized as follows: syenitic composite intrusions (Lebel stock and Murdock Creek intrusion), granitic composite intrusions (McElroy stock) and syenitic to granitic composite intrusions (Otto stock). The Gauthier diorite intrusion is composed of clinopyroxenite and quartz diorite and should be classified as a tholeiitic intrusion; its relation to the duality of magmatism is unclear. The syenitic composite intrusions are all nepheline- and olivine-normative. These undersaturated intrusions are subaluminous to metaluminous. The composite granitic McElroy stock is predominantly quartz-normative, except in the diorite samples which are very slightly nepheline-normative. The intrusion is peraluminous. For the tholeiitic Gauthier diorite intrusion, the clinopyroxenite unit contains hypersthene and diopside in the norm, and the more felsic quartz diorite unit contains olivine, and is metaluminous. The Otto stock is the only intrusion containing both syenitic and granitic units. Accordingly, normative mineralogy is varied. The most undersaturated units are both leucite- and nepheline-normative and are either peralkaline or subaluminous. The granitic units, which are nearly identical in texture and composition to the granitic rocks of domain 1, are quartz-normative and metaluminous to peraluminous. One unit , quartz syenite, contains sodic amphibole and is therefore peralkaline.

The following tables summarize the geochemical features observed in the syenitic and granitic suites of the Kirkland Lake area. They will be used to characterize and classify the rock types, in order to make interpretations on the origin, evolution and tectonic setting in the following chapter. Murdock Creek rocks have been studied in detail by Rowins et al. (1991, 1993), and have not been included in the tables. These rocks have been

described as shoshonitic, and in a few instances, as ultrapotassic (Rowins, 1993).

**Syenitic rocks ;**

| rock type | afms | afs | hs | lamp | Tvr | QS | LS | hsm |
|---|---|---|---|---|---|---|---|---|
| SiO2 range | 48.9-52.6 | 52.6-57 | 53.4 | 42.1-50.7 | 46.5-59.5 | 43-70.9 | 44.8-57.2 | 48.8-49.6 |
| Na2O+K2O | 7.58-9.46 | 10.4-11.7 | 8.51 | 3.73-8.48 | 5.29-10.8 | 2.12-12.1 | 5.24-8.66 | 4.44-4.97 |
| K2O/Na2O | 0.54-2.03 | 1.26-1.74 | 1.07 | 0.49-3.62 | 0.19-7.31 | 0.42-2.93 | 1.01-1.73 | 1.26-2.77 |
| K2Owt.% | 5.73-6.27 | 5.8-7.41 | 4.41 | 1.99-4.02 | 0.29-9.64 | 0.63-6.5 | 3.04-5.35 | 2.77-3.24 |
| Fe2O3/FeT | 0.36-0.43 | 0.27-0.45 | 0.39 | 0.22-0.73 | 0.21-0.83 | 0.23-0.73 | 0.34-0.49 | 0.29-0.33 |
| TiO2wt.% | 0.82-1.22 | 0.64-1.9 | 0.93 | 0.74-1.02 | 0.21-1.07 | 0.09-1.52 | 0.66-1.52 | 0.82-0.84 |
| Al2O3wt.% | 12.5-16.4 | 16-18.3 | 15.8 | 9.7-12 | 9.1-24.17 | 5.4-17.26 | 7.3-14.5 | 9.5-10.6 |
| Fe/(Fe+Mg) | 0.39-0.54 | 0.48-0.72 | 0.54 | 0.26-0.44 | 0.27-0.71 | 0.32-0.52 | 0.43-0.46 | 0.33-0.34 |
| Zr/Y | 6.0-7.5 | 10.56 | 7.27 | 5.91-10.0 | 3.88-13.5 | 2.39-20.1 | 3.5-9.44 | 2.36-4.0 |
| Rb/Sr | 0.11-0.33 | 0.17 | 0.07 | 0.04-0.20 | 0.02-0.40 | 0.03-0.30 | 0.07-0.36 | 0.09-0.13 |
| Ni ppm | 68-121 | 27 | 10 | 66-330 | 0-120 | 4-212 | 4-73 | 140-160 |
| Cr ppm | 250-366 | 100 | 55 | 91-890 | 0-460 | 9-1045 | 87-180 | 560-710 |

**Granitic and tholeiitic rocks :**

| rock type | qmd | grd | McVS | MLI | KCI | McFS | GDI |
|---|---|---|---|---|---|---|---|
| SiO2 range | 58.6-65.3 | 65.0-69.4 | 67.4 | 61-65.9 | 61.0 | 48.8-60.9 | 49.2-57.3 |
| Na2O+K2O | 5.23-9.02 | 8.78-9.26 | 7.97 | 7.91-9.7 | 6.59 | 4.97-8.69 | 1.65-6.41 |
| K2O/Na2O | 0.31-0.87 | 0.43-0.71 | 0.33 | 0.02-0.61 | 0.14 | 0.21-0.53 | 0.11-0.56 |
| K2O wt.% | 1.23-4.12 | 2.78-3.75 | 1.97 | 0.2-3.01 | 0.79 | 1.47-3.09 | 0.19-2.31 |
| Fe2O3/Fe(T) | 0.24-0.54 | 0.35-0.50 | 0.52 | 0.11-0.45 | 0.06 | 0.45-0.54 | 0.20-0.30 |
| TiO2 wt.% | 0.33-0.80 | 0.19-0.42 | 0.39 | 0.4-0.51 | 0.38 | 0.52-0.97 | 0.67-1.02 |
| Al2O3 wt.% | 13.9-15.2 | 14.9-16.0 | 15.7 | 15.6-19.5 | 15.4 | 15.7-17.6 | 5.7-16.5 |
| FeO/FeO+MgO) | 0.39-0.58 | 0.43-0.60 | 0.48 | 0.48-0.56 | 0.55 | 0.33-0.40 | 0.45-0.56 |
| Zr/Y | 3.52-15 | 9.41-19.4 | 10.59 | 8.5-11.76 | 6.32 | 2.8-13.1 | 4.67-6.88 |
| Rb/Sr | 0.04-0.17 | 0.01-0.15 | 0.04 | 0.02-0.07 | 0.02 | 0.03-0.07 | 0.05-0.06 |
| Ni ppm | 17-110 | 2-36 | 12 | 10-32 | 45 | 21-52 | 16-230 |
| Cr ppm | 50-210 | 37-91 | 42 | 55-64 | 77 | 45-180 | 26-1300 |

Syenitic rocks are characterized by higher $K_2O/Na_2O$, Rb/Sr, $K_2O$, $TiO_2$, Ni and Cr, and lower $SiO_2$ and Zr/Y relative to the granitic rocks. $Fe_2O_3/Fe(T)$, $Al_2O_3$ and FeO/(FeO+MgO) remain constant throughout the rocks of the Kirkland Lake area. The high Cr and Ni values, notably in the lamprophyre, Otto stock, hornblendite and Gauthier Diorite intrusion, indicate that these rocks were derived from parental magmas originating in the mantle (Wilson, 1989). $K_2O + Na_2O$ values are also fairly constant in both suites of rocks. Syenitic rocks have $Fe_2O_3/ Fe_2O_3+FeO$ ratios that gradually increase from 0.30 to 0.50 with increasing $SiO_2$; granitic rocks of domain 1 have similar ratios. The granitic rocks of domain 2 have widely ranging ratios: in the least-altered samples, such as the Kinabik Creek intrusion, the ratios are about 0.05, while in the more altered (e.g. hematitized) samples, such as the McVittie stock, it varies between 0.45 and 0.50. The lowest FeO/(FeO+MgO) ratios are found in the mafic marginal units of the syenitic intrusions of domain 3 (Fig. 27A). Ratios that exceed 0.70 are from altered rocks from the Timiskaming Group volcanic rocks and the granitic rocks of domain 2, and probably reflect postmagmatic alteration (hematitization). The ratio does not vary significantly with differentiation (Fig. 27A). The high ratios for the granitic rocks of domain 2 are largely controlled by amphibole and magnetite crystallization.

Granitic rocks have higher Zr/Y ratios than syenitic rocks (Fig. 27B). The presence of zircon crystals and the scarcity of apatite (which accomodates Y) in the granitic rocks ($P_2O_5 < 0.4$ wt.%) explain why these ratios are higher in granitic rocks compared to syenitic rocks. The high Zr/Y ratios for syenitic and granitic rocks are a further indication that garnet was present in the source region where parental magmas were

Figure 27. A) FeO/FeO+MgO versus Larsen index. The ratio does not vary significantly with differentiation. It is lowest in the mafic marginal units of syenitic intrusion of domain 3, and highest in the granitic rocks of domain 2. The high ratios observed for the granitic rocks of domain 2 are controlled by amphibole and magnetite crystallization. B) Zr/Y versus Larsen Index. Granitic rocks have higher ratios than syenitic rocks. The lowest ratios come from the rocks of the mafic margins of the Otto stock and Murdock Creek intrusion, which contain the most apatite into which Y is concentrated. Highest ratios are in the granitic rocks where zircon is present and apatite is absent. These ratios suggest the presence of garnet as a refractory phase in the source region.
Larsen index = $0.33*SiO_2 + K_2O - MgO - FeO - CaO$.

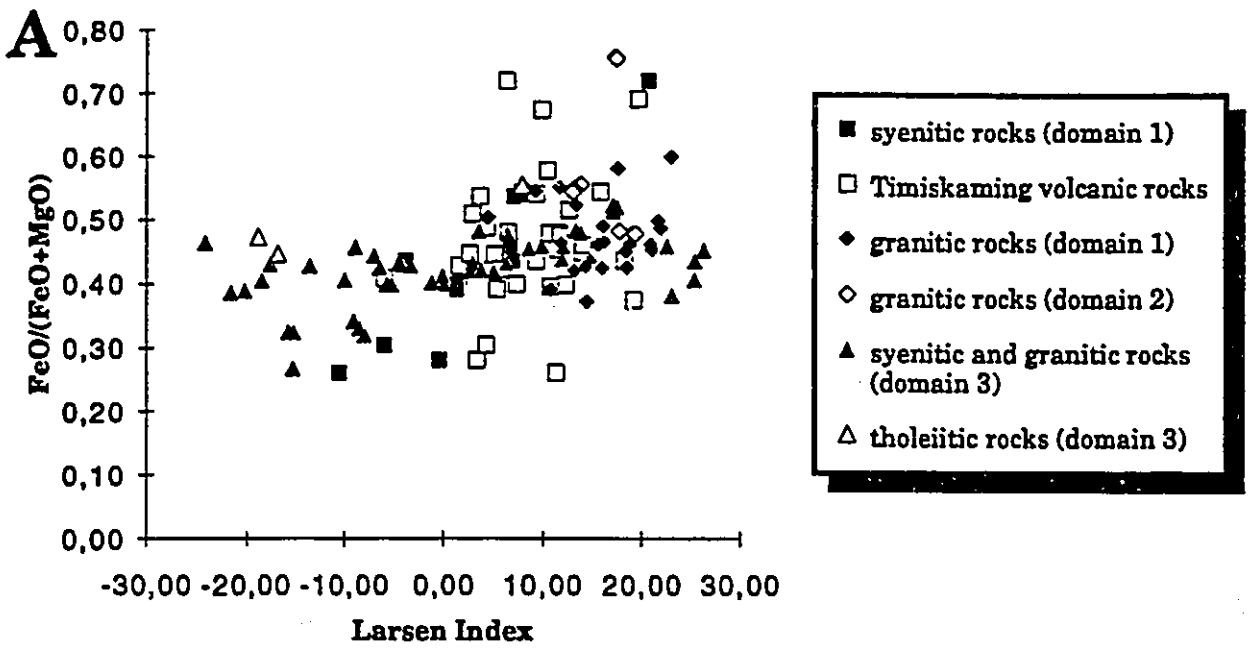
A
0,80
0,70
0,60
0,50
0,40
0,30
0,20
0,10
0,00
FeO/(FeO+MgO)
-30,00 -20,00 -10,00 0,00 10,00 20,00 30,00
Larsen Index
syenitic rocks (domain 1)
Timiskaming volcanic rocks
granitic rocks (domain 1)
granitic rocks (domain 2)
syenitic and granitic rocks (domain 3)
tholeiitic rocks (domain 3)

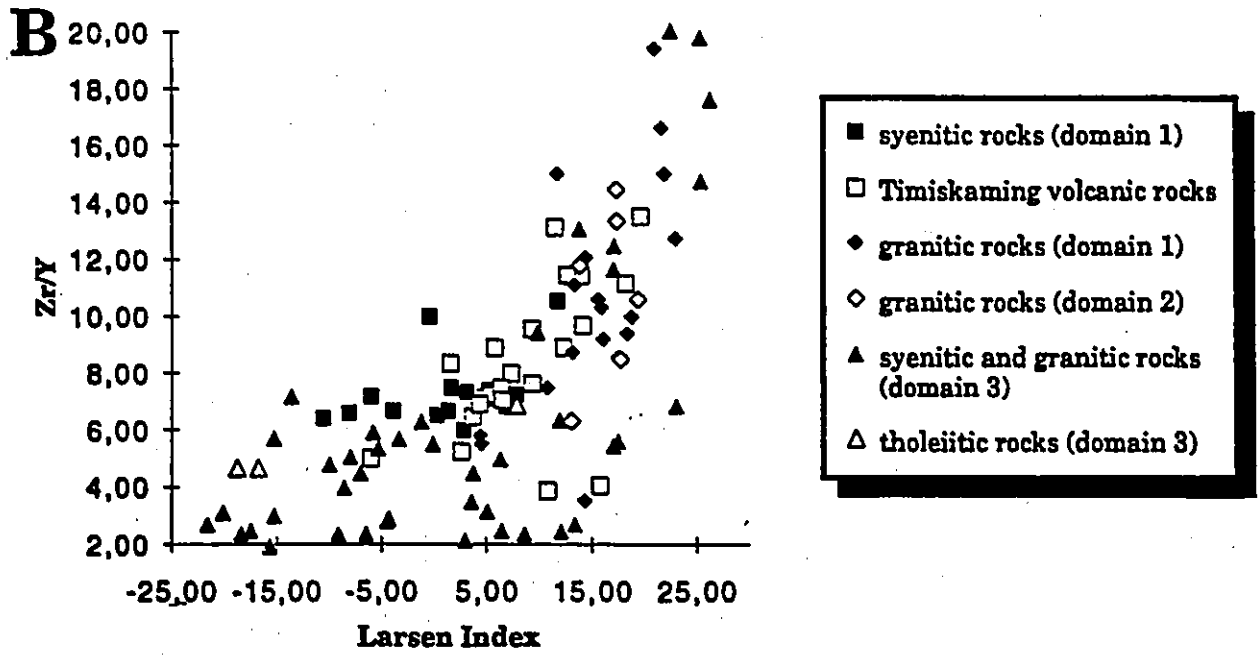
B
20,00
18,00
16,00
14,00
12,00
10,00
8,00
6,00
4,00
2,00
Zr/Y
-25,00 -15,00 -5,00 5,00 15,00 25,00
Larsen Index
syenitic rocks (domain 1)
Timiskaming volcanic rocks
granitic rocks (domain 1)
granitic rocks (domain 2)
syenitic and granitic rocks (domain 3)
tholeiitic rocks (domain 3)

formed, as did the high $(La/Lu)_{ch}$ and $(Sm/Yb)_{ch}$ ratios described in section 3.4. The lower Zr/Y ratios of the syenitic rocks fall in the range of rocks formed by continental magmatism (Ujike, 1985), although one sample from the Otto stock has abundant zircon (A13 , Ben Othman, 1990), uncommon for the syenitic rocks of the Kirkland Lake area. The high Rb/Sr ratios of the syenitic rocks occur as a result of the predominance of K-feldspar and biotite, in which Rb substitutes for K ; conversely, the lower ratios in granitic rocks can be explained by the dominance of plagioclase, in which Sr is accomodated, over K-feldspar in granitic rocks (Wilson, 1989). Thus, major and trace element geochemistry of the duality of magmatism reflects the mineralogical differences between both suites of rocks.

The duality of magmatism observed in the Kirkland Lake area can be illustrated by three different diagrams (Fig 28A, B, C). In the first diagram, the dividing line between alkaline and subalkaline fields is after MacDonald and Katsura (1964); the syenitic rocks fall above this line in the alkaline field, while granitic and tholeiitic rocks fall below, in the subalkaline or calc-alkaline field (Fig. 28A). The second diagram (Fig. 28B), from Wheller et al. (1987), divides shoshonitic rocks (above the line) and calc-alkaline rocks (below). The majority of Timiskaming volcanic rocks are classified as alkaline in Figure 28A, but in this diagram, about one-third of all Timiskaming rocks fall in the calc-alkaline field. This feature reflects the sodic nature of the more evolved volcanic rocks (soda trachyte of Cooke and Moorhouse, 1969). In the third diagram (Fig. 28C), half of the volcanic rocks of the Timiskaming Group fall in the calc-alkaline field, confirming their sodic nature and less syenitic rocks fall in the shoshonite field (dividing line after Morrison, 1980).

Figure 28. Major element alkaline/calc-alkaline classification diagrams. A) The classic diagram from MacDonald and Katsura (1964). All syenitic rocks fall above the dividing line (alkaline field), while granitic and tholeiitic rocks fall below (calc-alkaline field). B) The shoshonitic-calc-alkaline diagram from Wheller et al. (1987). As in the first diagram, most syenitic rocks fall in the shoshonitic field (above the line) and granitic and tholeiitic rocks fall below. Note that about one-third of Timiskaming volcanic rocks fall in the calc-alkaline field, compared to one-tenth in the first diagram. C) In this diagram, even less syenitic rocks fall in the upper shoshonite field (dividing line after Morrison, 1980). Half of all Timiskaming Group volcanic rocks fall below the dividing line in the calc-alkaline field. D) The total alkali-silica diagram of Le Bas et al. (1986). Most rocks fall in the trachybasalt to trachyandesite suite; one sample is an andesite, while pseudoleucite rocks fall in the tephrite basanite and phonotephrite fields. Fields (sodic equivalents in parentheses) : 1= trachybasalt (hawaiite), 2= basaltic trachyandesite (mugearite), 3= trachyandesite (benmoreite), 4= andesite, 5= tephrite basanite, 6= phonotephrite.

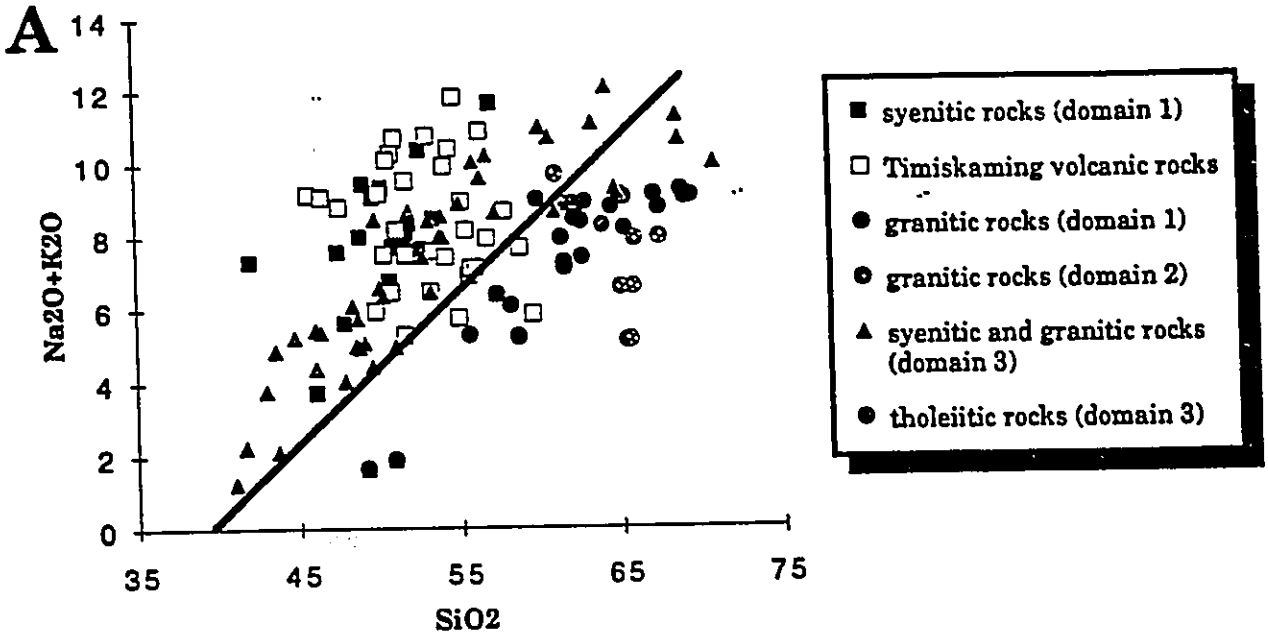
A
14
12
10
8
6
4
2
0
Na2O+K2O
35
45
55
65
75
SiO2
syenitic rocks (domain 1)
Timiskaming volcanic rocks
granitic rocks (domain 1)
granitic rocks (domain 2)
syenitic and granitic rocks (domain 3)
tholeiitic rocks (domain 3)

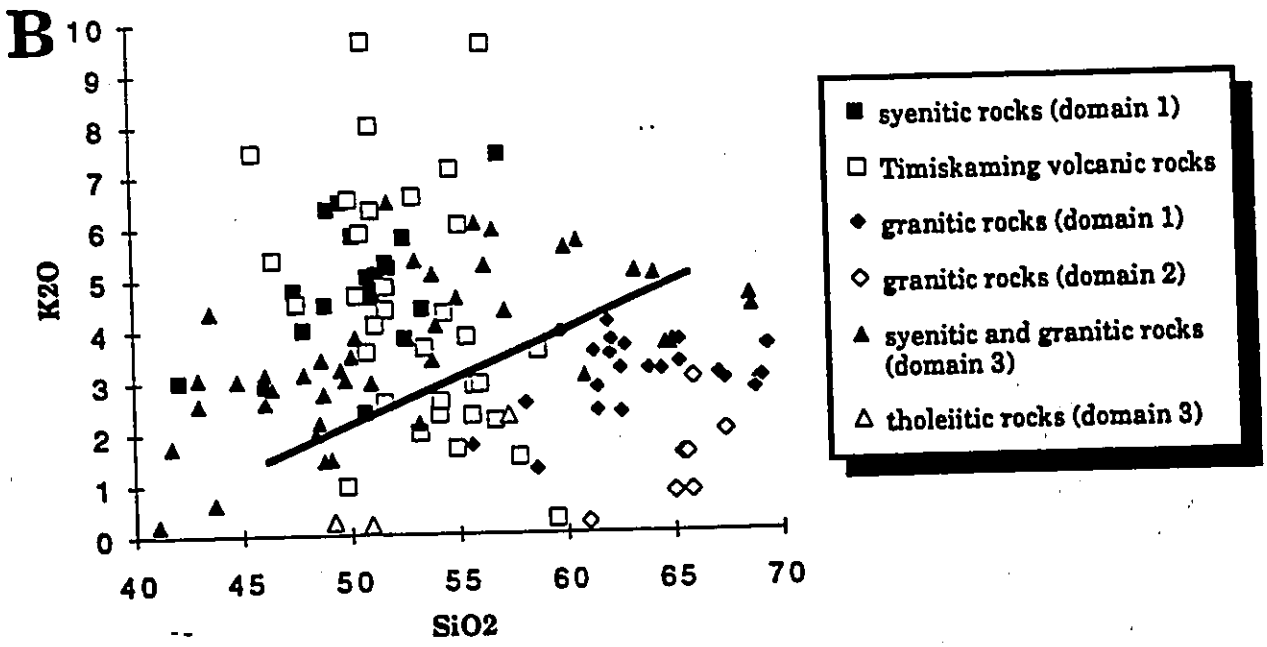
B
10
9
8
7
6
5
4
3
2
1
0
K2O
40
45
50
55
60
65
70
SiO2
syenitic rocks (domain 1)
Timiskaming volcanic rocks
granitic rocks (domain 1)
granitic rocks (domain 2)
syenitic and granitic rocks (domain 3)
tholeiitic rocks (domain 3)

C

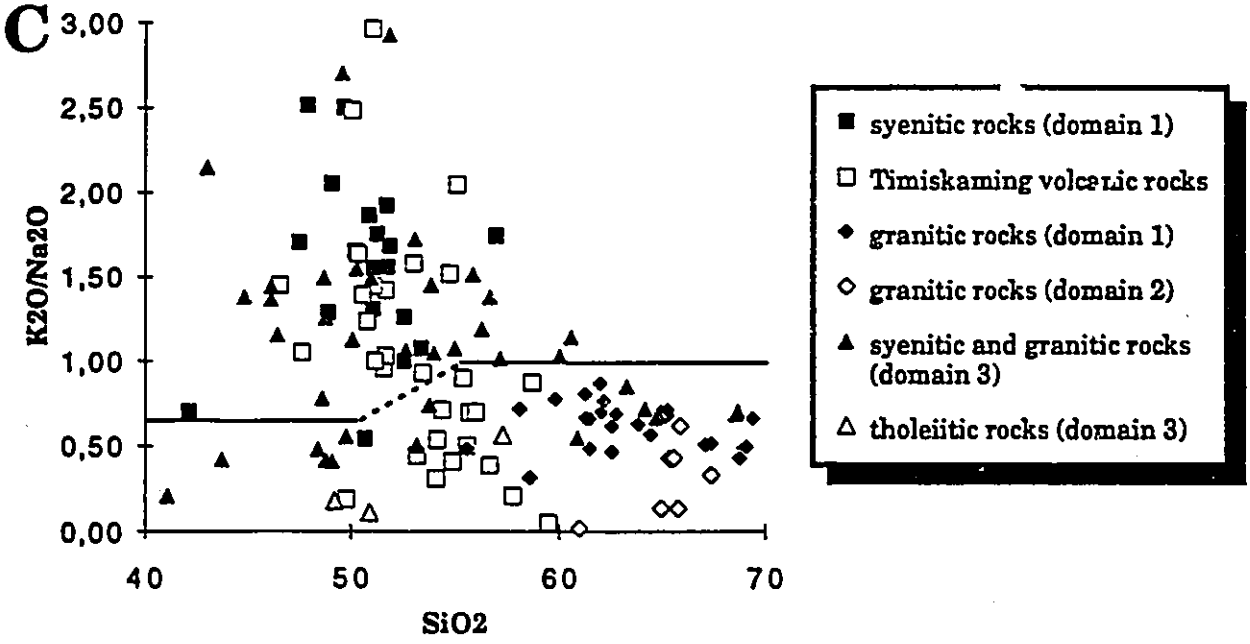
3,00
2,50
2,00
1,50
1,00
0,50
0,00
K2O/Na2O
40
50
60
70
SiO2
syenitic rocks (domain 1)
Timiskaming volcanic rocks
granitic rocks (domain 1)
granitic rocks (domain 2)
syenitic and granitic rocks (domain 3)
tholeiitic rocks (domain 3)

D

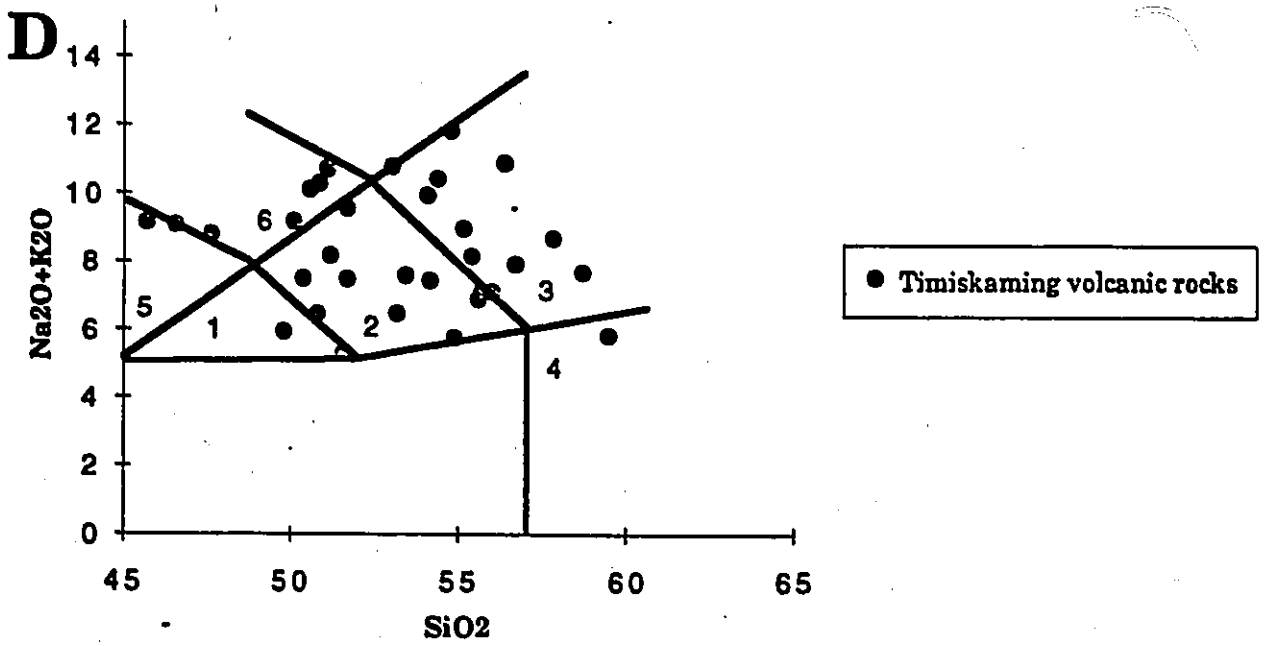
14
12
10
8
6
4
2
0
Na2O+K2O
45
50
55
60
65
SiO2
1
2
3
4
5
6
Timiskaming volcanic rocks

Nevertheless, all three diagrams are in general agreement in discriminating alkaline from calc-alkaline rocks. Figure 28D presents the widely-used classification diagram of volcanic rocks after LeBas et al. (1986). The rocks fall mainly in the trachybasalt to trachyandesite group (fields 1 to 3) and are more appropriately named hawaiite, mugearite and benmoreite, when they are more sodic (Irvine and Baragar, 1971). One sample falls in the andesite field and the pseudoleucite-bearing rocks fall in the tephrite basanite to phonotephrite fields.

All major elements display a compositional continuity between the syenitic and granitic suite. This is demonstrated on diagrams where major elements are plotted versus the Larsen differentiation index, which is defined by the following formula: L.I. = $0.33*SiO_2 + K_2O - MgO - FeO - CaO$ (Fig. 29). FeO decreases steadily with differentiation (Fig. 29), with the highest content found in the Gauthier diorite intrusion and the mafic marginal units of the composite syenite intrusions of domain 3. The lowest content is found in the granitic rocks of domains 1 and 2 and the quartz-bearing extrusive rocks of domain 1. $Fe_2O_3$ presents a slightly different decreasing trend (Fig 29B). As expected for rocks that evolved under oxidizing conditions, contents are less variable than for FeO and are in fact fairly constant with differentiation, at about 2 to 4 wt.%, suggesting that a fixed proportion of $Fe^{2+}$ was transformed to Fe . Consequently, oxidizing conditions would have been nearly constant throughout the formation of these rocks; this is agreement with the findings of Rowins et al. (1991) who suggest that oxidizing conditions were constant at $f_{O_2} \approx 10^{-12}$ bars throughout the evolution of the Murdock Creek intrusion. Less evolved rocks of domain 3 have the highest content of $Fe_2O_3$ (up to 7 wt.%) and the

Figure 29. Major elements versus Larsen index. All diagrams produce smooth continuous linear trends: FeO (A), $Fe_2O_3$ (B), MgO (C), CaO (D) and $TiO_2$ (E) all decrease with differentiation, while $Al_2O_3$ (F) increase. Note that the trend displayed by $Fe_2O_3$ is less regular than the others; the majority of samples fall between 2 and 4 wt.% $Fe_2O_3$ .
Larsen index = $0.33*SiO_2 + K_2O - MgO - FeO - CaO$.

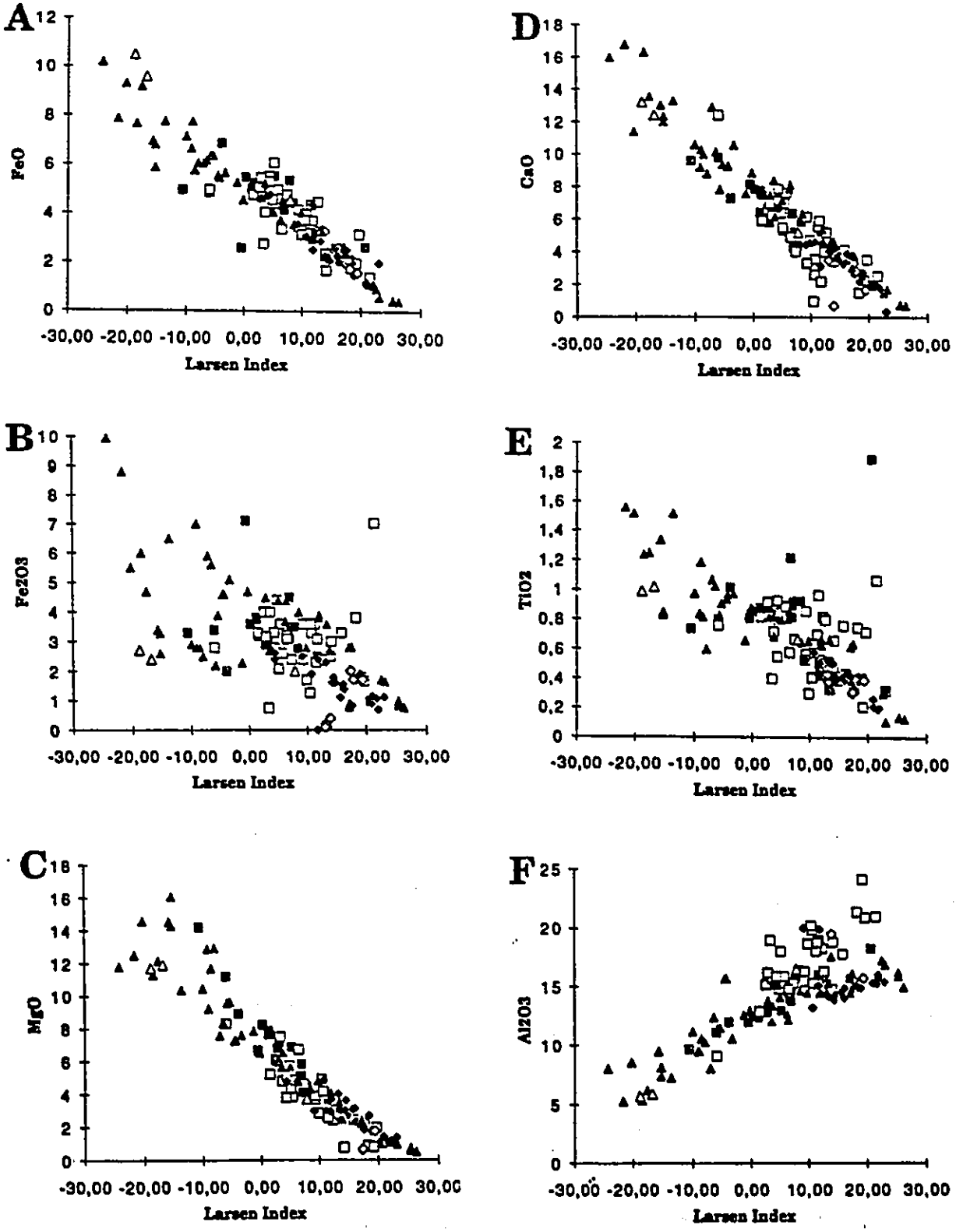
A
FeO
Larsen Index
B
Fe2O3
Larsen Index
C
MgO
Larsen Index
D
CaO
Larsen Index
E
TiO2
Larsen Index
F
Al2O3
Larsen Index
-30,00 -20,00 -10,00 0,00 10,00 20,00 30,00
syenitic rocks (domain 1)
Timiskaming volcanic rocks
granitic rocks (domain 1)
granitic rocks (domain 2)
syenitic and granitic rocks (domain 3)
tholeiitic rocks (domain 3)

granitic rocks of the Kirkland Lake area have the lowest $Fe_2O_3$ content (< 2 wt.%). Some samples may have been subjected to postmagmatic alteration and display anomalous $Fe_2O_3$ values (up to 10 wt.%).

MgO (Fig 29C) and CaO (Fig. 29D) decrease steadily with progressive differentiation, as indicated by increasing values of the Larsen index. These trends reflect continual removal of clinopyroxene (in syenitic rocks) and amphibole (in granitic rocks) from the crystallizing magma. For the Murdock Creek intrusion, Rowins et al. (1993) have demonstrated that clinopyroxene fractionation was the dominant mechanism for ferromagnesian fractionation. Since amphibole appears in igneous rocks at approximately 55 wt.% $SiO_2$ (Jakes and White, 1972; Anderson, 1980) and > 4 wt % $H_2O$ (Czamanske and Wones, 1973; Noyes et al., 1983), fractionation of these minerals is probably a controlling factor in the evolution of the granitic rocks of the Kirkland Lake area. Clinopyroxene and amphibole are probably important in controlling the decreasing trends exhibited by $Fe_2O_3$ and FeO; biotite and magnetite are minor phases affecting these two trends (Rowins et al., 1993). $TiO_2$ also decreases with differentiation (Fig. 29E), following the trends defined by CaO, MgO and FeO. $K_2O$, $Na_2O$ and $Al_2O_3$ (Fig. 29F) all increase with differentiation, reflecting the predominance of alkali-feldspar (K-feldspar and albite) in the more evolved rocks of the Kirkland Lake area. Timiskaming Group volcanic rocks characteristically have higher $Al_2O_3$ than other rock types (Fig. 29F).

The syenitic suite contains rocks that are predominantly equigranular to slightly porphyritic, composed of perthitic alkali-

feldpsar, where clinopyroxene and biotite are the main ferromagnesian minerals. The rocks are silica-undersaturated, with nepheline and olivine as the characteristic normative minerals. The suite is subaluminous to metaluminous. Many lines of petrographic and geochemical evidence indicate that the syenitic suite crystallized under high oxygen fugacity ($fO_2$): the presence of magnetite as both phenocryst and groundmass phases, relatively low Fe/(Fe+Mg) ratios (0.35-0.50) in biotite and clinopyroxene and high whole-rock $Fe_2O_3$/ $Fe_2O_3$+FeO ratios at 0.4 to 0.5. The $K_2O/Na_2O$ ratio commonly exceeds unity, $K_2O+Na_2O$ is usually greater than 5 wt.%, $TiO_2$ content is almost always below 1.5 wt.% , $Al_2O_3$ content varies between 10 and 20 wt.% and all syenitic rocks are enriched in LREE. All of these characteristics indicate a strong affinity to the shoshonite association (Morrison, 1980) and in some cases to the ultrapotassic clan (see Rowins et al., 1993). The high Ni and Cr contents indicate the primitive nature (unfractionated) of the syenitic rocks.

The granitic suite contains rocks that are predominantly porphyritic containing both plagioclase and alkali-feldspar phenocrysts, where amphibole is the dominant ferromagnesian mineral. The suite is metaluminous to peraluminous. The rocks are either silica-saturated (quartz in the norm) or quartz-bearing (as a phenocryst phase or in the groundmass). Whole-rock $Fe_2O_3$/ $Fe_2O_3$+FeO ratios are very similar to those of the syenitic rocks, but can be considerably lower (0.05) in the granitic rocks of domain 2. $TiO_2$ content is usually less than 0.6 wt.%. $Al_2O_3$ content

is usually greater than 15 wt.%. $K_2O/Na_2O$ ratios are generally less than 0.5, and total alkalies ($K_2O+Na_2O$) vary between 5 and 10 wt.%. Elevated Ni and Cr contents in quartz monzodiorite indicate its primitive nature. The latter rock type has been described as a "sanukitoid" with Mg# = 60 (Stern et al., 1989), which are closely associated to evolved granodiorite; these features are also observed in the granitic rocks of the Kirkland Lake area. All of these characteristics are consistent with those of the high-K, high-Mg calc-alkaline andesite-dacite group (Hyndman, 1985; Stern et al., 1989; Wilson, 1989).

Even though the syenitic and granitic rocks have contrasting mineralogical and textural characteristics, they share many common major, minor and trace element geochemical features: high $Al_2O_3$ and whole-rock $Fe_2O_3/ Fe_2O_3+FeO$ ratios, low $TiO_2$, high total alkalies, high Ni and Cr content, highly fractionated REE patterns, low Fe/(Fe+Mg) ratios in ferromagnesian minerals. Larsen diagrams also demonstrate the close relationship between both suites, by displaying smooth continuous linear trends. All of this evidence outlines the compositional continuity of the duality of magmatism in the Kirkland Lake area.

## 4. Petrogenesis and tectonic setting of the duality of magmatism

The association of syenitic and granitic rocks has been documented in several occurrences worldwide. Some of the better known localities are the northwestern Alps, Italy (Venturelli et al., 1984); Hercynides, SW Europe (Fourcade et Allègre, 1981); Eolian islands (Keller, 1982); Vitiaz arc, Fiji (Gill and Whelan, 1989); Nigeria-Niger Province (Bowden and Turner, 1974); Sunda-Banda arc, Indonesia (Wheller et al., 1987); Oslo graben, Norway (Barth, 1954; Williams, 1982); East-African rift, Kenya (Baker, 1972); Mboutou complex, Cameroon (Parsons et al., 1986); White Mountains, New Hampshire (Eby, 1987; Size, 1972); Mexican volcanic belt, Mexico (Luhr et al., 1989); Ach'uaine hybrids, northern Scotland (Fowler, 1988); Spanish Peaks, Colorado (Johnson, 1968); Central Bohemian pluton, Czechoslovaskia (Nemec, 1988). The syenite- granite association is not exclusive to one tectonomagmatic setting; in fact, this association can be found in tectonic settings varying from island arcs to anorogenic ring complexes.

Petrogenetic models of the syenitic rocks in the Kirkland Lake area are equivocal: mantle-derived melts from a subduction setting are preferred by Cooke and Moorhouse (1969), Ben Othman et al. (1990), Sutcliffe et al. (1990), Laflèche et al. (1991) and Hattori and Hart (1990), while melts of metasomatized mantle formed in an extensional setting are favored by Cameron (1990, in prep.) and Rowins et al. (1993). Petrogenetic models that deal with calc-alkaline granitic rocks of the Superior Province invoke mantle derivation and subduction processes (Stern et al., 1989; Feng and Kerrich, 1992). Studies

which attempt to reconcile the diversity of plutonic rocks (i.e. granitoids) of the southern Abitibi greenstone belt with one of the tectonic settings above illustrate the complexity of late Archean magmatism (Sutcliffe and Beakhouse, 1990; Rive et al., 1990; Feng and Kerrich, 1992). Mechanisms suggested for the generation of these granitoids include partial melting of subducted basaltic crust or enriched mantle, crustal assimilation, remelted mafic parent magmas in and around subduction zones (ibid.) and partial melting of a LILE- and LREE-rich mantle emplaced in strike-slip tensional fractures at convergent margins (Feng and Kerrich, 1992).

Clearly, the evolution of the southern Abitibi greenstone belt in the late Archean presents a complex relationship between magmatism and tectonism. It is apparent that the variety of igneous rocks found in the southern part of the Abitibi greenstone belt was produced in a complex tectonic environment, which is consistent with the complexity of accretionary tectonics believed to have operated late in the Archean (Card, 1990; Hoffman, 1989, 1990; Jackson, 1992). The generation of syenitic rocks of domain 3 have been conflictingly presented as products of subduction processes for the Otto stock (Sutcliffe et al., 1990) and to extension processes for the Murdock Creek intrusion (Rowins et al., 1993). The strong similarities between these two intrusions preclude the simultaneous verity of both models; conversely, these syenitic rocks may exhibit features common to both subduction and extensional tectonic settings. The preferred model should explain the majority of the characteristics exhibited by the duality of magmatism of the Kirkland Lake area.

## 4.1 Petrogenesis of the duality of magmatism

A duality of magmatism is observed along the Kirkland Lake-Larder Lake fault zone. This duality is defined by the intimate association of a syenitic suite and a granitic suite. Both suites are represented by a broad spectrum of rock types. The syenitic suite includes lamprophyre, clinopyroxenite, alkali-feldspar melasyenite and syenite, various types of trachytes and hornblendite, while quartz monzodiorite, quartz monzonite, granodiorite, diorite and some trachyte flows belong to the granitic suite. Interestingly, Kirkland Lake is the locus of syenitic magmatism; syenitic rocks are less common in the eastern portion of the KLF. Three distinct magmatic domains occur along the KLF: domain 1 is located within the deformation zone and consists of thin and elongated hypabyssal granitic intrusions and syenite bodies that occur both as hypabyssal intrusions and extrusive flows (which are known as the Timiskaming Group volcanic rocks). Domain 2 comprises the country north of the KLF: it contains elongated hypabyssal granitic intrusions. Domain 3 is the country south of the KLF and is composed of large rounded composite syenitic and granitic intrusions. Among these, two are exclusively syenitic (Lebel stock and Murdock Creek intrusion), one is exclusively granitic (McElroy stock) and one contains both syenitic and granitic phases (Otto stock).

The syenitic rocks of domain 1 possess many textural, mineralogical and geochemical similarities to the syenitic rocks of domain 3. Similarly, granitic rocks found in all three domains share strong similarities to one another. Chapter 2 illustrated the field and petrographic similarities, while chapter 3 demonstrated the strong mineralogical and geochemical resemblance between

the syenitic rocks of domain 1 and 3, as well as those of granitic rocks of all three domains. Syenitic rocks display these remarkably similar characteristics:

I. they are equigranular, with clinopyroxene, biotite and magnetite as ubiquitous mafic minerals, are hypersolvus (one feldspar, perthitic), have Ne+Ol in the norm, are subaluminous to metaluminous. Contacts between rock types are commonly gradational.

II. clinopyroxene that: 1) is diopsidic in composition, 2) displays Mg-enrichment, 3) has low and uniformly decreasing Fe/(Fe+Mg) ratios, 4) uniformly increasing Mg content, 5) constant Ca and Si content, 6) high $Fe^{3+}$/total iron ratios.

III. biotite that has : 1) low and uniform Fe/(Fe+Mg) ratios, 2) constant Mg content, 3) overlapping uniformly decreasing $Al^{iv}$ content, 4) low Ti content, 5) high $Fe^{3+}$/total iron ratios.

IV. high ΣREE, $(La/Lu)_{ch}$ and $(Sm/Yb)_{ch}$ ratios and no significant Eu anomaly.

V. high total alkalies, $Al_2O_3$, Ni, Cr, and $K_2O/Na_2O$ ratios, low $TiO_2$, uniform Zr/Y and Rb/Sr ratios for whole rock compositions.

Granitic rocks of all three domains share the following characteristics:

I. they are porphyritic, with amphibole and biotite as the dominant mafic minerals, are subsolvus (two feldspars, plagioclase and K-feldspar), have Qtz in the norm, are metaluminous to peraluminous. Contacts between rock types are commonly gradational.

II. amphibole that: 1) is calcic (edenite to pargasite to hastingsite), with compositions slightly varying only in the amount of ferric iron and Na+K

present, 2) has low Fe/(Fe+Mg) ratios that decrease with increasing $Si^{4+}$ in domains 1 and 3, but increase in domain 2, 3) uniform Na and Ca content, 4) has overlapping uniformly decreasing
$Al^{iv}$ content, 5) has a fairly high $Fe^{3+}$/total iron ratios in domain 1, but low ratios in domain 2.

III. lower ΣREE, $(La/Lu)_{ch}$ and $(Sm/Yb)_{ch}$ ratios and no or slightly positive Eu-anomaly, with REE patterns that are spoon-shaped for HREE.

IV. high total alkalies, $Al_2O_3$, lower Ni, Cr, and $K_2O/Na_2O$ ratios, low $TiO_2$, uniform Zr/Y and Rb/Sr ratios for whole rock compositions.

This evidence clearly indicates that the rocks of the syenitic suite are consanguineous; a similar conclusion can be reached for the rocks of the granitic suite. The intimate spatial association between the two suites is unequivocal (Thomson, 1950; Levesque, 1989; Levesque et al., 1991; Corfu et al., 1989, 1991). Furthermore, it is apparent that, in spite of broad textural and mineralogical differences, the syenitic suite also shares strong similarities to the granitic suite. These similarities include :

I. low and uniform or decreasing Fe/(Fe+Mg) ratios in ferromagnesian minerals, except ratios in the granites of domain 2 increase.

II. consistently high $Fe^{3+}$/total iron ratios in ferromagnesian minerals; ratios are lowest in amphibole of domain 2.

III. high total alkalies, $Al_2O_3$, $Fe^{3+}$/total iron ratios, low $TiO_2$ and Fe/(Fe+Mg) ratios, lack of Fe-enrichment in whole rock compositions.

IV. smooth continuous linear trends displayed on differentiation diagrams.

V. low Nb and Ta content (T-N-T anomaly), very similar trace element ratios (Zr/Y, Ni/Cr, Rb/Sr)

VI. coherent REE fractionated patterns, without Eu anomalies, and commonly displaying the spoon shape for HREE.

These similarities make a strong case for a genetic relationship between the syenitic rocks and granitic rocks of the Kirkland Lake area. The syenitic suite has strong shoshonitic affinities (Morrison, 1980) and the granitic suite is virtually identical to the sanukitoid suite (high-Mg trachyandesites and monzodiorites) of Shirey and Hanson (1984) and Stern et al. (1989). Recent work on the petrogenesis of the calc-alkaline/alkaline rock association in various localities around the world underlines the importance of two processes: partial melting in the mantle ± subducted slab and sediments, and assimilation-fractional crystallization (AFC). Partial melting of the mantle, which may include a subducted slab component and/or crustal material, is the preferred mechanism in the following settingss: 1) the onset of strike-slip faulting shortly after subduction ceased in the Aeolian Islands, Italy (Ellam et al., 1988); 2) eastward migrating arcs colliding with the Australian plate in the Sunda-Banda Arc, Indonesia (Wheller et al., 1987); 3) extensional tectonics following termination of subduction in Papua New Guinea (MacKenzie and Chappell, 1972; McInnes, 1992).

Assimilation-fractional crystallization models (AFC) have been used to explain the formation of the calc-alkaline/ alkaline rock association in: 1) the Independence volcano, Montana, where shoshonites are derived from calc-alkaline basalts, while crustal anatexis seemingly produced quartz monzodiorite-granodiorite rocks (Meen, 1987a); 2) the Oxford Lake area, Manitoba, where terminal magmatism occurs in an Archean arc (Brooks et al, 1982); 3) the Dolomites of northern Italy, where shoshonites emplaced along strike-slip faults

were derived from basaltic magmas (Sloman, 1989); 4) the Scottish Caledonides, where shoshonites and granitic rocks were derived from basic parental magmas late in the subduction history or immediately following continental collision (Thompson and Fowler, 1986; Fowler, 1988); 5) the British Caledonides by different histories of melting-freezing-remixing of fractionated melts along strike-slip faults (Bowes and Kosler, 1993). Mantle partial melting and AFC processes discussed above are proposed to have operated conjunctly in the following localities: 1) the western Mexican volcanic belt, where the magmas are emplaced within three intersecting rift zones above the subducted Cocos plate (Luhr et al., 1989; Verma and Nelson, 1989); 2) the northwestern Alps of Italy, where magmas were emplaced in an extensional setting, during the closure of the Thetyan ocean (Venturelli et al., 1984). Magmas generated by these two processes can have similar compositions (Fig. 30), emphasizing the difficulty in selecting one mechanism over the other to explain the petrogenesis of these rock suites.

It would therefore seem logical that mantle partial melting and AFC processes were responsible for the formation of the duality of magmatism of the Kirkland Lake area. Fractional crystallization has clearly been an important mechanism in the evolution of the syenitic suite: the role of clinopyroxene fractionation (± plagioclase) was dominant in the formation of the Murdock Creek intrusion (Rowins et al., 1993), while field and contact relationships between alkali-feldspar melasyenite and alkali-feldspar syenite unequivocally show that both are related by progressive removal of clinopyroxene. The same mechanism also operated in the granitic suite: amphibole fractionation is responsible for the steeper REE patterns of the granodiorite versus quartz monzodiorite units of domains 1 and 2, and recent work suggests this

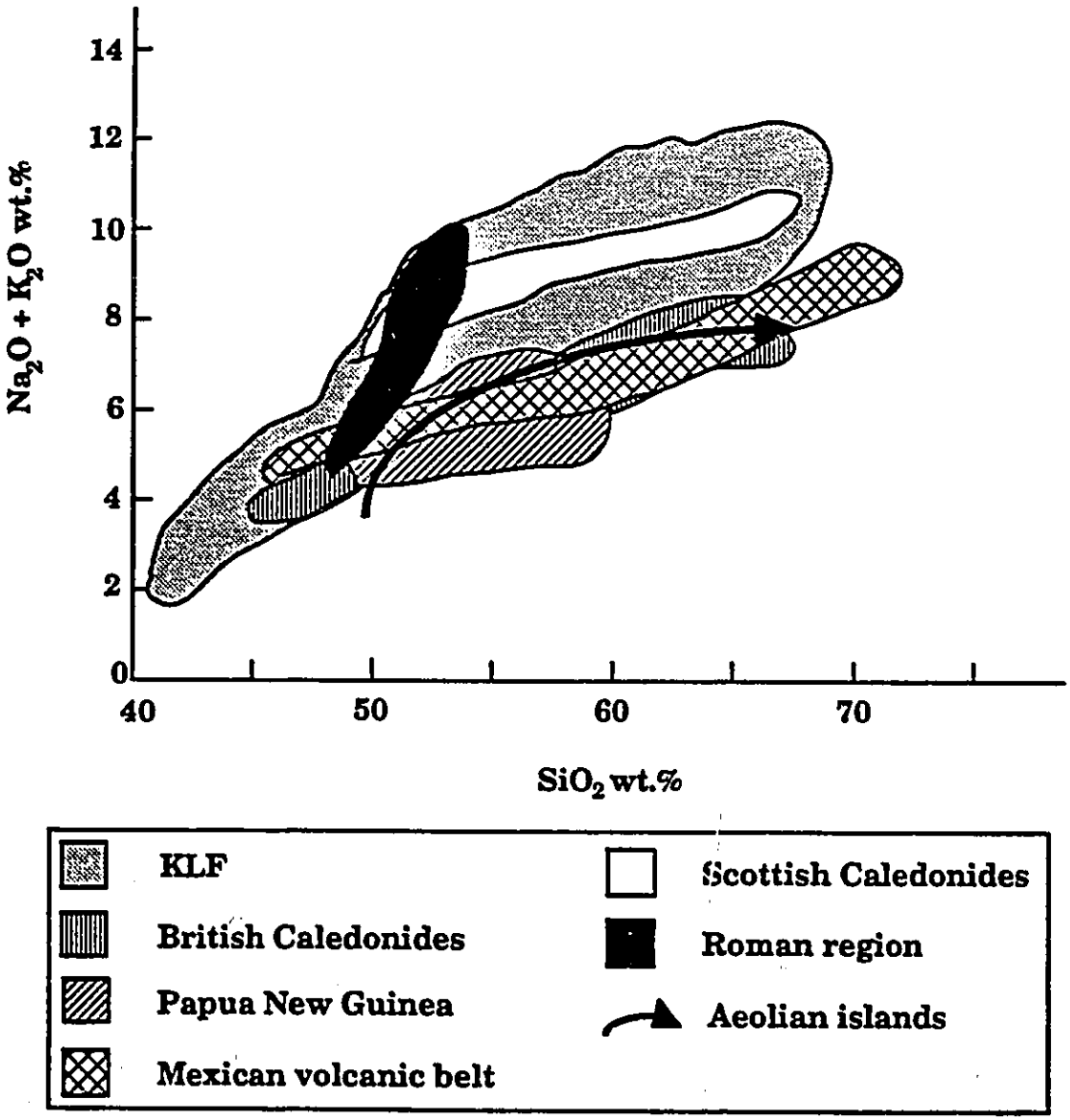


Figure 30. Total alkalies vs. silica diagram of rock suites comparable to the duality of magmatism of the KLF. Most of these localities share the syenitic-granitic association found in the KLF. All of these suites were generated in areas of extensional tectonics where subduction had ceased shortly before.
Source of data: Scottish Caledonides (Fowler, 1988); Mexican volcanic belt (Verma and Nelson, 1989); Papua-New Guinea (MacKenzie and Chappell, 1972); British Caledonides (Bowes and Kosler, 1993); Aeolian islands (Elllam et al., 1988); Roman volcanic province (Beccaluva et al., 1991).

mechanism (± plagioclase) was dominant in the evolution of late Archean granitoid rocks (Sutcliffe et al., 1990) and in the more evolved units of the sanukitoid suite (Shirey and Hanson, 1984). The variability of amphibole compositions, from pargasite to magnesio-hornblende has been observed in andesites of southwestern British Columbia by Green (1982). He attributed this variability to the presence of a zoned magma chamber, in which pargasite crystallized early at higher temperatures, while magnesiohornblende crystallized at lower temperatures. Thus, **intrasuite** evolution (from mafic to felsic units of either the syenitic or granitic suite) was controlled by fractional crystallization of clinopyroxene ± plagioclase in the syenitic rocks, and amphibole in the granitic rocks.

The mechanism for **intersuite** evolution (from syenitic magmatism to granitic magmatism) is less well constrained. Three possibilities exist: 1) granitic rocks were formed by crustal anatexis in the region where hot syenitic melts were emplaced; 2) syenitic and granitic rocks were formed by different degrees (and areas) of partial melting in the upper mantle; 3) granitic rocks were derived from syenitic rocks by AFC processes. Although these possibilities can be best constrained through isotopic evidence, several lines of major, trace and rare earth element geochemical evidence can also be used effectively.

The generation of alkaline magmas by metasomatism (LILE-enrichment) of the upper mantle is now widely accepted. In this process, garnet peridotite, which is enriched in LILE and associated elements by a metasomatizing agent which can either be a melt or a fluid, undergoes low degrees of partial melting to form alkaline magmas (Lloyd and Bailey, 1975; Wendlandt and Eggler, 1980; Bailey, 1987; Foley et al., 1987; Foley and Peccerillo, 1992). In many cases, the

generation of alkaline magmas from volatile-rich peridotite is coincidental with the production or release of $CO_2$ (Meen, 1987b). Evidence for the mantle derivation of the syenitic rocks of the Kirkland Lake area is overwhelming (Basu et al., 1984; Ben Othman et al., 1990; Cameron, 1990; Hattori and Hart, 1990; Sutcliffe et al., 1990; Rowins et al., 1993).

The melting of lower crustal granulites and upper crustal metasedimentary rocks are two important mechanisms for the generation of granitic rocks (Hyndman, 1985; Hall, 1987). It does not seem, however, that the melting of crustal components is responsible for the generation of the granitic rocks of the Kirkland Lake area. Several geochemical features of the granitic rocks argue against this mode of formation:

1) smooth linear major element variation trends: it is unlikely that the trends would be continuous (no gaps) between syenitic and granitic rocks, unless extensive magma mixing occurred. No evidence of this can be found in the Kirkland Lake area.
2) similar fractionated REE patterns of syenitic and granitic rocks without Eu-anomalies: it would be unlikely for a crustal melt to possess the same REE characteristics of a mantle-derived mafic magma to which it is spatially but not genetically-related.
3) high MgO, Ni and Cr content in granitic rocks, the similarity between granitic and syenitic rocks in total alkalies, $Fe^{3+}$/total iron, Fe/(Fe+Mg) and trace element ratios are not consistent with an anatectic origin.
4) the occurrence of the McElroy stock in domain 3 indicates that large amounts of granitic melt were generated at depth coevally with syenitic plutons.

Shirey and Hanson (1984) equally argue against this process since rocks of the sanukitoid suite have higher Ce/Yb ratios higher than the surrounding crust which could have been the contaminants, and Sutcliffe et al. (1990) confirm that monzodiorites have higher LREE and Sr content than most Superior Province supracrustal rocks. The assimilation of a minor amount of crustal material is probable, since pluton margins are commonly diffuse into the encasing basaltic country rocks. Therefore, it seems that the granitic rocks of the Kirkland Lake area are related to a mantle origin. Either the granitic rocks formed as a result of fractional crystallization of the syenitic rocks, or that they represent partial melts from the upper mantle or from a subducted slab.

Mantle derivation of granitic rocks has been convincingly demonstrated by Shirey and Hanson (1984) and Stern et al. (1989) for their sanukitoid suite, against which the granitic rocks of domains 1 and 2 seem virtually identical. They propose partial melting of upper mantle peridotite under hydrous conditions at pressures of 10 to 15 kilobars. Alternatively, granitic rocks in the Archean can be formed by direct melting of a subducted slab (Martin, 1986). In the Archean, hydrated subducted slabs were believed to be young and warm, and thus reached melting temperatures before dehydration reactions could occur; these slabs had garnet amphibolite compositions, so that partial melting of these rocks would generate granitic melts in which HREE are depleted, indicating that amphibole and garnet were refractory phases in the source region (Barker and Arth, 1976; Martin, 1986; Condie, 1989). Indeed, this is the case for the granitic rocks of the Kirkland Lake area, where hornblende (and garnet) was present in the source region of melting.

The porphyritic granitic rocks of the Otto stock are unique in the Kirkland Lake area in that they contain sodic amphibole and sodic clinopyroxene. These peralkaline rocks have lower Ni, Cr, Sr, $Al_2O_3$, ΣREE, and higher $Na_2O$, MgO, CaO and FeO than corresponding granitic rocks in domains 1 and 2. This unit represents the most evolved unit of the Otto stock, that probably represents the end result of clinopyroxene (rather than amphibole, as suggested by Sutcliffe et al. (1990)) fractionation operating in the Otto stock,which would result in the Na-enrichment observed in this unit. The similarities with other granitic rocks are therefore strictly textural, having been emplaced in shallow levels of the crust. The quartz monzonite unit of the McElroy stock contains amphibole crystals that commonly have granulated cores of clinopyroxene (± epidote), indicating that the latter was dominant in the early development of the stock. Amphibole in this unit crystallized late in the evolution of the stock and was formed by reaction of clinopyroxene with liquid, which is commonly observed in hydrous melts at high pressures in the region of continental margins (Hess, 1989). The geochemical features, as well as the intimate association between diorite, monzonite and hornblendite units in the McElroy stock suggest that it belongs to the sanukitoid suite. Shirey and Hanson (1984) indicate that the more evolved members of the sanukitoid suite were produced by early clinopyroxene and amphibole crystallization of sanukitoid parent melts. Early amphibole crystallization is represented by the associated hornblendite unit; this amphibole is not to be confused with the late crystallizing phase replacing clinopyroxene in the quartz monzonite unit.

Evidence for the origin of the granitic rocks (domains 1 and 2 and McElroy stock) of the Kirkland Lake area is conflicting: evidence suggests that they were either 1) produced directly by partial melting in the mantle, or 2) by fractional

crystallization of the syenitic magmas. Of the evidence which support the first model, the high Mg numbers, Ni and Cr content of these rocks suggest that they have not undergone extensive fractionation and were derived from primary melts. Total alkalies contents are nearly identical in both the syenitic and granitic suites, a feature inconsistent with extensive crystal fractionation. Fractional crystallization would produce an increase in incompatible element abundances in the granitic rocks: for elements such as Zr, Y, their abundances are virtually identical in both rock types except for granodiorite, in which Y values are lower. However, two important lines of evidence suggests that crystal fractionation was important in the generation of the duality of magmatism: all major element variation diagrams exhibit smooth linear trends that are continuous between syenitic and granitic rocks. These trends would be difficult to reproduce for two suites of rocks that are not related by fractionation processes. Fractional crystallization would also explain the intersuite geochemical characteristics (LILE- and LREE-enriched, no Eu-anomaly, high $Fe_2O_3$/total iron and low Fe/(Fe+Mg) ratios), since both suites would originate from the same source.

It is clear that an intersuite genetic relationship exists; the exact nature of this relationship is ambiguous. It can best be resolved if both suites of rocks were both derived from mafic melts produced in the upper mantle. Two such candidates are the hornblendite and lamprophyre units. Hornblendite compositions are remarkably similar in geochemistry and mineralogy to calc-alkaline lamprophyres (Rock, 1991). It has been suggested that hornblendite may represent the parent magma to the Murdock Creek intrusion (Rowins et al., 1993) and to the Otto stock (Sutcliffe et al., 1990). In the Scottish Caledonides, appinites are thought to represent mafic parental melts to which

calc-alkaline and shoshonitic (+ultrapotassic) rocks are related by fractional crystallization (Thompson and Fowler, 1986; Fowler, 1988; Bowes and Kosler, 1993). Appinites are identical in mineralogy and geochemistry to the hornblendite units of domain 3 and have been described as coarse-grained, volatile-rich plutonic equivalent to calc-alkaline lamprophyres (Rock, 1991). Appinites commonly occur in a suite of mafic to felsic rocks that include appinite, pyroxenite, diorite, syenite and granodiorite.

Why are hornblendite and lamprophyre such good candidates to be the parental magmas to both syenitic and granitic rocks of the Kirkland Lake area? There are several reasons: 1) high MgO, Ni, Cr, Ba and low Zr and Sr indicate an upper mantle origin, and both possess the proper abundances of these elements to be a parental magma to both suites of rocks (Thompson and Fowler, 1986; Rock, 1991); 2) the potential for both to produce rocks that have high total alkalies abundances over a wide-range of silica saturation (Frey et al., 1978; Yagi and Takeshita, 1987); 3) both occur at depth coevally with the intrusions of domain 3; 4) both contain all of the mineral phases encountered in the Kirkland Lake area: amphibole, clinopyroxene, biotite, magnetite, plagioclase and K-feldspar; 5) removal of amphibole in a hornblendite melt leaves only the interstitial phases listed in 4), which correspond exactly to the mineralogy of all syenitic rocks (Rowins et al., 1993); 6) both were produced under hydrous (hornblendite) or volatile-rich (lamprophyre) conditions; this is in agreement with the source region for the sanukitoid suite (Stern et al., 1989); 7) the REE characteristics for both suites of the Kirkland Lake area reflect their origin: hornblendite and lamprohyre were derived from the upper mantle so that REE patterns reflect the presence of amphibole and/or garnet in the source region where the syenitic and granitic melts were formed; alternatively, amphibole

fractionation could produce the REE patterns observed in the granitic rocks (Frey et al., 1978); 8) the volatile-rich nature of this rock can account for the intrinsic magmatic oxidation displayed by the ferromagnesian minerals of domains 1 and 3; domain 2 intrusions were formed far from the locus of volatile release along the LLF and probably escaped the oxidation effects; 9) it can also explain features common to both lamprophyres and granitic rocks: the presence of lamprophyre-type mica (composition and texture) in the granitic rocks of domain 1, originally attributed to lamprophyre alteration (Hattori and Levesque, 1989), and the presence of a Ho-anomaly in both rock types.

The petrogenesis of the duality of magmatism in the Kirkland Lake area can be summarized as follows (Fig. 31):

1. Patial melting of garnet peridotite or garnet amphibolite under hydrous or volatile-rich conditions occurred in the upper mantle to produce mafic melts; this could have been triggered by metasomatisizing fluids or melts released from a subducted slab.
2. These volatile-rich mafic melts are represented by hornblendite, which formed in the upper part of the upper mantle under hydrous conditions, and lamprophyre, which formed in the lower part of the upper mantle under volatile-rich (water-poor) conditions.
3. Amphibole removal from hornblendite leaves a melt composed of clinopyroxene+ biotite + plagioclase + magnetite + K-feldspar. Fractionation of these minerals produces the syenitic suite of the Kirkland Lake area.
4. Fractionation or partial melting of the amphibole residua (± interstitial phases) produces the granitic suite of the Kirkland Lake area.

5. Fractionation and partial melting of lamprophyric melts can also produce the range of syenitic rocks of the KLF.

### 4.2 Tectonomagmatic model and gold mineralization

The termination of subduction or the beginning of continental collision seems to be essential to the development of the calc-alkaline/alkaline association (e.g. Italy, Papua New Guinea, Scottish Caledonides). Both these events would be predominant in the late stages of island arc accretion, the preferred mechanism in the formation of the Superior Province (Card, 1990; Hoffman, 1989, 1990, Desrochers et al., 1993). It follows that petrogenetic models of igneous rocks would emphasize either of these two settings. Which one is responsible for the formation of the duality of magmatism? The best answer is provided by a tectonomagmatic model in which **both** subduction and strike-slip faulting are essential.

The Larder Lake fault represents a strike-slip fault formed during oblique convergence (Hubert et al., 1984). Its western termination, the KLF, is intimately associated with the sedimentary and alkaline volcanic rocks of the Timiskaming Group and syenitic and granitic intrusions (Fig. 1). The morphology and physical make-up (e.g, narrow elongate fault zones, pull-apart basins) of the KLF is typical of strike-slip belts (Williams, 1982; Sylvester, 1988), and its relatively discontinous, small amount of magmatism is reminescent of low volcanicity zones of rift environments (Barberi et al., 1982). As a consequence to strike-slip movements, magmatism is almost exclusively associated to the transtensional phase, while uplift and deformation, accompanied by reverse faulting are associated to the transpressive phase (Sylvester, 1988). Bailey

(1983) further characterized continental rift magmatism as alkali- ,volatile (halogens and carbon gases)-, LREE- and LILE- rich features common to Kirkland Lake area rocks. However, the latter fail to show other salient features of rift magmatism: high titanium, zirconium and niobium, low alumina, positive Eu anomalies (Barberi et al., 1982; Wilson, 1989).

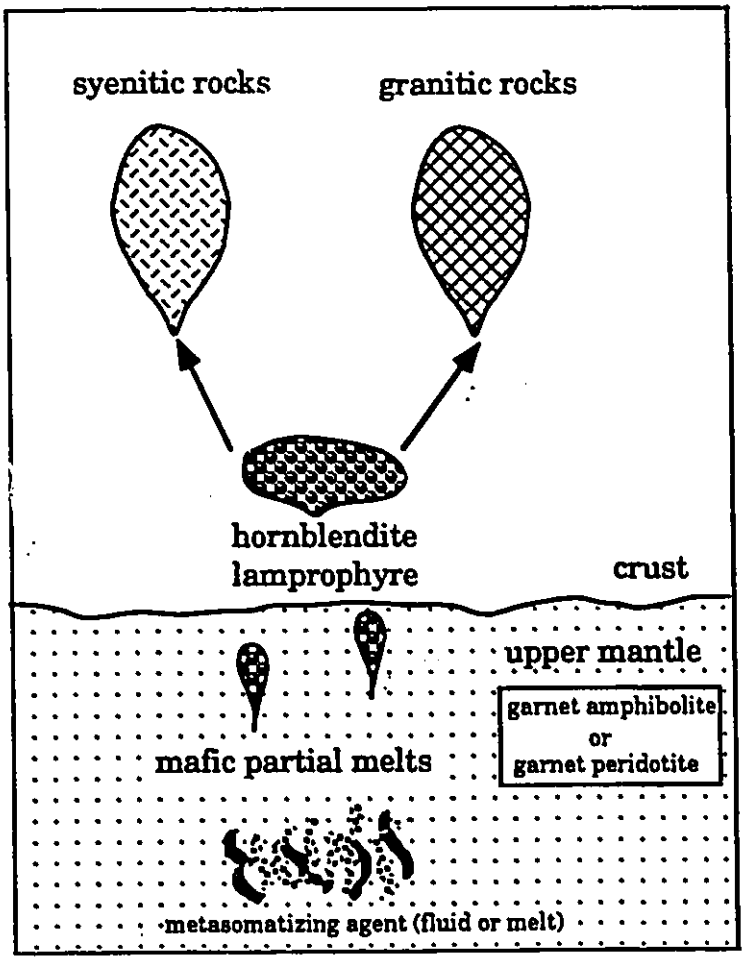


**Figure 31. Cartoon representing the petrogenesis of the duality of magmatism of the Kirkland Lake area. A metasomatizing agent induces partial melting of the upper mantle. Hornblendite and lamprophyre form from these mafic melts and differentiate to produce both syenitic and granitic suites.**

The common regime in the overriding plate of a subduction setting is one of extension (incipient barck-arc spreading,...) and not of shortening or compression (Hamilton, 1988). Subduction processes are intimately linked to the production of large amounts of extrusive and intrusive rocks by various means involving the subducted slab and its derived fluids (Arculus and Powell, 1986; Tatsumi, 1986, 1989; McCulloch and Gamble, 1991; Hawkesworth et al., 1993). The amount of magmatic activity usually decreases away from the volcanic front, so that in mature island arcs, the volume of rocks generated is less. Rocks from mature island arcs (Aeolian islands) or continental margins (Mexican volcanic belt, Sunda-Banda arc) commonly display the transition from the calc-alkaline to the shoshonite association (Wheller et al., 1987; Ellam et al., 1989; Luhr et al., 1989). Rocks from the calc-alkaline-shoshonite associations of continental margins are characterized by more highly evolved rock types, high alkalies, LILE, LREE, Ni, Cr and alumina, low titanium, steady increase of silica with differentiation, high $Fe^{3+}$/total iron ratios and little or no iron-enrichment (Baker, 1982; Condie, 1982; Hamilton, 1988); these features are consistent with those of the Kirkland Lake area rocks. Amphibole predominates over clinopyroxene in calc-alkaline rocks of continental margins (Jakes and White, 1972), while clinopyroxene is the dominant ferromagnesian mineral in shoshonitic rocks (Morrison, 1980). The characteristic Ti-Nb-Ta depletion occurring in island arc rocks and in those of the Kirkland Lake area has been the source of recent debate (Foley and Wheller, 1990; Rowins et al., 1993), since this feature is also observed in continental potassic rocks.

A continental margin setting, where subduction has recently ceased seems to be the most appropriate environment for the Kirkland Lake area

rocks. Rocks from this setting would display both subduction and rift zone characteristics. Geochemical discrimination diagrams for shoshonitic rocks recently developped by Muller et al. (1992) indicate that these were emplaced along a continental margin (Fig. 32); the authors emphasize the importance of oblique convergence in the genesis of these rocks. Although these diagrams were developped for Cenozoïc potassic rocks, the geochemical criteria for the identification of shoshonites is identical whether young (Cenozoïc) or old (Archean); these diagrams are most likely applicable to the rocks of the Kirkland Lake area. The diagrams reveal that the majority of rocks were emplaced in a continental arc setting, while some rocks may have formed in post-collisional arcs or within plate setting, which could possibly represent the continent-ward migration of shoshonitic magmatism during active collision.

Two features of the Kirkland Lake area that remain to be explained are the paucity of syenitic rock in the western portion of the study area (Fig. 1) and the existence of three distinct magmatic domains (Fig. 2). The calc-alkaline to shoshonite transition observed in many island arc occurs as a result of mineralogical changes in the subducted slab (Tatsumi, 1986; 1989). The subducted crust drags down altered peridotite along its surface: amphibole is stable in the upper part (depth to 75 km) (Martin, 1986), while phlogopite is stable in the deeper part (depth up to 200 km) (Tatsumi, 1989). Consequently, hornblendite could have been produced by metasomatizing agents in the upper part, while lamprophyre was produced in the deeper portion of the subducted slab. Thus, the concentration of syenitic magmatism in the western portion of the study area may be related to the depth and the composition of the subducted slab which releases the metasomatizing agents that trigger partial melting in the upper mantle (Tatsumi, 1986).

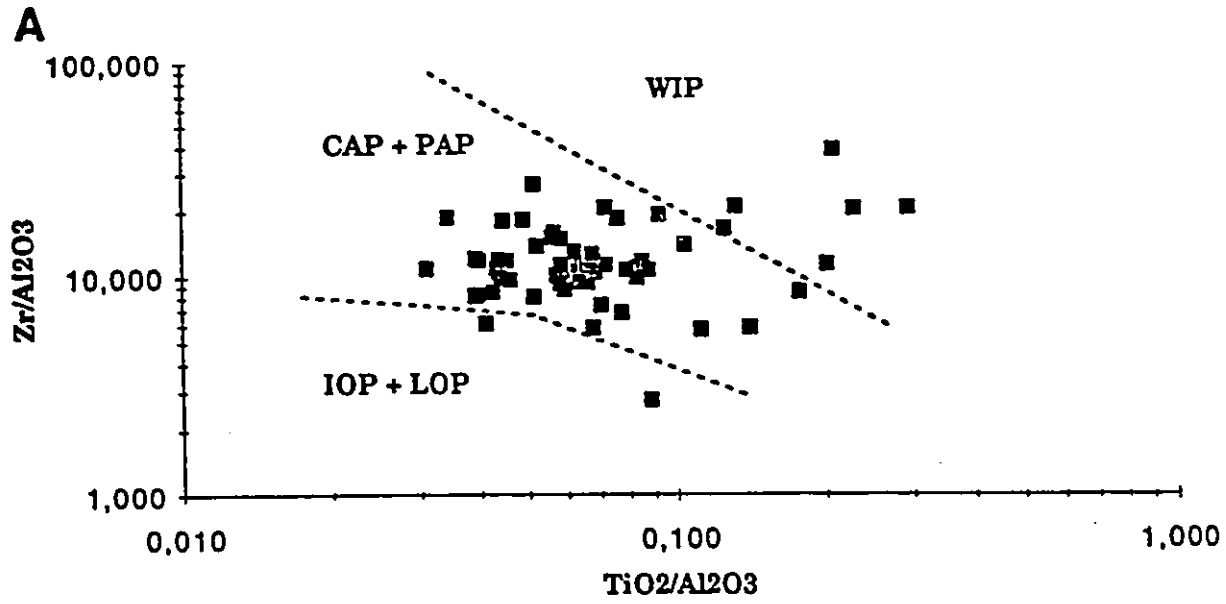


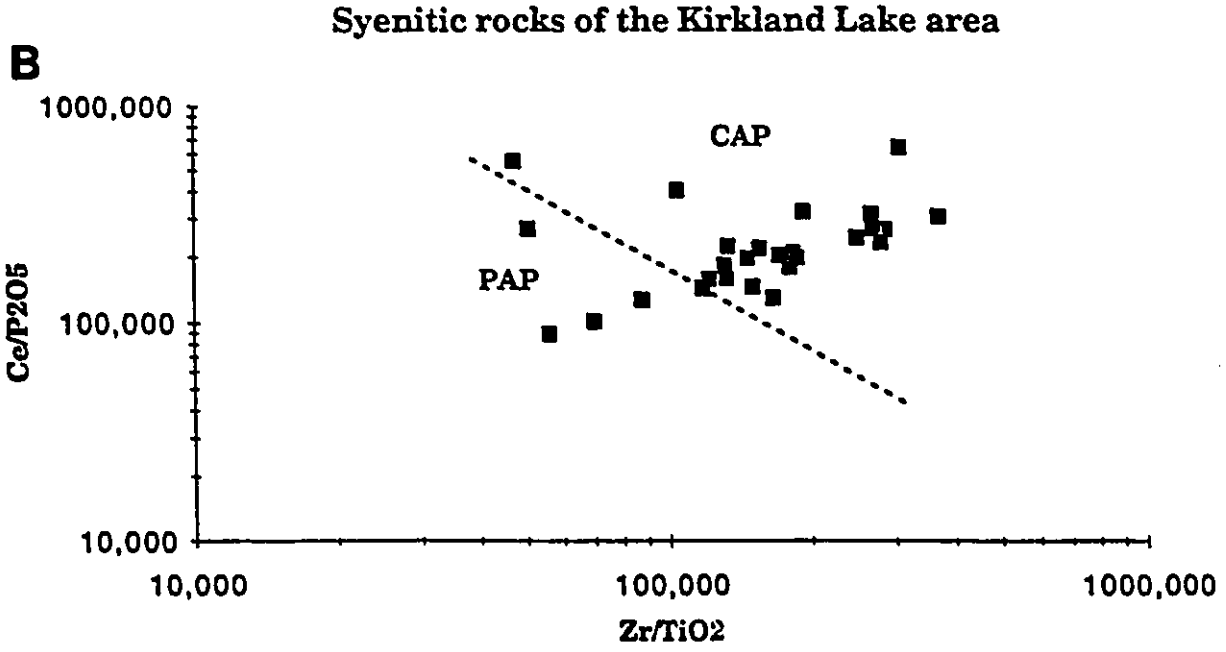


Figure 32. Tectonic discrimination diagrams for shoshonitic rocks and intrusive equivalents. A) Dicrimination diagram between island arc (IOP or LOP), continental arc (CAP or PAP) and within plate (WIP) settings. The majority of analyses fall in the continental arc field and a few in the wihtin plate field. B) Discrimination diagram between continental arc (CAP) or post-collisional arc (PAP). Most analyses fall in the continental arc field. The transition from continental arc to post collisional arc to within plate settings can be envisaged in the proposed tectonomagmatic model.

Domains 1 and 2 contain rocks that were emplaced either as hypabyssal intrusions or as extrusive flows; domain 3 is characterized by large rounded intrusions. Initially, small amounts of lithospheric extension, causing asthenospheric upwelling and triggerring small degrees of partial melting, was thought to be the driving mechanism behind alkaline rift magmatism (McKenzie and Bickle, 1988). This mechanism was postulated for the generation of alkaline magmas at Kirkland Lake (Cameron, 1990). However, recent observations indicate that alkaline magmatism commonly predates rifting (LeBas, 1987), so that rifts could be produced as a consequence, and not the cause of alkaline rift magmatism. In keeping with the first scenario of lithospheric extension, intrusions rise diapirically through the crust and are emplaced at mid- to shallow levels in domains 2 and 3. The difference in emplacement depth between these domains is largely a reflection of erosion level, domain 3 having been uplifted by reverse faulting (south-side up movement) along the LLF (Thomson , 1950), thus exposing the deeper portion of the intrusions in domain 3. The intrusions of the Kirkland Lake area were emplaced along a zone of extension in the crust created by accretion and oblique subduction. This ultimately resulted in the formation of the LLF and KLF, where both syenitic and granitic rocks were emplaced as hypabyssal bodies or extrusive flows. It is highly probable that the formation of the LLF and KLF was concurrent with the initiation of uplift and partial melting caused by strike-slip faulting.

The following tectonomagmatic model for the Kirkland Lake area can be pictured (Fig. 33):

1. Oblique convergence resulted in the termination of subduction and the initiation of continental collision in the Abitibi greenstone belt.

2. The termination of active subduction was followed by magmatism along the continental margin: areas where granitic rocks predominate were probably underlain by shallow subducted crust (amphibole stable), while areas marked by syenitic rocks were derived from deeper subducted crust (phlogopite stable). Consequently, granitic rocks may be slightly older than syenitic rocks, a fact confirmed by the studies of Corfu et al. (1991).

3. Metasomatizing agents (fluids and/or melts) triggered partial melting in the upper mantle, generating hornblendite and lamprophyre. From these mafic melts originate granitic magmas that were emplaced as hypabyssal intrusions in the thinner crust of domain 2, and syenitic magmas that rose forcefully and were emplaced as diapirs within the thicker crust of the continental margin.

4. The production of strike-slip faults by continued oblique convergence (collision) in the continental margin focused passively emplaced syenitic and granitic rocks and volatiles within extensional fractures. This represents the transtensional phase.

5. A later transpressive phase, marked by reverse faulting (thrusting) along the LLF and KLF, uplifted domain 3 (south side up) relative to the other domains.

How does this model relate to gold mineralization in the Kirkland Lake area? Recent studies on the genesis of mesothermal gold deposits (MGD) underline the importance of oblique convergence (accretion) and crustal stabilization (Hodgson and Hamilton, 1989; Fyon et al., 1989; Wyman and Kerrich, 1989; Rock et al., 1989; Kerrich and Wyman, 1990; Cameron, 1990). Oblique convergence and accretion inevitably leads to crustal thickening in the region where it occurs: this is the first step towards cratonization and the genesis of MGD. The hydrothermal fluids responsible for the dissolution, transport and deposition of gold originate at the base of the crust. The ultimate

source of these fluids has been attributed to 1) oxidative metamorphism of the lower crust during passage of $CO_2$-rich fluids of mantle origin (Cameron, 1988) 2) metamorphism of underplated oceanic crust (+ sediments) beneath the continental margin (Hodgson and Hamilton, 1989; Kerrich and Wyman, 1990; Kerrich and Feng, 1992). Since many Archean gold deposits were formed from $CO_2$ -rich oxidized hydrothermal fluids (Cameron and Hattori, 1987), it is unlikely that fluids derived from oceanic crust + sediments would be oxidized enough, given that sediments contain graphite that acts as a reducing buffer for these fluids (Cameron, 1989a). Thus the formation of granulites at the base of the crust provides us with a mechanism that can generate these $CO_2$ -rich oxidized fluids; such fluids exist in the Bamble belt of Norway (Cameron, 1989b).

The oxidized nature of the hydrothermal fluids responsible for the formation of MGD matches the oxidized nature of the syenitic and granitic magmas of the Kirkland Lake area. The oxidized nature of the magmas are characterized by the early crystallization of magnetite (Plate 6A) and titanite, low Fe/(Fe+Mg) ratios in mafic silicates and high $Fe^{3+}$/total iron ratios in whole rock compositions. Gold deposition may be related to the fault reactivation model of Sibson et al. (1988). High-angle reverse normal faults act as valves that promote gold deposition by pressure release of upward migrating supralithostatic fluids. Evidence of high-angle reverse faulting at Kirkland Lake is two-fold: uplift of the rocks south of the KLF is confirmed by the exposure of diapiric intrusions and fault plane surfaces along the Kirkland Lake main break clearly indicate fault reactivation (three sets of superimposed slickensides) shown by horizontal (strike-slip) and vertical (slip) slickenside orientation (Plate 6B).

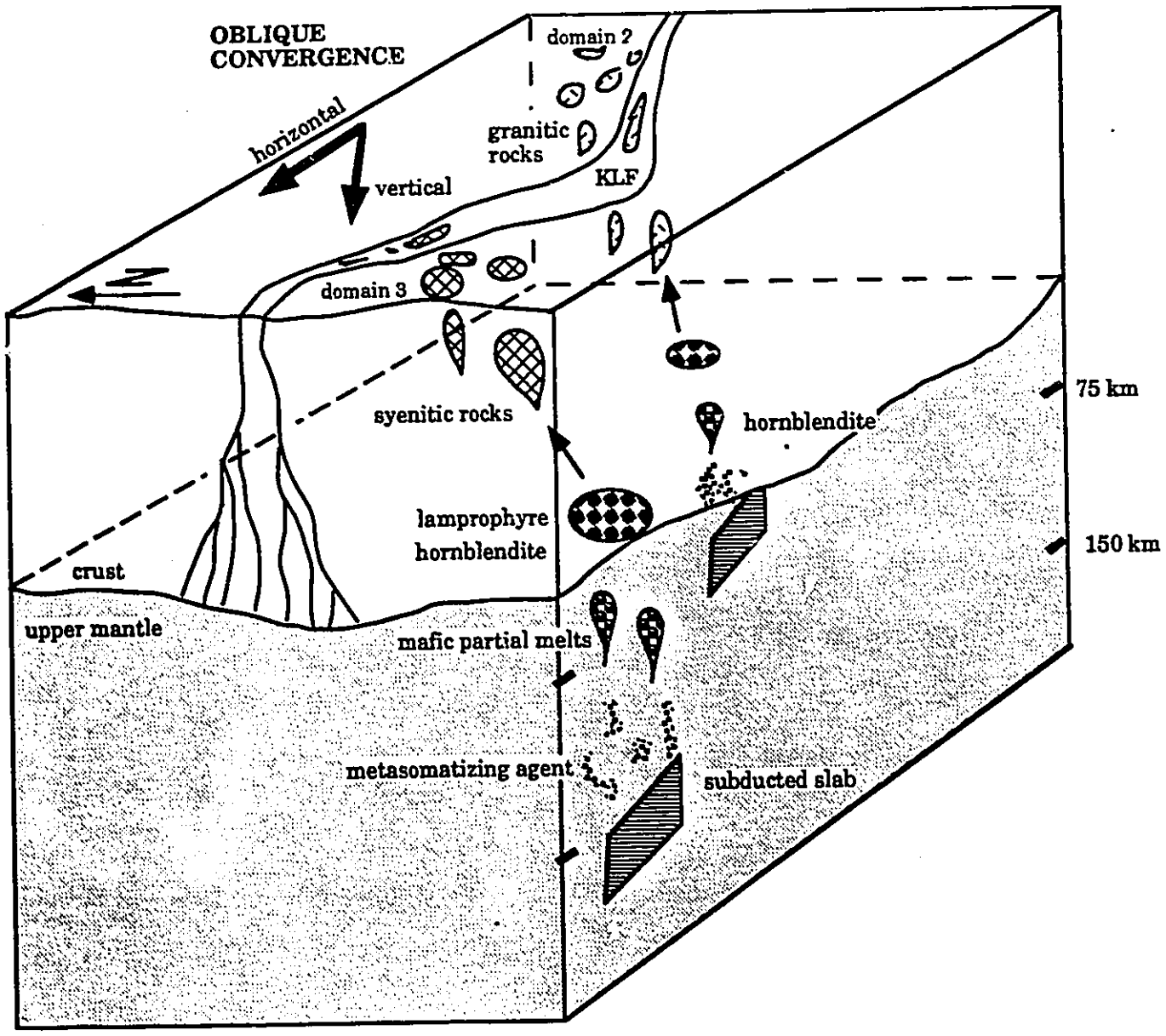


**Figure 33.** Tectonomagmatic model of the Kirkland Lake area. Oblique convergence of a south-dipping slab from the northeast explains both the regionality of granitic and syenitic rocks and the interpreted sinistral strike-slip movement along the LLF and KLF. The KLF was formed simultaneously with, or immediately following, the onset of magmatism.

Plate 6. Mineralogical and structural features associated to gold mineralization. A) The early crystallization of magnetite (black grains) within clinopyroxene indicates the oxidized nature of the magmas at Kirkland Lake. This matches the oxidized nature of the gold mineralizing fluids. Crossed polars, field of view is 5 mm. B) At least three generations of perpendicular slickenside sets can be identified along the prolific Kirkland Lake main break. These slickensides agree with fault reactivation models that are essential in the deposition of gold. Slickensides indicate that fault movements were strike-slip (horizontal) and normal or reverse slip.

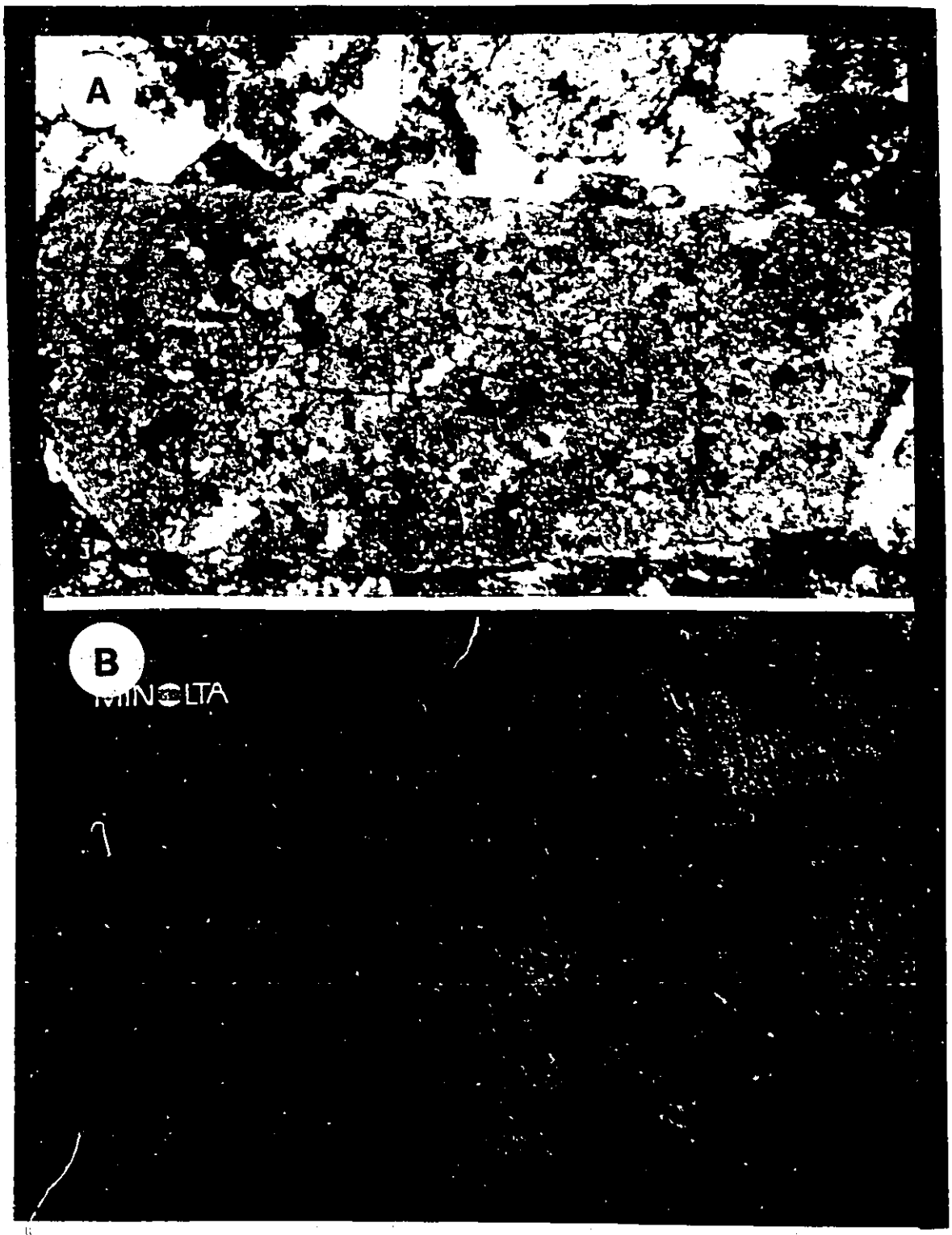
A
B
MINOLTA

## Conclusions

The Kirkland Lake- Larder Lake fault zone is the site of prolific gold mineralization and of a magmatic duality. The spatial, temporal and possible genetic relationship between these two features has prompted many studies, including this dissertation. Here are the main conclusions of this research:

1. Rocks from the syenitic suite and the granitic suite are emplaced along the KLF in three distinct magmatic domains: domain 1 is the KLF proper and contains granitic bodies emplaced as hypabyssal bodies, while syenitic rocks were emplaced as both hypabyssal bodies and extrusive flows (Timiskaming Group volcanic rocks). Domain 2 is the country north of the KLF and contains only granitic rocks emplaced as hypabyssal bodies. Domain 3 is the country south of the KLF and is characterized by large rounded intrusions. Among these, two are exclusively syenitic (Murdock Creek intrusion and Lebel stock), one is tholeiitic (Gauthier diorite intrusion), one is granitic (McElroy stock) and one contains both syenitic and granitic units (Otto stock).
2. Mineral chemistry indicates that the rocks of domains 1 and 3 evolved under oxidized conditions, while those of domain 2 evolved under unoxidized conditions.
3. Syenitic magmatism can be characterized as shoshonitic and granitic magmatism is associated to the sanukitoid suite of Shirey and Hanson (1984).
4. The coherent nature of fractionated REE patterns suggest that both suites evolved from a common source. The most likely parents are the hornblendite and lamprophyre units which are intimately associated both syenitic and granitic suites, especially to the Murdock Creek intrusion and the McElroy and Otto stocks in domain 3.

5. Both suites of rocks were derived from partial melting of upper mantle rocks under hydrous (granitic suite) or volatile-rich (syenitic suite) conditions. Metasomatizing agents (fluids or melts) from a subducted slab probably triggered melting in the upper mantle. These mafic partial melts produced granitic rocks were generated in the zone where amphibole was stable and syenitic rocks, where phlogopite was stable, by a combination of fractional crystallization and partial melting.

6. The regional distribution of syenitic and granitic rocks may yield information on the relative position of the subducted slab: oblique convergence from a south dipping, southwestern moving plate can account for the distribution of granitic and syenitic rocks and the formation of a sinistral strike-slip fault.

7. Syenitic and granitic magmatism along the continental margin is a product of oblique convergence and accretionary tectonics; these mechanisms are now believed to be essential in the formation of mesothermal gold deposits.

8. The tectonomagmatic model proposed for the Kirkland Lake area is similar to those inferred for the Cripple Creek area (Lindgren and Ransom, 1906; Mutschler et al., 1985, 1987), Papua NewGuinea (McInnes, 1992), and many other Phanerozoic areas (Kerrich and Wyman, 1990); these are also areas of important gold mineralization.

## References


Abraham, E.M., 1950, Geology of McElroy and part of Boston townships; Ontario Department of Mines, Annual Report, v. 59, Part 6, 66 p.

Anders, E. and Grevesse, N, 1989, Abundances of the elements: Meteoritic and solar; Geochimica et Cosmochimica Acta, v. 53, p. 197-214.

Anderson, A. T., 1980, Significance of hornblende in calc-alkaline andesites and basalts; American Mineralogist, v. 65, p. 837-851.

Arculus, R.J. and Powell, R., 1986, Source component mixing in the regions of arc magma generation; Journal of Geophysical Research, v. 91, p. 5913-5926.

Aurissichio, C., Federico, M. and Gianfagna, A., 1988, Clinopyroxene chemistry of the high-potassium suite from the Alban Hills, Italy; Mineralogy and Petrology, v. 39, p. 1-19.

Bailey, D.K., 1976, Applications of experiments to alkaline rocks; in *Alkaline Igneous Rocks*, edited by J.G. Fitton and B.G.J. Upton, Geological Society Special Publication nº 30, p. 1-13.

_____, 1983, The chemical and thermal evolution of rifts; Tectonophysics, v. 94, p 585-597.

_____, 1987, Mantle metasomatism- perspective and prospect; in *Alkaline Igneous Rocks*, J.G. Fitton and B.G.J. Upton, eds., Geological Society Special Publication No. 30, p. 1-13.

Baker, P.E., 1972, Volcanism at destructive plate margins, Journal of Earth Sciences, v. 8, p. 183-195.

_____, 1982, Evolution and classification of orogenic volcanic rocks; in *Andesites*, R.S Thorpe, ed., John Wiley and Sons, New York, 724 p.

_____, Gass, I.G., Harris, P.G. and Lemaître, R.W., 1964, The volcanological report of the Royal Society expedition to Tristan de Cunha, 1962; Philosophical Transactions of the Royal Society of London, 256A, p. 439-575.

Barberi, F., Santacroce, R. and Varet, J., 1982, Chemical aspects of rift magmatism; in *Continental and Oceanic Rifts*, American Geophysical Union Geodynamics Series, ed. G. Palmason, v. 8, p. 259-270.

Barker, F. and arth, J.G., 1976, Generation of trondhjemitic-tonalitic liquids and Archean bimodal trondhjemite-basalt suites; Geology, v. 4, p. 596-600.

Barnes, R.P., Rock, N.M.S., and Gaskarth, W.J., 1986, Late Caledonian dike-swarms of southern Scotland: New petrological and geochemical data from the Wigtown peninsula, Galloway; Journal of Geology, v. 21, p. 101-125.

Barth, T.F.W., 1954, The igneous rock complex of the Oslo region. XIV. Provenance of the Oslo magmas, Nor. Vidensk. Akad. Oslo, I, Math. Naturvidensk., p. 3-20.

Basu, A.R., Goodwin, A.M. and Tatsumoto, M., 1984, Sm-Nd study of Archean alkalic rocks from the Superior Province of the Canadian Shield; Earth and Planetary science Letters, v. 70, p. 40-46.

Bell, K., Anglin, C.D., and Franklin, J.M., 1989, Sm-Nd and Rb-Sr isotope systematics of scheelites: Possible implications for the age and genesis of vein-hosted gold deposits; Geology, v.17, p. 500-504.

Ben Othman, D., Arndt, N.A., White, W.M. and Jochum, K.P., 1990, Geochemistry and age of Timiskaming alkali volcanics and the Otto syenite stock, Abitibi, Ontario; Canadian Journal of Earth Sciences, v. 27, p. 1304-1311.

Bowden, P. and Turner, D.C., 1974, Peralkaline and associated ring-complexes in the Nigeria-Niger Province, west Africa; in *The Alkaline Rocks*, ed. H. Sørensen, Wiley and Sons, New York, p. 330-351.

Bowes, D.R. and Kosler, J., 1993, Geochemical comparison of the subvolcanic appinite suite of the British Caledonides and the durbachite suite of the Central European Hercynides: evidence for assoicated shoshonitic and granitic magmatism; Mineralogy and Petrology, v. 48, p. 47-63.

Brooks, C., Ludden, J., Pigeon, Y. and Hubregtse, J.J.M.W., 1982, Volcanism of shoshonite to high-K andesite affinity in an Archean arc environment, Oxford Lake, Manitoba; Canadian Journal of Earth Sciences, v. 19, p. 55-67.

Burrows, A.G. and Hopkins, P.E., 1923, Kirkland Lake gold area; Ontario Department of Mines, Annual Report for 1923, v. 32, Part 4, 96 p.

Burrows, D.R., Wood, P.C., and Spooner, E.T.C., 1986, Carbon isotope evidence for a magmatic origin for Archaean gold-quartz vein ore deposits; Nature, v. 321, p. 851-854.

_____ and Spooner, E.T.C., 1989, Relationships between Archean gold quartz vein-shear zone mineralization and igneous intrusions in the Val d'Or and Timmins areas, Abitibi Subprovince, Canada; Economic Geology, Monograph 6, p. 424-444.

Cameron, E.M.C., 1988, Archean gold: relation to granulite formation and redox zoning in the crust; Geology, v. 16, p. 109-112.

_____, 1989a, Derivation of gold by oxidative metamorphism of a deep ductile shear zone: Part 1. Conceptual model; Journal of Geochemical Exploration, v. 31, p. 135-147.

_____, 1989b, Derivation of gold by oxidative metamorphism of a deep ductile shear zone: Part 2. Evidence from the Bambkle Belt, south Norway; Journal of Geochemical Exploration, v. 31, p. 135-147.

_____, 1990, Alkaline magmatism at Kirkland Lake, Ontario: Product of strike-slip orogenesis; in *Current Research*, Part C, Geological Survey of Canada, Paper 90-1C, p. 261-269.

_____ and Carrigan, W.J., 1987, Oxygen fugacity of Archean felsic magmas: relationship to gold mineralization; in *Current Research*, part A, Geological Survey of Canada, Paper 87-1A, p. 281-298.

_____, and Hattori, K., 1987, Archean gold mineralization and oxidized hydrothermal fluids; Economic Geology, v. 82, p. 1177-1191.

Card, K.D., 1990, A review of the Superior Province of the Canadian Shield, a product of Archean accretion; Precambrian Research, v. 48, p. 99-156.

Cawthorn, R.G., 1976, Some chemical controls on igneous amphibole compositions; Geochimica et Cosmochimica Acta, v. 40, p 1319-1328.

Cherry, M.E., 1983, The association of gold and felsic intrusions-examples from the Abitibi belt; in *The Geology of Gold in Ontario*, edited by A.C. Colvine, Ontario Geological Survey, Miscellaneous Paper 110, p. 48-55.

Claoué-Long, J.C., King, R.W., and Kerrich, R., 1990, Archaean hydrothermal zircon in the Abitibi greenstone belt: Constraints on the timing of gold deposits; Earth and Planetary Science Letters, v. 98, p. 109-128.

Colvine, A.C., Fyon, A.J., Heather, K.B., Marmont, S., Smith P.M., and Troop, D.G., 1988, Archean lode gold deposits in Ontario; Ontario Geological Survey, Miscellaneous Paper 139, 136 p.

Condie, K.C., 1982, Archean andesites; in *Andesites*, R.S. Thorpe, ed., John Wiley and Sons, New York, 724 p.

_____, 1989, Geochemical changes in basalts and andesites across the Archean-Proterozoic boundary: Identification and significance; Lithos, v. 23, p. 1-18.

Cooke, D.L., and Moorhouse, W.W., 1969, Timiskaming volcanism in the Kirkland Lake area, Ontario, Canada; Canadian Journal of Earth Sciences, v. 6, p. 117-132.

Corfu, F., Krogh, T.E., Kwok, Y.Y., and Jensen, L.S., 1989, U-Pb zircon geochronology in the southwestern Abitibi greenstone belt, Superior Province; Canadian Journal of Earth Sciences, v. 26, p. 1747-1763.

_____, Jackson, S.L., and Sutcliffe, R.H., 1991, U-Pb ages and tectonic significance of late Archean alkalic magmatism and nonmarine sedimentation: Timiskaming Group, southern Abitibi belt, Ontario; Canadian Journal of Earth Sciences, v. 28, p. 489-503.

_____ and Noble, S.R., 1992, Genesis of the southern Abitibi greenstone belt, Superior Province, Canada: Evidence from zircon Hf isotope analyses using a single filament technique; Geochimica et Cosmochimica Acta, v. 56, p. 2081-2097.

Cullers, R.L. and Graf, J.L., 1984a, Rare earth elements in igneous rocks of the continental crust: predominantly basic and ultrabasic rocks; in *Rare Earth Element Geochemistry*, P. Henderson, ed., Chapter 7, p. 237-274.

_____ and _____, 1984b, Rare earth elements in igneous rocks of the continental crust: intermediate and silicic rocks- ore petrogenesis; in *Rare Earth Element Geochemistry*, Chapter 8, p. 275-308.

Czamanske, G.E. and Wones, D.R., 1973, Oxidation during magmatic differentiation, Finnmarka complex, Oslo area, Norway: Part 2, the mafic silicates; Journal of Petrology, v. 14, p. 349-380.

Davies, R.M. and Ballantyne, G.H., 1987, Geology of the Ladolam gold deposit, Lihir Island, Papua New Guinea; in *Pacific Rim Congress '87*, Australasian Institute of Minig and Metallurgy, p. 943-949.

Deer, W.A., Howie, R.A., and Zussman, J., 1966, *An Introduction to the Rock Forming Minerals*; Longmans, England, 528 p.

_____, _____, and _____, 1972, *Rock Forming Minerals, Volume 3: Sheet Silicates*; Longmans, England, 270 p.

_____, _____, and _____, 1978, *Rock Forming Minerals. Volume 2A. Single-chain silicates*; Wiley and sons, New York, 668 p.

Desrochers, J.-P., Hubert, C., Ludden, J.N. and Pilote, P., 1993, Accretion of Archean oceanic plateau fragments in the Abitibi greenstone belt, Canada; Geology, v. 21, p. 451-454.

Dimroth, E., Imreh, L., Goulet, N., and Rocheleau, M., 1983, Evolution ofthe south-central segment of the Archean Abitibi belt, Québec. Part III:

plutonic and metamorphic evolution and geotectonic model; Canadian Journal of Earth Sciences, v. 20, p. 1374-1388.

Dodge, F.C.W. and Moore, J.G., 1968, Occurrence and composition of biotites from the Cartridge Pass pluton of the Sierra Nevada batholith, California; United States Geological Survey Professionnal Paper 600-B, p. B6-B10.

Eby, G.N., 1987, The Monteregian and White Mountain alkaline igneous provinces, eastern North America; in *Alkaline Igneous Rocks*, J.G. Fitton and B.G.J. Upton, eds.; Geologcial Society Special Publication No. 30, p. 433-447.

Edgar, A.D., Sutcliffe, R.H., Collison, M.S., Clegg, M., Barron, K., 1991, Mineralogy, petrology and geochemistry of alkaline metavolcanic rocks and their relationship to gold mineralization in the Kirkland Lake area; in Abstracts, Ontario Mines and Minerals Symposium, p. 30.

Ellam, R.M., Menzies, M.A., Hawkesworth, C.J., Leeman, W.P., Rosi, M. and Serri, G., 1988, The transition from calc-alkaline to potassic orogenic magmatism in the Aeolian Islands, Southern Italy; Bulletin of Volcanology, v. 50, p. 386-398.

_____, Hawkeswoth, C.J., Menzies, M.A. and Rogers, N.W., 1989, The volcanism of southern Italy: role of subduction and the relationship between potassic and sodic alkaline magmatism; Journal of Geophysical Research, v. 94, p. 4589-4601.

Feng, R. and Kerrich, R., 1992, Geochemical evolution of granitoids from the Archean Abitibi southern volcanic zone and the Pontiac subprovince, Superior Province, Canada: implications for tectonic history and source regions; Chemical Geology, v. 98, p. 23-70.

Foley, S.F., Venturelli, G., Green, D.H. and Toscani, L., 1987, The ultrapotassic rocks: characteristics, classification and constraints for petrogenetic models; Earth Science Reviews, v. 24, p. 81-134.

_____and Wheller, G.E., 1990, Parallels in the origin of the geochemical signatures of island arc volcanics and continental potassic igneous rocks: the role of residual titanates; Chemical Geology, v. 85, p. 1-18.

_____ and Peccerillo, A., 1992, Potassic and ultrapotassic magmas and their origin; Lithos, v. 28, p. 181-185.

Fourcade, S. and Allègre, C.J., 1981, Trace element behaviour in granite genesis: a case study. The calc-alkaline plutonic association from the Querigut Complex (Pyrénées, France); Contributions to Mineralogy and Petrology, v.76, p. 177-195.

Fowler, M.B., 1988, Ach'uaine hybrid appinite pipes: evidence for mantle-derived shoshonitic parent magmas in Caledonian granite genesis, Geology, v. 16, p. 1026-1030.

Frey, F.A., Chappell, B.W. and Roy, S.D., 1978, Fractionation of rare-earth elements in the Tuolumne Intrusive Series, Sierra Nevada batholith, California, Geology, v. 6, p. 239-242.

Fyon, J.A., Troop, D.G., Marmont, S., and MacDonald, A.J., 1989, Introduction of gold into Archean crust, Superior Province, Ontario-Coupling between mantle-initiated magmatsim and lower crustal thermal maturation; Economic Geology, Monograph 6, p. 479-490.

Gill, J. and Whelan, P., Early rifting of an oceanic island arc (Fiji) produced shoshonitic to tholeiitic basalts, Journal of Geophysical Research, v. 94, p. 4561-4578.

Gott, G.B., McCarthy Jr., J.H., VanSickle, G.H., and McHugh, J.B., 1969, Distribution of gold and other metals in the Cripple Creek district, Colorado; U.S. Geological Survey, Professional Paper 625-A, p. A1-A17.

Green, N.L., 1982, Co-existing calcic amphiboles in calc-alkaline andesites: possible evidence of a zoned magma chamber; Journal of Volcanology and Geothermal Research, v. 12, p. 57-76.

Hall, A, 1987, *Igneous Petrology*; Longman Scientific, New York, 573 p.

Hamilton, W.B., 1988, Plate tectonics and island arcs; Geological Society of America Bulletin, v. 100, p. 1503-1527.

Hanson, G.N., 1980, Rare earth elements in petrogenetic studies of igneous systems; Annual Review of Earth and Planetary Sciences, v. 8, p. 371-406.

Hattori, K, 1989, Pervasive Alteration Related to Lamprophyre Intrusion in the Kirkland Lake Gold Camp, Abitibi Greenstone Belt, Abst. Joint Meeting Geological Association of Canada and the Mineralogical Association of Canada, p. A80.

_____ and Cameron, E.M.C., 1986, Archean magmatic sulfate; Nature, v. 319, p. 45-47.

_____ and Levesque, G., 1989, Hydrothermal activity in the Kirkland Lake intrusive complex; in *Geoscience Research Grant Program*, Summary of Research 1988-89, Ontario Geological Survey, Miscellaneous Paper 143, p. 59-67.

_____ and Hart, S.R., 1990, Fast recycling model inferred from isotope and trace element study of pyroxenes and feldspars in Timiskaming-type

alkaline rocks, southern Abitibi greenstone belt; Extended Abstract Volume, 3rd International Archean Symposium, Perth, p. 267-269.

Hawkesworth, C.J., Gallagher, K,. Hergt, J.M. and McDermott, F., 1993, Mantle and slab contributions in arc magmas; Annual Review of Earth and Planetary Sciences, v. 21, p. 175-204.

Hess, P.C., 1989, *Origins of Igneous Rocks*; Harvard University Press, Cambridge, Massachusetts,336 p.

Hewitt, D.F., 1963, The Timiskaming Series of the Kirkland Lake area; Canadian Mineralogist, v. 7, p. 497-523.

Hicks, K. D., 1990, Magmatic-Hydrothermal Wall Rock Alteration at the Lakeshore Gold Deposit, Kirkland Lake, Ontario;Unpublished M.Sc. thesis, University of Ottawa, Ottawa, Ontario, 195 p.

_____ and Hattori, K., 1988, Magmatic-hydrothermal and wallrock alteration petrology at the Lakeshore gold deposit, Kirkland Lake, Ontario; in *Geoscience Research Grant Program*, Summary of Research 1987-1988 (V.G. Milne, ed.); Ontario Geological Survey Miscellaneous Paper 140, p. 192-204.

Hodgson, C.J., 1986, Place of gold ore formation in the geological development of the Abitibi greenstone belt, Ontario, Canada; Transactions of the Institute of Mineralogy and Metallurgy, v. 95, p. B183-B194.

Hodgson, C.J., and MacGeehan, P.J., 1982, A review of the geological characteristics of "gold-only" deposits in the Superior Province of the Canadian Shield; in *The Geology of Canadian Gold Deposits*, Canadian Institute of Mining and Metallurgy, Special Volume 24, p. 211-228.

_____ and Hamilton, J.V., 1989, Gold mineralization in the Abitibi greenstone belt: End-stage result of Archean collisional tectonics?; Economic Geology, Monograph 6, p. 86-100.

_____, Hamilton, J.V., and Guimond, R.P., 1991, Relationship between gold deposits and the tectonic framework of the Abitibi greenstone belt in the Kirkland Lake-Larder Lake area; Ontario Geological Survey, Open File Report 5782, 60 p.

Hoffman, P. F., 1989, Precambrian geology and tectonic history of North America; in *The Geology of North America-An Overview*, edited by A.W. Bally and A.R. Palmer, Geological Society of America, The Geology of North America, Volume A.

_____, 1990, On accretion of granite-greenstone terranes; in *NUNA Conference on Greenstone Gold and Crustal Evolution*, F. Robert, P.A. Sheahan, S.D. Green, eds., Val d' Or, p. 32-45.

Hubert, C., Trudel, P. and Gélinas, L., 1984, Archean wrench fault tectonics and structural evolution of the Blake River Group, Abitibibelts, Québec; Canadian Journal of Earth Sciences, v. 21, p. 1024-1032.

Hyde, R.S., 1980, Sedimentary facies in the Archean Timiskaming Group, Abitibi greenstone belt, northeastern Ontario, Canada; Precambrian Research, v. 12, p. 161-195.

Hyndman, D.W., 1985, *Petrology of Igneous and Metamorphic Rocks*, McGraw-Hill, New York, 786 p.

Irvine, T.N. and Baragar, W.R.A., 1971, A guide to the chemical classification of the common volcanic rocks; Canadian Journal of Earth Sciences, v. 8, p. 523-548.

Jackson, 1992, Terminal tectonics of a late Archean greenstone belt: The sedimentary record and post-sedimentary structural history of the southern Abitibi greenstone belt near Larder Lake, Ontario; in *Program with Abstracts*, Geological Association of Canada, v. 17, p. A52.

_____, S.L., Sutcliffe, R.H., Ludden, J.N., Hubert, C., Green A.G., Milkereit, B., Mayrand, L., West, G.F., and Verplaest, P., 1990, Southern Abitibi greenstone belt: Archean crustal structure from seismic-reflection profiles, Geology, v. 18, p. 1086-1090.

_____ and Fyon, J.A., 1991, Abitibi greenstone belt supracrustal assemblages in Ontario: Products of arc volcanism, arc rifting, and terminal collision?; in *Program with Abstracts*, Geological Association of Canada, v. 16, p. A60.

Jakes, P. and White, A.J.R., 1972, Hornblende from calc-alkaline volcanic rocks of island arcs and continental margins; American Mineralogist, v. 57, p. 887- 902.

Jemielita, R.A., Davis, D.W., and Krogh, T.E., 1990, U-Pb evidence for Abitibi gold mineralization postdating greenstone magmatism and metamorphism; Nature, v. 346, p. 831-834.

Jensen. L.S., 1985, Stratigraphy and petrogenesis of Archean metavolcanic sequences, southwestern Abitibi Subprovince, Ontario; in *Evolution of Supracrustal Sequences*, edited by L.D. Ayres, K.D. Card and W. Weber, Geological Association of Canada Special Paper 28, p. 65-87.

Johnson, R.B., 1968, Geology of the igneous rocks of the Spanish Peaks region, Colorado, U.S. Geological Survey Professionnal Paper 594-G, p. G1-G47.

Keller, J., 1982, Mediterranean island arcs; in *Andesites: orogenic andesites and related rocks*, ed. R.S. Thorpe, Wiley and Sons, London, p. 307-325.

Kerrich, R., 1989, Archean gold: Relation to granulite formation or felsic intrusions?; Geology, v. 17, p. 1011-1015.

_____ and Wyman, D., 1990, Geodynamic setting of mesothermal gold deposits: an association with accretionary tectonic regimes; Geology, v. 18, p. 882-885.

_____ and Feng, R., 1992, Archean geodynamics and the Abitibi-Pontiac collision: implications for advection of fluids at transpressive collisional boundaries and the origin of giant quartz vein systems; Earth-Science Reviews, v. 32, p 33-60.

Laflèche, M.R., Dupuy, C. and Dostal, J., 1991, Archaean orogenic ultrapotassic magmatism: an example from the southern Abitibi greenstone belt; Precambrian Research, v. 52, p. 71-96.

Lalonde, A.E., 1992, Composition and pleochroic colour of biotite associated with gold deposits at Kirkland Lake; in *Geoscience Research Grant Program*, Summary of Research 1991-1992, V.G. Milne, ed.; Ontario Geological Survey Miscellaneous Paper 159, p. 104-110.

_____ and Martin, R.F., 1983, The Baie-des-Moutons syenitic complex, La Tabatière, Québec II. The ferromagnesian minerals; Canadian Mineralogist, v. 21, p. 81-91.

Leake, B. E., 1978, Nomenclature of amphiboles; Canadian Mineralogist, v. 16, p. 501-520.

LeBas, M.J., 1987, Ultra-alkaline magmatism with or without rifting; Tectonophysics, v. 13, p. 75-84.

_____, Le Maître, R.W., Streckeisen, A. and Zanettin, B., 1986, A chemical classification of volcanic rocks based on the total alkali-silica diagram; Journal of Petrology, v. 27, p. 745-750.

Levesque, G., 1989, *The Kirkland Lake Intrusive Complex: a petrogaphical and chemical approach*; unpublished B.Sc. thesis, University of Ottawa, 83 p.

Levesque, G.S. and Hattori, K., 1989, Late Archaean alkaline intrusive complex hosting the Kirkland Lake gold camp; in *Program with Abstracts*, Geological Association of Canada, v. 14, p. A81.

_____, Cameron, E.M., and Lalonde, A.E., 1991, Duality of magmatism along the Kirkland Lake-Larder Lake fault zone, Ontario; in *Current Research*, Part C, Geological Survey of Canada, Paper 91-1C, p. 17-24.

Lindgren, W. and Ransome, F.L., 1906, Geology and gold deposits of the Cripple Creek district, Colorado; U.S. Geological Survey, Professional Paper 54, 516 p.

Lloyd, F.E. and Bailey, D.K., 1975, Light element metasomatism of the continental mantle: the evidence and the consequences; Physics and Chemsitry of the Earth, v. 9, p. 389-416.

Lovell, H.L., 1972, Geology of the Eby and Otto area, district of Timiskaming, Ontario; Ontario Department of Mines and Northern Affairs, Geological Report 99, 34 p.

Ludden, J., Hubert, C., and Gariépy, C., 1986, The tectonic evolution of the Abitibi greenstone belt of Canada; Geological Magazine, v. 123, p. 153-166.

Luhr, J.F., Allan, J.F., Carmicheal, I.S.E., Nelson, S.A. and Hasenaka, T., 1989,Primitive calc-alkaline and alkaline rock types from the western Mexican volcanic belt; Journal of Geophysical Research, v. 94, p. 4515-4530.

MacDonald, G.A. and Katsura, T., 1964, Chemical compositon of Hawaiian lavas; Journal of Petrology, v. 5, p. 82-133.

MacLean, A., 1944, Map of Lebel township; Ontario Department of Mines, Annual Report, v. 53, Part 2.

_____, 1956, Geology of Lebel township; Ontario Department of Mines, Bulletin, 150, p. 1-63.

MacKenzie, D.E and Chappell, B.W., 1972, Shoshonitic and calc-alkaline lavas from the Highlands of Papua New Guinea; Contributions to Mineralogy and Petrology, v. 35, p. 50-62.

Marmont, S. and Corfu, F., 1989, Timing of gold introduction in the late Archean tectonic framework of the Canadian Shield: Evidence from U-Pb zircon geochronology of the Abitibi Subprovince; Economic Geology, Monograph 6, p. 101-111.

Martin, R.F., 1973, Controls of ordering and subsolidus phase relations in the alkali feldspars; in The Feldspars, Proceedings of a NATO Advanced Study Institute, Manchester, England, Manchester University Press, p. 313-336.

Martin, H., 1986, Effect of steeper Archean geothermal gradient on geochemistry of subduction-zone magmas; Geology, v. 14, p. 753-756.

Mason, D.R. and MacDonald, J.A., 1978, Intrusive rocks and porphyry copper occurrences of the Papua New Guinea-Solomon Islands region; Economic Geology, v. 73, p. 857-877.

McCulloch, M.T. and Gamble, J.A., 1991, Geochemical and geodynamical constraints on subduction zone magmatism; Earth and Planetary Science Letters, v. 102, p. 358-374.

McInnes, B.,1992, A Glimpse of Ephemeral Subduction Zone Processes from Simberi Island, Papua New Guinea; Unpublished Ph.D. thesis, University of Ottawa, Ottawa, Ontario, 253 p.

McKenzie, D. and Bickle, M.J., 1988, The volume and composition of melt generated by extension of the lithosphere; Journal of Petrology, v. 29, p. 625-679.

McNeil, A.M. and Kerrich, R. 1986, Archean lamprophyre dykes and gold mineralization, Matheson, Ontario: the conjunction of LILE-enriched mafic magmas, deep crustal structures, and Au concentration; Canadian Journal of Earth Sciences, v. 23, p. 324-343.

Meen, J.K., 1987a, Formation of shoshonites from calc-alkaline basalt magmas: geochemical and experimental constraints from the type locality; Contributions to Mineralogy and Petrology, v. 97, p. 333-351.

_____, 1987b, Mantle metasomatism and carbonatites; an experimental study of a complex relationship; Geological Society of America Special Paper 215, p. 91-100.

Mitchell, R.H., 1972, Composition of nepheline, pyroxene and biotite in ijolite from the Seabrook Lake complex, Ontario, Canada; Neues Jahrb. Min. , p. 415-432.

_____, 1990, A review of the compositional variation of amphiboles in alkaline plutonic complexes; Lithos, v. 26, p. 135-156.

Morimoto, N, 1989, Nomenclature of pyroxenes; Canadian Mineralogist, v.27, p. 143-156.

Morrison, G.W., 1980, Characteristics and tectonic setting of the shoshonite rock association; Lithos, v. 13, p. 97-108.

Muller, D., Rock, N.M.S. ans Groves, D.I., 1992, Geochemical discrimination between shoshonitic and potassic volcanic rocks in different tectonic settings: a pilot study; Mineralogy and Petrology, v. 46m p. 259-289.

Mutschler, F.E., Griffin, M.E., Stevens, D.S., and Shannon Jr., S.S., 1985, Precious metal deposits related to alkaline rocks in the North American

Cordillera-An interpretive review; Geological Society of South Africa Transactions, v. 88, p. 355-377.

_____, Larson, E.E. and Bruce, R.M., 1987, Laramide and younger magmatism in Colorado- New petrologic and tectonic variations on old themes; Colorado School of Mines Quarterly, v. 82, p. 1-47.

Nash, W.P. and Wilkinson, J.F.G., 1970, Shonkin Sag laccolith, Montana. I. Mafic minerals and estimates of temperature, pressure, oxygen fugacity and silica activity; Contributions to Mineralogy and Petrology, v. 25, p. 241-269.

Nemec, D., 1988, Origin of syenite porphyries in the Central Bohemian Pluton by magma mixing; Neues Jahrbuch Miner. Abh, v. 159, p. 59-71.

Noyes, H.J., Wones, D.R. and Frey, F.A., 1983, A tale of two plutons: petrographic and mineralogical constraints of the Red Lake and Eagle Creek plutons, Central Sierra Nevada, California, Journal of Geology, v. 91, p. 353-379.

Parsons, I., 1977, Feldspars and fluids in cooling plutons; Mineralogical Magazine, v. 42, p. 1-17.

_____, 1979, The Klokken gabbro-syenite complex, south Greenland: cryptic variation and origin of inversely graded layering; Journal of Petrology, v. 20, p. 653-694.

_____, Brown, W.L., and Jacquemin, H., 1986, Mineral chemistry and crystallizing conditions of the Mboutou layered gabbro-syenite-granite complex, north Cameroon; Journal of Petrology, v. 27, p. 1305-1329.

Perkins, C., McDougall, I., and Walshe, J.L., 1992, Timing of shoshonitic magmatism and gold mineralization, Sheahan-Grants and Glendale, New South Wales; Australian Journal of Earth Sciences, v. 39, p. 99-110.

Peterson, J.W. and Newton, R.C., 1990, $CO_2$-enhanced crustal melting: A possible link among porphyritic granites, lamprophyres and gold deposits; in *NUNA Conference on Greenstone Gold and Crustal Evolution*, F. Robert, P.A. Sheahan, S.D. Green, eds., Val d' Or, p. 67-72.

Ploeger, F.R. and Crocket, J.H., 1982, Relationship of gold to syenitic intrusive rocks in Kirkland Lake; in The Geology of Cnadian Gold Deposits, Canadian Institute of Mining and Metallurgy, Special Volume 24, p. 69-71.

Rancourt, D. G., Dang, M.Z., and Lalonde, A.E., 1992, Mössbauer spectroscopy of tetrahedral $Fe^{3+}$ in trioctahedral micas; American Mineralogist, v. 77, p. 34-43.

Richards, J.P., 1990, Petrology and geochemistry of alkalic intrusives at the Porgera gold deposit, Papua New Guinea; Journal of Geochemical Exploration, v. 35, p. 141-199.

Rive, M., Pintson, H. and Ludden, J.N., 1990, Characteristics of late Archean plutonic rocks from the Abitibi and Pontiac subprovinces, Superior Province, Canada; Canadian Institute of Mining and Metallurgy, Special Volume 43, p. 47-61.

Robert, F., 1989, Internal structure of the Cadillac tectonic zone southeast of Val d'Or, Abitibi greenstone belt, Québec; Canadian Journal of Earth Sciences, v. 26, p. 2661-2675.

_____, 1990, Dating old gold deposits; Nature, v.346, p. 792-793.

Robinson, P. , 1980, The compositional space of terrestrial pyroxenes-internal and external limits; in *Pyroxenes*, C.T. Prewitt, ed., Reviews in Mineralogy, Volume 7, Mineralogical Society of America, p. 419-494.

Rock, N.M.S., 1987, The nature and origin of lamprophyres: An overview; in Fitton, J.G., and Upton, B.G.J., eds., *Alkaline Igneous Rocks*; Geological Society of London Special Publication 30, p. 191-226.

_____, 1991, *Lamprophyres*, Blackie and Sons, London, 285 p.

Rock, N.M.S., and Hunter, R.H., 1987, Late Caledonian dike-swarms of northern Britain; spatial and temporal intimacy between lamprophyric and granitic magmatism; Geologische Rundschau, v. 76, p. 807-826.

_____, and Groves D.I., 1988, Can lamprophyres resolve the genetic controversy over mesothermal gold deposits?; Geology, v. 16, p. 538-541.

_____, _____, Perring, C.S., and Golding, S.D., 1989, Gold, lamprophyres, and porphyries: What does their association mean?; Economic Geology, Monograph 6, p. 609-625.

Rowins, S.M., 1990, Mineralogy and geochemistry of the Murdock Creek intrusion, Kirkland Lake, Ontario; unpublished M.Sc. thesis, University of Ottawa, 196 p.

_____, Lalonde, A.E.,and Cameron, E.M., 1989, Geology of the Archean Murdock Creek intrusion, Kirkland Lake, Ontario; in *Current Research*, Part C, Geological Survey of Canada, Paper 89-1C, p. 313-323.

_____, _____, and _____, 1991, Magmatic oxidation in the syenitic Murdock Creek intrusion, Kirkland Lake, Ontario: Evidence from the ferromagnesian silicates; Journal of Geology, v. 99, p. 395-414.

_____, Cameron, E.M., Lalonde, A.E. and Ernst, R.E., 1993, Petrogenesis of the late Archean syenitic Murdock Creek pluton, Kirkland Lake, Ontario: evidence for an extensional tectonic setting; Canadian Mineralogist, v. 31, p. 219-244.

Shirey, S.B. and Hanson, G.N., 1984, Mantle-derived Archaean monzodiorites and trachyandesites; Nature, v. 310, p. 22-224.

Sibson, R.H., Robert, F., and Poulsen K.H., 1988, High-angle reverse faults, fluid-pressure cycling, and mesothermal gold-quartz deposits; Geology, v. 16, p. 551-555.

Size, W.B., 1972, Petrology of the Red Hill syenite complex, New Hampshire; Geological Society of America Bulletin, v. 83, p. 3747-3760.

Sloman, L.E., 1989, Triassic shoshonites from the Dolomites, northern Italy: alkaline arc rocks in a strike-slip setting; Journal of Geophysical Research, v. 94, p. 4655-4666.

Smith, A.R. and Sutcliffe, R.H., 1988, Plutonic rocks of the Abitibi Subprovince; Project 88-08, Ontario Geological Survey, Miscellaneous Paper 141, p. 188-196.

Speer, A., 1984, Micas in igneous rocks; in *Micas*, S.W. Bailey, ed.Reviews in Mineralogy, Volume 13, Mineralogical Society of America, p. 299-356.

Spera, F.J., 1984, Carbon dioxide in igneous petrogenesis: III. Role of volatiles in the ascent of alkaline magmas with special reference to xenolith-bearing mafic lavas; Contributions to Mineralogy and Petrology, v. 88, p. 217-232.

Stern, R.A., Hanson, G.N. and Shirey, S.B., 1989, Petrogenesis of mantle-derived, LILE-enriched Archean monzodiorites and trachyandesite (sanukitoids) in southwestern Superior Province; Canadian Journal of Earth Sciences, v. 26, p. 1688-1712.

Streckeisen, A., 1976, To each plutonic rock its proper name; Earth Science Reviews, v. 12, p. 1-33.

_____, 1979, Classification and nomenclature of volcanic rocks, lamprophyres, carbonatites, and melilitic rocks: recommendations and suggestions of the IUGS subcommission on the systematics of igneous rocks; Geology, v. 7, p. 331-335.

Stricker, S.J., 1978, The Kirkland-Larder stratiform carbonatite, Mineralium Deposita, v. 13, p. 355-367.

Sutcliffe. R.H. and Beakhouse, G.P., 1988, Archean plutonic rocks in the southern part of the Superior Province: magmatism during arc

construction and arc accretion; in *Summary of Field Work and Other Activities*, Ontario Geological Survey Miscellaneous Paper 151, p. 91-98

Sutcliffe, R.H., Smith, A.R., Doherty, W., and Barnett, R.L., 1990, Mantle derivation of Archean amphibole-bearing granitoid and associated mafic rocks: Evidence from the southern Superior Province, Canada; Contributions to Mineralogy and Petrology, v. 105, p. 255-274.

Sylvester, A.G., 1988, Strike-slip faults; Geological Society of America Bulletin, v. 100, p. 1666-1703.

Tatsumi, Y., 1986, Formation of the volcanic front in subduction zones, Geophysical Research Letters, v. 13, p. 717-720.

_____, 1989, Migration of fluid phases and genesis of basalt magmas in subduction zones; Journal of Geophysical Research, v. 94B, p. 4697-4707.

Thomson, J.E., 1941, Geology of McGarry and McVittie townships, Larder Lake area; Ontario Department of Mines, Annual Report, v. 50, Part 7, 94 p.

_____, 1950, Geology of Teck township and Kenogami Lake area, Kirkland Lake gold belt; Ontario Department of Mines, Annual Report for 1948, v. 57, Part 5, p. 1-53. Reprinted 1989.

Thomson, J.E. and Griffis, A.T., 1941, Geology of Gauthier township, east Kirkland Lake area; Ontario Department of Mines, Annual Report, Part 8, 26 p.

_____, Charlewood, C.H., Griffin, K., Hawley, J.E., Hopkins, H., MacIntosh, C.G., Ogryzlo, S.P., Perry, O.S.,and Ward, W., 1950, Geology of the main ore zone at Kirkland Lake; Ontario Department of Mines, Annual Report for 1948, v. 57, Part 5, p. 54-196.

Thompson, R.N. and Fowler, M.B., 1986, Subduction-related shoshonitic and ultrapotassic magmatism: a study of Siluro-Ordovician syenites from the Scottish Caledonides; Contributions to Mineralogy and Petrology, v. 94, p. 507-522.

Todd, E.W., 1928, Kirkland Lake gold area-A detailed study of the Central Zone and vicinity; Ontario Department of Mines, Annual Report, v. 37, Part 2, p. 1-176.

Ujike, O, 1985, Geochemistry of Archean alkalic volcanic rocks from the Crystal Lake area, east of Kirkland Lake, Ontario, Canada; Earth and Planetary Science Letters, v. 73, p. 333-344.

Venturelli, G., Thorpe, R.S., Dal Piaz, G.V., Del Moro, A., and Potts, P.J., 1984, Petrogenesis of calc-alkaline, shoshonitic ans associated ultrapotassic

Oligocene volcanic rocks from the northwestern Alps, Italy, Contributions to Mineralogy and Petrology, v. 86, p. 209-220.

Verma, S.P. and Nelson, S.A., 1989, Isotopic and trace element constraints on the origin and evolution of alkaline and calc-alkaline magmas in the northwestern Mexican volcanic belt; Journal of Geophysical Research, v. 94, p. 4531-4544.

Wendlandt, R.F. and Eggler, D.H., 1980, The origins of potassic magmas: 1. Melting relations in the system $KAlSiO_4$ - $Mg_2SiO_4$ - $SiO_2$ and $KAlSiO_4$ - MgO - $SiO_2$ to 30 kilobars; American Journal of Earth Sciences, v. 280, p. 385-420.

Wheller, G.E., Varne, R., Foden, J.D. and Abbott, M.J., 1987, Geochemistry of Quaternary volcanism in the Sunda-Banda arc, Indonesia, and three-component genesis of island-arc basaltic magmas; Journal of Volcanology and Geothermal Research, v. 32, p. 137-160.

Williams, L.A.J., 1982, Physical aspects of magmatism in continental rifts; in *Continental and Oceanic Rifts*, American Geophysical Union Geodynamics Series, ed. G. Palmason, v. 8, p. 193-222.

Wilson, A.D., 1960, The micro-determination of ferrous iron in silicate minerals by a volumetric and colorimetric method; Analyst, v. 85, p. 823-827.

Wilson, M.E., 1956, Early Precambrian rocks of the Timiskaming region, Québec and Ontario, Canada; Bulletin of the Geological Society of America, v. 67, p. 1397-1430.

_____, 1989, *Igneous Petrogenesis*, Unwin Hyman, London, 466 p.

Wones, D.R. and Gilbert, M.C., 1982, Amphiboles in the igneous environment; in *Amphiboles: Petrology and Experimental Phase Relations*, D.R. Veblen and P.H. Ribbe, eds, Mineralogical Society of America, Reviews in Mineralogy, Volume 9B, p. 355-390

Wyman, D.A. and Kerrich, R., 1988, Alkaline magmatism, major structures, and gold deposits: Implications for greenstone belt metallogeny; Economic Geology, v. 83, p. 454-461.

_____ and _____, 1989, Archean shoshonitic lamprophyres associated with Superior Province gold deposits: Distribution, tectonic setting, noble metal abundances, and significance for gold mineralization; Economic Geology, Monograph 6, p. 651-667.

Yagi, K and Takeshita, H, 1987, Impact of hornblende crystallization for the genesis of calc-alkaline andesites; in *Magmatic Processes: Physicochemical Principles*, Mysen, B.O., ed., Geochemical Society Special Publication 1, p. 183-190.

# Appendix A

## Geochemical data for the rocks of the Kirkland Lake area

### A.1 Whole rock and trace element data

### A.2 Rare earth element data

### A.3 Electron microprobe mineral analyses

#### A.3.1 Clinopyroxene
#### A.3.2 Biotite
#### A.3.3 Amphibole

## A.1 Whole rock and trace element data

Whole rock analyses of glass disks (fusion with a mixture of lithium metaborate and lithium carbonate) by wavelength dispersive X-ray fluorescence spectroscopy were performed at the Geological Survey of Canada and at the University of Ottawa. The results were calibrated against standard rock samples. The following are the estimates of validity of results, with ranges in absolute (first value) and relative (second value) variation from true value :

Major elements :

| | |
|---|---|
| $SiO_2$, $Al_2O_3$ : | ± 0.4 % + 1% of concentration |
| $TiO_2$ $P_2O_5$ : | ± 0.02 % + 1% of concentration |
| $Fe_2O_3(t)$ , MgO, CaO: | ± 0.1 % + 1% of concentration |
| MnO : | ± 0.01 % + 2% of concentration |
| $Na_2O$ : | ± 0.5 % + 1% of concentration |
| $K_2O$ : | ± 0.05 % + 1% of concentration |
| FeO : | ± 0.2 % + 5% of concentration |
| $H_2O(t)$ : | ± 0.1 % + 5% of concentration |
| $CO_2$ : | ± 0.1 % + 3% of concentration |
| S(t) : | ± 0.04 % + 5% of concentration |

Minor elements :

| | |
|---|---|
| Ba, Pb, Sr, Zr : | ± 20 ppm+ 10% of concentration |
| Be, Sc, Yb : | ± 0.5 ppm+ 5% of concentration |
| Co, V, Y, Zn : | ± 5 ppm+ 5% of concentration |
| Cr, Cu, La, Ni : | ± 10 ppm+ 5% of concentration |
| Nb : | ± 30 ppm+ 10% of concentration |
| Rb : | ± 20 ppm+ 2% of concentration |

All samples analyzed contained Nb values lower than accuracy estimates and are reported as zero. FeO was determined by iron titration following the method of Wilson (1960). $Fe_2O_3$ was calculated using measured FeO values. $H_2O(t)$ was determined by the furnace method, $CO_2$ was determined by combustion and infrared detection, while S(t) was determined by ion chromatography.

(n.d. indicates not determined)

| | AFMS, Dom1 LC-1 | AFMS, Dom1 LC-9 | AFMS, Dom1 LC-10 | AFMS, Dom1 GL89046/LH4 | AFMS, Dom1 GL90032 | AFMS, Dom1 GL90058 | AFMS, Dom1 GL90163 | AFMS, Dom1 Thomson, 50 | AFMS, Dom1 Ker&Wat | AFMS, Dom1 AvgKer&Wat | AFMS, Dom1 Ker&Wat | AFMS, Dom1 CAM&CAR 87 |
|---|---|---|---|---|---|---|---|---|---|---|---|---|
| SiO2 (wt.%) | 51,3 | 50,9 | 51,9 | 47,5 | 50,7 | 51,8 | 49,1 | 50,24 | 48,9 | 51,74 | 49,7 | 52,6 |
| TiO2 | 0,83 | 0,86 | 0,84 | 0,85 | 1,02 | 0,85 | 0,82 | 0,93 | 0,85 | 1,22 | 0,81 | 0,92 |
| Al2O3 | 12,9 | 12,5 | 13,3 | 12,8 | 12 | 12,9 | 13,8 | 16,43 | 12,4 | 14,01 | 13 | 15,4 |
| Fe2O3T | 9,1 | 9,7 | 8,9 | 8,6 | 9,7 | 9,5 | 7,8 | 7,75 | 9,4 | 8,03 | 9,8 | 8,83 |
| Fe2O3 | 3,2 | 3,6 | 3,1 | 2,9 | 2 | 3,8 | 3,1 | 2,77 | 3,76 | 3,18 | 3,6 | 3,5 |
| FeO | 5,3 | 5,5 | 5,2 | 5,1 | 6,9 | 5,1 | 4,2 | 4,48 | 5,08 | 4,36 | 5,58 | 4,8 |
| MnO | 0,14 | 0,15 | 0,14 | 0,13 | 0,14 | 0,15 | 0,13 | 0,16 | 0,14 | 0,11 | 0,13 | 0,14 |
| MgO | 7,68 | 8,25 | 7,15 | 6,8 | 8,92 | 7,8 | 5,14 | 3,8 | 7,9 | 5,1 | 6,9 | 4,13 |
| CaO | 7,51 | 7,88 | 6,93 | 5,8 | 7,28 | 7,77 | 6,39 | 5,84 | 6,4 | 6,36 | 5,3 | 5,22 |
| Na2O | 2,9 | 2,7 | 3,1 | 2,8 | 4,4 | 3,1 | 3,1 | 3,54 | 3,5 | 2,76 | 2,6 | 3,83 |
| K2O | 5,09 | 5,03 | 5,22 | 4,78 | 2,39 | 4,83 | 6,36 | 5,84 | 4,5 | 5,31 | 6,5 | 3,84 |
| H2OT | 1,1 | 1,2 | 1,1 | 1,7 | 1,7 | 1 | 1,4 | 1,9 | 4,3 | 5,4 | 4,5 | 2,1 |
| CO2T | 0,4 | 0,2 | 0,4 | 7,5 | 2 | 0,4 | 4,3 | 3,35 | 3,2 | 4,5 | 3,5 | 2,5 |
| P2O5 | 0,57 | 0,61 | 0,58 | 0,58 | 0,46 | 0,6 | 0,54 | 0,51 | 0,54 | 0,46 | 0,6 | 0,55 |
| S | 0 | 0 | 0 | 0,01 | 0,2 | 0,05 | 0,03 | 0 | n.d | n.d | n.d | 0,04 |
| Ba (ppm) | 2200 | 2200 | 2200 | 2000 | 860 | 1900 | 1900 | n.d | 1166 | 1894 | 2183 | n.d |
| Be | 2,3 | 2,2 | 2,7 | 2,9 | 1,7 | 2,5 | 3,2 | n.d | n.d | n.d | n.d | n.d |
| Co | 36 | 36 | 35 | 31 | 34 | 34 | 35 | n.d | 53 | 25 | 52 | n.d |
| Cr | 270 | 270 | 250 | 250 | 380 | 250 | 210 | n.d | 366 | 238 | 332 | n.d |
| Cu | 93 | 92 | 92 | 79 | 69 | 71 | 74 | n.d | 15 | n.d | 16 | n.d |
| La | 36 | 35 | 36 | 39 | 28 | 36 | 33 | n.d | n.d | n.d | n.d | n.d |
| Nb | 0 | 0 | 0 | 0 | 0 | 0 | 0 | n.d | 6 | n.d | 20 | n.d |
| Ni | 84 | 86 | 75 | 68 | 93 | 81 | 58 | n.d | 118 | 57 | 121 | n d |
| Rb | 190 | 190 | 170 | 130 | 110 | 160 | 230 | n.d | 209 | n.d | 312 | n.d |
| Sc | 21 | 22 | 19 | 19 | 24 | 22 | 17 | n.d | 4,6 | n.d | 23 | n.d |
| Sr | 1400 | 1300 | 1300 | 1200 | 540 | 1200 | 1200 | n.d | 629 | n.d | 1622 | n.d |
| V | 160 | 170 | 150 | 160 | 160 | 160 | 140 | n.d | 350 | n.d | 390 | n.d |
| Y | 20 | 20 | 19 | 20 | 21 | 21 | 19 | n.d | 22 | n.d | 23 | n.d |
| Yb | 1,5 | 1,5 | 1,4 | 1,5 | 1,6 | 1,6 | 1,5 | n.d | n.d | n.d | n.d | n.d |
| Zn | 84 | 83 | 79 | 78 | 100 | 100 | 80 | n.d | 125 | 106 | 136 | n.d |
| Zr | 150 | 130 | 140 | 120 | 140 | 140 | 130 | n.d | 145 | n.d | 170 | n.d |
| Ti ppm | 5187,5 | 5375 | 5250 | 5312,5 | 6375 | 5312,5 | 5125 | 5812,5 | 5312,5 | 7625 | 5062,5 | 5750 |
| Total | 99,4 | 99,6 | 99,4 | 99,7 | 100,4 | 100,6 | 98,9 | 99,79 | 98,8 | 99,8 | 99,8 | 99,8 |
| Larsen Index | 1,68 | 0,35 | 3,22 | 2,90 | -3,83 | 1,41 | 6,98 | 8,45 | -8,00 | 6,72 | 5,27 | 7,21 |
| Na2O+K2O | 7,99 | 7,73 | 8,32 | 7,58 | 6,79 | 7,93 | 9,46 | 9,38 | 8 | 8,07 | 9,1 | 7,67 |
| K2O/Na2O | 1,76 | 1,86 | 1,68 | 1,71 | 0,54 | 1,56 | 2,05 | 1,65 | 1,29 | 1,92 | 2,50 | 1,00 |
| Fe2O3/FeT | 0,38 | 0,40 | 0,37 | 0,36 | 0,22 | 0,43 | 0,42 | 0,38 | 0,43 | 0,42 | 0,39 | 0,42 |
| Fet/(Fet+Mg) | 0,53 | 0,52 | 0,54 | 0,54 | 0,50 | 0,53 | 0,59 | 0,66 | 0,53 | 0,60 | 0,57 | 0,67 |
| Zr/Y | 7,50 | 6,50 | 7,37 | 6,00 | 6,67 | 6,67 | 6,84 | | 6,59 | | 7,39 | |
| Ni/Cr | 0,31 | 0,32 | 0,30 | 0,27 | 0,24 | 0,32 | 0,28 | | 0,32 | 0,24 | 0,36 | |
| Rb/Sr | 0,14 | 0,15 | 0,13 | 0,11 | 0,20 | 0,13 | 0,19 | | 0,33 | | 0,19 | |
| Rb/Zr | 1,27 | 1,46 | 1,21 | 1,08 | 0,79 | 1,14 | 1,77 | | 1,44 | | 1,84 | |
| Ti/V | 32,42 | 31,62 | 35,00 | 33,20 | 39,84 | 33,20 | 36,61 | | 15,18 | | 12,98 | |

| | AFMS, Dom1 Cam^Car 67 | AFS, Dom1 Thomson, 50 | AFS, Dom1 GL8857 | HybS, Dom1 GL8856 | Lamp. Dom1 GL8858 | Lamp, Dom1 GL90016 | Lamp, Dom1 GL90079 | IntBrec, Dom1 GL90202 | IntBrec, Dom1 GL90034 | IntBrec, Dom1 GL90038 | Trach, Dom1 GL90019 | Trach, Dom1 GL90067 |
|---|---|---|---|---|---|---|---|---|---|---|---|---|
| SiO2 (wt.%) | 51,1 | 57,02 | 52,6 | 53,4 | 42,1 | 47,9 | 46,1 | 51,6 | 55,6 | 51,7 | 49,8 | 54,4 |
| TiO2 | 0,9 | 1,9 | 0,64 | 0,93 | 0,81 | 0,8 | 0,74 | 0,76 | 0,67 | 0,85 | 0,82 | 0,75 |
| Al2O3 | 14,7 | 18,3 | 16 | 15,8 | 12 | 11,1 | 9,7 | 9,1 | 15,3 | 14,8 | 12,9 | 21,4 |
| Fe2O3T | 9,50 | 3,95 | 5,8 | 9,5 | 10 | 8,8 | 8,9 | 6,4 | 7,7 | 9,5 | 8,6 | 5,8 |
| Fe2O3 | 4,5 | 0,98 | 2,5 | 3,5 | 7,1 | 3,4 | 3,3 | 2,8 | 2,4 | 4,4 | 3,3 | 3,8 |
| FeO | 4,5 | 2,67 | 3 | 5,4 | 2,6 | 4,9 | 5 | 5 | 4,8 | 4,6 | 4,8 | 1,8 |
| MnO | 0,09 | 0,17 | 0,1 | 0,15 | 0,17 | 0,13 | 0,16 | 0,18 | 0,11 | 0,17 | 0,12 | 0,1 |
| MgO | 5,82 | 1,04 | 3,24 | 4,52 | 6,67 | 11,2 | 14,2 | 8,33 | 4,61 | 5,73 | 5,22 | 0,87 |
| CaO | 4,28 | 1,99 | 5,29 | 4,42 | 8,15 | 9,8 | 9,6 | 12,4 | 4,04 | 6,39 | 5,91 | 1,53 |
| Na2O | 3,55 | 4,25 | 4,6 | 4,1 | 4,3 | 1,6 | 0,8 | 2,7 | 4,6 | 3,1 | 5 | 6,1 |
| K2O | 4,65 | 7,41 | 5,8 | 4,41 | 3,03 | 4,02 | 2,93 | 2,59 | 2,32 | 4,4 | 0,95 | 4,33 |
| H2OT | 2,3 | 0,95 | 1,5 | 1,9 | 0,7 | 2,5 | 4,2 | 0,9 | 2,6 | 1,7 | 1,9 | 1,7 |
| CO2T | 2,5 | 3,06 | 3,9 | 0,9 | 11,9 | 1,1 | 2,1 | 2,5 | 2,3 | 0,9 | 8,2 | 2,5 |
| P2O5 | 0,65 | 0,23 | 0,35 | 0,52 | 0,3 | 0,73 | 0,63 | 0,35 | 0,3 | 0,36 | 0,56 | 0,16 |
| S | 0,04 | 0 | 0,01 | 0,01 | 0,04 | 0,01 | 0,02 | 0,03 | 0,03 | 0 | 0,03 | 0,07 |
| Ba (ppm) | n.d | n.d | 1200 | 2400 | 900 | 1300 | 1800 | 610 | 1900 | 2400 | 1100 | 3600 |
| Be | n.d | n.d | 3,8 | 2,1 | 2,7 | 2,7 | 2,5 | 1,8 | 2 | 1,7 | 2,1 | 6,8 |
| Co | n.d | n.d | 18 | 29 | 32 | 38 | 45 | 34 | 29 | 31 | 30 | 12 |
| Cr | n.d | n.d | 100 | 55 | 91 | 500 | 890 | 460 | 110 | 100 | 260 | 4 |
| Cu | n.d | n.d | 74 | 40 | 53 | 100 | 20 | 40 | 66 | 25 | 88 | 87 |
| La | n.d | n.d | 41 | 43 | 13 | 79 | 67 | 23 | 38 | 42 | 36 | 100 |
| Nb | n.d | n.d | 0 | 0 | 0 | 0 | 0 | 0 | 0 | 0 | 0 | 0 |
| Ni | n.d | n.d | 27 | 10 | 66 | 160 | 330 | 95 | 24 | 21 | 97 | 0 |
| Rb | n.d | n.d | 140 | 91 | 230 | 120 | 94 | 71 | 52 | 97 | 19 | 400 |
| Sc | n.d | n.d | 10 | 17 | 32 | 22 | 21 | 26 | 19 | 25 | 19 | 4,2 |
| Sr | n.d | n.d | 840 | 1300 | 1300 | 1200 | 1200 | 710 | 1300 | 1300 | 1000 | 990 |
| V | n.d | n.d | 81 | 160 | 200 | 140 | 130 | 130 | 160 | 180 | 150 | 200 |
| Y | n.d | n.d | 18 | 22 | 14 | 32 | 28 | 20 | 20 | 21 | 18 | 34 |
| Yb | n.d | n.d | 1,7 | 1,7 | 1,3 | 1,7 | 1,6 | 1,5 | 1,9 | 1,8 | 1,4 | 2,2 |
| Zn | n.d | n.d | 65 | 100 | 83 | 72 | 100 | 62 | 85 | 91 | 150 | 160 |
| Zr | n.d | n.d | 190 | 160 | 140 | 230 | 180 | 100 | 160 | 150 | 150 | 380 |
| Tl ppm | 5625 | 11875 | 4000 | 5812,5 | 5062,5 | 5000 | 4625 | 4750 | 4187,5 | 5312,5 | 5125 | 4087,5 |
| Total | 100,4 | 99,97 | 99,8 | 100,4 | 100,2 | 99,5 | 100 | 99,5 | 100 | 99,5 | 99,8 | 100,1 |
| Larsen index | 7,07 | 20,70 | 11,79 | 7,85 | -0,37 | -5,93 | -10,52 | -5,96 | 7,38 | 4,90 | 1,80 | 18,25 |
| Na2O+K2O | 8,2 | 11,66 | 10,4 | 8,51 | 7,33 | 5,62 | 3,73 | 5,29 | 6,92 | 7,5 | 5,95 | 10,43 |
| K2O/Na2O | 1,31 | 1,74 | 1,26 | 1,08 | 0,70 | 2,51 | 3,66 | 0,96 | 0,50 | 1,42 | 0,19 | 0,71 |
| Fe2O3/FeT | 0,50 | 0,27 | 0,45 | 0,39 | 0,73 | 0,41 | 0,40 | 0,36 | 0,33 | 0,49 | 0,41 | 0,68 |
| Fet/(Fet+Mg) | 0,61 | 0,78 | 0,63 | 0,66 | 0,59 | 0,43 | 0,37 | 0,48 | 0,61 | 0,61 | 0,61 | 0,87 |
| Zr/Y | | | 10,56 | 7,27 | 10,00 | 7,19 | 6,43 | 5,00 | 8,00 | 7,14 | 8,33 | 11,18 |
| Ni/Cr | | | 0,27 | 0,18 | 0,73 | 0,32 | 0,37 | 0,21 | 0,22 | 0,21 | 0,37 | 0,00 |
| Rb/Sr | | | 0,17 | 0,07 | 0,18 | 0,10 | 0,08 | 0,10 | 0,04 | 0,07 | 0,02 | 0,40 |
| Rb/Zr | | | 0,74 | 0,57 | 1,64 | 0,52 | 0,52 | 0,71 | 0,33 | 0,65 | 0,13 | 1,05 |
| Ti/V | | | 49,38 | 36,33 | 25,31 | 35,71 | 35,58 | 36,54 | 26,17 | 29,51 | 34,17 | 23,44 |

| | Trach, Dom1 GL90070 | Trach, Dom1 GL90085 | Trach, Dom1 GL90091 | Trach, Dom1 GL90092 | Trach,Dom1 GL90099 | Trach, Dom1 GL90109 | Trach, Dom1 GL90134 | Trach, Dom1 GL90135 | Trach, Dom1 GL90141 | Trach, Dom1 GL90160 | Trach, Dom1 GL90160 dup | Trach, Dom1 GL90198 |
|---|---|---|---|---|---|---|---|---|---|---|---|---|
| SiO2 (wt.%) | 55,4 | 51,7 | 58,7 | 45,7 | 47,6 | 54,1 | 50,8 | 53,2 | 57,8 | 55,7 | 56 | 51,1 |
| TiO2 | 0,63 | 0,82 | 0,46 | 0,86 | 0,8 | 0,66 | 0,92 | 0,72 | 0,57 | 0,56 | 0,58 | 0,76 |
| Al2O3 | 15,3 | 18,3 | 14,8 | 14,7 | 15,3 | 18,6 | 15,2 | 15,7 | 16,3 | 14,6 | 14,6 | 17,8 |
| Fe2O3T | 7,5 | 6,1 | 5,2 | 7,5 | 8,2 | 4,9 | 9,7 | 8,6 | 7,1 | 7 | 6,9 | 6,2 |
| Fe2O3 | 3,3 | 2,4 | 2,5 | 3,6 | 3,6 | 3 | 4 | 4 | 2,4 | 3,2 | 3,1 | 3,3 |
| FeO | 3,8 | 3,3 | 2,4 | 3,5 | 4,1 | 1,7 | 5,1 | 4,1 | 4,2 | 3,4 | 3,4 | 2,6 |
| MnO | 0,11 | 0,15 | 0,08 | 0,22 | 0,14 | 0,16 | 0,17 | 0,14 | 0,12 | 0,13 | 0,13 | 0,17 |
| MgO | 4,16 | 2,41 | 3,28 | 3,68 | 3,85 | 0,76 | 6,13 | 4,8 | 3,88 | 6,73 | 6,72 | 2,44 |
| CaO | 3,58 | 4,03 | 3,45 | 6,16 | 6,98 | 3,76 | 6,58 | 7,09 | 3,32 | 4,93 | 4,92 | 4,16 |
| Na2O | 4,3 | 4,7 | 4,1 | 1,7 | 4,3 | 7,6 | 2,9 | 4,5 | 7,2 | 4,2 | 4,2 | 2,7 |
| K2O | 3,87 | 4,85 | 3,59 | 7,47 | 4,52 | 2,35 | 3,58 | 1,99 | 1,5 | 2,92 | 2,94 | 7,99 |
| H2OT | 2 | 2 | 1,4 | 1,3 | 1,6 | 1 | 2,5 | 2,1 | 1,4 | 2,1 | 2,1 | 1,5 |
| CO2T | 2 | 3 | 4,8 | 8,6 | 5,6 | 4,3 | 0,4 | 1,4 | 0,7 | 0,2 | 0,2 | 2,7 |
| P2O5 | 0,52 | 0,3 | 0,29 | 0,57 | 0,55 | 0,22 | 0,46 | 0,37 | 0,32 | 0,27 | 0,26 | 0,3 |
| S | 0,19 | 0,05 | 0,01 | 0,14 | 0,05 | 0,13 | 0 | 0 | 0 | 0 | 0 | 0,26 |
| Ba (ppm) | 3500 | 4100 | 1300 | 2800 | 2100 | 5300 | 1400 | 720 | 460 | 1100 | 1100 | 6100 |
| Be | 2,4 | 6,2 | 2,3 | 3,5 | 2,9 | 4,6 | 1,4 | 1,8 | 2,5 | 1,8 | 1,8 | 6,1 |
| Co | 24 | 18 | 18 | 19 | 24 | 14 | 29 | 27 | 21 | 32 | 32 | 19 |
| Cr | 85 | 84 | 110 | 97 | 58 | 4 | 83 | 69 | 77 | 320 | 330 | 78 |
| Cu | 11 | 170 | 19 | 980 | 77 | 120 | 3 | 7 | 19 | 3 | 3 | 450 |
| La | 75 | 96 | 38 | 90 | 100 | 91 | 32 | 31 | 29 | 34 | 34 | 91 |
| Nb | 0 | 0 | 0 | 0 | 0 | 0 | 0 | 0 | 0 | 0 | 0 | 0 |
| Ni | 0 | 0 | 25 | 0 | 3 | 0 | 16 | 18 | 26 | 110 | 120 | 0 |
| Pb | 92 | 170 | 120 | 210 | 91 | 160 | 93 | 46 | 32 | 85 | 82 | 240 |
| Sc | 15 | 7,9 | 12 | 19 | 16 | 3,1 | 24 | 21 | 17 | 19 | 19 | 7,5 |
| Sr | 4000 | 1400 | 390 | 1500 | 2200 | 870 | 860 | 990 | 660 | 1100 | 1100 | 4500 |
| V | 120 | 160 | 77 | 170 | 160 | 110 | 170 | 150 | 110 | 110 | 110 | 160 |
| Y | 24 | 37 | 14 | 23 | 29 | 34 | 21 | 17 | 17 | 16 | 17 | 37 |
| Yb | 1,7 | 2,6 | 1,2 | 1,9 | 1,9 | 2,4 | 1,6 | 1,4 | 1,5 | 1,5 | 1,5 | 2,4 |
| Zn | 89 | 190 | 86 | 120 | 170 | 65 | 96 | 79 | 69 | 58 | 63 | 190 |
| Zr | 93 | 330 | 160 | 220 | 210 | 330 | 110 | 110 | 130 | 120 | 120 | 150 |
| Ti ppm | 3937,5 | 5125 | 2875 | 5375 | 5000 | 4125 | 5750 | 4500 | 3562,5 | 3625 | 3625 | 4750 |
| Total | 100 | 98,7 | 100,1 | 98,8 | 99,6 | 99,3 | 100,4 | 100,4 | 99,9 | 99,3 | 99,7 | 99 |
| Larsen index | 10,76 | 12,33 | 14,01 | 9,35 | 5,44 | 14,15 | 2,69 | 3,72 | 9,35 | 6,41 | 6,55 | 15,81 |
| Na2O+K2O | 8,17 | 9,55 | 7,69 | 9,17 | 8,82 | 9,95 | 6,48 | 6,49 | 8,7 | 7,12 | 7,14 | 10,69 |
| K2O/Na2O | 0,90 | 1,03 | 0,88 | 4,39 | 1,05 | 0,31 | 1,23 | 0,44 | 0,21 | 0,70 | 0,70 | 2,96 |
| Fe2O3/FeT | 0,46 | 0,42 | 0,51 | 0,51 | 0,47 | 0,64 | 0,44 | 0,49 | 0,36 | 0,48 | 0,48 | 0,56 |
| Fel/(Fel+Mg) | 0,63 | 0,70 | 0,60 | 0,66 | 0,67 | 0,86 | 0,60 | 0,63 | 0,63 | 0,50 | 0,49 | 0,71 |
| Zr/Y | 3,88 | 8,92 | 11,43 | 9,57 | 7,24 | 9,71 | 5,24 | 6,47 | 7,65 | 7,50 | 7,06 | 4,05 |
| Ni/Cr | 0,00 | 0,00 | 0,23 | 0,00 | 0,05 | 0,00 | 0,19 | 0,26 | 0,34 | 0,34 | 0,36 | 0,00 |
| Rb/Sr | 0,02 | 0,12 | 0,31 | 0,14 | 0,04 | 0,18 | 0,11 | 0,05 | 0,05 | 0,08 | 0,07 | 0,05 |
| Rb/Zr | 0,99 | 0,52 | 0,75 | 0,95 | 0,43 | 0,48 | 0,85 | 0,42 | 0,25 | 0,71 | 0,68 | 1,60 |
| Ti/V | 32,81 | 32,03 | 37,34 | 31,62 | 31,25 | 37,50 | 33,82 | 30,00 | 32,39 | 32,95 | 32,95 | 29,69 |

| | Trach, Dom1 Thoms, 1941 | Trach, Dom1 C&M, 1 | Trach, Dom1 C&M 2 | Trach, Dom1 C&M 3 | Trach, Dom1 C&M 4 | Trach, Dom1 C&M 5 | Trach, Dom1 C&M 6 | Trach, Dom1 C&M 7 | Trach, Dom1 C&M 8 | Trach, Dom1 C&M 9 | Trach, Dom1 C&M 10 | Trach, Dom1 UJKE, 1 |
|---|---|---|---|---|---|---|---|---|---|---|---|---|
| SiO2 (wt.%) | 54,9 | 46,54 | 50,1 | 50,86 | 53,05 | 50,37 | 51,19 | 53,46 | 54,16 | 56,69 | 59,48 | 51,11 |
| TiO2 | 0,4 | 0,55 | 0,7 | 1,07 | 0,21 | 0,82 | 0,85 | 0,64 | 0,3 | 0,53 | 0,41 | 0,89 |
| Al2O3 | 18,95 | 15,24 | 18,07 | 21,02 | 24,17 | 16,19 | 18,02 | 19,86 | 18,67 | 18,96 | 20,23 | 15,86 |
| Fe2O3T | 3,85 | 9,50 | 7,61 | 8,60 | 4,01 | 9,28 | 8,88 | 8,07 | 5,22 | 7,26 | 5,45 | 8,17 |
| Fe2O3 | 0,76 | 3,31 | 3,59 | 7,01 | 1,8 | 3,17 | 2,08 | 3,6 | 1,7 | 3,09 | 1,27 | 2,6 |
| FeO | 2,78 | 5,57 | 3,62 | 1,43 | 1,99 | 5,5 | 6,12 | 4,02 | 3,17 | 3,75 | 3,76 | 5,01 |
| MnO | 0,01 | 0,16 | 0,14 | 0,17 | 0,11 | 0,15 | 0,15 | 0,09 | 0,14 | 0,1 | 0,08 | 0,13 |
| MgO | 7,53 | 3,81 | 2,71 | 1,09 | 0,81 | 6,05 | 4,35 | 4,17 | 2,85 | 3,41 | 4,91 | 4,87 |
| CaO | 6,25 | 7,14 | 5,59 | 2,56 | 2,29 | 6,94 | 5,5 | 2,62 | 4,73 | 2,18 | 0,99 | 7,63 |
| Na2O | 4,08 | 3,71 | 2,64 | 0,65 | 4,18 | 2,85 | 4,09 | 3,94 | 4,85 | 5,72 | 5,56 | 4,39 |
| K2O | 1,68 | 5,38 | 6,55 | 9,64 | 6,6 | 4,67 | 4,1 | 3,66 | 2,6 | 2,22 | 0,29 | 6,33 |
| H2OT | 1,73 | 2,6 | 1,79 | 1,85 | 2,04 | 2,16 | 2,2 | 2,7 | 1,79 | 2,42 | 3,04 | n.d |
| CO2T | n.d | 5,2 | 4,9 | 1,99 | 3,07 | 1,29 | 1,43 | 1,1 | 4,83 | 1,03 | 0,11 | n.d |
| P2O5 | 0,63 | 0,35 | 0,11 | 0,37 | 0,16 | 0,49 | 0,47 | 0,38 | 0,35 | 0,24 | 0,17 | 0,6 |
| S | 0,26 | n.d | n.d | n.d | n.d | n.d | n.d | n.d | n.d | n.d | n.d | n.d |
| Ba (ppm) | n.d | n.d | n.d | n.d | n.d | n.d | n.d | n.d | n.d | n.d | n.d | 1900 |
| Be | n.d | n.d | n.d | n.d | n d | n.d | n.d | n.d | n.d | n.d | n.d | n.d |
| Co | n.d | n.d | n.d | n.d | n.d | n.d | n.d | n.d | n.d | n.d | n.d | 25 |
| Cr | n.d | n.d | n.d | n.d | n.d | n.d | n.d | n.d | n.d | n.d | n.d | 61 |
| Cu | n.d | n.d | n.d | n.d | n.d | n.d | n.d | n.d | n.d | n.d | n.d | n.d |
| La | n.d | n.d | n.d | n.d | n.d | n.d | n.d | n.d | n.d | n.d | n.d | 88,8 |
| Nb | n.d | n.d | n.d | n.d | n.d | n.d | n.d | n.d | n.d | n.d | n.d | n.d |
| Ni | n.d | n.d | n.d | n.d | n.d | n.d | n.d | n.d | n.d | n.d | n.d | 19 |
| Pb | n.d | n.d | n.d | n.d | n.d | n.d | n.d | n.d | n.d | n.d | n.d | 118 |
| Sc | n.d | n.d | n.d | n.d | n.d | n.d | n.d | n.d | n.d | n.d | n.d | 19,2 |
| Sr | n.d | n.d | n.d | n.d | n.d | n.d | n.d | n.d | n.d | n.d | n.d | 1420 |
| V | n.d | n.d | n.d | n.d | n.d | n.d | n.d | n.d | n.d | n.d | n.d | 185 |
| Y | n.d | n.d | n.d | n.d | n.d | n.d | n.d | n.d | n.d | n.d | n.d | 27 |
| Yb | n.d | n.d | n.d | n.d | n.d | n.d | n.d | n.d | n.d | n.d | n.d | 2,58 |
| Zn | n.d | n.d | n.d | n.d | n.d | n.d | n.d | n.d | n.d | n.d | n.d | n.d |
| Zr | n.d | n.d | n.d | n.d | n.d | n.d | n.d | n.d | n.d | n.d | n.d | 240 |
| Ti ppm | 2500 | 3437,5 | 4375 | 6687,5 | 1312,5 | 5125 | 5312,5 | 4000 | 1875 | 3312,5 | 2562,5 | 5562,5 |
| Total | 100,06 | 99,56 | 100,51 | 99,71 | 100,48 | 100,65 | 100,55 | 100,24 | 100,14 | 100,34 | 100,3 | n.d |
| Larsen index | 3,40 | 4,36 | 11,31 | 21,50 | 19,18 | 2,95 | 5,18 | 10,65 | 9,89 | 11,76 | 10,44 | 5,84 |
| Na2O+K2O | 5,76 | 9,09 | 9,19 | 10,29 | 10,78 | 7,52 | 8,19 | 7,6 | 7,45 | 7,94 | 5,85 | 10,72 |
| K2O/Na2O | 0,41 | 1,45 | 2,48 | 14,83 | 1,58 | 1,64 | 1,00 | 0,93 | 0,54 | 0,39 | 0,05 | 1,44 |
| Fe2O3/FeT | 0,21 | 0,37 | 0,50 | 0,83 | 0,47 | 0,37 | 0,25 | 0,47 | 0,35 | 0,45 | 0,25 | 0,34 |
| Fet/(Fet+Mg) | 0,32 | 0,70 | 0,73 | 0,89 | 0,82 | 0,59 | 0,65 | 0,65 | 0,63 | 0,67 | 0,51 | 0,61 |
| Zr/Y | | | | | | | | | | | | 8,89 |
| Ni/Cr | | | | | | | | | | | | 0,31 |
| Rb/Sr | | | | | | | | | | | | 0,08 |
| Rb/Zr | | | | | | | | | | | | 0,49 |
| Ti/V | | | | | | | | | | | | 30,07 |

| | Trach, Dom1 UJKE, 6 | Trach, Dom1 UJKE, 3 | Trach, Dom1 UJKE, 10 | Trach, Dom1 UJKE, 12 | FP, Dom1 GL90166 | FP, Dom1 GL89036 | FP, Dom1 GL89037 | FP, Dom1 GL89037 dup | FP, Dom1 GL89038 | FP, Dom1 GL89047/LH5 | FP, Dom1 GL90068 | FP, Dom1 GL90116 |
|---|---|---|---|---|---|---|---|---|---|---|---|---|
| SiO2 (wt.%) | 50,58 | 54,78 | 56,37 | 55,15 | 69,4 | 62,1 | 58,6 | 58,6 | 61,5 | 63,9 | 61,3 | 61,5 |
| TiO2 | 0,93 | 0,8 | 0,72 | 0,97 | 0,32 | 0,52 | 0,8 | 0,8 | 0,51 | 0,41 | 0,33 | 0,58 |
| Al2O3 | 15,86 | 16,3 | 20,92 | 18,79 | 15,4 | 14,4 | 15,1 | 15,2 | 15,1 | 14,9 | 14,2 | 13,2 |
| Fe2O3T | 8,72 | 7,4 | 5,2 | 7,19 | 3,3 | 5,5 | 7,7 | 7,9 | 4,6 | 3,5 | 3,9 | 5,3 |
| Fe2O3 | 2,79 | 2,37 | 1,66 | 2,3 | 1,1 | 2,3 | 2,4 | 2,6 | 0 | 1,8 | 0,1 | 1,9 |
| FeO | 5,34 | 4,53 | 3,19 | 4,40 | 2 | 2,9 | 4,8 | 4,8 | 4,4 | 1,5 | 3,4 | 3,1 |
| MnO | 0,15 | 0,12 | 0,15 | 0,22 | 0,02 | 0,1 | 0,13 | 0,13 | 0,05 | 0,06 | 0,08 | 0,08 |
| MgO | 5,14 | 3 | 1,96 | 2,57 | 1,34 | 3,99 | 4,73 | 4,75 | 3,58 | 1,75 | 3,1 | 4,84 |
| CaO | 7,86 | 5,19 | 3,56 | 5,92 | 0,35 | 4,04 | 6,65 | 6,73 | 3,14 | 2,41 | 4,03 | 4,62 |
| Na2O | 4,23 | 4,7 | 1,31 | 2,95 | 5,5 | 5 | 4 | 4 | 4,9 | 5,1 | 4,4 | 4,3 |
| K2O | 5,89 | 7,13 | 9,58 | 6,03 | 3,62 | 3,48 | 1,23 | 1,25 | 2,38 | 3,19 | 3,54 | 2,84 |
| H2OT | n.d | n.d | n.d | n.d | 0,9 | 0,8 | 1,2 | 1,3 | 1,9 | 1 | 1,8 | 1,2 |
| CO2T | n.d | n.d | n.d | n.d | 0 | 0,2 | 0,1 | 0,2 | 1,9 | 3,1 | 2,8 | 1 |
| P2O5 | 0,64 | 0,59 | 0,24 | 0,23 | 0,16 | 0,37 | 0,27 | 0,28 | 0,2 | 0,21 | 0,23 | 0,3 |
| S | n.d | n.d | n.d | n.d | 0,12 | 0 | 0,02 | 0,01 | 0,49 | 0,06 | 0,65 | 0,01 |
| Ba (ppm) | 1880 | 3240 | 6390 | 5200 | 1800 | 1800 | 780 | 820 | 830 | 2200 | 2200 | 1700 |
| Be | n.d | n.d | n.d | n.d | 1,9 | 2,4 | 1,5 | 1,5 | 1,2 | 2,5 | 1,9 | 1,7 |
| Co | 25 | 20 | 7 | 13 | 15 | 24 | 29 | 28 | 22 | 13 | 20 | 28 |
| Cr | 86 | 32 | 0 | 0 | 54 | 120 | 120 | 110 | 140 | 50 | 110 | 210 |
| Cu | n.d | n.d | n.d | n.d | 46 | 15 | 17 | 15 | 18 | 4 | 17 | 37 |
| La | 102,9 | 94,5 | 101,5 | 137,2 | 29 | 34 | 11 | 13 | 32 | 37 | 24 | 51 |
| Nb | n.d | n.d | n.d | n.d | 0 | 0 | 0 | 0 | 0 | 0 | 0 | 0 |
| Ni | 26 | 18 | 9 | 11 | 12 | 26 | 38 | 34 | 62 | 7 | 17 | 110 |
| Rb | 129 | 140 | 280 | 302 | 86 | 93 | 28 | 30 | 48 | 150 | 110 | 63 |
| Sc | 21,4 | 14,2 | 3,4 | 5,2 | 4,2 | 13 | 17 | 17 | 9,4 | 6,8 | 9,1 | 13 |
| Sr | 1270 | 1110 | 1830 | 1160 | 570 | 1000 | 640 | 630 | 500 | 870 | 1600 | 1000 |
| V | 253 | 201 | 203 | 369 | 30 | 85 | 120 | 120 | 67 | 37 | 50 | 83 |
| Y | 26 | 26 | 29 | 38 | 11 | 16 | 20 | 19 | 8 | 14 | 9 | 16 |
| Yb | 2,55 | 2,33 | 2,93 | 3,26 | 0,9 | 1,3 | 1,9 | 1,9 | 0,6 | 1,2 | 0,7 | 1,2 |
| Zn | n.d | n.d | n.d | n.d | 38 | 56 | 57 | 56 | 49 | 46 | 57 | 56 |
| Zr | 180 | 298 | 392 | 499 | 140 | 140 | 110 | 110 | 120 | 140 | 100 | 120 |
| Ti ppm | 5812,5 | 5000 | 4500 | 6062,5 | 2000 | 3250 | 5000 | 5000 | 3187,5 | 2562,5 | 2062,5 | 3625 |
| Total | n.d | n.d | n.d | n.d | 100,5 | 100,5 | 100,2 | 100,8 | 100 | 99,8 | 100,4 | 99,8 |
| Larsen index | 4,40 | 12,66 | 19,65 | 11,50 | 23,04 | 13,23 | 4,56 | 4,48 | 11,74 | 18,81 | 13,42 | 10,76 |
| Na2O+K2O | 10,12 | 11,83 | 10,89 | 8,98 | 9,12 | 8,48 | 5,23 | 5,25 | 7,28 | 8,29 | 7,94 | 7,14 |
| K2O/Na2O | 1,39 | 1,52 | 7,31 | 2,04 | 0,66 | 0,70 | 0,31 | 0,31 | 0,49 | 0,63 | 0,80 | 0,66 |
| Fe2O3/FeT | 0,34 | 0,34 | 0,34 | 0,34 | 0,35 | 0,44 | 0,33 | 0,35 | 0,00 | 0,55 | 0,03 | 0,38 |
| Fet/(Fet+Mg) | 0,61 | 0,70 | 0,71 | 0,72 | 0,70 | 0,57 | 0,60 | 0,61 | 0,55 | 0,65 | 0,53 | 0,51 |
| Zr/Y | 6,92 | 11,46 | 13,52 | 13,13 | 12,73 | 8,75 | 5,50 | 5,79 | 15,00 | 10,00 | 11,11 | 7,50 |
| Ni/Cr | 0,30 | 0,56 | | | 0,22 | 0,22 | 0,32 | 0,31 | 0,44 | 0,14 | 0,15 | 0,52 |
| Rb/Sr | 0,10 | 0,13 | 0,15 | 0,26 | 0,15 | 0,09 | 0,04 | 0,05 | 0,10 | 0,17 | 0,07 | 0,06 |
| Rb/Zr | 0,72 | 0,47 | 0,71 | 0,61 | 0,61 | 0,66 | 0,25 | 0,27 | 0,40 | 1,07 | 1,10 | 0,53 |
| Ti/V | 22,97 | 24,88 | 22,17 | 16,43 | 66,67 | 38,24 | 41,67 | 41,67 | 47,57 | 69,26 | 41,25 | 43,67 |

| | FP< Dom1 Thomson, 50 | FP, Dom1 W&K,12-14 | FP, Dom1 Cam&Car,67 | FP, Dom1 Cam&Car,87 | FP, Dom1 Cooke&Moor | FP, Dom1 Cooke&Moor | FP, Dom1 Hicks, 018 | FP, Dom1 Hicks, 017 | FP, Dom1 Hicks, 134 | FP, Dom1 Hicks, 139 | FP, Dom1 GL90192 | QFP, Dom1 GL90035 |
|---|---|---|---|---|---|---|---|---|---|---|---|---|
| SiO2 (wt.%) | 62,19 | 62,6 | 62,6 | 65,3 | 55,6 | 58,12 | 62,03 | 59,83 | 64,48 | 61,34 | 62,8 | 65 |
| TiO2 | 0,44 | 0,43 | 0,4 | 0,4 | 0,53 | 0,43 | 0,39 | 0,42 | 0,33 | 0,39 | 0,41 | 0,42 |
| Al2O3 | 14,85 | 14,01 | 14,3 | 14,9 | 20,02 | 19,88 | 14,16 | 13,86 | 14,78 | 14,22 | 14,5 | 14,9 |
| Fe2O3T | 3,64 | 4,00 | 3,93 | 3,68 | 6,48 | 5,22 | 4,06 | 4,09 | 3,64 | 4,14 | 4 | 4 |
| Fe2O3 | 1,38 | 1,54 | 1,6 | 1,9 | 2,51 | 2,4 | 1,52 | 1,6 | 0,82 | 1,77 | 1,1 | 1,8 |
| FeO | 2,03 | 2,21 | 2,1 | 1,6 | 3,57 | 2,54 | 2,29 | 2,24 | 2,54 | 2,13 | 2,8 | 2 |
| MnO | 0,13 | 0,07 | 0,07 | 0,06 | 0,05 | 0,09 | 0,07 | 0,08 | 0,05 | 0,07 | 0,07 | 0,07 |
| MgO | 2,33 | 2,3 | 2,72 | 1,74 | 2,97 | 2,94 | 3,11 | 3,01 | 1,83 | 3,6 | 3,04 | 2,7 |
| CaO | 3,88 | 3,4 | 3,56 | 2,74 | 4,44 | 4,51 | 3,39 | 4,26 | 2,67 | 3,74 | 3,26 | 2,2 |
| Na2O | 4,92 | 5,2 | 5,06 | 4,9 | 3,56 | 3,56 | 4,76 | 5,08 | 5,61 | 5,35 | 5,3 | 5,4 |
| K2O | 3,76 | 3,2 | 2,35 | 3,31 | 1,73 | 2,54 | 4,12 | 3,94 | 3,18 | 3,54 | 3,64 | 3,75 |
| H2OT | 1,05 | 2,6 | 1,1 | 1,2 | 2,72 | 1,29 | n.d | n.d | n.d | n.d | 0,8 | 0,9 |
| CO2T | 2,79 | 1,8 | 2,5 | 1,7 | 2,7 | 1,54 | n.d | n.d | n.d | n.d | 1,3 | 0,4 |
| P2O5 | 0,37 | 0,23 | 0,3 | 0,21 | 0,32 | 0,31 | 0,39 | 0,43 | 0,22 | 0,38 | 0,29 | 0,28 |
| S | 0 | n.d | 0,09 | 0,06 | n.d | n.d | 0,05 | 0,04 | 0,04 | 0,03 | 0,01 | 0,02 |
| Ba (ppm) | n.d | 2176 | n.d | n.d | n.d | n.d | 2409 | 2647 | 2042 | 2152 | 2400 | 2400 |
| Be | n.d | n.d | n.d | n.d | n.d | n.d | n.d | n.d | n.d | n.d | 2,8 | 2,9 |
| Co | n.d | 43 | n.d | n.d | n.d | n.d | n.d | n.d | n.d | n.d | 20 | 21 |
| Cr | n.d | 197 | n.d | n.d | n.d | n.d | 177 | 186 | 99 | 196 | 130 | 91 |
| Cu | n.d | 11 | n.d | n.d | n.d | n.d | n.d | n.d | n.d | n.d | 13 | 21 |
| La | n.d | n.d | n.d | n.d | n.d | n.d | n.d | n.d | n.d | n.d | 45 | 35 |
| Nb | n.d | 6 | n.d | n.d | n.d | n.d | n.d | n.d | n.d | n.d | 0 | 0 |
| Ni | n.d | 47 | n.d | n.d | n.d | n.d | 62 | 60 | 21 | 86 | 43 | 36 |
| Rb | n.d | 89 | n.d | n.d | n.d | n.d | 126 | 124 | 74 | 140 | 71 | 78 |
| Sc | n.d | 14 | n.d | n.d | n.d | n.d | n.d | n.d | n.d | n.d | 7,8 | 7,6 |
| Sr | n.d | 1629 | n.d | n.d | n.d | n.d | 1738 | 1511 | 1365 | 1286 | 1300 | 940 |
| V | n.d | 111 | n.d | n.d | n.d | n.d | 66 | 71 | 49 | 59 | 45 | 44 |
| Y | n.d | 19 | n.d | n.d | n.d | n.d | 19 | 60 | 21 | 17 | 17 | 17 |
| Yb | n.d | n.d | n.d | n.d | n.d | n.d | n.d | n.d | n.d | n.d | 1,3 | 1,5 |
| Zn | n.d | 60 | n.d | n.d | n.d | n.d | 60 | 67 | 50 | 70 | 54 | 52 |
| Zr | n.d | 175 | n.d | n.d | n.d | n.d | 196 | 211 | 180 | 205 | 180 | 160 |
| Ti ppm | 2750 | 2687,5 | 2500 | 2500 | 3312,5 | 2687,5 | 2437,5 | 2625 | 2062,5 | 2437,5 | 2562,5 | 2625 |
| Total | 100,12 | 98,8 | 99,3 | 100,4 | 100,72 | 100,15 | 96,58 | 95,16 | 96,95 | 96,87 | 99,6 | 100,2 |
| Larsen index | 16,23 | 16,14 | 14,82 | 18,97 | 9,26 | 11,90 | 15,99 | 14,35 | 17,61 | 14,50 | 15,65 | 18,50 |
| Na2O+K2O | 8,68 | 8,4 | 7,41 | 8,21 | 5,29 | 6,1 | 8,88 | 9,02 | 8,79 | 8,89 | 8,94 | 9,15 |
| K2O/Na2O | 0,76 | 0,62 | 0,46 | 0,68 | 0,49 | 0,71 | 0,87 | 0,78 | 0,57 | 0,66 | 0,69 | 0,69 |
| Fe2O3/FeT | 0,40 | 0,41 | 0,43 | 0,54 | 0,41 | 0,49 | 0,40 | 0,42 | 0,24 | 0,45 | 0,30 | 0,47 |
| Fet/(Fet+Mg) | 0,59 | 0,62 | 0,58 | 0,67 | 0,67 | 0,63 | 0,55 | 0,56 | 0,65 | 0,52 | 0,55 | 0,58 |
| Zr/Y | | 9,21 | | | | | 10,32 | 3,52 | 8,57 | 12,06 | 10,59 | 9,41 |
| Ni/Cr | | 0,24 | | | | | 0,35 | 0,32 | 0,21 | 0,44 | 0,33 | 0,40 |
| Rb/Sr | | 0,05 | | | | | 0,07 | 0,08 | 0,05 | 0,11 | 0,05 | 0,08 |
| Rb/Zr | | 0,51 | | | | | 0,64 | 0,59 | 0,41 | 0,68 | 0,39 | 0,49 |
| Ti/V | | 24,21 | | | | | 36,93 | 36,97 | 42,09 | 41,31 | 56,94 | 59,66 |

| | QFP, Dom1 GL90035 dup | QFP, Dom1 GL90185 | QFP, Dom1 GL90185 dup | QFP, Dom1 GL90187 | QFP, Dom1 Hicks, 119 | Vindicator St n.d | McVittie stock GL89006 | Beaverhouse L GL90210 | Beaverhouse L GL90210 dup | Monocle L GL90211 | Monocle L GL90213 | Kinabik Creek GL90215 |
|---|---|---|---|---|---|---|---|---|---|---|---|---|
| SiO2 (wt.%) | 65,3 | 69 | 69,1 | 67,4 | 67,13 | 68,8 | 67,4 | 65,4 | 65,6 | 65,9 | 61 | 65,8 |
| TiO2 | 0,41 | 0,2 | 0,2 | 0,26 | 0,21 | 0,19 | 0,39 | 0,3 | 0,31 | 0,4 | 0,51 | 0,36 |
| Al2O3 | 15 | 15,7 | 16 | 15,3 | 15,31 | 15,21 | 15,7 | 15,8 | 15,7 | 15,6 | 19,5 | 15,4 |
| Fe2O3T | 4,1 | 1,9 | 1,9 | 2,2 | 2,36 | 2,24 | 3,5 | 4,2 | 4,2 | 4 | 4,1 | 3,9 |
| Fe2O3 | 1,7 | 0,7 | 0,7 | 0,9 | 1,13 | 1,07 | 1,7 | 2 | 2 | 1,7 | 0,4 | 0,2 |
| FeO | 2,2 | 1,1 | 1,1 | 1,2 | 1,11 | 1,05 | 1,6 | 2 | 2 | 2,1 | 3,3 | 3,3 |
| MnO | 0,07 | 0,03 | 0,03 | 0,03 | 0,04 | 0,03 | 0,05 | 0,08 | 0,08 | 0,07 | 0,04 | 0,07 |
| MgO | 2,68 | 1,15 | 1,16 | 1,4 | 1,34 | 1,06 | 1,75 | 0,64 | 0,65 | 2,26 | 2,64 | 2,72 |
| CaO | 2,18 | 1,75 | 1,79 | 1,89 | 1,94 | 1,87 | 1,67 | 3,35 | 3,33 | 2,84 | 0,7 | 3,52 |
| Na2O | 5,3 | 6,1 | 6,1 | 5,8 | 6,07 | 6,48 | 6 | 3,6 | 3,6 | 4,9 | 9,5 | 5,8 |
| K2O | 3,75 | 2,97 | 3 | 2,98 | 3,08 | 2,78 | 1,97 | 1,53 | 1,54 | 3,01 | 0,2 | 0,79 |
| H2OT | 0,9 | 0,5 | 0,4 | 0,6 | n.d | n.d | 1,1 | 2 | 1,9 | 1 | 1,6 | 1,3 |
| CO2T | 0,3 | 0,4 | 0,4 | 0,4 | n.d | n.d | 0,3 | 3,2 | 3,1 | 0,2 | 0,1 | 0,6 |
| P2O5 | 0,27 | 0,11 | 0,11 | 0,13 | 0,15 | 0,11 | 0,17 | 0,12 | 0,13 | 0,2 | 0,21 | 0,19 |
| S | 0,01 | 0,03 | 0,03 | 0,11 | 0,08 | 0,08 | 0,02 | 0 | 0 | 0 | 0 | 0,66 |
| Ba (ppm) | 2400 | 2200 | 2200 | 2600 | 2475 | 2366 | 1400 | 300 | 290 | 1800 | 90 | 770 |
| Be | 2,9 | 2,8 | 2,8 | 2,6 | n.d | n.d | 2 | 0,9 | 0,9 | 2,2 | 1 | 1,7 |
| Co | 20 | 17 | 18 | 20 | n.d | n.d | 33 | 15 | 14 | 43 | 20 | 22 |
| Cr | 85 | 37 | 37 | 46 | 90 | 46 | 42 | 3 | 3 | 55 | 64 | 77 |
| Cu | 16 | 6 | 9 | 4 | n.d | n.d | 19 | 0 | 1 | 6 | 0 | 3 |
| La | 34 | 22 | 21 | 24 | n.d | n.d | 24 | 10 | 11 | 35 | 6 | 25 |
| Nb | 0 | 0 | 0 | 0 | n.d | 5 | 0 | 3 | 0 | 0 | 0 | 0 |
| Ni | 28 | 2 | 5 | 6 | 16 | 5 | 12 | 3 | 3 | 10 | 32 | 45 |
| Pb | 83 | 78 | 80 | 72 | 77 | 58 | 51 | 42 | 42 | 78 | 6 | 14 |
| Sc | 7,5 | 3 | 3 | 3,7 | n.d | n.d | 6,4 | 3,2 | 3,3 | 7,4 | 5,3 | 7,1 |
| Sr | 980 | 2500 | 2500 | 4000 | 4291 | 1571 | 1300 | 200 | 200 | 1100 | 300 | 920 |
| V | 42 | 13 | 13 | 18 | 41 | 8 | 38 | 6 | 8 | 42 | 36 | 38 |
| Y | 17 | 8 | 8 | 9 | 10 | 8 | 17 | 9 | 9 | 20 | 17 | 19 |
| Yb | 1,3 | 0,6 | 0,6 | 0,6 | n.d | n.d | 1,7 | 0,8 | 0,9 | 1,9 | 1,5 | 1,8 |
| Zn | 48 | 29 | 30 | 33 | 31 | 86 | 42 | 38 | 32 | 46 | 36 | 55 |
| Zr | 160 | 120 | 120 | 0 | 194 | 133 | 180 | 130 | 120 | 170 | 200 | 120 |
| Ti ppm | 2562,5 | 1250 | 1250 | 1625 | 1312,5 | 1187,5 | 2437,5 | 1875 | 1937,5 | 2500 | 3187,5 | 2375 |
| Total | 100,4 | 100,2 | 100,6 | 99,1 | 98,12 | 99,34 | 100,2 | 100,1 | 100 | 100,5 | 99,8 | 101 |
| Larsen index | 18,43 | 21,95 | 21,96 | 20,93 | 21,04 | 21,71 | 19,39 | 17,32 | 17,40 | 17,75 | 13,87 | 13,16 |
| Na2O+K2O | 9,05 | 9,07 | 9,1 | 8,78 | 9,15 | 9,26 | 7,97 | 5,13 | 5,14 | 7,91 | 9,7 | 6,59 |
| K2O/Na2O | 0,71 | 0,49 | 0,49 | 0,51 | 0,51 | 0,43 | 0,33 | 0,43 | 0,43 | 0,61 | 0,02 | 0,14 |
| Fe2O3/FeT | 0,44 | 0,39 | 0,39 | 0,43 | 0,50 | 0,50 | 0,52 | 0,50 | 0,50 | 0,45 | 0,11 | 0,06 |
| Fet/(Fet+Mg) | 0,59 | 0,61 | 0,61 | 0,60 | 0,63 | 0,67 | 0,65 | 0,86 | 0,86 | 0,63 | 0,58 | 0,56 |
| Zr/Y | 9,41 | 15,00 | 15,00 | 0,00 | 19,40 | 16,63 | 10,59 | 14,44 | 13,33 | 8,50 | 11,76 | 6,32 |
| Ni/Cr | 0,33 | 0,05 | 0,14 | 0,13 | 0,18 | 0,11 | 0,29 | 1,00 | 1,00 | 0,18 | 0,50 | 0,58 |
| Rb/Sr | 0,08 | 0,03 | 0,03 | 0,01 | 0,02 | 0,04 | 0,04 | 0,21 | 0,21 | 0,07 | 0,02 | 0,02 |
| Rb/Zr | 0,52 | 0,65 | 0,67 | | 0,40 | 0,44 | 0,28 | 0,32 | 0,35 | 0,46 | 0,03 | 0,12 |
| Ti/V | 61,01 | 96,15 | 96,15 | 90,28 | 32,01 | 148,44 | 64,14 | 312,50 | 242,19 | 59,52 | 88,54 | 62,50 |

| | Kinabik Creek GL90215 dup | Otto Stock SMR-12 | Otto Stock GL89XX | Otto Stock GL89017 | Otto Stock GL89018 | Otto stock GL89019 | Otto stock GL89019 dup | Otto Stock GL89025 | Otto Stock GL89025 dup | Otto Stock SUT, 881108 | Otto Stock SUT 8899 | Otto Stock SUT 88120 |
|---|---|---|---|---|---|---|---|---|---|---|---|---|
| SiO2 (wt.%) | 65 | 68,6 | 55,9 | 43 | 48,7 | 60,02 | 60,61 | 64,9 | 64,7 | 64,2 | 68,7 | 51,9 |
| TiO2 | 0,43 | 0,14 | 0,67 | 1,24 | 1,07 | 0,62 | 0,64 | 0,43 | 0,39 | 0,11 | | 0,86 |
| Al2O3 | 15,2 | 16,2 | 14,5 | 5,4 | 8,1 | 15,76 | 16,12 | 14,5 | 14,5 | 16,9 | 15,9 | 12,2 |
| Fe2O3T | 3,7 | 1,6 | 7,4 | 14,6 | 12,7 | 5,43 | 5,48 | 3,8 | 3,8 | 2,32 | 1,36 | 9,27 |
| Fe2O3 | 0,1 | 1 | 3,8 | 6 | 5,9 | 2,8 | 2,82 | 0,8 | 0,9 | 1,65 | 0,84 | 4,39 |
| FeO | 3,2 | 0,5 | 3,2 | 7,7 | 6,1 | 2,37 | 2,39 | 2,7 | 2,6 | 0,6 | 0,47 | 4,39 |
| MnO | 0,06 | 0,03 | 0,12 | 0,28 | 0,24 | 0,12 | 0,12 | 0,08 | 0,07 | 0,04 | 0,03 | 0,18 |
| MgO | 2,69 | 0,73 | 4,09 | 11,3 | 7,62 | 2,24 | 2,2 | 2,46 | 2,44 | 0,97 | 0,61 | 4,78 |
| CaO | 3,49 | 0,85 | 5,4 | 16,3 | 12,9 | 3,86 | 3,81 | 3,06 | 3,08 | 1,75 | 0,8 | 8,12 |
| Na2O | 5,8 | 6,7 | 4 | 1,2 | 2,3 | 5,42 | 5,01 | 5,5 | 5,6 | 7,04 | 6,26 | 2,22 |
| K2O | 0,78 | 4,62 | 6,06 | 2,58 | 3,44 | 5,59 | 5,72 | 3,7 | 3,71 | 5,06 | 4,41 | 6,5 |
| H2OT | 1,3 | 0 | 0,5 | 1,3 | 0,7 | n.d | n.d | 0,3 | 0,4 | 0,18 | 0,16 | 1,14 |
| CO2T | 0,2 | 0 | 0,7 | 0,2 | 0 | n.d | n.d | 0 | 0 | 0,08 | 0,18 | 0,26 |
| P2O5 | 0,19 | 0,05 | 0,61 | 1,98 | 1,19 | 0,36 | 0,38 | 0,26 | 0,27 | 0 | 0,02 | 1,03 |
| S | 0,65 | 0 | 0 | 0,06 | 0,01 | 0 | 0 | 0,04 | 0,04 | 0,01 | 0,18 | 0,03 |
| Ba (ppm) | 760 | 1000 | 3000 | 2800 | 7000 | 2825 | 2463 | 2000 | 2000 | n.d | n.d | n.d |
| Be | 1,8 | 2,9 | 1,9 | 1,6 | 1,4 | n.d | n.d | 2,7 | 2,7 | n.d | n.d | n.d |
| Co | 22 | 17 | 26 | 51 | 41 | n.d | n.d | 22 | 23 | n.d | n.d | n.d |
| Cr | 77 | 28 | 64 | 220 | 190 | 21 | 34 | 76 | 76 | 45 | 19 | 69 |
| Cu | 4 | 3 | 64 | 29 | 30 | n.d | n.d | 14 | 16 | n.d | n.d | n.d |
| La | 27 | 7 | 69 | 220 | 180 | n.d | n.d | 26 | 27 | 6,03 | 10,3 | 190 |
| Nb | 0 | 5 | 0 | 0 | 0 | 17 | 17 | 0 | 0 | n.d | n.d | n.d |
| Ni | 45 | 12 | 4 | 77 | 24 | 30 | 35 | 15 | 14 | 25 | 12 | 24 |
| Pb | 15 | 130 | 140 | 110 | 74 | 162 | 160 | 90 | 97 | 59 | 110 | 151 |
| Sc | 7,2 | 1,9 | 14 | 36 | 27 | n.d | n.d | 7,8 | 7,7 | n.d | n.d | n.d |
| Sr | 930 | 430 | 2000 | 2200 | 2900 | 1758 | 1754 | 1100 | 1100 | 336 | 371 | 2616 |
| V | 39 | 18 | 120 | 180 | 190 | 136 | 105 | 50 | 49 | n.d | n.d | n.d |
| Y | 19 | 5 | 22 | 46 | 38 | 35 | 34 | 12 | 12 | 7 | 8 | 36 |
| Yb | 1,9 | 0,5 | 1,5 | 2,2 | 2,2 | n.d | n.d | 0,9 | 0,9 | 0,34 | 0,6 | 2,22 |
| Zn | 59 | 34 | 83 | 150 | 120 | 107 | 106 | 42 | 41 | n.d | n.d | n.d |
| Zr | 120 | 99 | 140 | 110 | 170 | 191 | 191 | 140 | 150 | 48 | 118 | 90 |
| Ti ppm | 2687,5 | 875 | 4187,5 | 7750 | 6687,5 | 3875 | 4000 | 2687,5 | 2437,5 | 687,5 | 0 | 5375 |
| Total | 99,3 | 99,6 | 100,2 | 99,2 | 99,4 | 100,04 | 100,55 | 99,1 | 99,1 | 98,6 | 98,5 | 98 |
| Larsen Index | 13,05 | 25,38 | 11,98 | -18,40 | -6,96 | 17,11 | 17,50 | 17,09 | 17,14 | 23,12 | 25,41 | 6,49 |
| Na2O+K2O | 6,58 | 11,32 | 10,06 | 3,78 | 5,74 | 11,01 | 10,73 | 9,2 | 9,31 | 12,1 | 10,67 | 8,72 |
| K2O/Na2O | 0,13 | 0,69 | 1,52 | 2,15 | 1,50 | 1,03 | 1,14 | 0,67 | 0,66 | 0,72 | 0,70 | 2,93 |
| Fe2O3/FeT | 0,03 | 0,67 | 0,54 | 0,44 | 0,49 | 0,54 | 0,54 | 0,23 | 0,26 | 0,73 | 0,64 | 0,50 |
| Fet/(Fet+Mg) | 0,55 | 0,67 | 0,63 | 0,55 | 0,61 | 0,70 | 0,70 | 0,59 | 0,59 | 0,70 | 0,68 | 0,65 |
| Zr/Y | 6,32 | 19,80 | 6,36 | 2,39 | 4,47 | 5,46 | 5,62 | 11,67 | 12,50 | 6,86 | 14,75 | 2,50 |
| Ni/Cr | 0,58 | 0,43 | 0,06 | 0,35 | 0,13 | 1,43 | 1,03 | 0,20 | 0,18 | 0,56 | 0,63 | 0,35 |
| Rb/Sr | 0,02 | 0,30 | 0,07 | 0,05 | 0,03 | 0,09 | 0,09 | 0,08 | 0,09 | 0,18 | 0,30 | 0,06 |
| Rb/Zr | 0,13 | 1,31 | 1,00 | 1,00 | 0,44 | 0,85 | 0,84 | 0,64 | 0,65 | 1,23 | 0,93 | 1,68 |
| Ti/V | 68,91 | 48,61 | 34,90 | 43,06 | 35,20 | 28,49 | 38,10 | 53,75 | 49,74 | | | |

| | Otto Stock SUT 88103 | Otto Stock SUT 88104 | Otto Stock SUT 88114 | Otto Stock Othman A13 | Otto Stock Othman A14 | Lebel stock GL89013 | Lebel stock GL89029 | Lebel stock GL89030 | Lebel stock GL89031 | Gauthier dio SMR27 | Gauthier dio GL89034 | Gauthier dio GL90089 |
|---|---|---|---|---|---|---|---|---|---|---|---|---|
| SiO2 (wt.%) | 48,6 | 46,1 | 43,7 | 63,32 | 70,88 | 57,2 | 44,8 | 53,9 | 53,1 | 57,3 | 49,2 | 50,9 |
| TiO2 | 0,98 | 0,85 | 1,52 | 0,3 | 0,13 | 0,66 | 1,52 | 0,81 | 0,62 | 0,67 | 0,99 | 1,02 |
| Al2O3 | 11,2 | 8,16 | 8,58 | 17,26 | 14,97 | 14,5 | 7,3 | 12,7 | 12,1 | 16,5 | 5,7 | 5,9 |
| Fe2O3T | 10,90 | 10,90 | 15,86 | 2,77 | 1,25 | 7,4 | 15,2 | 7,9 | 8,6 | 7,1 | 14,4 | 13,1 |
| Fe2O3 | 2,91 | 3,29 | 5,5 | 1,71 | 0,77 | 2,8 | 6,5 | 3,7 | 2,7 | 2 | 2,7 | 2,4 |
| FeO | 7,19 | 6,85 | 9,32 | 0,95 | 0,43 | 4,1 | 7,8 | 3,8 | 5,3 | 4,6 | 10,5 | 9,6 |
| MnO | 0,19 | 0,17 | 0,18 | 0,05 | 0,03 | 0,12 | 0,34 | 0,19 | 0,17 | 0,12 | 0,2 | 0,2 |
| MgO | 10,5 | 14,3 | 14,6 | 1,12 | 0,52 | 4,82 | 10,4 | 4,99 | 5,67 | 3,68 | 11,7 | 11,9 |
| CaO | 10,6 | 12 | 11,4 | 1,54 | 0,75 | 4,62 | 13,3 | 7,91 | 8,42 | 5,2 | 13,2 | 12,4 |
| Na2O | 2,82 | 1,8 | 1,49 | 6 | 5,6 | 4,3 | 2,2 | 3,5 | 3,1 | 4,1 | 1,4 | 1,7 |
| K2O | 2,2 | 2,6 | 0,63 | 5,11 | 4,41 | 4,36 | 3,04 | 5,08 | 5,35 | 2,31 | 0,25 | 0,19 |
| H2OT | 1,45 | 1,58 | 2,44 | 0,83 | 0,41 | 1,1 | 1,4 | 1 | 0,7 | 2,1 | 1,8 | 1,7 |
| CO2T | 0,06 | 0,11 | 0,55 | 0,51 | 0,02 | 0,5 | 0,2 | 0,3 | 0,1 | 0,6 | 1,6 | 1,2 |
| P2O5 | 0,36 | 0,37 | 0,03 | 0,11 | 0,03 | 0,4 | 1,37 | 0,77 | 0,81 | 0,23 | 0,07 | 0,06 |
| S | 0,03 | 0,13 | 0,22 | n.d | n.d | 0,06 | 0,01 | 0,01 | 0 | 0 | 0,03 | 0,03 |
| Ba (ppm) | n.d | n.d | n.d | 2130 | 1000 | 1800 | 1100 | 2800 | 4300 | 880 | 100 | 50 |
| Be | n.d | n.d | n.d | n.d | n.d | 1,9 | 4,2 | 2,1 | 1,2 | 1,3 | 0,6 | 0,7 |
| Co | n.d | n.d | n.d | n.d | n.d | 26 | 51 | 29 | 37 | 27 | 65 | 57 |
| Cr | 515 | 1045 | 595 | 9 | 12 | 170 | 180 | 87 | 120 | 26 | 1300 | 1200 |
| Cu | n.d | n.d | n.d | 16 | 3 | 15 | 390 | 87 | 15 | 4 | 200 | 40 |
| La | 22,5 | 33,2 | 5,38 | 64 | 12 | 23 | 130 | 76 | 70 | 22 | 0 | 0 |
| Nb | n.d | n.d | n.d | 14 | 10 | 0 | 0 | 0 | 0 | 0 | 0 | 0 |
| Ni | 114 | 212 | 32 | 8 | 5 | 32 | 73 | 13 | 4 | 16 | 220 | 230 |
| Rb | 68 | 100 | 14 | 128 | 142 | 61 | 210 | 100 | 140 | 60 | 5 | 5 |
| Sc | n.d | n.d | n.d | n.d | n.d | 13 | 34 | 19 | 20 | 14 | 34 | 35 |
| Sr | 1045 | 512 | 342 | 1150 | 501 | 920 | 580 | 2000 | 3000 | 940 | 100 | 91 |
| V | n.d | n.d | n.d | 45 | 20 | 100 | 250 | 140 | 150 | 100 | 180 | 180 |
| Y | 25 | 20 | 23 | 19 | 8 | 18 | 39 | 24 | 20 | 16 | 12 | 12 |
| Yb | 1,9 | 1,42 | 1,55 | 2,4 | 0,9 | 1,1 | 2,7 | 1,6 | 1,3 | 1,5 | 0,7 | 0,8 |
| Zn | n.d | n.d | n.d | 42 | 14 | 74 | 250 | 610 | 100 | 62 | 100 | 71 |
| Zr | 120 | 114 | 72 | 381 | 141 | 170 | 280 | 120 | 70 | 110 | 56 | 56 |
| Ti ppm | 6125 | 5312,5 | 9500 | 1875 | 812,5 | 4125 | 9500 | 5062,5 | 5125 | 4187,5 | 6187,5 | 6375 |
| Total | 99,1 | 98,4 | 100,1 | 98,9 | 99,2 | 99,2 | 100,6 | 99,3 | 99,2 | 99,6 | 99,6 | 99,4 |
| Larsen Index | -9,91 | -15,20 | -20,14 | 22,59 | 26,31 | 9,87 | -13,54 | 6,33 | 3,64 | 7,91 | -18,77 | -16,76 |
| Na2O+K2O | 5,02 | 4,4 | 2,12 | 11,11 | 10,01 | 8,66 | 5,24 | 8,58 | 8,45 | 6,41 | 1,65 | 1,69 |
| K2O/Na2O | 0,78 | 1,44 | 0,42 | 0,85 | 0,79 | 1,01 | 1,38 | 1,45 | 1,73 | 0,56 | 0,18 | 0,11 |
| Fe2O3/FeT | 0,29 | 0,32 | 0,37 | 0,64 | 0,64 | 0,41 | 0,45 | 0,49 | 0,34 | 0,30 | 0,20 | 0,20 |
| Fet/(Fet+Mg) | 0,49 | 0,41 | 0,50 | 0,70 | 0,70 | 0,59 | 0,58 | 0,60 | 0,59 | 0,64 | 0,53 | 0,50 |
| Zr/Y | 4,80 | 5,70 | 3,13 | 20,05 | 17,63 | 9,44 | 7,18 | 5,00 | 3,50 | 6,88 | 4,67 | 4,67 |
| Ni/Cr | 0,22 | 0,20 | 0,05 | 0,89 | 0,42 | 0,19 | 0,41 | 0,15 | 0,03 | 0,62 | 0,17 | 0,19 |
| Rb/Sr | 0,07 | 0,20 | 0,04 | 0,11 | 0,28 | 0,07 | 0,36 | 0,05 | 0,05 | 0,06 | 0,05 | 0,05 |
| Rb/Zr | 0,57 | 0,88 | 0,19 | 0,34 | 1,01 | 0,36 | 0,75 | 0,83 | 2,00 | 0,55 | 0,09 | 0,09 |
| Ti/V | | | | 41,67 | 40,63 | 41,25 | 38,00 | 36,16 | 34,17 | 41,88 | 34,38 | 35,42 |

| | McElroy st SMR24 | McElroy st SMR37 | McElroy SMR37 dup | McElroy st Thomson, 47 | Hornblendite GL6853 | Hornblendite GL6854 | Lamp, Dom3 GL89020 | Lamp, Dom3 Sut 881112 | Murdock Cr AS, 87101 | Murdock Cr AS, 87117 | Murdock Cr As, 87134 | Murdock Cr MAS, 88216 |
|---|---|---|---|---|---|---|---|---|---|---|---|---|
| SiO2 (wt.%) | 60,9 | 49,1 | 48,8 | 41,08 | 49,6 | 48,8 | 48,4 | 49,8 | 56,3 | 56,7 | 55 | 50,3 |
| TiO2 | 0,52 | 0,97 | 0,94 | | 0,84 | 0,82 | 0,83 | 0,66 | 0,63 | 0,07 | 0,65 | 0,98 |
| Al2O3 | 17,6 | 15,7 | 15,7 | 8,07 | 9,5 | 10,6 | 11,5 | 12,6 | 14,5 | 15,3 | 14,7 | 10,6 |
| Fe2O3T | 5,3 | 10,7 | 10,8 | 21,28 | 10,2 | 9,2 | 9,3 | 8,18 | 7,6 | 7,2 | 8 | 11,3 |
| Fe2O3 | 2,7 | 4,6 | 4,6 | 9,94 | 2,8 | 2,8 | 2,2 | 2,28 | 3,9 | 3,6 | 4 | 5,1 |
| FeO | 2,3 | 5,5 | 5,6 | 10,2 | 6,7 | 5,8 | 6,4 | 5,31 | 3,3 | 3,3 | 3,6 | 5,7 |
| MnO | 0,1 | 0,17 | 0,17 | n.d | 0,17 | 0,14 | 0,2 | 0,15 | 0,14 | 0,12 | 0,15 | 0,23 |
| MgO | 2,49 | 7,29 | 7,28 | 11,8 | 12,9 | 11,7 | 9,6 | 7,87 | 3,88 | 3,52 | 4,3 | 7,62 |
| CaO | 4,66 | 9,3 | 9,25 | 16 | 9,21 | 10 | 7,83 | 7,6 | 4,7 | 4,61 | 6,39 | 10,58 |
| Na2O | 5,6 | 3,6 | 3,5 | 1,04 | 1,2 | 2,2 | 4,1 | 5,44 | 4,4 | 4,3 | 4,3 | 2,5 |
| K2O | 3,09 | 1,49 | 1,47 | 0,22 | 3,24 | 2,77 | 1,99 | 3,04 | 5,24 | 5,94 | 4,62 | 3,87 |
| H2OT | 0,4 | 1,9 | 2 | 0,83 | 2,4 | 1,7 | 2,4 | 1,61 | 0,9 | 0,7 | 0,9 | 0,7 |
| CO2T | 0 | 0,1 | 0 | 0,56 | 0,5 | 1,4 | 2,9 | 3,09 | 1,3 | 1 | 0,6 | 0,1 |
| P2O5 | 0,23 | 0,43 | 0,41 | n.d | 0,49 | 0,56 | 0,58 | 0,5 | 0,54 | 0,56 | 0,49 | 0,84 |
| S | 0 | 0,01 | 0,01 | n.d | 0 | 0 | 0,01 | 0,21 | n.d | n.d | n.d | n.d |
| Ba (ppm) | 1300 | 690 | 690 | n.d | 1800 | 1400 | 560 | n.d | 2785 | 2886 | 3176 | 3039 |
| Be | 1,6 | 1,3 | 1,2 | n.d | 1,5 | 1,4 | 3,1 | n.d | n.d | n.d | n.d | n.d |
| Co | 26 | 40 | 38 | n.d | 52 | 47 | 39 | n.d | 27 | 29 | 29 | 44 |
| Cr | 45 | 180 | 170 | n.d | 710 | 560 | 420 | 394 | 160 | 130 | 200 | 250 |
| Cu | 22 | 43 | 39 | n.d | 17 | 14 | 38 | n.d | n.d | n.d | n.d | n.d |
| La | 31 | 20 | 17 | n.d | 16 | 25 | 56 | 60 | 78 | 88 | 72 | 74 |
| Nb | 0 | 0 | 0 | n.d | 0 | 0 | 0 | n.d | 0 | 0 | 0 | 10 |
| Ni | 21 | 52 | 47 | n.d | 160 | 140 | 87 | 75 | 32 | 34 | 38 | 62 |
| Pb | 78 | 30 | 28 | n.d | 76 | 79 | 100 | 110 | 119 | 152 | 97 | 83 |
| Sc | 7,7 | 26 | 26 | n.d | 30 | 33 | 26 | n.d | 14 | 14 | 18 | n.d |
| Sr | 1200 | 1100 | 1100 | n.d | 590 | 840 | 2400 | 1063 | 1804 | 1853 | 1861 | 1934 |
| V | 81 | 200 | 190 | n.d | 170 | 170 | 170 | n.d | n.d | n.d | n.d | 260 |
| Y | 13 | 20 | 20 | n.d | 11 | 18 | 22 | 25 | 64 | 67 | 61 | 36 |
| Yb | 1,3 | 1,7 | 1,7 | n.d | 0,6 | 1,2 | 1,6 | n.d | 1 | 1 | 2 | 3 |
| Zn | 72 | 100 | 96 | n.d | 110 | 100 | 140 | n.d | 160 | 130 | 140 | 120 |
| Zr | 170 | 58 | 56 | n.d | 26 | 72 | 130 | 157 | 158 | 182 | 145 | 205 |
| Ti ppm | 3250 | 6062,5 | 5875 | 0 | 5250 | 5125 | 5187,5 | 4125 | 3937,5 | 4187,5 | 4062,5 | 6125 |
| Total | 101 | 100,4 | 100 | 99,73 | 99,9 | 99,6 | 99,3 | 100,1 | 99,73 | 99,92 | 99,7 | 99,12 |
| Larsen index | 13,90 | -4,25 | -4,41 | -24,10 | -9,05 | -8,48 | -5,72 | -1,16 | 12,11 | 13,39 | 8,65 | -3,28 |
| Na2O+K2O | 8,69 | 5,09 | 4,97 | 1,26 | 4,44 | 4,97 | 6,09 | 8,48 | 9,64 | 10,24 | 8,92 | 6,37 |
| K2O/Na2O | 0,55 | 0,41 | 0,42 | 0,21 | 2,70 | 1,26 | 0,49 | 0,56 | 1,19 | 1,38 | 1,07 | 1,55 |
| Fe2O3/FeT | 0,54 | 0,46 | 0,45 | 0,49 | 0,29 | 0,33 | 0,26 | 0,30 | 0,54 | 0,52 | 0,53 | 0,47 |
| Fet/(Fet+Mg) | 0,67 | 0,58 | 0,58 | 0,63 | 0,42 | 0,42 | 0,47 | 0,49 | 0,65 | 0,66 | 0,64 | 0,59 |
| Zr/Y | 13,08 | 2,90 | 2,80 | | 2,36 | 4,00 | 5,91 | 6,28 | 2,47 | 2,72 | 2,38 | 5,69 |
| Ni/Cr | 0,47 | 0,29 | 0,28 | | 0,23 | 0,25 | 0,21 | 0,19 | 0,20 | 0,26 | 0,19 | 0,25 |
| Rb/Sr | 0,07 | 0,03 | 0,03 | | 0,13 | 0,09 | 0,04 | 0,10 | 0,07 | 0,08 | 0,05 | 0,04 |
| Rb/Zr | 0,46 | 0,52 | 0,50 | | 2,92 | 1,10 | 0,77 | 0,70 | 0,75 | 0,84 | 0,67 | 0,40 |
| Ti/V | 40,12 | 30,31 | 30,92 | | 30,88 | 30,15 | 30,51 | | | | | 23,56 |

| | Murdock Cr MS, 87131 | Murdock Cr MS, 87133 | Murdock Cr MS, 89292 | Murdock Cr MM, 88295 | Murdock Cr MM, 89227 | Murdock Cr MD, 87132 | Murdock Cr MD, 89248A | Murdock Cr CP, 87130 | Murdock Cr CP, 89221 | Murdock Cr CP, 89298 | Murdock Cr HB, 89509 | Murdock Cr HB, 89327 |
|---|---|---|---|---|---|---|---|---|---|---|---|---|
| SiO2 (wt.%) | 54 | 52,7 | 53,8 | 46,1 | 53,2 | 46,4 | 50,1 | 41,7 | 43,6 | 43 | 47,9 | 51 |
| TiO2 | 0,8 | 0,82 | 0,69 | 1,19 | 0,88 | 1,03 | 0,91 | 1,56 | 1,34 | 1,25 | 0,83 | 0,6 |
| Al2O3 | 14,1 | 13,8 | 13,4 | 9,5 | 13 | 12,4 | 11,5 | 5,3 | 9,5 | 6,2 | 7,4 | 10,3 |
| Fe2O3T | 8,9 | 9,7 | 8,1 | 15,6 | 9,8 | 12,4 | 11 | 17,4 | 14,6 | 14,9 | 9,1 | 9,2 |
| Fe2O3 | 4,4 | 4,5 | 2,8 | 7 | 4,7 | 5,6 | 3,9 | 8,8 | 3,4 | 4,7 | 2,6 | 2,5 |
| FeO | 4,1 | 4,7 | 4,8 | 7,8 | 4,6 | 6,2 | 6,4 | 7,9 | 7 | 9,2 | 5,9 | 6,1 |
| MnO | 0,16 | 0,18 | 0,15 | 0,21 | 0,17 | 0,2 | 0,19 | 0,28 | 0,2 | 0,26 | 0,15 | 0,17 |
| MgO | 5,67 | 6,17 | 6,56 | 9,26 | 6,54 | 8,36 | 9,66 | 12,51 | 14,54 | 12,17 | 16,1 | 12,95 |
| CaO | 7,18 | 7,5 | 6,16 | 10,29 | 8,86 | 10,15 | 9,4 | 16,78 | 13,02 | 13,56 | 12,33 | 8,82 |
| Na2O | 3,9 | 3,6 | 4,6 | 2,3 | 4,3 | 2,5 | 3,1 | 0,5 | 0,5 | 0,7 | 0,9 | 2 |
| K2O | 4,09 | 3,84 | 3,41 | 3,15 | 2,18 | 2,89 | 3,49 | 1,75 | 4,38 | 3,09 | 3,15 | 2,98 |
| H2OT | 1,1 | 1,3 | 2,6 | 1,3 | 0,9 | 2 | 1,1 | 1,2 | 1 | 0,8 | 1,2 | 1,9 |
| CO2T | 0,1 | 0,1 | n.d | 0,7 | n.d | 0,9 | n.d | 0,3 | n.d | n.d | n.d | n.d |
| P2O5 | 0,52 | 0,54 | 0,45 | 0,63 | 0,61 | 0,78 | 0,6 | 1,46 | 1,29 | 0,89 | 0,13 | 0,22 |
| S | n.d | n.d | n.d | n.d | n.d | n.d | n.d | n.d | n.d | n.d | n.d | n.d |
| Ba (ppm) | 2159 | 3655 | 2300 | 1850 | 1303 | 1565 | 1665 | 2141 | 2117 | 1894 | 121 | 1533 |
| Be | n.d | n.d | n.d | n.d | n.d | n.d | n.d | n.d | n.d | n.d | n.d | n.d |
| Co | 37 | 40 | n.d | 52 | n.d | 56 | n.d | 90 | n.d | n.d | n.d | n.d |
| Cr | 300 | 320 | 319 | 310 | 242 | 450 | 468 | 440 | 819 | 534 | 1230 | 1078 |
| Cu | n.d | n.d | n.d | n.d | n.d | n.d | n.d | n.d | n.d | n.d | n.d | n.d |
| La | 75 | 64 | n.d | 44 | n.d | 61 | n.d | 74 | n.d | n.d | n.d | n.d |
| Nb | 0 | 0 | 0 | 19 | 2 | 0 | 0 | 0 | 7 | 2 | 0 | 5 |
| Ni | 51 | 64 | 73 | 57 | 44 | 100 | 95 | 90 | 256 | 94 | 262 | 271 |
| Rb | 131 | 90 | 81 | 112 | 92 | 88 | 154 | 70 | 196 | 124 | 112 | 59 |
| Sc | 22,6 | 24,8 | n.d | n.d | n.d | 28,5 | n.d | 64,5 | n.d | n.d | n.d | n.d |
| Sr | 1587 | 2196 | 1412 | 769 | 2881 | 3013 | 1614 | 669 | 424 | 224 | 277 | 485 |
| V | n.d | n.d | n.d | 370 | 218 | n.d | 250 | n.d | 214 | 379 | 202 | 161 |
| Y | 71 | 56 | 24 | 70 | 30 | 51 | 23 | 40 | 28 | 28 | 14 | 19 |
| Yb | 3 | 1 | n.d | 3 | n.d | 1 | n.d | 3 | n.d | n.d | n.d | n.d |
| Zn | 140 | 220 | 172 | 130 | 139 | 200 | 195 | 210 | 163 | 161 | 70 | 105 |
| Zr | 225 | 121 | 108 | 158 | 165 | 122 | 123 | 109 | 55 | 70 | 42 | 96 |
| Ti ppm | 5000 | 5125 | 4312,5 | 7437,5 | 5500 | 6437,5 | 5667,5 | 9750 | 8375 | 7812,5 | 5187,5 | 3750 |
| Total | 100,12 | 99,75 | 99,42 | 99,43 | 99,94 | 99,41 | 100,35 | 100,04 | 97,77 | 99,09 | 98,59 | 99,54 |
| Larsen index | 5,12 | 3,02 | 3,81 | -8,85 | -0,10 | -6,37 | -5,29 | -21,55 | -15,66 | -17,52 | -15,23 | -7,91 |
| Na2O+K2O | 7,99 | 7,44 | 8,01 | 5,45 | 6,48 | 5,39 | 6,59 | 2,25 | 4,88 | 3,79 | 4,05 | 4,98 |
| K2O/Na2O | 1,05 | 1,07 | 0,74 | 1,37 | 0,51 | 1,16 | 1,13 | 3,50 | 8,76 | 4,41 | 3,50 | 1,49 |
| Fe2O3/FeT | 0,52 | 0,49 | 0,37 | 0,47 | 0,51 | 0,47 | 0,38 | 0,53 | 0,33 | 0,34 | 0,31 | 0,29 |
| Fet/(Fet+Mg) | 0,60 | 0,60 | 0,54 | 0,62 | 0,59 | 0,59 | 0,52 | 0,57 | 0,42 | 0,53 | 0,35 | 0,40 |
| Zr/Y | 3,17 | 2,16 | 4,50 | 2,26 | 5,50 | 2,39 | 5,35 | 2,73 | 1,96 | 2,50 | 3,00 | 5,05 |
| Ni/Cr | 0,17 | 0,20 | 0,23 | 0,18 | 0,18 | 0,22 | 0,20 | 0,20 | 0,31 | 0,18 | 0,21 | 0,25 |
| Rb/Sr | 0,08 | 0,04 | 0,06 | 0,14 | 0,03 | 0,03 | 0,10 | 0,10 | 0,46 | 0,55 | 0,40 | 0,12 |
| Rb/Zr | 0,58 | 0,74 | 0,75 | 0,71 | 0,56 | 0,72 | 1,25 | 0,64 | 3,56 | 1,77 | 2,67 | 0,61 |
| Ti/V | | | | 20,10 | 25,23 | | 22,75 | | 39,14 | 20,61 | 25,68 | 23,29 |

## A.2 Rare earth element data

Rare earth element analyses were performed on samples usually containing less than 1.0 wt.% $CO_2$, chosen as an arbitrary upper limit for least-altered specimens of the KLF, except in the case of some syenitic extrusive rocks (up to 2.5 wt.%), and lamprophyres (up to 2.9 wt.%) which normally have higher primary $CO_2$ contents (Rock, 1991).

Samples submitted for neutron activation analysis were carefully prepared: approximately 120 grams of each sample was crushed and sieved over nylon mesh to the 200 mesh fraction to ensure homogeneity, and 15 to 25 grams of each sample was submitted for analysis. Weathered rinds of samples chosen for rare earth analyses were removed before crushing in a tungsten carbide shatterbox. Before each crushing run, the crushers and shatterbox were precontaminated. Rare earth and selected trace elements were analyzed by instrumental neutron activation (INAA) at l'École polytechnique de l'Université de Montréal. All reported values are precise to within ± 5 % of reported concentrations of the following elements : Sc, Co, La, Ce, Nd, Sm, Eu, Tb, Dy, Ho, Yb, Lu, Hf, Ta, Th, U.

(n.d indicates not determined)

| | AFMS, Dom1 LC-9 | AFMS, Dom1 LC-5 | AFMS, Dom1 LC-6 | Lamp, Dom1 Hatt | Lamp avg Rock, 1991 | Lamp. Dom1 GL90016 | Trach, Dom1 GL90160 | Trach, Dom1 GL90141 | Int Brec Dom1 GL90202 | Hy. Sye, Dom1 GL8856 |
|---|---|---|---|---|---|---|---|---|---|---|
| Sc | 23,5 | 27,9 | 18 | 21,8 | 20 | 24,1 | 20,8 | 18,1 | 29,7 | 20,8 |
| Co | 37,8 | n.d | n.d | n.d | 36 | 41,9 | 33,8 | 21,1 | 38,8 | n.d |
| La | 42 | 42,6 | 30,7 | 87,7 | 53 | 91 | 39 | 34,2 | 31,4 | 44,9 |
| Ce | 89 | 102 | 75 | 202,9 | 110 | 195 | 76 | 64,8 | 63,9 | 105 |
| Nd | 45 | 49 | 35 | 108,8 | 56 | 98 | 33 | 30,8 | 36,6 | 50 |
| Sm | 9,1 | 10,2 | 6,9 | 21,3 | 10,5 | 17,8 | 6,1 | 5,6 | 6,9 | 10,1 |
| Eu | 2,51 | 2,52 | 1,74 | 5,2 | 3,1 | 4,86 | 1,74 | 1,63 | 2,09 | 2,5 |
| Tb | 0,86 | 1,04 | 0,69 | 1,93 | 1,1 | 1,68 | 0,63 | 0,55 | 0,81 | 1,04 |
| Dy | 4,1 | 5,1 | 3,7 | 6,7 | 3,7 | 7,3 | 3,2 | 3 | 4,3 | 5,4 |
| Ho | 0,9 | 0,92 | 0,65 | 1,3 | 0,9 | 1,32 | 0,66 | 0,62 | 0,79 | 0,92 |
| Yb | 1,84 | 2,02 | 1,45 | 1,23 | 1,8 | 2,02 | 1,86 | 1,86 | 1,96 | 1,98 |
| Lu | 0,29 | 0,31 | 0,24 | 0,19 | 0,26 | 0,28 | 0,29 | 0,29 | 0,29 | 0,33 |
| Hf | 3,2 | 3,5 | 2,6 | 6,7 | 5,2 | 5,2 | 3,5 | 3,6 | 3 | 4,2 |
| Ta | 0,59 | 0,31 | 0,26 | 0,59 | 0,9 | 0,42 | 1 | 0,69 | 0,93 | 0,4 |
| Th | 6,5 | 6,8 | 5,3 | 6,5 | 9 | 11,2 | 10 | 6 | 4 | 8,5 |
| U | 1,74 | 1,69 | 1,29 | 0,8 | 3 | 2,85 | 2,23 | 1,78 | 1,1 | 1,74 |
| ΣREE | 195,6 | 215,71 | 156,07 | 437,25 | 240,36 | 419,26 | 162,48 | 143,35 | 149,04 | 222,17 |
| Normalized with C1 values of Anders and Grevesse (1989) | | | | | | | | | | |
| La | 178,952 | 181,508 | 130,805 | 373,669 | 225,820 | 387,729 | 166,170 | 145,718 | 133,788 | 191,308 |
| Ce | 147,546 | 169,098 | 124,337 | 336,373 | 182,361 | 323,276 | 125,995 | 107,427 | 105,935 | 174,072 |
| Nd | 99,469 | 108,311 | 77,365 | 240,495 | 123,784 | 216,622 | 72,944 | 68,081 | 80,902 | 110,522 |
| Sm | 61,863 | 69,341 | 46,907 | 144,799 | 71,380 | 121,006 | 41,468 | 38,069 | 46,907 | 68,661 |
| Eu | 44,821 | 45,000 | 31,071 | 92,857 | 55,357 | 86,786 | 31,071 | 29,107 | 37,321 | 44,643 |
| Tb | 23,691 | 28,650 | 19,008 | 53,168 | 30,303 | 46,281 | 17,355 | 15,152 | 22,314 | 28,650 |
| Dy | 16,893 | 21,014 | 15,245 | 27,606 | 15,245 | 30,078 | 13,185 | 12,361 | 17,717 | 22,250 |
| Ho | 16,187 | 16,547 | 11,691 | 23,381 | 16,187 | 23,741 | 11,871 | 11,151 | 14,209 | 16,547 |
| Yb | 11,323 | 12,431 | 8,923 | 7,569 | 11,077 | 12,431 | 11,446 | 11,446 | 12,062 | 12,185 |
| Lu | 11,983 | 12,810 | 9,917 | 7,851 | 10,744 | 11,570 | 11,983 | 11,983 | 11,983 | 13,636 |
| ΣREE | 612,73 | 664,71 | 475,27 | 1307,77 | 742,26 | 1259,52 | 503,49 | 450,50 | 483,14 | 682,47 |
| La/Lu | 14,93 | 14,17 | 13,19 | 47,59 | 21,02 | 33,51 | 13,87 | 12,16 | 11,16 | 14,03 |
| Eu/Sm | 0,72 | 0,65 | 0,66 | 0,64 | 0,78 | 0,72 | 0,75 | 0,76 | 0,80 | 0,65 |
| Sm/Yb | 5,46 | 5,58 | 5,26 | 19,13 | 6,44 | 9,73 | 3,62 | 3,33 | 3,89 | 5,64 |

| | FP, Dom1 GL89037 | FP, Dom1 GL90192 | QFP, Dom1 GL90185 | QFP, Dom1 Vindicator St | Kinabik Creek GL90215 | McVittie Stock GL89006 | Gauthier Dio GL90089 | McElroy Stock GL89035 | Hornblendite GL8854 | Lebel Stock GL89029 |
|---|---|---|---|---|---|---|---|---|---|---|
| Sc | 17,5 | 8 | 3,1 | 3,3 | 7,7 | 6,7 | 38,8 | 8,5 | 35,6 | 34,7 |
| Co | 28,8 | 19 | 16,9 | n.d | 23,9 | 34,2 | 66,8 | 32,8 | 50,1 | 54,5 |
| La | 17,8 | 47 | 23,9 | 23,9 | 31 | 25,6 | 4,4 | 33,6 | 31,9 | 141 |
| Ce | 36,3 | 93 | 41,5 | 50,2 | 62 | 49,4 | 11,6 | 65,5 | 70,8 | 285 |
| Nd | 20,4 | 42 | 19 | 21,7 | 29 | 24,3 | 10,1 | 31,9 | 43,1 | 132 |
| Sm | 4,5 | 7,3 | 3,7 | 4,2 | 5,3 | 4,9 | 2,8 | 5,6 | 9,8 | 22,2 |
| Eu | 1,39 | 1,94 | 1,11 | 1,06 | 1,53 | 1,39 | 1,11 | 1,68 | 2,47 | 5,62 |
| Tb | 0,62 | 0,63 | 0,32 | 0,41 | 0,62 | 0,57 | 0,49 | 0,51 | 0,95 | 1,77 |
| Dy | 3,4 | 3,3 | 1,5 | 1,8 | 3,4 | 3,2 | 2,8 | 2,6 | 4,4 | 8,3 |
| Ho | 0,69 | 0,66 | 0,38 | 0,57 | 0,77 | 0,64 | 0,52 | 0,53 | 0,68 | 1,35 |
| Yb | 2,14 | 1,51 | 0,77 | 0,62 | 1,98 | 1,93 | 1,32 | 1,28 | 1,28 | 3,2 |
| Lu | 0,33 | 0,23 | 0,11 | 0,11 | 0,32 | 0,31 | 0,19 | 0,21 | 0,2 | 0,52 |
| Hf | 3,2 | 4,5 | 3,5 | 3,6 | 3,8 | 4,5 | 1,64 | 3,9 | 2,9 | 7 |
| Ta | 0,9 | 1,18 | 1,61 | 1,31 | 1,25 | 1,69 | 0,59 | 1,2 | 0,43 | 0,56 |
| Th | 2,4 | 8,3 | 4,9 | 5,1 | 5,5 | 6,7 | 0,27 | 5,7 | 4,6 | 8,5 |
| U | 0,76 | 3,21 | 2,92 | 2,97 | 1,76 | 2,26 | 0,08 | 1,36 | 0,95 | 1,48 |
| ΣREE | 87,57 | 197,57 | 92,29 | 104,57 | 135,92 | 112,24 | 35,33 | 143,41 | 165,58 | 600,96 |
| Normalized wit | | | | | | | | | | |
| La | 75,841 | 200,256 | 101,832 | 101,832 | 132,084 | 109,075 | 18,747 | 143,161 | 135,918 | 600,767 |
| Ce | 60,179 | 154,178 | 68,800 | 83,223 | 102,785 | 81,897 | 19,231 | 108,588 | 117,374 | 472,480 |
| Nd | 45,093 | 92,838 | 41,998 | 47,966 | 64,103 | 53,714 | 22,325 | 70,513 | 95,270 | 291,777 |
| Sm | 30,591 | 49,626 | 25,153 | 28,552 | 36,030 | 33,311 | 19,035 | 38,069 | 66,621 | 150,918 |
| Eu | 24,821 | 34,643 | 19,821 | 18,929 | 27,321 | 24,821 | 19,821 | 30,000 | 44,107 | 100,357 |
| Tb | 17,080 | 17,355 | 8,815 | 11,295 | 17,080 | 15,702 | 13,499 | 14,050 | 26,171 | 48,760 |
| Dy | 14,009 | 13,597 | 6,180 | 7,417 | 14,009 | 13,185 | 11,537 | 10,713 | 18,129 | 34,199 |
| Ho | 12,410 | 11,871 | 6,835 | 10,252 | 13,849 | 11,511 | 9,353 | 9,532 | 12,230 | 24,281 |
| Yb | 13,169 | 9,292 | 4,738 | 3,815 | 12,185 | 11,877 | 8,123 | 7,877 | 7,877 | 19,692 |
| Lu | 13,636 | 9,504 | 4,545 | 4,545 | 13,223 | 12,810 | 7,851 | 8,678 | 8,264 | 21,488 |
| ΣREE | 306,83 | 593,16 | 288,72 | 317,83 | 432,67 | 367,90 | 149,52 | 441,18 | 531,96 | 1764,72 |
| La/Lu | 5,56 | 21,07 | 22,40 | 22,40 | 9,99 | 8,51 | 2,39 | 16,50 | 16,45 | 27,96 |
| Eu/Sm | 0,81 | 0,70 | 0,79 | 0,66 | 0,76 | 0,75 | 1,04 | 0,79 | 0,66 | 0,66 |
| Sm/Yb | 2,32 | 5,34 | 5,31 | 7,48 | 2,96 | 2,80 | 2,34 | 4,83 | 8,46 | 7,66 |

| | Otto Stock GL89019 | Otto Stock Sut 881108 | Otto Stock Sut 8899 | Otto Stock Sut 88120 | Otto Stock Sut 88103 | Otto Stock Sut 88104 | Otto Stock Sut 88114 | Otto Stock Othman,A12 | Otto Stock Othman, A13 | Otto Stock, Othman, A14 |
|---|---|---|---|---|---|---|---|---|---|---|
| Sc | 7,8 | n.d | n.d | n.d | n.d | n.d | n.d | n.d | n.d | n.d |
| Co | 18,2 | n.d | n.d | n.d | n.d | n.d | n.d | n.d | n.d | n.d |
| La | 117 | 6,03 | 10,3 | 190 | 22,5 | 33,2 | 5,38 | 156 | 64 | 12 |
| Ce | 229 | 15,9 | 22,6 | 417 | 56,7 | 82,2 | 16,6 | 333 | 119 | 25 |
| Nd | 95 | 8,08 | 8,25 | 192 | 35,3 | 51,3 | 15,5 | 172 | 61 | 12 |
| Sm | 15,4 | 1,69 | 1,53 | 32,5 | 7,57 | 10,1 | 4,41 | 29 | 10 | 2 |
| Eu | 3,82 | 0,362 | 0,38 | 7,47 | 2,05 | 2,43 | 1,32 | 9,5 | 3,3 | 0,8 |
| Tb | 1,22 | 0,127 | 0,128 | 2,05 | 0,786 | 0,79 | 0,628 | n.d | n.d | n.d |
| Dy | 5,8 | 0,707 | 0,823 | 9,63 | 4,56 | 4,38 | 4,2 | n.d | n.d | n.d |
| Ho | 1,04 | 0,115 | 0,16 | 1,43 | 0,828 | 0,722 | 0,755 | 1,5 | 0,8 | 0,2 |
| Yb | 1,81 | 0,335 | 0,595 | 2,22 | 1,9 | 1,42 | 1,55 | 3,3 | 2,4 | 0,9 |
| Lu | 0,27 | 0,045 | 0,085 | 0,345 | 0,257 | 0,208 | 0,216 | 0,6 | 0,3 | 0,1 |
| Hf | 5,1 | n.d | n.d | n.d | n.d | n.d | n.d | 7 | 11 | 5 |
| Ta | 1,82 | n.d | n.d | n.d | n.d | n.d | n.d | n.d | n.d | n.d |
| Th | 16,1 | n.d | n.d | n.d | n.d | n.d | n.d | 8 | 21 | 18 |
| U | 1,5 | n.d | n.d | n.d | n.d | n.d | n.d | 1 | 3 | 4 |
| ΣREE | 470,36 | 33,391 | 44,851 | 854,645 | 132,451 | 186,75 | 50,559 | 704,9 | 260,8 | 53 |
| Normalized wil | | | | | | | | | | |
| La | 498,509 | 25,692 | 43,886 | 809,544 | 95,867 | 141,457 | 22,923 | 664,678 | 272,689 | 51,129 |
| Ce | 379,642 | 26,359 | 37,467 | 691,313 | 93,999 | 136,273 | 27,520 | 552,056 | 197,281 | 41,446 |
| Nd | 209,991 | 17,860 | 18,236 | 424,403 | 78,028 | 113,395 | 34,262 | 380,195 | 134,836 | 26,525 |
| Sm | 104,691 | 11,489 | 10,401 | 220,938 | 51,462 | 68,661 | 29,980 | 197,145 | 67,981 | 13,596 |
| Eu | 68,214 | 6,464 | 6,786 | 133,393 | 36,607 | 43,393 | 23,571 | 169,643 | 58,929 | 14,286 |
| Tb | 33,609 | 3,499 | 3,526 | 56,474 | 21,653 | 21,763 | 17,300 | n.d | n.d | n.d |
| Dy | 23,898 | 2,913 | 3,391 | 39,679 | 18,789 | 18,047 | 17,305 | n.d | n.d | n.d |
| Ho | 18,705 | 2,068 | 2,878 | 25,719 | 14,892 | 12,986 | 13,579 | 26,978 | 14,388 | 3,597 |
| Yb | 11,138 | 2,062 | 3,662 | 13,662 | 11,692 | 8,738 | 9,538 | 20,308 | 14,769 | 5,538 |
| Lu | 11,157 | 1,860 | 3,512 | 14,256 | 10,620 | 8,595 | 8,926 | 24,793 | 12,397 | 4,132 |
| ΣREE | 1359,55 | 100,27 | 133,74 | 2429,38 | 433,61 | 573,31 | 204,90 | 2035,80 | 773,27 | 160,25 |
| La/Lu | 44,68 | 13,82 | 12,49 | 56,79 | 9,03 | 16,46 | 2,57 | 26,81 | 22,00 | 12,37 |
| Eu/Sm | 0,65 | 0,56 | 0,65 | 0,60 | 0,71 | 0,63 | 0,79 | 0,86 | 0,87 | 1,05 |
| Sm/Yb | 9,40 | 5,57 | 2,84 | 16,17 | 4,40 | 7,86 | 3,14 | 9,71 | 4,60 | 2,45 |

| | Murdock Cr. AS, 87101 | Murdock Cr. AS, 87118 | Murdock Cr. MS, 87133 | Murdock Cr. MS, 87131 | Murdock Cr. MD,87132 | Murdock Cr. CP, 87130 | Murdock Cr. CP, 87135 | Trach, Dom1 Ujike, 1 | Trach, Dom1 Ujike, 3 | Trach, Dom1 Ujike, 6 |
|---|---|---|---|---|---|---|---|---|---|---|
| Sc | 14 | 15 | 24,8 | 22,6 | 28,5 | 64,5 | 50,4 | 19,2 | 14,2 | 21,4 |
| Co | 27 | 29 | 40 | 37 | 56 | 90 | 73 | 25 | 20 | 25 |
| La | 78 | 92 | 64 | 75 | 61 | 74 | 120 | 88,8 | 94,5 | 102,9 |
| Ce | 132 | 153 | 106 | 121 | 112 | 147 | 205 | 189 | 180,7 | 205,2 |
| Nd | n.d | n.d | n.d | n.d | n.d | n.d | n.d | 80,9 | 79 | 88,9 |
| Sm | 11 | 12 | 11 | 10 | 11 | 18 | 20,4 | 15,8 | 14,9 | 16,9 |
| Eu | 4 | 3 | 3 | 2 | 3 | 5 | 5 | 4,25 | 3,42 | 3,94 |
| Tb | 1,3 | 1,4 | 1,2 | 1,4 | 1,4 | 2,5 | 2,5 | 1,19 | 1,1 | 1,29 |
| Dy | n.d | n.d | n.d | n.d | n.d | n.d | n.d | n.d | n.d | n.d |
| Ho | n.d | n.d | n.d | n.d | n.d | n.d | n.d | 1,54 | 1,62 | 1,47 |
| Yb | 1 | 1 | 1 | 3 | 1 | 3 | 3 | 2,58 | 2,33 | 2,55 |
| Lu | 0,3 | 0,3 | 0,3 | 0,4 | 0,2 | 0,5 | 0,5 | 0,34 | 0,34 | 0,4 |
| Hf | 4 | 4 | 2 | 5 | 0,5 | 3 | 6 | 6,3 | 6,2 | 4,7 |
| Ta | 0,5 | 0,7 | 0,5 | 0,6 | 0,5 | 0,5 | 0,5 | 0,5 | 0,4 | 0,5 |
| Th | 4,5 | 7,4 | 1,7 | 11 | 1,1 | 2,1 | 8,4 | 13,7 | 18,6 | 18,7 |
| U | 1,4 | 1,5 | 0,1 | 2,5 | 0,1 | 0,3 | 1,3 | 3,2 | 4,6 | 2,4 |
| ∑REE | 227,6 | 262,7 | 186,5 | 212,8 | 189,6 | 250 | 356,4 | 384,4 | 377,91 | 423,55 |
| Normalized wit | | | | | | | | | | |
| La | 332,339 | 391,990 | 272,689 | 319,557 | 259,906 | 315,296 | 511,291 | 378,355 | 402,642 | 438,432 |
| Ce | 218,833 | 253,647 | 175,729 | 200,597 | 185,676 | 243,700 | 339,854 | 313,329 | 299,569 | 340,186 |
| Nd | n.d | n.d | n.d | n.d | n.d | n.d | n.d | 178,824 | 174,624 | 196,508 |
| Sm | 74,779 | 81,577 | 74,779 | 67,981 | 74,779 | 122,366 | 138,681 | 107,410 | 101,292 | 114,888 |
| Eu | 71,429 | 53,571 | 53,571 | 35,714 | 53,571 | 89,286 | 89,286 | 75,893 | 61,071 | 70,357 |
| Tb | 35,813 | 38,567 | 33,058 | 38,567 | 38,567 | 68,871 | 68,871 | 32,782 | 30,303 | 35,537 |
| Dy | n.d | n.d | n.d | n.d | n.d | n.d | n.d | n.d | n.d | n.d |
| Ho | n.d | n.d | n.d | n.d | n.d | n.d | n.d | 27,698 | 29,137 | 26,439 |
| Yb | 6,154 | 6,154 | 6,154 | 18,462 | 6,154 | 18,462 | 18,462 | 15,877 | 14,338 | 15,692 |
| Lu | 12,397 | 12,397 | 12,397 | 16,529 | 8,264 | 20,661 | 20,661 | 14,050 | 14,050 | 16,529 |
| ∑REE | 751,74 | 837,90 | 628,38 | 697,41 | 626,92 | 878,64 | 1187,11 | 1144,22 | 1127,03 | 1254,57 |
| La/Lu | 26,81 | 31,62 | 22,00 | 19,33 | 31,45 | 15,26 | 24,75 | 26,93 | 28,66 | 26,53 |
| Eu/Sm | 0,96 | 0,66 | 0,72 | 0,53 | 0,72 | 0,73 | 0,64 | 0,71 | 0,60 | 0,61 |
| Sm/Yb | 12,15 | 13,26 | 12,15 | 3,68 | 12,15 | 6,63 | 7,51 | 6,77 | 7,06 | 7,32 |

| | Trach, Dom1 Ujike, 9 | Trach, Dom1 Ujike, 12 | Lebel Stock Hatt |
|---|---|---|---|
| Sc | 9 | 5,2 | 14,5 |
| Co | 21 | 13 | n.d |
| La | 104,6 | 137,2 | 32,4 |
| Ce | 193,6 | 272,1 | 69,4 |
| Nd | 76,6 | 101,1 | 30,8 |
| Sm | 13 | 21,6 | 5,8 |
| Eu | 3,47 | 5,04 | 1,72 |
| Tb | 0,87 | 1,93 | 0,64 |
| Dy | n.d | n.d | 2,9 |
| Ho | 0,98 | 2,05 | n.d |
| Yb | 2,03 | 3,26 | 1,37 |
| Lu | 0,3 | 0,41 | 0,25 |
| Hf | 4,7 | 10,6 | 5,3 |
| Ta | 0,7 | 0,7 | 0,79 |
| Th | 26,6 | 36,3 | 5,3 |
| U | 2,9 | 8,3 | 1,88 |
| ΣREE | 395,45 | 544,69 | 145,28 |
| Normalized witl | | | |
| La | 445,675 | 584,576 | 138,049 |
| Ce | 320,955 | 451,094 | 115,053 |
| Nd | 169,319 | 223,475 | 68,081 |
| Sm | 88,375 | 146,839 | 39,429 |
| Eu | 61,964 | 90,000 | 30,714 |
| Tb | 23,967 | 53,168 | 17,631 |
| Dy | n.d | n.d | 11,949 |
| Ho | 17,626 | 36,871 | n.d |
| Yb | 12,492 | 20,062 | 8,431 |
| Lu | 12,397 | 16,942 | 10,331 |
| ΣREE | 1152,77 | 1623,03 | 439,67 |
| La/Lu | 35,95 | 34,50 | 13,36 |
| Eu/Sm | 0,70 | 0,61 | 0,78 |
| Sm/Yb | 7,07 | 7,32 | 4,68 |

## A.3 Electron microprobe analyses of minerals

All electron microprobe mineral analyses were carried out by wavelength dispersive X-ray spectroscopy on the Camebax electron microprobe at McGill University using the ONQUANT software package and a series of natural and synthetic standards. The instrument parameters were as follows: acceleration potential was 15 kV, beam current was 8 nA, beam size ranged from 5 to 8 μm, counting times were 25s for major elements and varied between 25 and 100 s for F and Cl. Mineral analyses were recalculated using the MINFILE public domain software package. Clinopyroxene analyses were calculated on the basis of 4 cations, following the method of Morimoto (1989). Amphibole and biotite analyses were recalculated on the basis of 22 oxygens + 2 (OH, F, Cl).

Clinopyroxene, amphibole and biotite separates from 12 representative samples were obtained by a combination of magnetic and heavy liquid separation techniques. Amphibole and clinopyroxene were then analyzed for ferrous iron by the modified Wilson cold acid method, after Wilson (1960). Measured ferric and ferrous iron are an important line of evidence in the documentation of magmatic oxidation. By obtaining $Fe^{3+}/(Fe^{3+}+Fe^{2+})$ molar ratios for ferromagnesian minerals of 12 representative of the rocks of the Kirkland Lake area, these ratios can be used to calculate FeO and $Fe_2O_3$ of ferromagnesian minerals in similar rock units, providing a better estimate than simple charge balancing in mineral formula calculations.

(n.d indicates not determined)

## A.3.1 Clinopyroxene

| | LC-6 | LC-6 | LC-6 | LC-6 | LC-6 | LC-6 | LC-6 | LC-5 | LC-5 | LC-5 |
|---|---|---|---|---|---|---|---|---|---|---|
| SiO2 | 49.75 | 50.08 | 50.33 | 50.84 | 50.78 | 50.23 | 51.48 | 51.07 | 51.37 | 51.00 |
| TiO2 | 0.85 | 0.84 | 0.75 | 0.81 | 0.70 | 0.85 | 0.72 | 0.80 | 0.77 | 0.80 |
| Al2O3 | 4.63 | 3.77 | 3.23 | 3.15 | 2.73 | 3.41 | 2.67 | 3.13 | 2.69 | 3.10 |
| Cr2O3 | 0.05 | 0.03 | 0.05 | 0.04 | 0.01 | 0.02 | 0.04 | - | 0.01 | 0.01 |
| Fe2O3 | 2.49 | 2.46 | 2.21 | 2.17 | 2.26 | 2.28 | 2.24 | 2.22 | 2.37 | 2.33 |
| FeO | 6.46 | 6.37 | 5.73 | 5.61 | 5.85 | 5.91 | 5.80 | 5.74 | 6.14 | 6.03 |
| MnO | 0.25 | 0.20 | 0.23 | 0.19 | 0.26 | 0.21 | 0.27 | 0.18 | 0.23 | 0.20 |
| NiO | - | - | - | - | - | - | - | - | - | - |
| MgO | 13.55 | 13.61 | 14.15 | 14.24 | 13.84 | 13.32 | 13.74 | 13.98 | 13.50 | 13.70 |
| CaO | 21.04 | 21.64 | 22.24 | 22.38 | 22.08 | 22.06 | 22.20 | 22.40 | 22.16 | 21.40 |
| Na2O | 0.75 | 0.52 | 0.47 | 0.46 | 0.56 | 0.82 | 0.59 | 0.49 | 0.61 | 0.65 |
| K2O | 0.02 | 0.01 | 0.03 | - | 0.06 | 0.18 | 0.03 | 0.02 | 0.02 | 0.01 |
| Total | 99.84 | 99.53 | 99.42 | 99.89 | 99.13 | 99.29 | 99.78 | 100.03 | 99.87 | 99.23 |
| #Si IV | 1.85 | 1.87 | 1.88 | 1.89 | 1.90 | 1.88 | 1.92 | 1.89 | 1.91 | 1.91 |
| #Al IV | 0.15 | 0.13 | 0.12 | 0.11 | 0.10 | 0.12 | 0.08 | 0.11 | 0.09 | 0.09 |
| T site | 2.00 | 2.00 | 2.00 | 2.00 | 2.00 | 2.00 | 2.00 | 2.00 | 2.00 | 2.00 |
| #Al VI | 0.05 | 0.04 | 0.02 | 0.02 | 0.02 | 0.03 | 0.03 | 0.03 | 0.03 | 0.05 |
| #Ti | 0.02 | 0.02 | 0.02 | 0.02 | 0.02 | 0.02 | 0.02 | 0.02 | 0.02 | 0.02 |
| #Cr | 0.00 | 0.00 | 0.00 | 0.00 | 0.00 | 0.00 | 0.00 | - | 0.00 | 0.00 |
| #Fe +3 | 0.07 | 0.07 | 0.06 | 0.06 | 0.06 | 0.06 | 0.06 | 0.06 | 0.07 | 0.07 |
| #Fe +2 | 0.20 | 0.20 | 0.18 | 0.17 | 0.18 | 0.18 | 0.18 | 0.18 | 0.19 | 0.19 |
| #Mn +2 | 0.01 | 0.01 | 0.01 | 0.01 | 0.01 | 0.01 | 0.01 | 0.01 | 0.01 | 0.01 |
| #Ni | - | - | - | - | - | - | - | - | - | - |
| #Mg | 0.75 | 0.76 | 0.79 | 0.79 | 0.77 | 0.74 | 0.76 | 0.77 | 0.75 | 0.76 |
| #Ca | 0.84 | 0.87 | 0.89 | 0.89 | 0.89 | 0.88 | 0.89 | 0.89 | 0.88 | 0.86 |
| #Na | 0.05 | 0.04 | 0.03 | 0.03 | 0.04 | 0.06 | 0.04 | 0.04 | 0.04 | 0.05 |
| #K | 0.00 | 0.00 | 0.00 | - | 0.00 | 0.01 | 0.00 | 0.00 | 0.00 | 0.00 |
| M1,M2 | 2.00 | 2.00 | 2.00 | 2.00 | 2.00 | 2.00 | 2.00 | 2.00 | 2.00 | 2.00 |
| #O | 5.98 | 5.99 | 5.98 | 5.99 | 5.99 | 5.97 | 6.01 | 6.00 | 6.01 | 6.01 |

| | LC-5 | LC-5 | LC-5 | LC-5 | LC-5 | LC-5 | LC-5 | LC-5 | LC-5 | LC-5 |
|---|---|---|---|---|---|---|---|---|---|---|
| SiO2 | 53.97 | 54.47 | 54.26 | 51.70 | 50.66 | 51.34 | 51.10 | 54.16 | 52.99 | 52.82 |
| TiO2 | 0.24 | 0.17 | 0.18 | 0.70 | 0.80 | 0.82 | 0.80 | 0.22 | 0.14 | 0.37 |
| Al2O3 | 1.02 | 1.13 | 1.44 | 3.23 | 3.75 | 3.11 | 3.51 | 1.26 | 2.10 | 2.72 |
| Cr2O3 | 0.28 | 0.25 | 0.77 | 0.03 | 0.05 | 0.03 | 0.04 | 0.14 | - | 0.02 |
| Fe2O3 | 1.18 | 1.48 | 1.14 | 2.22 | 2.46 | 2.09 | 2.23 | 1.66 | 1.76 | 2.23 |
| FeO | 3.04 | 3.84 | 2.95 | 5.75 | 6.36 | 5.40 | 5.77 | 4.30 | 4.56 | 5.78 |
| MnO | 0.05 | 0.10 | 0.04 | 0.21 | 0.20 | 0.15 | 0.18 | 0.15 | 0.29 | 0.30 |
| NiO | - | - | - | - | - | - | - | 0.05 | 0.05 | - |
| MgO | 13.59 | 16.84 | 17.11 | 14.22 | 13.59 | 14.42 | 14.01 | 17.31 | 17.07 | 14.92 |
| CaO | 21.38 | 21.86 | 22.04 | 21.88 | 21.38 | 22.24 | 22.80 | 20.95 | 18.80 | 20.77 |
| Na2O | 0.72 | 0.54 | 0.53 | 0.62 | 0.72 | 0.50 | 0.43 | 0.46 | 0.42 | 0.63 |
| K2O | 0.01 | 0.04 | - | 0.02 | 0.01 | 0.02 | 0.02 | - | 1.05 | - |
| Total | 95.48 | 100.72 | 100.46 | 100.58 | 99.98 | 100.12 | 100.89 | 100.66 | 99.23 | 100.56 |
| #Si IV | 2.08 | 1.98 | 1.97 | 1.90 | 1.88 | 1.90 | 1.88 | 1.97 | 1.95 | 1.94 |
| #Al IV | - | 0.02 | 0.03 | 0.10 | 0.12 | 0.10 | 0.12 | 0.03 | 0.05 | 0.06 |
| T site | 2.08 | 2.00 | 2.00 | 2.00 | 2.00 | 2.00 | 2.00 | 2.00 | 2.00 | 2.00 |
| #Al VI | 0.05 | 0.03 | 0.03 | 0.04 | 0.05 | 0.03 | 0.03 | 0.02 | 0.04 | 0.06 |
| #Ti | 0.01 | 0.00 | 0.00 | 0.02 | 0.02 | 0.02 | 0.02 | 0.01 | 0.00 | 0.01 |
| #Cr | 0.01 | 0.01 | 0.02 | 0.00 | 0.00 | 0.00 | 0.00 | 0.00 | - | 0.00 |
| #Fe +3 | 0.03 | 0.04 | 0.03 | 0.06 | 0.07 | 0.06 | 0.06 | 0.05 | 0.05 | 0.06 |
| #Fe +2 | 0.10 | 0.12 | 0.09 | 0.18 | 0.20 | 0.17 | 0.18 | 0.13 | 0.14 | 0.18 |
| #Mn +2 | 0.00 | 0.00 | 0.00 | 0.01 | 0.01 | 0.00 | 0.01 | 0.00 | 0.01 | 0.01 |
| #Ni | - | - | - | - | - | - | - | 0.00 | 0.00 | - |
| #Mg | 0.78 | 0.91 | 0.93 | 0.78 | 0.75 | 0.79 | 0.77 | 0.94 | 0.94 | 0.82 |
| #Ca | 0.88 | 0.85 | 0.86 | 0.86 | 0.85 | 0.88 | 0.90 | 0.82 | 0.74 | 0.82 |
| #Na | 0.05 | 0.04 | 0.04 | 0.04 | 0.05 | 0.04 | 0.03 | 0.03 | 0.03 | 0.04 |
| #K | 0.00 | 0.00 | - | 0.00 | 0.00 | 0.00 | 0.00 | - | 0.05 | - |
| M1,M2 | 1.92 | 2.00 | 2.00 | 2.00 | 2.00 | 2.00 | 2.00 | 2.00 | 2.00 | 2.00 |
| #O | 6.11 | 6.01 | 6.01 | 6.00 | 6.00 | 6.00 | 5.99 | 6.01 | 5.98 | 6.02 |

| | LC-5 | LC-5 | LC-5 | LC-7 | LC-7 | LC-7 | LC-7 | LC-7 | 90190 | 90190 |
|---|---|---|---|---|---|---|---|---|---|---|
| SiO2 | 53.49 | 51.41 | 51.15 | 51.44 | 54.40 | 53.01 | 51.32 | 52.13 | 52.80 | 52.94 |
| TiO2 | 0.27 | 0.69 | 0.76 | 0.82 | 0.17 | 0.37 | 0.63 | 0.64 | 0.37 | 0.35 |
| Al2O3 | 1.76 | 3.34 | 3.57 | 3.49 | 0.74 | 2.23 | 3.58 | 2.70 | 1.50 | 1.86 |
| Cr2O3 | - | 0.06 | 0.06 | - | 0.03 | 0.07 | - | - | 0.10 | 0.08 |
| Fe2O3 | 1.75 | 2.44 | 2.34 | 2.58 | 1.38 | 1.85 | 2.54 | 2.81 | 1.87 | 1.76 |
| FeO | 4.52 | 6.31 | 6.07 | 6.68 | 3.56 | 4.79 | 6.57 | 7.26 | 4.85 | 4.56 |
| MnO | 0.16 | 0.25 | 0.31 | 0.31 | 0.13 | 0.17 | 0.26 | 0.31 | 0.21 | 0.13 |
| NiO | - | - | 0.01 | 0.02 | 0.09 | 0.02 | - | - | 0.04 | 0.01 |
| MgO | 15.99 | 13.82 | 14.15 | 13.97 | 16.77 | 15.14 | 14.11 | 13.44 | 14.38 | 15.70 |
| CaO | 22.09 | 21.10 | 21.33 | 20.56 | 22.94 | 21.91 | 20.42 | 20.39 | 22.25 | 22.77 |
| Na2O | 0.45 | 0.65 | 0.57 | 0.70 | 0.30 | 0.50 | 0.70 | 0.94 | 0.39 | 0.30 |
| K2O | - | - | 0.02 | 0.02 | - | 0.01 | 0.01 | - | - | - |
| Total | 100.48 | 100.07 | 100.34 | 100.59 | 100.51 | 100.07 | 100.14 | 100.62 | 98.76 | 100.46 |
| #Si IV | 1.96 | 1.91 | 1.89 | 1.90 | 1.98 | 1.95 | 1.90 | 1.93 | 1.98 | 1.94 |
| #Al IV | 0.04 | 0.09 | 0.11 | 0.10 | 0.02 | 0.05 | 0.10 | 0.07 | 0.02 | 0.06 |
| T site | 2.00 | 2.00 | 2.00 | 2.00 | 2.00 | 2.00 | 2.00 | 2.00 | 2.00 | 2.00 |
| #Al VI | 0.03 | 0.06 | 0.05 | 0.05 | 0.01 | 0.05 | 0.06 | 0.05 | 0.05 | 0.02 |
| #Ti | 0.01 | 0.02 | 0.02 | 0.02 | 0.00 | 0.01 | 0.02 | 0.02 | 0.01 | 0.01 |
| #Cr | - | 0.00 | 0.00 | - | 0.00 | 0.00 | - | - | 0.00 | 0.00 |
| #Fe +3 | 0.05 | 0.07 | 0.07 | 0.07 | 0.04 | 0.05 | 0.07 | 0.08 | 0.05 | 0.05 |
| #Fe +2 | 0.14 | 0.20 | 0.19 | 0.21 | 0.11 | 0.15 | 0.20 | 0.22 | 0.15 | 0.14 |
| #Mn +2 | 0.00 | 0.01 | 0.01 | 0.01 | 0.00 | 0.01 | 0.01 | 0.01 | 0.01 | 0.00 |
| #Ni | - | - | 0.00 | 0.00 | 0.00 | 0.00 | - | - | 0.00 | 0.00 |
| #Mg | 0.87 | 0.77 | 0.78 | 0.77 | 0.91 | 0.83 | 0.78 | 0.74 | 0.80 | 0.86 |
| #Ca | 0.87 | 0.84 | 0.85 | 0.81 | 0.90 | 0.86 | 0.81 | 0.81 | 0.89 | 0.89 |
| #Na | 0.03 | 0.05 | 0.04 | 0.05 | 0.02 | 0.04 | 0.05 | 0.07 | 0.03 | 0.02 |
| #K | - | - | 0.00 | 0.00 | - | 0.00 | 0.00 | - | - | - |
| M1,M2 | 2.00 | 2.00 | 2.00 | 2.00 | 2.00 | 2.00 | 2.00 | 2.00 | 2.00 | 2.00 |
| #O | 6.01 | 6.01 | 6.00 | 6.01 | 6.01 | 6.02 | 6.01 | 6.01 | 6.04 | 6.01 |

| | 90190 | 90190 | 90190 | 90153 | 90153 | 90153 | 90153 | 90160 | 90160 | 90202 |
|---|---|---|---|---|---|---|---|---|---|---|
| SiO2 | 52.99 | 49.56 | 50.02 | 55.89 | 57.54 | 57.61 | 56.81 | 56.19 | 56.40 | 52.98 |
| TiO2 | 0.32 | 0.89 | 0.97 | 0.01 | 0.02 | - | 0.03 | - | 0.05 | 0.32 |
| Al2O3 | 2.17 | 4.41 | 4.20 | 1.03 | 0.35 | 0.47 | 0.67 | 0.99 | 0.69 | 1.68 |
| Cr2O3 | 0.05 | - | - | 0.04 | 0.04 | 0.03 | - | - | 0.03 | 0.61 |
| Fe2O3 | 1.89 | 2.62 | 2.56 | 4.82 | 4.57 | 3.79 | 4.29 | 4.76 | 4.65 | 1.41 |
| FeO | 4.90 | 6.77 | 6.63 | 5.30 | 5.03 | 4.16 | 4.72 | 5.24 | 5.12 | 3.64 |
| MnO | 0.19 | 0.26 | 0.30 | 0.23 | 0.34 | 0.16 | 0.32 | 0.30 | 0.41 | 0.11 |
| NiO | - | 0.05 | - | 0.02 | 0.11 | 0.03 | 0.05 | 0.01 | 0.02 | 0.03 |
| MgO | 15.31 | 13.37 | 13.17 | 19.00 | 19.13 | 20.12 | 18.73 | 18.42 | 18.31 | 16.87 |
| CaO | 22.50 | 21.13 | 21.20 | 12.22 | 12.72 | 12.56 | 12.62 | 12.43 | 12.68 | 22.36 |
| Na2O | 0.48 | 0.71 | 0.65 | 0.22 | 0.11 | 0.90 | 0.27 | 0.27 | 0.25 | 0.42 |
| K2O | - | - | - | 0.10 | 0.02 | 0.03 | 0.04 | 0.05 | 0.04 | 0.02 |
| Total | 100.80 | 99.77 | 99.70 | 98.88 | 99.98 | 99.86 | 98.55 | 98.66 | 98.65 | 100.45 |
| #Si IV | 1.94 | 1.85 | 1.87 | 2.08 | 2.12 | 2.10 | 2.12 | 2.10 | 2.11 | 1.93 |
| #Al IV | 0.06 | 0.15 | 0.13 | - | - | - | - | - | - | 0.07 |
| T site | 2.00 | 2.00 | 2.00 | 2.08 | 2.12 | 2.10 | 2.12 | 2.10 | 2.11 | 2.00 |
| #Al VI | 0.03 | 0.04 | 0.05 | 0.05 | 0.02 | 0.02 | 0.03 | 0.04 | 0.03 | 0.00 |
| #Ti | 0.01 | 0.02 | 0.03 | 0.00 | 0.00 | - | 0.00 | - | 0.00 | 0.01 |
| #Cr | 0.00 | - | - | 0.00 | 0.00 | 0.00 | - | - | 0.00 | 0.02 |
| #Fe +3 | 0.05 | 0.07 | 0.07 | 0.14 | 0.13 | 0.10 | 0.12 | 0.13 | 0.13 | 0.04 |
| #Fe +2 | 0.15 | 0.21 | 0.21 | 0.17 | 0.16 | 0.13 | 0.15 | 0.16 | 0.16 | 0.11 |
| #Mn +2 | 0.01 | 0.01 | 0.01 | 0.01 | 0.01 | 0.00 | 0.01 | 0.01 | 0.01 | 0.00 |
| #Ni | - | 0.00 | - | 0.00 | 0.00 | 0.00 | 0.00 | 0.00 | 0.00 | 0.00 |
| #Mg | 0.83 | 0.74 | 0.73 | 1.06 | 1.05 | 1.09 | 1.04 | 1.03 | 1.02 | 0.92 |
| #Ca | 0.88 | 0.84 | 0.85 | 0.49 | 0.50 | 0.49 | 0.50 | 0.50 | 0.51 | 0.87 |
| #Na | 0.03 | 0.05 | 0.05 | 0.02 | 0.01 | 0.06 | 0.02 | 0.02 | 0.02 | 0.03 |
| #K | - | - | - | 0.00 | 0.00 | 0.00 | 0.00 | 0.00 | 0.00 | 0.00 |
| M1,M2 | 2.00 | 2.00 | 2.00 | 1.92 | 1.88 | 1.90 | 1.88 | 1.90 | 1.89 | 2.00 |
| #O | 6.00 | 5.98 | 6.00 | 6.16 | 6.19 | 6.13 | 6.19 | 6.18 | 6.18 | 5.99 |

| | 90202 | 90202 | 90202 | 90016 | 90016 | 90016 | 90192 | 90192 |
|---|---|---|---|---|---|---|---|---|
| SiO2 | 54.10 | 52.98 | 51.55 | 53.82 | 53.82 | 53.28 | 54.74 | 55.15 |
| TiO2 | 0.18 | 0.17 | 0.46 | 0.16 | 0.20 | 0.24 | 0.30 | 0.20 |
| Al2O3 | 1.13 | 1.43 | 2.49 | 0.84 | 1.06 | 1.12 | 2.78 | 2.99 |
| Cr2O3 | 0.35 | 0.88 | 0.45 | 0.01 | 0.10 | 0.21 | 0.06 | 0.05 |
| Fe2O3 | 1.32 | 1.20 | 1.74 | 1.17 | 1.08 | 0.96 | 3.25 | 3.55 |
| FeO | 3.41 | 3.09 | 4.50 | 4.22 | 3.83 | 3.44 | 3.57 | 3.90 |
| MnO | 0.15 | 0.13 | 0.16 | 0.11 | 0.13 | 0.15 | 0.12 | 0.18 |
| NiO | 0.03 | - | 0.01 | - | 0.02 | 0.01 | 0.06 | 0.06 |
| MgO | 17.89 | 17.85 | 15.85 | 17.74 | 16.52 | 17.07 | 20.23 | 19.96 |
| CaO | 21.50 | 21.66 | 22.27 | 21.20 | 23.43 | 22.67 | 10.70 | 11.03 |
| Na2O | 0.44 | 0.48 | 0.35 | 0.38 | 0.40 | 0.37 | 1.78 | 1.53 |
| K2O | - | - | 0.02 | 0.02 | 0.01 | - | 0.50 | 0.43 |
| Total | 100.50 | 99.87 | 99.85 | 99.67 | 100.60 | 99.52 | 98.09 | 99.03 |
| #Si IV | 1.96 | 1.93 | 1.90 | 1.97 | 1.96 | 1.95 | 2.00 | 2.00 |
| #Al IV | 0.04 | 0.06 | 0.10 | 0.03 | 0.04 | 0.05 | 0.00 | - |
| T site | 2.00 | 1.99 | 2.00 | 2.00 | 2.00 | 2.00 | 2.00 | 2.00 |
| #Al VI | 0.01 | - | 0.01 | 0.00 | 0.00 | 0.00 | 0.12 | 0.13 |
| #Ti | 0.00 | 0.00 | 0.01 | 0.00 | 0.01 | 0.01 | 0.01 | 0.01 |
| #Cr | 0.01 | 0.03 | 0.01 | 0.00 | 0.00 | 0.01 | 0.00 | 0.00 |
| #Fe +3 | 0.04 | 0.03 | 0.05 | 0.03 | 0.03 | 0.03 | 0.09 | 0.10 |
| #Fe +2 | 0.10 | 0.09 | 0.14 | 0.13 | 0.12 | 0.11 | 0.11 | 0.12 |
| #Mn +2 | 0.00 | 0.00 | 0.00 | 0.00 | 0.00 | 0.00 | 0.00 | 0.01 |
| #Ni | 0.00 | - | 0.00 | - | 0.00 | 0.00 | 0.00 | 0.00 |
| #Mg | 0.97 | 0.97 | 0.87 | 0.97 | 0.90 | 0.93 | 1.10 | 1.08 |
| #Ca | 0.83 | 0.85 | 0.88 | 0.83 | 0.91 | 0.89 | 0.42 | 0.43 |
| #Na | 0.03 | 0.03 | 0.02 | 0.03 | 0.03 | 0.03 | 0.13 | 0.11 |
| #K | - | - | 0.00 | 0.00 | 0.00 | - | 0.02 | 0.02 |
| M1,M2 | 2.00 | 2.01 | 2.00 | 2.00 | 2.00 | 2.00 | 2.00 | 2.00 |
| #O | 6.00 | 5.98 | 5.98 | 5.99 | 5.99 | 5.99 | 6.04 | 6.06 |

| | OSBS | OSBS | 89017 | 89017 | 89017 | 89019 | 89019 | SSHORN | SSALK | MCBS |
|---|---|---|---|---|---|---|---|---|---|---|
| SiO2 | 51.85 | 51.76 | 50.50 | 51.20 | 50.61 | 50.85 | 50.71 | 53.54 | 52.26 | 53.14 |
| TiO2 | 0.17 | 0.54 | 0.49 | 0.55 | 0.49 | 0.56 | 0.49 | 0.07 | 0.16 | 0.04 |
| Al2O3 | 1.78 | 2.15 | 1.91 | 1.32 | 1.77 | 2.26 | 2.01 | 0.75 | 0.55 | 2.14 |
| Cr2O3 | 0.04 | 0.01 | 0.03 | 0.04 | 0.02 | 0.02 | 0.04 | - | - | 0.03 |
| Fe2O3 | 6.35 | 4.97 | 5.50 | 5.42 | 6.09 | 5.09 | 5.16 | 2.88 | 14.02 | 3.65 |
| FeO | 6.98 | 5.46 | 6.05 | 5.96 | 6.70 | 5.60 | 5.67 | 4.19 | 5.79 | 4.02 |
| MnO | 0.53 | 0.41 | 0.29 | 0.34 | 0.34 | 0.42 | 0.37 | 0.22 | 0.48 | 0.29 |
| NiO | - | - | - | 0.02 | - | 0.02 | - | - | - | - |
| MgO | 9.90 | 11.99 | 11.10 | 11.36 | 10.81 | 11.76 | 11.60 | 14.70 | 7.17 | 13.27 |
| CaO | 19.88 | 20.95 | 21.13 | 20.98 | 20.91 | 20.97 | 21.10 | 23.41 | 15.25 | 21.97 |
| Na2O | 2.34 | 1.94 | 2.01 | 2.05 | 1.99 | 1.79 | 1.85 | 0.75 | 5.23 | 1.61 |
| K2O | 0.01 | - | - | - | 0.01 | - | - | - | - | - |
| Total | 99.83 | 100.18 | 99.01 | 99.24 | 99.74 | 99.34 | 99.00 | 100.51 | 100.91 | 100.16 |
| #Si IV | 1.96 | 1.93 | 1.91 | 1.93 | 1.91 | 1.91 | 1.92 | 1.97 | 1.97 | 1.96 |
| #Al IV | 0.04 | 0.07 | 0.09 | 0.06 | 0.08 | 0.09 | 0.08 | 0.03 | 0.02 | 0.04 |
| T site | 2.00 | 2.00 | 2.00 | 1.99 | 1.99 | 2.00 | 2.00 | 2.00 | 2.00 | 2.00 |
| #Al VI | 0.04 | 0.02 | - | - | - | 0.01 | 0.00 | 0.00 | - | 0.05 |
| #Ti | 0.00 | 0.02 | 0.01 | 0.02 | 0.01 | 0.02 | 0.01 | 0.00 | 0.00 | 0.00 |
| #Cr | 0.00 | 0.00 | 0.00 | 0.00 | 0.00 | 0.00 | 0.00 | - | - | 0.00 |
| #Fe +3 | 0.18 | 0.14 | 0.16 | 0.15 | 0.17 | 0.14 | 0.15 | 0.08 | 0.40 | 0.10 |
| #Fe +2 | 0.22 | 0.17 | 0.19 | 0.19 | 0.21 | 0.18 | 0.18 | 0.13 | 0.18 | 0.12 |
| #Mn +2 | 0.02 | 0.01 | 0.01 | 0.01 | 0.01 | 0.01 | 0.01 | 0.01 | 0.02 | 0.01 |
| #Ni | - | - | - | 0.00 | - | 0.00 | - | - | - | - |
| #Mg | 0.56 | 0.67 | 0.63 | 0.64 | 0.61 | 0.66 | 0.65 | 0.81 | 0.40 | 0.73 |
| #Ca | 0.81 | 0.84 | 0.86 | 0.85 | 0.85 | 0.85 | 0.85 | 0.92 | 0.62 | 0.87 |
| #Na | 0.17 | 0.14 | 0.15 | 0.15 | 0.15 | 0.13 | 0.14 | 0.05 | 0.38 | 0.12 |
| #K | 0.00 | - | - | - | 0.00 | - | - | - | - | - |
| M1,M2 | 2.00 | 2.00 | 2.00 | 2.01 | 2.01 | 2.00 | 2.00 | 2.00 | 2.00 | 2.00 |
| #O | 6.01 | 5.99 | 5.97 | 5.98 | 5.98 | 5.99 | 5.98 | 6.00 | 6.00 | 6.00 |

| | MCBS | MCBS | MCBS | MCSR | MCSR | MCSR | MCSR | MCSR | MCSR | MCSR |
|---|---|---|---|---|---|---|---|---|---|---|
| SiO2 | 53.01 | 52.21 | 52.89 | 53.87 | 51.81 | 51.25 | 52.97 | 52.50 | 51.83 | 50.79 |
| TiO2 | 0.54 | 0.62 | 0.34 | 0.05 | 0.25 | 0.49 | 0.14 | 0.15 | 0.23 | 0.41 |
| Al2O3 | 2.10 | 2.67 | 2.26 | 0.36 | 1.92 | 2.90 | 1.96 | 1.29 | 1.65 | 2.31 |
| Cr2O3 | - | 0.01 | 0.03 | 0.05 | 0.03 | 0.02 | - | - | - | - |
| Fe2O3 | 3.49 | 3.63 | 3.75 | 2.08 | 4.91 | 5.28 | 1.84 | 4.01 | 5.02 | 5.84 |
| FeO | 3.84 | 3.99 | 4.12 | 3.89 | 5.17 | 4.26 | 6.57 | 5.43 | 3.18 | 3.66 |
| MnO | 0.32 | 0.25 | 0.30 | 0.19 | 0.34 | 0.33 | 0.35 | 0.39 | 0.40 | 0.48 |
| NiO | - | - | - | - | - | - | - | - | - | - |
| MgO | 13.43 | 13.76 | 13.28 | 14.75 | 11.84 | 12.34 | 13.51 | 13.41 | 14.08 | 12.88 |
| CaO | 22.02 | 22.00 | 21.73 | 24.57 | 21.90 | 22.44 | 22.22 | 22.57 | 22.60 | 22.28 |
| Na2O | 1.55 | 1.38 | 1.70 | 0.53 | 1.61 | 1.37 | 0.86 | 0.90 | 0.98 | 1.17 |
| K2O | 0.01 | - | 0.01 | 0.04 | 0.01 | 0.01 | - | 0.03 | - | 0.01 |
| Total | 100.31 | 100.52 | 100.41 | 100.38 | 99.79 | 100.69 | 100.42 | 100.68 | 99.97 | 99.83 |
| #Si IV | 1.95 | 1.92 | 1.95 | 1.98 | 1.94 | 1.90 | 1.96 | 1.94 | 1.92 | 1.90 |
| #Al IV | 0.05 | 0.08 | 0.05 | 0.02 | 0.06 | 0.10 | 0.04 | 0.06 | 0.07 | 0.10 |
| T site | 2.00 | 2.00 | 2.00 | 2.00 | 2.00 | 2.00 | 2.00 | 2.00 | 1.99 | 2.00 |
| #Al VI | 0.04 | 0.03 | 0.04 | - | 0.02 | 0.03 | 0.04 | 0.00 | - | - |
| #Ti | 0.01 | 0.02 | 0.01 | 0.00 | 0.01 | 0.01 | 0.00 | 0.00 | 0.01 | 0.01 |
| #Cr | - | 0.00 | 0.00 | 0.00 | 0.00 | 0.00 | - | - | - | - |
| #Fe +3 | 0.10 | 0.10 | 0.10 | 0.06 | 0.14 | 0.15 | 0.05 | 0.11 | 0.14 | 0.16 |
| #Fe +2 | 0.12 | 0.12 | 0.13 | 0.12 | 0.16 | 0.13 | 0.20 | 0.17 | 0.10 | 0.11 |
| #Mn +2 | 0.01 | 0.01 | 0.01 | 0.01 | 0.01 | 0.01 | 0.01 | 0.01 | 0.01 | 0.02 |
| #Ni | - | - | - | - | - | - | - | - | - | - |
| #Mg | 0.74 | 0.75 | 0.73 | 0.81 | 0.66 | 0.68 | 0.74 | 0.74 | 0.78 | 0.72 |
| #Ca | 0.87 | 0.87 | 0.86 | 0.97 | 0.88 | 0.89 | 0.88 | 0.90 | 0.90 | 0.89 |
| #Na | 0.11 | 0.10 | 0.12 | 0.04 | 0.12 | 0.10 | 0.06 | 0.06 | 0.07 | 0.08 |
| #K | 0.00 | - | 0.00 | 0.00 | 0.00 | 0.00 | - | 0.00 | - | 0.00 |
| M1,M2 | 2.00 | 2.00 | 2.00 | 2.00 | 2.00 | 2.00 | 2.00 | 2.00 | 2.01 | 2.00 |
| #O | 6.01 | 5.99 | 6.00 | 6.00 | 6.00 | 6.00 | 6.00 | 6.00 | 6.00 | 6.00 |

| | MCSR | MCSR | MCSR | MCSR | 90089 | 90089 | 90089 | 90089 | 90089 | 89035 |
|---|---|---|---|---|---|---|---|---|---|---|
| SiO2 | 53.03 | 52.93 | 52.70 | 51.64 | 52.95 | 51.79 | 51.83 | 52.61 | 53.63 | 52.82 |
| TiO2 | 0.13 | 0.54 | 0.42 | 0.26 | 0.28 | 0.49 | 0.57 | 0.34 | 0.29 | 0.01 |
| Al2O3 | 1.42 | 2.41 | 2.44 | 1.01 | 0.76 | 1.38 | 1.60 | 1.12 | 0.99 | 0.63 |
| Cr2O3 | - | - | - | - | 0.38 | 0.37 | 0.32 | 0.53 | 0.53 | 0.01 |
| Fe2O3 | 6.67 | 3.25 | 3.21 | 5.81 | 2.06 | 2.41 | 2.02 | 1.80 | 1.44 | 2.21 |
| FeO | 6.79 | 3.90 | 4.70 | 4.95 | 5.56 | 6.51 | 5.45 | 4.86 | 3.88 | 5.98 |
| MnO | 0.53 | 0.32 | 0.37 | 0.46 | 0.24 | 0.22 | 0.17 | 0.14 | 0.17 | 0.61 |
| NiO | - | - | - | - | 0.02 | - | 0.02 | 0.04 | 0.04 | - |
| MgO | 9.66 | 13.07 | 12.71 | 12.39 | 15.04 | 14.55 | 16.29 | 16.61 | 16.51 | 13.16 |
| CaO | 18.77 | 21.49 | 21.43 | 21.49 | 21.48 | 21.07 | 20.86 | 21.26 | 21.29 | 22.98 |
| Na2O | 3.22 | 1.88 | 1.76 | 1.50 | 0.30 | 0.39 | 0.32 | 0.28 | 0.33 | 0.67 |
| K2O | - | - | 0.01 | - | - | 0.04 | - | - | - | - |
| Total | 100.22 | 99.79 | 99.75 | 99.51 | 99.07 | 99.22 | 99.45 | 99.59 | 99.10 | 99.08 |
| #Si IV | 1.99 | 1.95 | 1.95 | 1.94 | 1.98 | 1.94 | 1.92 | 1.94 | 1.99 | 1.99 |
| #Al IV | 0.01 | 0.05 | 0.05 | 0.04 | 0.02 | 0.06 | 0.07 | 0.05 | 0.01 | 0.01 |
| T site | 2.00 | 2.00 | 2.00 | 1.99 | 2.00 | 2.00 | 1.99 | 1.99 | 2.00 | 2.00 |
| #Al VI | 0.05 | 0.06 | 0.06 | - | 0.02 | 0.00 | - | - | 0.03 | 0.02 |
| #Ti | 0.00 | 0.01 | 0.01 | 0.01 | 0.01 | 0.01 | 0.02 | 0.01 | 0.01 | 0.00 |
| #Cr | - | - | - | - | 0.01 | 0.01 | 0.01 | 0.02 | 0.02 | 0.00 |
| #Fe +3 | 0.19 | 0.09 | 0.09 | 0.16 | 0.06 | 0.07 | 0.06 | 0.05 | 0.04 | 0.06 |
| #Fe +2 | 0.21 | 0.12 | 0.15 | 0.16 | 0.17 | 0.20 | 0.17 | 0.15 | 0.12 | 0.19 |
| #Mn +2 | 0.02 | 0.01 | 0.01 | 0.01 | 0.01 | 0.01 | 0.01 | 0.00 | 0.01 | 0.02 |
| #Ni | - | - | - | - | 0.00 | - | 0.00 | 0.00 | 0.00 | - |
| #Mg | 0.54 | 0.72 | 0.70 | 0.69 | 0.84 | 0.81 | 0.90 | 0.91 | 0.91 | 0.74 |
| #Ca | 0.75 | 0.85 | 0.85 | 0.87 | 0.86 | 0.85 | 0.83 | 0.84 | 0.84 | 0.93 |
| #Na | 0.23 | 0.13 | 0.13 | 0.11 | 0.02 | 0.03 | 0.02 | 0.02 | 0.02 | 0.05 |
| #K | - | - | 0.00 | - | - | 0.00 | - | - | - | - |
| M1,M2 | 2.00 | 2.00 | 2.00 | 2.01 | 2.00 | 2.00 | 2.01 | 2.01 | 2.00 | 2.00 |
| #O | 6.00 | 6.00 | 6.00 | 6.00 | 6.03 | 6.01 | 5.99 | 6.00 | 6.03 | 6.01 |

| | 89035 | 89035 | 89030 | 89030 | 89030 | 89030 | 89030 | 89030 | 89030 | 89030 |
|---|---|---|---|---|---|---|---|---|---|---|
| SiO2 | 52.55 | 52.80 | 52.42 | 51.01 | 51.34 | 50.87 | 51.76 | 52.72 | 51.08 | 52.55 |
| TiO2 | 0.04 | 0.05 | 0.45 | 0.49 | 0.46 | 0.41 | 0.50 | 0.43 | 0.39 | 0.39 |
| Al2O3 | 0.78 | 0.93 | 1.81 | 2.27 | 2.03 | 1.89 | 2.10 | 1.92 | 1.92 | 1.94 |
| Cr2O3 | 0.03 | 0.02 | - | 0.03 | 0.01 | 0.01 | - | 0.01 | - | 0.03 |
| Fe2O3 | 2.38 | 2.22 | 3.63 | 5.78 | 3.84 | 6.11 | 4.80 | 3.60 | 6.12 | 3.61 |
| FeO | 6.44 | 5.99 | 4.33 | 6.90 | 4.58 | 7.29 | 5.72 | 4.29 | 7.30 | 4.30 |
| MnO | 0.71 | 0.68 | 0.34 | 0.40 | 0.32 | 0.36 | 0.29 | 0.32 | 0.39 | 0.19 |
| NiO | - | 0.05 | - | - | - | 0.06 | - | 0.07 | - | 0.05 |
| MgO | 13.24 | 13.23 | 13.54 | 10.28 | 13.00 | 9.90 | 11.68 | 13.82 | 9.73 | 13.78 |
| CaO | 22.74 | 23.00 | 21.73 | 19.80 | 21.36 | 20.70 | 20.05 | 20.85 | 19.47 | 20.70 |
| Na2O | 0.80 | 0.57 | 1.70 | 2.71 | 1.90 | 2.47 | 2.20 | 1.67 | 2.45 | 1.75 |
| K2O | - | - | - | 0.01 | 0.02 | - | - | 0.03 | 0.01 | - |
| Total | 99.71 | 99.54 | 99.95 | 99.68 | 98.86 | 100.07 | 99.10 | 99.73 | 98.86 | 99.29 |
| #Si IV | 1.97 | 1.98 | 1.94 | 1.92 | 1.92 | 1.92 | 1.95 | 1.95 | 1.95 | 1.95 |
| #Al IV | 0.03 | 0.02 | 0.06 | 0.08 | 0.08 | 0.08 | 0.05 | 0.05 | 0.05 | 0.05 |
| T site | 2.00 | 2.00 | 2.00 | 2.00 | 2.00 | 2.00 | 2.00 | 2.00 | 2.00 | 2.00 |
| #Al VI | - | 0.02 | 0.01 | 0.02 | 0.01 | 0.00 | 0.04 | 0.03 | 0.04 | 0.04 |
| #Ti | 0.00 | 0.00 | 0.01 | 0.01 | 0.01 | 0.01 | 0.01 | 0.01 | 0.01 | 0.01 |
| #Cr | 0.00 | 0.00 | - | 0.00 | 0.00 | 0.00 | - | 0.00 | - | 0.00 |
| #Fe +3 | 0.07 | 0.06 | 0.10 | 0.16 | 0.11 | 0.17 | 0.14 | 0.10 | 0.18 | 0.10 |
| #Fe +2 | 0.20 | 0.19 | 0.13 | 0.22 | 0.14 | 0.23 | 0.18 | 0.13 | 0.23 | 0.13 |
| #Mn +2 | 0.02 | 0.02 | 0.01 | 0.01 | 0.01 | 0.01 | 0.01 | 0.01 | 0.01 | 0.01 |
| #Ni | - | 0.00 | - | - | - | 0.00 | - | 0.00 | - | 0.00 |
| #Mg | 0.74 | 0.74 | 0.75 | 0.58 | 0.72 | 0.56 | 0.65 | 0.76 | 0.55 | 0.76 |
| #Ca | 0.91 | 0.92 | 0.86 | 0.80 | 0.86 | 0.84 | 0.81 | 0.83 | 0.80 | 0.82 |
| #Na | 0.06 | 0.04 | 0.12 | 0.20 | 0.14 | 0.18 | 0.16 | 0.12 | 0.18 | 0.13 |
| #K | - | - | - | 0.00 | 0.00 | - | - | 0.00 | 0.00 | - |
| M1,M2 | 2.00 | 2.00 | 2.00 | 2.00 | 2.00 | 2.00 | 2.00 | 2.00 | 2.00 | 2.00 |
| #O | 5.99 | 6.01 | 5.98 | 5.97 | 5.96 | 5.97 | 5.99 | 5.99 | 6.00 | 5.99 |

| | 89030 | 89029 | 89029 | 89029 | 89029 | 89029 |
|---|---|---|---|---|---|---|
| SiO2 | 51.72 | 50.14 | 50.44 | 50.27 | 50.86 | 50.97 |
| TiO2 | 0.39 | 0.53 | 0.52 | 0.45 | 0.47 | 0.49 |
| Al2O3 | 2.04 | 2.53 | 2.70 | 2.26 | 2.42 | 2.92 |
| Cr2O3 | - | 0.04 | 0.05 | 0.03 | 0.02 | 0.06 |
| Fe2O3 | 4.71 | 7.60 | 7.41 | 7.29 | 7.33 | 7.31 |
| FeO | 5.62 | 6.06 | 5.92 | 5.82 | 5.85 | 5.84 |
| MnO | 0.22 | 0.35 | 0.36 | 0.34 | 0.34 | 0.36 |
| NiO | - | 0.02 | - | - | - | - |
| MgO | 11.43 | 9.81 | 9.66 | 9.86 | 9.99 | 9.88 |
| CaO | 19.69 | 19.60 | 19.24 | 19.89 | 19.38 | 19.97 |
| Na2O | 2.22 | 2.77 | 3.01 | 2.56 | 2.81 | 3.03 |
| K2O | 0.05 | - | - | 0.03 | - | - |
| Total | 98.09 | 99.45 | 99.31 | 98.80 | 99.47 | 100.83 |
| #Si IV | 1.96 | 1.90 | 1.91 | 1.92 | 1.92 | 1.90 |
| #Al IV | 0.04 | 0.10 | 0.09 | 0.08 | 0.08 | 0.10 |
| T site | 2.00 | 2.00 | 2.00 | 2.00 | 2.00 | 2.00 |
| #Al VI | 0.05 | 0.01 | 0.03 | 0.02 | 0.03 | 0.02 |
| #Ti | 0.01 | 0.02 | 0.01 | 0.01 | 0.01 | 0.01 |
| #Cr | - | 0.00 | 0.00 | 0.00 | 0.00 | 0.00 |
| #Fe +3 | 0.13 | 0.22 | 0.21 | 0.21 | 0.21 | 0.20 |
| #Fe +2 | 0.18 | 0.19 | 0.19 | 0.19 | 0.18 | 0.18 |
| #Mn +2 | 0.01 | 0.01 | 0.01 | 0.01 | 0.01 | 0.01 |
| #Ni | - | 0.00 | - | - | - | - |
| #Mg | 0.65 | 0.55 | 0.54 | 0.56 | 0.56 | 0.55 |
| #Ca | 0.80 | 0.80 | 0.78 | 0.81 | 0.78 | 0.80 |
| #Na | 0.16 | 0.20 | 0.22 | 0.19 | 0.21 | 0.22 |
| #K | 0.00 | - | - | 0.00 | - | - |
| M1,M2 | 2.00 | 2.00 | 2.00 | 2.00 | 2.00 | 2.00 |
| #O | 6.00 | 5.98 | 5.98 | 5.99 | 5.99 | 5.97 |

## A.3.2 Biotite

| | CT-6 | CT-6 | CT-6 | CT-6 | CT-2 | CT-2 | CT-2 | CT-2 | CT-2 | CT-6G |
|---|---|---|---|---|---|---|---|---|---|---|
| SiO2 | 36.84 | 36.80 | 36.19 | 35.86 | 35.57 | 35.74 | 35.57 | 36.36 | 36.17 | 41.56 |
| TiO2 | 2.69 | 4.66 | 3.52 | 6.37 | 5.16 | 5.30 | 6.42 | 3.49 | 3.37 | 0.94 |
| Al2O3 | 15.34 | 14.09 | 15.40 | 13.93 | 13.70 | 13.92 | 13.49 | 14.14 | 14.27 | 13.53 |
| Cr2O3 | - | - | - | - | - | 0.01 | - | - | - | - |
| Fe2O3 | 5.14 | 4.95 | 5.10 | 4.93 | 4.54 | 4.58 | 4.42 | 4.61 | 4.61 | 0.00 |
| FeO | 13.89 | 13.36 | 13.78 | 13.31 | 12.26 | 12.38 | 11.93 | 12.46 | 12.44 | 14.91 |
| MnO | - | - | - | - | 0.17 | 0.18 | 0.14 | 0.12 | 0.11 | - |
| MgO | 15.22 | 15.42 | 14.26 | 13.97 | 14.05 | 13.79 | 14.34 | 14.56 | 14.41 | 16.56 |
| Li2O | - | - | - | - | - | - | - | - | - | - |
| BaO | - | - | - | - | - | - | - | - | - | - |
| CaO | 0.05 | - | - | 0.52 | - | - | 0.03 | - | 0.01 | - |
| Na2O | - | - | - | 0.07 | 0.05 | 0.05 | 0.05 | 0.02 | 0.04 | - |
| K2O | 9.90 | 9.41 | 9.75 | 9.34 | 10.17 | 10.18 | 10.09 | 10.39 | 10.29 | 10.80 |
| Rb2O | - | - | - | - | - | - | - | - | - | - |
| Cs2O | - | - | - | - | - | - | - | - | - | - |
| H2O | 4.00 | 4.01 | 3.99 | 3.99 | 4.00 | 4.00 | 4.00 | 4.00 | 4.00 | 3.83 |
| F | - | - | - | - | - | - | - | - | - | 0.44 |
| Cl | - | - | 0.03 | - | - | - | - | - | - | 0.06 |
| O=F | - | - | - | - | - | - | - | - | - | 0.19 |
| O=Cl | - | - | 0.01 | - | - | - | - | - | - | 0.01 |
| Total | 103.07 | 102.70 | 102.01 | 102.29 | 99.67 | 100.13 | 100.48 | 100.15 | 99.72 | 102.43 |
| #Si IV | 5.36 | 5.35 | 5.32 | 5.26 | 5.36 | 5.35 | 5.30 | 5.44 | 5.43 | 6.00 |
| #Al IV | 2.63 | 2.42 | 2.67 | 2.41 | 2.43 | 2.46 | 2.37 | 2.49 | 2.53 | 2.00 |
| #Fe IV | 0.02 | 0.23 | 0.01 | 0.33 | 0.21 | 0.19 | 0.33 | 0.07 | 0.04 | - |
| #Ti IV | - | - | - | - | - | - | - | - | - | - |
| T site | 8.00 | 8.00 | 8.00 | 8.00 | 8.00 | 8.00 | 8.00 | 8.00 | 8.00 | 8.00 |
| #Al VI | - | - | - | - | - | - | - | - | - | 0.30 |
| #Ti VI | 0.29 | 0.51 | 0.39 | 0.70 | 0.58 | 0.60 | 0.72 | 0.39 | 0.38 | 0.10 |
| #Cr | - | - | - | - | - | 0.00 | - | - | - | - |
| #Fe +3 | 0.55 | 0.31 | 0.55 | 0.21 | 0.30 | 0.33 | 0.17 | 0.45 | 0.48 | 0.00 |
| #Fe +2 | 1.69 | 1.62 | 1.69 | 1.63 | 1.54 | 1.55 | 1.49 | 1.56 | 1.56 | 1.80 |
| #Mn +2 | - | - | - | - | 0.02 | 0.02 | 0.02 | 0.02 | 0.01 | - |
| #Mg | 3.30 | 3.34 | 3.13 | 3.05 | 3.15 | 3.08 | 3.19 | 3.25 | 3.23 | 3.56 |
| #Li | - | - | - | - | - | - | - | - | - | - |
| O site | 5.83 | 5.79 | 5.76 | 5.60 | 5.60 | 5.58 | 5.58 | 5.67 | 5.67 | 5.76 |
| #Ba | - | - | - | - | - | - | - | - | - | - |
| #Ca | 0.01 | - | - | 0.08 | - | - | 0.00 | - | 0.00 | - |
| #Na | - | - | - | 0.02 | 0.01 | 0.01 | 0.01 | 0.01 | 0.01 | - |
| #K | 1.84 | 1.75 | 1.83 | 1.75 | 1.95 | 1.95 | 1.92 | 1.98 | 1.97 | 1.99 |
| #Rb | - | - | - | - | - | - | - | - | - | - |
| #Cs | - | - | - | - | - | - | - | - | - | - |
| A site | 1.84 | 1.75 | 1.83 | 1.85 | 1.97 | 1.96 | 1.94 | 1.99 | 1.99 | 1.99 |
| #O | 20.00 | 20.00 | 20.00 | 20.00 | 20.00 | 20.00 | 20.00 | 20.00 | 20.00 | 20.00 |
| #OH | 4.00 | 4.00 | 3.99 | 4.00 | 4.00 | 4.00 | 4.00 | 4.00 | 4.00 | 3.78 |
| #F | - | - | - | - | - | - | - | - | - | 0.20 |
| #Cl | - | - | 0.01 | - | - | - | - | - | - | 0.01 |

| | CT-6G | LC-5G | LC-5G | LC-7G | 90016 | 90016 | 90079 | 90079 | 90079 | 90192 |
|---|---|---|---|---|---|---|---|---|---|---|
| SiO2 | 39.79 | 40.31 | 41.03 | 41.07 | 39.17 | 40.28 | 39.64 | 40.39 | 40.40 | 38.06 |
| TiO2 | 0.80 | 0.38 | 0.37 | 0.34 | 1.23 | 0.78 | 0.84 | 0.98 | 0.97 | 1.29 |
| Al2O3 | 13.63 | 12.51 | 12.34 | 11.98 | 13.76 | 13.38 | 14.02 | 13.60 | 13.34 | 13.52 |
| Cr2O3 | - | 0.02 | 0.08 | - | 0.21 | 0.83 | 1.29 | 0.13 | 0.90 | 1.74 |
| Fe2O3 | - | - | 0.00 | 0.00 | 2.61 | 1.51 | 1.56 | 2.11 | 1.77 | 5.29 |
| FeO | 15.63 | 14.87 | 14.27 | 15.79 | 4.98 | 2.88 | 2.98 | 4.04 | 3.39 | 11.10 |
| MnO | - | 0.19 | 0.25 | 0.21 | 0.10 | - | - | 0.08 | 0.03 | 0.18 |
| MgO | 17.46 | 17.17 | 17.09 | 16.67 | 23.04 | 25.15 | 24.30 | 23.76 | 24.21 | 15.65 |
| Li2O | - | - | - | - | - | - | - | - | - | - |
| BaO | - | - | - | - | - | - | - | - | - | - |
| CaO | 0.05 | 0.09 | 0.13 | 0.04 | - | - | 0.09 | 0.03 | 0.01 | 0.02 |
| Na2O | 0.06 | 0.03 | 0.02 | 0.03 | 0.30 | 0.08 | 0.10 | 0.06 | 0.07 | 0.04 |
| K2O | 9.85 | 9.69 | 9.45 | 9.75 | 9.94 | 10.33 | 9.46 | 9.44 | 8.75 | 9.28 |
| Rb2O | - | - | - | - | - | - | - | - | - | - |
| Cs2O | - | - | - | - | - | - | - | - | - | - |
| H2O | 3.91 | 3.80 | 3.78 | 3.71 | 3.07 | 3.51 | 3.67 | 3.27 | - | 3.58 |
| F | 0.25 | 0.52 | 0.61 | 0.67 | 2.27 | 1.46 | 1.15 | 1.96 | 1.96 | 0.94 |
| Cl | 0.05 | 0.01 | - | 0.01 | 0.01 | 0.01 | - | - | 95.89 | 0.01 |
| O=F | 0.11 | 0.22 | 0.26 | 0.28 | 0.96 | 0.61 | 0.48 | 0.83 | 0.83 | 0.40 |
| O=Cl | 0.01 | 0.00 | - | 0.00 | 0.00 | 0.00 | - | - | 21.64 | 0.00 |
| Total | 101.36 | 99.37 | 99.16 | 99.99 | 99.73 | 99.59 | 98.62 | 99.02 | 169.23 | 100.30 |
| #Si IV | 5.82 | 6.00 | 6.09 | 6.09 | 5.63 | 5.73 | 5.68 | 5.78 | 5.79 | 5.63 |
| #Al IV | 2.18 | 2.00 | 1.91 | 1.91 | 2.33 | 2.24 | 2.32 | 2.22 | 2.21 | 2.36 |
| #Fe IV | - | - | - | - | 0.03 | 0.03 | - | - | - | 0.01 |
| #Ti IV | - | - | - | - | - | - | - | - | - | - |
| T site | 8.00 | 8.00 | 8.00 | 8.00 | 8.00 | 8.00 | 8.00 | 8.00 | 8.00 | 8.00 |
| #Al VI | 0.17 | 0.19 | 0.24 | 0.18 | - | - | 0.05 | 0.07 | 0.04 | - |
| #Ti VI | 0.09 | 0.04 | 0.04 | 0.04 | 0.13 | 0.08 | 0.09 | 0.11 | 0.10 | 0.14 |
| #Cr | - | 0.00 | 0.01 | - | 0.02 | 0.09 | 0.15 | 0.01 | 0.10 | 0.20 |
| #Fe +3 | - | - | 0.00 | 0.00 | 0.25 | 0.14 | 0.17 | 0.23 | 0.19 | 0.57 |
| #Fe +2 | 1.91 | 1.85 | 1.77 | 1.96 | 0.60 | 0.34 | 0.36 | 0.48 | 0.41 | 1.37 |
| #Mn +2 | - | 0.02 | 0.03 | 0.03 | 0.01 | - | - | 0.01 | 0.00 | 0.02 |
| #Mg | 3.81 | 3.81 | 3.78 | 3.69 | 4.94 | 5.33 | 5.19 | 5.07 | 5.17 | 3.45 |
| #Li | - | - | - | - | - | - | - | - | - | - |
| O site | 5.98 | 5.92 | 5.87 | 5.89 | 5.96 | 5.99 | 6.00 | 5.98 | 6.02 | 5.77 |
| #Ba | - | - | - | - | - | - | - | - | - | - |
| #Ca | 0.01 | 0.01 | 0.02 | 0.01 | - | - | 0.01 | 0.00 | 0.00 | 0.00 |
| #Na | 0.02 | 0.01 | 0.01 | 0.01 | 0.08 | 0.02 | 0.03 | 0.02 | 0.02 | 0.01 |
| #K | 1.84 | 1.84 | 1.79 | 1.84 | 1.82 | 1.87 | 1.73 | 1.72 | 1.60 | 1.75 |
| #Rb | - | - | - | - | - | - | - | - | - | - |
| #Cs | - | - | - | - | - | - | - | - | - | - |
| A site | 1.86 | 1.86 | 1.81 | 1.86 | 1.91 | 1.90 | 1.77 | 1.74 | 1.62 | 1.77 |
| #O | 20.00 | 20.00 | 20.00 | 20.00 | 20.00 | 20.00 | 20.00 | 20.00 | -2E-01 | 20.00 |
| #OH | 3.87 | 3.75 | 3.71 | 3.68 | 2.96 | 3.34 | 3.48 | 3.11 | - | 3.56 |
| #F | 0.12 | 0.24 | 0.29 | 0.31 | 1.03 | 0.66 | 0.52 | 0.89 | 0.89 | 0.44 |
| #Cl | 0.01 | 0.00 | - | 0.00 | 0.00 | 0.00 | - | - | 23.29 | 0.00 |

| | 135-3 | 14-1 | 153-1 | 135-2 | 18-1 | 18-2 | 427-10 | 427-10 | 427-10 | 427-10 |
|---|---|---|---|---|---|---|---|---|---|---|
| SiO2 | 37.75 | 36.68 | 37.56 | 35.96 | 40.30 | 38.97 | 40.90 | 40.59 | 38.22 | 38.06 |
| TiO2 | 3.16 | 3.83 | 3.27 | 3.35 | 0.55 | 1.05 | 0.88 | 0.89 | 0.76 | 1.46 |
| Al2O3 | 12.79 | 13.10 | 13.07 | 14.08 | 13.88 | 13.26 | 13.05 | 13.21 | 14.40 | 16.62 |
| Cr2O3 | 0.11 | 0.18 | - | - | 1.57 | 0.52 | 0.21 | 0.17 | 2.20 | 0.11 |
| Fe2O3 | 5.44 | 5.35 | 5.31 | 5.64 | - | - | - | 0.00 | 0.00 | 0.00 |
| FeO | 11.42 | 11.24 | 11.15 | 11.85 | 4.46 | 14.19 | 4.90 | 5.12 | 13.97 | 11.47 |
| MnO | 0.07 | 0.16 | 0.09 | 0.17 | 0.06 | 0.09 | - | - | - | - |
| MgO | 14.77 | 14.22 | 14.92 | 14.83 | 25.47 | 18.68 | 25.54 | 25.65 | 17.59 | 19.89 |
| Li2O | - | - | - | - | - | - | - | - | - | - |
| BaO | - | - | - | - | - | - | - | - | - | - |
| CaO | - | - | - | 0.09 | 0.03 | - | - | - | - | - |
| Na2O | - | - | - | 0.49 | 0.07 | 0.08 | 0.06 | 0.07 | 0.06 | - |
| K2O | 9.33 | 9.84 | 9.23 | 8.10 | 9.89 | 9.55 | 10.16 | 10.14 | 9.54 | 9.35 |
| Rb2O | - | - | - | - | - | - | - | - | - | - |
| Cs2O | - | - | - | - | - | - | - | - | - | - |
| H2O | 4.05 | 4.02 | 4.05 | 4.04 | 3.67 | 3.70 | 3.18 | 2.99 | 3.36 | 3.43 |
| F | - | - | - | - | 1.13 | 0.73 | 2.14 | 2.52 | 1.41 | 1.43 |
| Cl | - | - | - | - | - | - | - | - | - | - |
| O=F | - | - | - | - | 0.48 | 0.31 | 0.90 | 1.06 | 0.59 | 0.60 |
| O=Cl | - | - | - | - | - | - | - | - | - | - |
| Total | 98.89 | 98.62 | 98.65 | 98.60 | 100.61 | 100.51 | 100.12 | 100.29 | 100.92 | 101.22 |
| #Si IV | 5.66 | 5.54 | 5.63 | 5.41 | 5.68 | 5.73 | 5.80 | 5.76 | 5.62 | 5.47 |
| #Al IV | 2.26 | 2.33 | 2.31 | 2.50 | 2.31 | 2.27 | 2.18 | 2.21 | 2.38 | 2.53 |
| #Fe IV | 0.08 | 0.12 | 0.06 | 0.09 | - | - | - | 0.00 | - | - |
| #Ti IV | - | - | - | - | 0.01 | - | 0.02 | 0.04 | - | - |
| T site | 8.00 | 8.00 | 8.00 | 8.00 | 8.00 | 8.00 | 8.00 | 8.00 | 8.00 | 8.00 |
| #Al VI | - | - | - | - | - | 0.03 | - | - | 0.11 | 0.29 |
| #Ti VI | 0.36 | 0.44 | 0.37 | 0.38 | 0.05 | 0.12 | 0.07 | 0.06 | 0.08 | 0.16 |
| #Cr | 0.01 | 0.02 | - | - | 0.18 | 0.06 | 0.02 | 0.02 | 0.26 | 0.01 |
| #Fe +3 | 0.53 | 0.49 | 0.54 | 0.55 | - | - | - | - | 0.00 | 0.00 |
| #Fe +2 | 1.43 | 1.42 | 1.40 | 1.49 | 0.53 | 1.75 | 0.58 | 0.61 | 1.72 | 1.38 |
| #Mn +2 | 0.01 | 0.02 | 0.01 | 0.02 | 0.01 | 0.01 | - | - | - | - |
| #Mg | 3.30 | 3.20 | 3.34 | 3.33 | 5.36 | 4.10 | 5.40 | 5.42 | 3.85 | 4.26 |
| #Li | - | - | - | - | - | - | - | - | - | - |
| O site | 5.65 | 5.59 | 5.66 | 5.77 | 6.11 | 6.06 | 6.08 | 6.11 | 6.02 | 6.10 |
| #Ba | - | - | - | - | - | - | - | - | - | - |
| #Ca | - | - | - | 0.01 | 0.00 | - | - | - | - | - |
| #Na | - | - | - | 0.14 | 0.02 | 0.02 | 0.02 | 0.02 | 0.02 | - |
| #K | 1.78 | 1.90 | 1.77 | 1.56 | 1.78 | 1.79 | 1.84 | 1.83 | 1.79 | 1.71 |
| #Rb | - | - | - | - | - | - | - | - | - | - |
| #Cs | - | - | - | - | - | - | - | - | - | - |
| A site | 1.78 | 1.90 | 1.77 | 1.71 | 1.80 | 1.82 | 1.85 | 1.85 | 1.81 | 1.71 |
| #O | 20.00 | 20.00 | 20.00 | 20.00 | 20.00 | 20.00 | 20.00 | 20.00 | 20.00 | 20.00 |
| #OH | 4.00 | 4.00 | 4.00 | 4.00 | 3.50 | 3.66 | 3.04 | 2.87 | 3.34 | 3.35 |
| #F | - | - | - | - | 0.50 | 0.34 | 0.96 | 1.13 | 0.66 | 0.65 |
| #Cl | - | - | - | - | - | - | - | - | - | - |

| | OSBS | OSBS | OSBS | 89017 | 89017 | 89XX | 89XX | 89XX | 89XX | 89XX |
|---|---|---|---|---|---|---|---|---|---|---|
| SiO2 | 38.87 | 38.74 | 39.29 | 35.50 | 35.24 | 36.31 | 35.98 | 35.91 | 35.79 | 35.71 |
| TiO2 | 1.99 | 1.81 | 1.47 | 1.18 | 0.98 | 2.91 | 2.89 | 2.84 | 3.26 | 2.15 |
| Al2O3 | 12.08 | 12.15 | 11.92 | 14.27 | 14.00 | 12.92 | 12.86 | 12.95 | 13.08 | 13.14 |
| Cr2O3 | - | - | - | - | - | - | - | - | - | - |
| Fe2O3 | 5.14 | 4.97 | 4.90 | 6.80 | 6.65 | 5.65 | 5.64 | 5.85 | 5.70 | 5.78 |
| FeO | 12.45 | 12.08 | 11.93 | 13.00 | 12.72 | 13.74 | 13.73 | 14.24 | 13.87 | 14.06 |
| MnO | 0.64 | 0.69 | 0.74 | 0.33 | 0.37 | 0.47 | 0.50 | 0.52 | 0.51 | 0.51 |
| MgO | 14.24 | 14.44 | 14.75 | 13.53 | 13.57 | 13.08 | 12.76 | 13.00 | 13.19 | 13.48 |
| Li2O | - | - | - | - | - | - | - | - | - | - |
| BaO | - | - | - | - | - | - | - | - | - | - |
| CaO | - | - | 0.02 | 0.02 | 0.05 | - | 0.14 | - | - | - |
| Na2O | 0.07 | 0.07 | 0.04 | 0.03 | 0.05 | 0.04 | 0.04 | 0.05 | 0.05 | 0.05 |
| K2O | 10.24 | 10.35 | 10.23 | 9.66 | 9.79 | 10.40 | 10.00 | 10.48 | 10.56 | 10.37 |
| Rb2O | - | - | - | - | - | - | - | - | - | - |
| Cs2O | - | - | - | - | - | - | - | - | - | - |
| H2O | 4.01 | 4.01 | 4.02 | 3.83 | 3.81 | 3.71 | 3.66 | 3.68 | 3.70 | 3.66 |
| F | - | - | - | 0.28 | 0.31 | 0.49 | 0.59 | 0.52 | 0.48 | 0.56 |
| Cl | - | - | - | - | 0.03 | 0.01 | 0.01 | - | - | 0.02 |
| O=F | - | - | - | 0.12 | 0.13 | 0.21 | 0.25 | 0.22 | 0.20 | 0.24 |
| O=Cl | - | - | - | - | 0.01 | 0.00 | 0.00 | - | - | 0.00 |
| Total | 99.73 | 99.31 | 99.31 | 98.32 | 97.43 | 99.52 | 98.55 | 99.82 | 99.99 | 99.25 |
| #Si IV | 5.83 | 5.83 | 5.90 | 5.45 | 5.47 | 5.54 | 5.54 | 5.48 | 5.45 | 5.48 |
| #Al IV | 2.14 | 2.16 | 2.10 | 2.55 | 2.53 | 2.32 | 2.33 | 2.33 | 2.35 | 2.38 |
| #Fe IV | 0.03 | 0.01 | - | - | - | 0.14 | 0.13 | 0.18 | 0.21 | 0.14 |
| #Ti IV | - | - | - | - | - | - | - | - | - | - |
| T site | 8.00 | 8.00 | 8.00 | 8.00 | 8.00 | 8.00 | 8.00 | 8.00 | 8.00 | 8.00 |
| #Al VI | - | - | 0.01 | 0.04 | 0.03 | - | - | - | - | - |
| #Ti VI | 0.22 | 0.20 | 0.17 | 0.14 | 0.11 | 0.33 | 0.33 | 0.33 | 0.37 | 0.25 |
| #Cr | - | - | - | - | - | - | - | - | - | - |
| #Fe +3 | 0.55 | 0.55 | 0.55 | 0.79 | 0.78 | 0.51 | 0.53 | 0.49 | 0.45 | 0.52 |
| #Fe +2 | 1.56 | 1.52 | 1.50 | 1.67 | 1.65 | 1.75 | 1.77 | 1.82 | 1.77 | 1.80 |
| #Mn +2 | 0.08 | 0.09 | 0.09 | 0.04 | 0.05 | 0.06 | 0.07 | 0.07 | 0.07 | 0.07 |
| #Mg | 3.18 | 3.24 | 3.30 | 3.10 | 3.14 | 2.97 | 2.93 | 2.96 | 2.99 | 3.08 |
| #Li | - | - | - | - | - | - | - | - | - | - |
| O site | 5.60 | 5.60 | 5.62 | 5.77 | 5.76 | 5.63 | 5.62 | 5.66 | 5.65 | 5.73 |
| #Ba | - | - | - | - | - | - | - | - | - | - |
| #Ca | - | - | 0.00 | 0.00 | 0.01 | - | 0.02 | - | - | - |
| #Na | 0.02 | 0.02 | 0.01 | 0.01 | 0.02 | 0.01 | 0.01 | 0.01 | 0.01 | 0.01 |
| #K | 1.96 | 1.99 | 1.96 | 1.89 | 1.94 | 2.02 | 1.96 | 2.04 | 2.05 | 2.03 |
| #Rb | - | - | - | - | - | - | - | - | - | - |
| #Cs | - | - | - | - | - | - | - | - | - | - |
| A site | 1.98 | 2.01 | 1.97 | 1.91 | 1.96 | 2.03 | 2.00 | 2.06 | 2.07 | 2.05 |
| #O | 20.00 | 20.00 | 20.00 | 20.00 | 20.00 | 20.00 | 20.00 | 20.00 | 20.00 | 20.00 |
| #OH | 4.00 | 4.00 | 4.00 | 3.86 | 3.84 | 3.76 | 3.71 | 3.75 | 3.77 | 3.72 |
| #F | - | - | - | 0.14 | 0.15 | 0.24 | 0.29 | 0.25 | 0.23 | 0.27 |
| #Cl | - | - | - | - | 0.01 | 0.00 | 0.00 | - | - | 0.01 |

| | MCSR | MCSR | MCSR | MCSR | 92 | MCSR | MCSR | MCSR | MCSR | MCSR |
|---|---|---|---|---|---|---|---|---|---|---|
| SiO2 | 37.18 | 37.90 | 37.59 | 38.00 | 38.24 | 35.75 | 38.33 | 36.55 | 37.04 | 36.69 |
| TiO2 | 2.64 | 2.77 | 2.43 | 1.85 | 2.12 | 3.10 | 2.38 | 3.95 | 2.78 | 3.57 |
| Al2O3 | 13.24 | 13.38 | 13.99 | 14.34 | 14.52 | 15.19 | 14.06 | 15.35 | 13.82 | 14.45 |
| Cr2O3 | - | 0.01 | 0.05 | 0.26 | 0.29 | - | - | - | 0.03 | - |
| Fe2O3 | 7.20 | 7.45 | 7.15 | 4.85 | 4.80 | 7.70 | 6.00 | 4.10 | 6.32 | 6.17 |
| FeO | 12.04 | 12.45 | 11.95 | 9.36 | 9.27 | 12.80 | 11.60 | 11.10 | 11.97 | 11.70 |
| MnO | 0.46 | 0.45 | 0.44 | 0.12 | 0.09 | 0.26 | 0.14 | 0.30 | 0.29 | 0.37 |
| MgO | 12.93 | 12.90 | 13.40 | 16.56 | 16.21 | 13.98 | 15.66 | 13.81 | 14.23 | 14.07 |
| Li2O | - | - | - | - | - | - | - | - | - | - |
| BaO | - | - | - | - | - | - | - | - | - | - |
| CaO | 0.10 | - | - | - | - | - | - | - | 0.03 | - |
| Na2O | 0.10 | 0.09 | 0.10 | 0.09 | 0.17 | 0.20 | 0.12 | 0.29 | 0.15 | 0.07 |
| K2O | 10.03 | 10.17 | 10.40 | 10.02 | 10.21 | 9.29 | 9.06 | 9.59 | 9.59 | 9.50 |
| Rb2O | - | - | - | - | - | - | - | - | - | - |
| Cs2O | - | - | - | - | - | - | - | - | - | - |
| H2O | 3.99 | 3.99 | 3.99 | 4.08 | 4.08 | 3.87 | 3.87 | 3.90 | 4.01 | 3.79 |
| F | - | - | - | - | - | 0.21 | 0.32 | 0.30 | - | 0.44 |
| Cl | - | - | - | - | - | 0.05 | 0.12 | 0.01 | - | 0.04 |
| O=F | - | - | - | - | - | 0.09 | 0.13 | 0.13 | - | 0.19 |
| O=Cl | - | - | - | - | - | 0.01 | 0.03 | 0.00 | - | 0.01 |
| Total | 99.91 | 101.56 | 101.49 | 99.53 | 100.00 | 102.30 | 101.49 | 99.12 | 100.26 | 100.67 |
| #Si IV | 5.59 | 5.61 | 5.56 | 5.61 | 5.62 | 5.26 | 5.59 | 5.46 | 5.52 | 5.44 |
| #Al IV | 2.35 | 2.33 | 2.44 | 2.39 | 2.38 | 2.63 | 2.41 | 2.54 | 2.43 | 2.52 |
| #Fe IV | 0.06 | 0.06 | 0.00 | - | - | 0.11 | - | - | 0.05 | 0.04 |
| #Ti IV | - | - | - | - | - | - | - | - | - | - |
| T site | 8.00 | 8.00 | 8.00 | 8.00 | 8.00 | 8.00 | 8.00 | 8.00 | 8.00 | 8.00 |
| #Al VI | - | - | - | 0.11 | 0.13 | - | 0.00 | 0.16 | - | - |
| #Ti VI | 0.30 | 0.31 | 0.27 | 0.21 | 0.23 | 0.34 | 0.26 | 0.44 | 0.31 | 0.40 |
| #Cr | - | 0.00 | 0.01 | 0.03 | 0.03 | - | - | - | 0.00 | - |
| #Fe +3 | 0.76 | 0.77 | 0.79 | 0.54 | 0.53 | 0.74 | 0.66 | 0.46 | 0.66 | 0.65 |
| #Fe +2 | 1.52 | 1.54 | 1.48 | 1.16 | 1.14 | 1.57 | 1.41 | 1.39 | 1.49 | 1.45 |
| #Mn +2 | 0.06 | 0.06 | 0.06 | 0.02 | 0.01 | 0.03 | 0.02 | 0.04 | 0.04 | 0.05 |
| #Mg | 2.90 | 2.85 | 2.95 | 3.64 | 3.55 | 3.06 | 3.40 | 3.07 | 3.16 | 3.11 |
| #Li | - | - | - | - | - | - | - | - | - | - |
| O site | 5.53 | 5.53 | 5.56 | 5.70 | 5.63 | 5.76 | 5.76 | 5.56 | 5.66 | 5.65 |
| #Ba | - | - | - | - | - | - | - | - | - | - |
| #Ca | 0.02 | - | - | - | - | - | - | - | 0.00 | - |
| #Na | 0.03 | 0.03 | 0.03 | 0.03 | 0.05 | 0.06 | 0.03 | 0.08 | 0.04 | 0.02 |
| #K | 1.93 | 1.92 | 1.96 | 1.89 | 1.91 | 1.74 | 1.68 | 1.83 | 1.82 | 1.80 |
| #Rb | - | - | - | - | - | - | - | - | - | - |
| #Cs | - | - | - | - | - | - | - | - | - | - |
| A site | 1.97 | 1.95 | 1.99 | 1.91 | 1.96 | 1.80 | 1.72 | 1.91 | 1.87 | 1.82 |
| #O | 20.00 | 20.00 | 20.00 | 20.00 | 20.00 | 20.00 | 20.00 | 20.00 | 20.00 | 20.00 |
| #OH | 4.00 | 4.00 | 4.00 | 4.00 | 4.00 | 3.89 | 3.82 | 3.86 | 4.00 | 3.78 |
| #F | - | - | - | - | - | 0.10 | 0.15 | 0.14 | - | 0.21 |
| #Cl | - | - | - | - | - | 0.01 | 0.03 | 0.00 | - | 0.01 |

| | MCSR | MCSR | MCSR | MCSR | MCSR | 89020 | 89020 | 89020 | 89020 | 89020 |
|---|---|---|---|---|---|---|---|---|---|---|
| SiO2 | 37.99 | 36.67 | 39.10 | 37.63 | 38.39 | 37.32 | 38.27 | 37.49 | 37.12 | 38.69 |
| TiO2 | 3.08 | 2.85 | 2.48 | 2.35 | 2.65 | 1.05 | 0.82 | 1.09 | 1.07 | 0.75 |
| Al2O3 | 14.39 | 13.73 | 12.84 | 13.53 | 13.20 | 12.84 | 12.67 | 13.08 | 13.16 | 13.53 |
| Cr2O3 | - | - | - | - | - | - | - | - | - | 1.03 |
| Fe2O3 | 5.90 | 5.79 | 5.10 | 5.03 | 4.84 | 5.63 | 5.15 | 5.95 | 5.80 | 5.06 |
| FeO | 10.00 | 13.66 | 12.10 | 11.86 | 11.83 | 10.77 | 9.85 | 11.38 | 11.09 | 9.68 |
| MnO | 0.34 | 0.40 | 0.64 | 0.58 | 0.51 | 0.28 | 0.23 | 0.25 | 0.29 | 0.27 |
| MgO | 13.44 | 13.65 | 14.78 | 13.63 | 12.77 | 15.29 | 17.45 | 15.36 | 15.28 | 16.06 |
| Li2O | - | - | - | - | - | - | - | - | - | - |
| BaO | - | - | - | - | - | - | - | - | - | - |
| CaO | 0.03 | 0.09 | 0.04 | 0.03 | - | 0.04 | 0.01 | - | - | - |
| Na2O | 0.09 | 0.17 | 0.09 | 0.14 | 0.05 | 0.02 | 0.06 | 0.05 | 0.05 | 0.04 |
| K2O | 9.87 | 9.16 | 9.27 | 9.78 | 10.23 | 9.92 | 10.46 | 10.56 | 10.41 | 10.12 |
| Rb2C | - | - | - | - | - | - | - | - | - | - |
| Cs2O | - | - | - | - | - | - | - | - | - | - |
| H2O | 3.74 | 3.67 | 3.76 | 3.76 | 3.80 | 3.44 | 3.45 | 3.50 | 3.53 | 3.60 |
| F | 0.57 | 0.62 | 0.56 | 0.51 | 0.45 | 1.17 | 1.22 | 1.02 | 0.97 | 0.95 |
| Cl | 0.15 | 0.05 | 0.04 | 0.03 | 0.01 | - | - | - | 0.01 | - |
| O=F | 0.24 | 0.26 | 0.24 | 0.21 | 0.19 | 0.49 | 0.51 | 0.43 | 0.41 | 0.40 |
| O=Cl | 0.03 | 0.01 | 0.01 | 0.01 | 0.00 | - | - | - | 0.00 | - |
| Total | 99.31 | 100.24 | 100.55 | 98.64 | 98.54 | 97.28 | 99.12 | 99.30 | 98.36 | 99.38 |
| #Si IV | 5.65 | 5.50 | 5.77 | 5.69 | 5.80 | 5.71 | 5.72 | 5.65 | 5.65 | 5.75 |
| #Al IV | 2.35 | 2.43 | 2.23 | 2.31 | 2.20 | 2.29 | 2.23 | 2.32 | 2.35 | 2.25 |
| #Fe IV | - | 0.07 | - | - | - | - | 0.05 | 0.02 | - | - |
| #Ti IV | - | - | - | - | - | - | - | - | - | - |
| T site | 8.00 | 8.00 | 8.00 | 8.00 | 8.00 | 8.00 | 8.00 | 8.00 | 8.00 | 8.00 |
| #Al VI | 0.18 | - | 0.00 | 0.10 | 0.16 | 0.03 | - | - | 0.00 | 0.12 |
| #Ti VI | 0.34 | 0.32 | 0.28 | 0.27 | 0.30 | 0.12 | 0.09 | 0.12 | 0.12 | 0.08 |
| #Cr | - | - | - | - | - | - | - | - | - | 0.12 |
| #Fe +3 | 0.66 | 0.58 | 0.57 | 0.57 | 0.55 | 0.65 | 0.53 | 0.65 | 0.66 | 0.57 |
| #Fe +2 | 1.24 | 1.71 | 1.49 | 1.50 | 1.50 | 1.38 | 1.23 | 1.44 | 1.41 | 1.20 |
| #Mn +2 | 0.04 | 0.05 | 0.08 | 0.07 | 0.07 | 0.04 | 0.03 | 0.03 | 0.04 | 0.03 |
| #Mg | 2.98 | 3.05 | 3.25 | 3.07 | 2.88 | 3.49 | 3.89 | 3.45 | 3.46 | 3.56 |
| #Li | - | - | - | - | - | - | - | - | - | - |
| O site | 5.45 | 5.72 | 5.67 | 5.58 | 5.45 | 5.70 | 5.77 | 5.70 | 5.70 | 5.68 |
| #Ba | - | - | - | - | - | - | - | - | - | - |
| #Ca | 0.00 | 0.01 | 0.01 | 0.00 | - | 0.01 | 0.00 | - | - | - |
| #Na | 0.03 | 0.05 | 0.03 | 0.04 | 0.01 | 0.01 | 0.02 | 0.01 | 0.01 | 0.01 |
| #K | 1.87 | 1.75 | 1.74 | 1.89 | 1.97 | 1.94 | 1.99 | 2.03 | 2.02 | 1.92 |
| #Rb | - | - | - | - | - | - | - | - | - | - |
| #Cs | - | - | - | - | - | - | - | - | - | - |
| A site | 1.90 | 1.82 | 1.78 | 1.93 | 1.99 | 1.95 | 2.01 | 2.05 | 2.03 | 1.93 |
| #O | 20.00 | 20.00 | 20.00 | 20.00 | 20.00 | 20.00 | 20.00 | 20.00 | 20.00 | 20.00 |
| #OH | 3.69 | 3.69 | 3.73 | 3.75 | 3.78 | 3.43 | 3.42 | 3.51 | 3.53 | 3.55 |
| #F | 0.27 | 0.29 | 0.26 | 0.24 | 0.22 | 0.57 | 0.58 | 0.49 | 0.47 | 0.45 |
| #Cl | 0.04 | 0.01 | 0.01 | 0.01 | 0.00 | - | - | - | 0.00 | - |

| | 89020 | 89020 | 89020 | 89029 | 89029 | 89029 | 89029 | 89029 | 89030 | 89030 |
|---|---|---|---|---|---|---|---|---|---|---|
| SiO2 | 39.18 | 38.65 | 38.18 | 36.16 | 35.92 | 35.76 | 37.00 | 37.12 | 36.03 | 35.95 |
| TiO2 | 0.86 | 0.95 | 1.27 | 2.53 | 2.41 | 2.61 | 2.29 | 2.51 | 2.13 | 2.05 |
| Al2O3 | 13.37 | 13.69 | 13.29 | 13.39 | 13.64 | 14.22 | 13.95 | 13.93 | 14.46 | 13.57 |
| Cr2O3 | 0.42 | 1.21 | 0.35 | - | - | - | 0.04 | - | - | - |
| Fe2O3 | 5.24 | 5.38 | 5.56 | 5.54 | 5.55 | 5.30 | 5.35 | 5.23 | 5.07 | 5.12 |
| FeO | 10.02 | 10.30 | 10.63 | 13.47 | 13.51 | 12.91 | 13.02 | 12.72 | 15.29 | 15.44 |
| MnO | 0.26 | 0.20 | 0.23 | 0.37 | 0.36 | 0.40 | 0.40 | 0.39 | 0.40 | 0.49 |
| MgO | 15.93 | 14.95 | 14.67 | 14.01 | 13.68 | 13.47 | 14.01 | 14.01 | 12.36 | 12.90 |
| Li2O | - | - | - | - | - | - | - | - | - | - |
| BaO | - | - | - | - | - | - | - | - | - | - |
| CaO | - | - | - | 0.01 | 0.02 | 0.29 | - | - | 0.17 | - |
| Na2O | 0.05 | 0.07 | 0.07 | 0.11 | 0.08 | 0.28 | 0.16 | 0.16 | 0.04 | 0.06 |
| K2O | 10.10 | 10.38 | 10.13 | 10.01 | 10.26 | 9.56 | 9.94 | 9.98 | 9.51 | 10.30 |
| Rb2O | - | - | - | - | - | - | - | - | - | - |
| Cs2O | - | - | - | - | - | - | - | - | - | - |
| H2O | 3.59 | 3.59 | 3.22 | 3.58 | 3.63 | 3.65 | 3.58 | 3.64 | 3.61 | 3.58 |
| F | 0.97 | 0.93 | 1.08 | 0.78 | 0.67 | 0.65 | 0.84 | 0.72 | 0.69 | 0.72 |
| Cl | - | - | 1.02 | 0.01 | 0.01 | 0.03 | - | 0.01 | 0.01 | - |
| O=F | 0.41 | 0.39 | 0.45 | 0.33 | 0.28 | 0.27 | 0.35 | 0.30 | 0.29 | 0.30 |
| O=Cl | - | - | 0.23 | 0.00 | 0.00 | 0.01 | - | 0.00 | 0.00 | - |
| Total | 99.58 | 99.91 | 99.01 | 99.64 | 99.45 | 98.85 | 100.23 | 100.12 | 99.48 | 99.87 |
| #Si IV | 5.80 | 5.74 | 5.76 | 5.49 | 5.47 | 5.45 | 5.54 | 5.56 | 5.49 | 5.49 |
| #Al IV | 2.20 | 2.26 | 2.24 | 2.39 | 2.45 | 2.55 | 2.46 | 2.44 | 2.51 | 2.44 |
| #Fe IV | - | - | - | 0.12 | 0.08 | 0.00 | - | - | - | 0.06 |
| #Ti IV | - | - | - | - | - | - | - | - | - | - |
| T site | 8.00 | 8.00 | 8.00 | 8.00 | 8.00 | 8.00 | 8.00 | 8.00 | 8.00 | 8.00 |
| #Al VI | 0.14 | 0.13 | 0.12 | - | - | - | 0.01 | 0.02 | 0.09 | - |
| #Ti VI | 0.10 | 0.11 | 0.14 | 0.29 | 0.28 | 0.30 | 0.26 | 0.28 | 0.24 | 0.24 |
| #Cr | 0.05 | 0.14 | 0.04 | - | - | - | 0.00 | - | - | - |
| #Fe +3 | 0.58 | 0.60 | 0.63 | 0.51 | 0.55 | 0.61 | 0.60 | 0.59 | 0.58 | 0.53 |
| #Fe +2 | 1.24 | 1.28 | 1.34 | 1.71 | 1.72 | 1.64 | 1.63 | 1.59 | 1.95 | 1.97 |
| #Mn +2 | 0.03 | 0.03 | 0.03 | 0.05 | 0.05 | 0.05 | 0.05 | 0.05 | 0.05 | 0.06 |
| #Mg | 3.52 | 3.31 | 3.30 | 3.17 | 3.11 | 3.06 | 3.13 | 3.13 | 2.81 | 2.94 |
| #Li | - | - | - | - | - | - | - | - | - | - |
| O site | 5.66 | 5.59 | 5.60 | 5.73 | 5.70 | 5.66 | 5.69 | 5.66 | 5.72 | 5.74 |
| #Ba | - | - | - | - | - | - | - | - | - | - |
| #Ca | - | - | - | 0.00 | 0.00 | 0.05 | - | - | 0.03 | - |
| #Na | 0.01 | 0.02 | 0.02 | 0.03 | 0.02 | 0.08 | 0.05 | 0.05 | 0.01 | 0.02 |
| #K | 1.91 | 1.97 | 1.95 | 1.94 | 1.99 | 1.86 | 1.90 | 1.91 | 1.85 | 2.01 |
| #Rb | - | - | - | - | - | - | - | - | - | - |
| #Cs | - | - | - | - | - | - | - | - | - | - |
| A site | 1.92 | 1.99 | 1.97 | 1.97 | 2.02 | 1.99 | 1.95 | 1.95 | 1.89 | 2.03 |
| #O | 20.00 | 20.00 | 20.00 | 20.00 | 20.00 | 20.00 | 20.00 | 20.00 | 20.00 | 20.00 |
| #OH | 3.55 | 3.56 | 3.22 | 3.62 | 3.67 | 3.68 | 3.60 | 3.66 | 3.66 | 3.65 |
| #F | 0.45 | 0.44 | 0.51 | 0.37 | 0.32 | 0.31 | 0.40 | 0.34 | 0.33 | 0.35 |
| #Cl | - | - | 0.26 | 0.00 | 0.00 | 0.01 | - | 0.00 | 0.00 | - |

| | 89030 | 8854 | 8854 | 8854 | 8854 | 8854 | 89019 | 89019 | 89019 | 89019 |
|---|---|---|---|---|---|---|---|---|---|---|
| SiO2 | 36.61 | 37.95 | 37.57 | 36.84 | 37.43 | 36.55 | 37.41 | 37.46 | 38.47 | 38.35 |
| TiO2 | 1.82 | 1.63 | 1.73 | 2.12 | 1.26 | 2.27 | 1.82 | 1.25 | 1.46 | 0.98 |
| Al2O3 | 14.01 | 14.84 | 15.25 | 14.69 | 14.62 | 14.48 | 12.70 | 12.88 | 12.88 | 13.38 |
| Cr2O3 | 0.05 | 0.10 | 0.01 | - | - | - | - | - | - | - |
| Fe2O3 | 5.07 | 5.14 | 5.10 | 5.17 | 5.44 | 5.28 | 4.92 | 4.94 | 4.58 | 4.63 |
| FeO | 15.26 | 9.83 | 9.76 | 9.90 | 10.41 | 10.09 | 11.97 | 12.03 | 11.15 | 11.27 |
| MnO | 0.34 | 0.18 | 0.16 | 0.17 | 0.17 | 0.22 | 0.61 | 0.70 | 0.48 | 0.52 |
| MgO | 12.68 | 14.63 | 14.02 | 14.91 | 14.77 | 14.96 | 15.04 | 15.33 | 15.06 | 15.36 |
| Li2O | - | - | - | - | - | - | - | - | - | - |
| BaO | - | - | - | - | - | - | - | - | - | - |
| CaO | 0.01 | - | - | 0.01 | 0.06 | 0.05 | - | 0.03 | - | 0.02 |
| Na2O | 0.07 | 0.03 | 0.03 | 0.05 | 0.05 | 0.07 | 0.04 | 0.04 | 0.04 | 0.09 |
| K2O | 10.10 | 10.11 | 10.16 | 10.26 | 10.69 | 10.06 | 10.26 | 10.25 | 10.10 | 10.23 |
| Rb2O | - | - | - | - | - | - | - | - | - | - |
| Cs2O | - | - | - | - | - | - | - | - | - | - |
| H2O | 3.59 | 3.97 | 3.98 | 3.87 | 3.85 | 3.84 | 3.02 | 2.98 | 3.14 | 3.12 |
| F | 0.73 | 0.20 | 0.18 | 0.36 | 0.38 | 0.37 | 1.98 | 2.07 | 1.81 | 1.85 |
| Cl | - | - | - | 0.01 | - | 0.07 | 0.01 | 0.01 | 0.02 | 0.01 |
| O=F | 0.31 | 0.08 | 0.08 | 0.15 | 0.16 | 0.16 | 0.83 | 0.87 | 0.76 | 0.78 |
| O=Cl | - | - | - | 0.00 | - | 0.02 | 0.00 | 0.00 | 0.00 | 0.00 |
| Total | 100.04 | 98.53 | 97.88 | 98.21 | 98.97 | 98.14 | 98.94 | 99.09 | 98.42 | 99.03 |
| #Si IV | 5.56 | 5.67 | 5.65 | 5.55 | 5.62 | 5.53 | 5.67 | 5.67 | 5.81 | 5.76 |
| #Al IV | 2.44 | 2.33 | 2.35 | 2.45 | 2.38 | 2.47 | 2.27 | 2.30 | 2.19 | 2.24 |
| #Fe IV | - | - | - | - | - | - | 0.06 | 0.03 | - | - |
| #Ti IV | - | - | - | - | - | - | - | - | - | - |
| T site | 8.00 | 8.00 | 8.00 | 8.00 | 8.00 | 8.00 | 8.00 | 8.00 | 8.00 | 8.00 |
| #Al VI | 0.06 | 0.29 | 0.36 | 0.16 | 0.21 | 0.10 | - | - | 0.10 | 0.13 |
| #Ti VI | 0.21 | 0.18 | 0.20 | 0.24 | 0.14 | 0.26 | 0.21 | 0.14 | 0.17 | 0.11 |
| #Cr | 0.01 | 0.01 | 0.00 | - | - | - | - | - | - | - |
| #Fe +3 | 0.58 | 0.58 | 0.58 | 0.59 | 0.61 | 0.60 | 0.50 | 0.54 | 0.52 | 0.52 |
| #Fe +2 | 1.94 | 1.23 | 1.23 | 1.25 | 1.31 | 1.28 | 1.52 | 1.52 | 1.41 | 1.42 |
| #Mn +2 | 0.04 | 0.02 | 0.02 | 0.02 | 0.02 | 0.03 | 0.08 | 0.09 | 0.06 | 0.07 |
| #Mg | 2.87 | 3.26 | 3.15 | 3.35 | 3.31 | 3.37 | 3.40 | 3.46 | 3.39 | 3.44 |
| #Li | - | - | - | - | - | - | - | - | - | - |
| O site | 5.70 | 5.57 | 5.53 | 5.61 | 5.60 | 5.64 | 5.71 | 5.75 | 5.64 | 5.69 |
| #Ba | - | - | - | - | - | - | - | - | - | - |
| #Ca | 0.00 | - | - | 0.00 | 0.01 | 0.01 | - | 0.00 | - | 0.00 |
| #Na | 0.02 | 0.01 | 0.01 | 0.01 | 0.01 | 0.02 | 0.01 | 0.01 | 0.01 | 0.03 |
| #K | 1.96 | 1.93 | 1.95 | 1.97 | 2.05 | 1.94 | 1.98 | 1.98 | 1.95 | 1.96 |
| #Rb | - | - | - | - | - | - | - | - | - | - |
| #Cs | - | - | - | - | - | - | - | - | - | - |
| A site | 1.98 | 1.94 | 1.96 | 1.99 | 2.07 | 1.97 | 2.00 | 2.00 | 1.96 | 1.99 |
| #O | 20.00 | 20.00 | 20.00 | 20.00 | 20.00 | 20.00 | 20.00 | 20.00 | 20.00 | 20.00 |
| #OH | 3.65 | 3.91 | 3.91 | 3.83 | 3.82 | 3.81 | 3.05 | 3.01 | 3.13 | 3.12 |
| #F | 0.35 | 0.09 | 0.09 | 0.17 | 0.18 | 0.18 | 0.95 | 0.99 | 0.86 | 0.88 |
| #Cl | - | - | - | 0.00 | - | 0.02 | 0.00 | 0.00 | 0.01 | 0.00 |

| | 90192 | 90192 |
|---|---|---|
| SiO2 | 38.65 | 38.03 |
| TiO2 | 1.12 | 3.53 |
| Al2O3 | 13.45 | 13.09 |
| Cr2O3 | 0.93 | - |
| Fe2O3 | 5.13 | 5.80 |
| FeO | 10.77 | 12.17 |
| MnO | 0.18 | 0.23 |
| MgO | 16.26 | 13.30 |
| Li2O | - | - |
| BaO | - | - |
| CaO | 0.05 | - |
| Na2O | 0.04 | 0.09 |
| K2O | 9.31 | 9.52 |
| Rb2O | - | - |
| Cs2O | - | - |
| H2O | 3.72 | 3.78 |
| F | 0.70 | 0.49 |
| Cl | 0.01 | 0.02 |
| O=F | 0.29 | 0.21 |
| O=Cl | 0.00 | 0.00 |
| Total | 100.02 | 99.84 |
| #Si IV | 5.70 | 5.68 |
| #Al IV | 2.30 | 2.30 |
| #Fe IV | - | 0.02 |
| #Ti IV | - | - |
| T site | 8.00 | 8.00 |
| #Al VI | 0.04 | - |
| #Ti VI | 0.12 | 0.40 |
| #Cr | 0.11 | - |
| #Fe +3 | 0.57 | 0.63 |
| #Fe +2 | 1.33 | 1.52 |
| #Mn +2 | 0.02 | 0.03 |
| #Mg | 3.58 | 2.96 |
| #Li | - | - |
| O site | 5.77 | 5.53 |
| #Ba | - | - |
| #Ca | 0.01 | - |
| #Na | 0.01 | 0.03 |
| #K | 1.75 | 1.81 |
| #Rb | - | - |
| #Cs | - | - |
| A site | 1.77 | 1.84 |
| #O | 20.00 | 20.00 |
| #OH | 3.67 | 3.76 |
| #F | 0.33 | 0.23 |
| #Cl | 0.00 | 0.01 |

## A.3.3 Amphibole

| | 8854 | 8854 | HSR | HSR | 89035 | 89035 | 89035 | 90202 | 90202 | 89006 |
|---|---|---|---|---|---|---|---|---|---|---|
| SiO2 | 41.70 | 49.40 | 46.33 | 45.13 | 48.11 | 48.03 | 48.31 | 42.71 | 42.45 | 44.68 |
| TiO2 | 1.52 | 0.67 | 0.80 | 0.89 | 1.03 | 1.03 | 0.27 | 2.09 | 1.46 | 1.44 |
| Al2O3 | 11.35 | 5.50 | 8.91 | 9.34 | 5.98 | 5.99 | 5.85 | 11.62 | 10.22 | 10.25 |
| Cr2O3 | - | - | 0.21 | 0.19 | - | - | - | 0.06 | 0.07 | 0.08 |
| Fe2O3 | 2.40 | 2.26 | 4.68 | 7.22 | 3.56 | 3.59 | 3.77 | 2.67 | 3.39 | 1.67 |
| FeO | 10.20 | 9.60 | 7.25 | 5.07 | 9.62 | 9.68 | 10.17 | 9.62 | 12.20 | 8.53 |
| MnO | 0.19 | 0.17 | 0.20 | 0.26 | 0.46 | 0.47 | 0.56 | 0.09 | 0.25 | 0.15 |
| MgO | 13.94 | 15.77 | 15.55 | 15.76 | 14.98 | 14.81 | 14.05 | 14.41 | 12.48 | 15.73 |
| ZnO | - | - | - | - | - | - | - | - | - | - |
| CaO | 11.68 | 12.15 | 12.02 | 11.56 | 11.48 | 11.48 | 11.40 | 11.54 | 11.52 | 10.76 |
| Na2O | 2.22 | 1.23 | 2.26 | 2.56 | 1.47 | 1.43 | 1.18 | 2.25 | 2.31 | 2.26 |
| K2O | 1.30 | 0.55 | 0.84 | 0.85 | 0.75 | 0.72 | 0.61 | 1.36 | 1.24 | 0.84 |
| H2O | 1.88 | 1.97 | 2.00 | 1.94 | 1.84 | 1.85 | 1.89 | 1.94 | 1.97 | 1.86 |
| F | 0.24 | 0.19 | 0.17 | 0.30 | 0.43 | 0.39 | 0.27 | 0.22 | 0.06 | 0.38 |
| Cl | 0.01 | 0.01 | 0.01 | 0.01 | 0.04 | 0.04 | 0.01 | 0.01 | 0.02 | - |
| O=F | 0.10 | 0.08 | 0.07 | 0.13 | 0.18 | 0.16 | 0.11 | 0.09 | 0.03 | 0.16 |
| O=Cl | 0.00 | 0.00 | 0.00 | 0.00 | 0.01 | 0.01 | 0.00 | 0.00 | 0.00 | - |
| Total | 98.53 | 99.39 | 101.16 | 100.95 | 99.56 | 99.34 | 98.23 | 100.50 | 99.61 | 98.47 |
| #Si IV | 6.25 | 7.18 | 6.65 | 6.49 | 7.03 | 7.04 | 7.15 | 6.25 | 6.36 | 6.56 |
| #Al IV | 1.75 | 0.82 | 1.35 | 1.51 | 0.97 | 0.96 | 0.85 | 1.75 | 1.64 | 1.44 |
| #Fe +3 | - | - | - | - | - | - | - | - | - | - |
| #Ti IV | - | - | - | - | - | - | - | - | - | - |
| T site | 8.00 | 8.00 | 8.00 | 8.00 | 8.00 | 8.00 | 8.00 | 8.00 | 8.00 | 8.00 |
| #Al VI | 0.26 | 0.12 | 0.16 | 0.08 | 0.06 | 0.07 | 0.18 | 0.25 | 0.17 | 0.34 |
| #Fe +3 | 0.27 | 0.25 | 0.51 | 0.78 | 0.39 | 0.40 | 0.42 | 0.29 | 0.38 | 0.18 |
| #Ti | 0.17 | 0.07 | 0.09 | 0.10 | 0.11 | 0.11 | 0.03 | 0.23 | 0.16 | 0.16 |
| #Cr | - | - | 0.02 | 0.02 | - | - | - | 0.01 | 0.01 | 0.01 |
| #Mg | 3.12 | 3.42 | 3.33 | 3.38 | 3.26 | 3.24 | 3.10 | 3.14 | 2.79 | 3.44 |
| #Fe +2 | 1.19 | 1.15 | 0.87 | 0.61 | 1.17 | 1.18 | 1.26 | 1.07 | 1.49 | 0.87 |
| #Zn | - | - | - | - | - | - | - | - | - | - |
| #Mn | - | - | 0.02 | 0.03 | - | - | 0.01 | - | - | - |
| #Ca | - | - | - | 0.00 | - | - | - | - | - | - |
| M1,2,3 | 5.00 | 5.00 | 5.00 | 5.00 | 5.00 | 5.00 | 5.00 | 5.00 | 5.00 | 5.00 |
| #Mg | - | - | - | - | - | - | - | - | - | - |
| #Fe +2 | 0.09 | 0.02 | - | - | 0.01 | 0.00 | - | 0.10 | 0.04 | 0.18 |
| #Zn | - | - | - | - | - | - | - | - | - | - |
| #Mn | 0.02 | 0.02 | 0.00 | - | 0.06 | 0.06 | 0.06 | 0.01 | 0.03 | 0.02 |
| #Ca | 1.88 | 1.89 | 1.85 | 1.78 | 1.80 | 1.80 | 1.81 | 1.81 | 1.85 | 1.69 |
| #Na | 0.01 | 0.07 | 0.15 | 0.22 | 0.14 | 0.14 | 0.13 | 0.08 | 0.08 | 0.11 |
| M4 site | 2.00 | 2.00 | 2.00 | 2.00 | 2.00 | 2.00 | 2.00 | 2.00 | 2.00 | 2.00 |
| #Ca | - | - | - | -7E-04 | - | - | - | - | - | - |
| #Na | 0.64 | 0.28 | 0.48 | 0.50 | 0.28 | 0.27 | 0.21 | 0.56 | 0.59 | 0.54 |
| #K | 0.25 | 0.10 | 0.15 | 0.16 | 0.14 | 0.13 | 0.12 | 0.25 | 0.24 | 0.16 |
| A site | 0.89 | 0.38 | 0.63 | 0.65 | 0.42 | 0.40 | 0.32 | 0.82 | 0.83 | 0.69 |
| #O | 22.00 | 22.00 | 22.00 | 22.00 | 22.00 | 22.00 | 22.00 | 22.00 | 22.00 | 22.00 |
| #OH | 1.88 | 1.91 | 1.92 | 1.86 | 1.79 | 1.81 | 1.87 | 1.90 | 1.97 | 1.82 |
| #F | 0.11 | 0.09 | 0.08 | 0.14 | 0.20 | 0.18 | 0.13 | 0.10 | 0.03 | 0.18 |
| #Cl | 0.00 | 0.00 | 0.00 | 0.00 | 0.01 | 0.01 | 0.00 | 0.00 | 0.01 | - |

| | 89006 | 89006 | 89006 | 89006 | 89006 | 89006 | 89006 | 89006 | 89006 | 89006 |
|---|---|---|---|---|---|---|---|---|---|---|
| SiO2 | 46.18 | 42.46 | 44.18 | 44.81 | 43.46 | 44.03 | 44.65 | 45.31 | 44.84 | 46.63 |
| TiO2 | 0.87 | 1.63 | 1.44 | 1.06 | 1.16 | 1.37 | 1.13 | 1.37 | 1.29 | 0.84 |
| Al2O3 | 8.93 | 11.03 | 10.22 | 8.62 | 10.39 | 9.84 | 9.42 | 9.20 | 9.74 | 7.89 |
| Cr2O3 | 0.04 | 0.06 | 0.08 | 0.02 | 0.04 | 0.09 | - | 0.15 | 0.13 | 0.03 |
| Fe2O3 | 2.40 | 2.04 | 1.95 | 2.79 | 2.55 | 1.85 | 2.83 | 1.92 | 1.87 | 2.55 |
| FeO | 12.22 | 10.39 | 9.95 | 14.20 | 12.99 | 9.44 | 14.44 | 9.81 | 9.51 | 13.02 |
| MnO | 0.36 | 0.13 | 0.17 | 0.32 | 0.26 | 0.17 | 0.36 | 0.21 | 0.16 | 0.34 |
| MgO | 13.10 | 15.22 | 14.54 | 11.95 | 12.35 | 15.40 | 11.46 | 14.98 | 15.26 | 13.07 |
| ZnO | - | - | - | - | - | - | - | - | - | - |
| CaO | 11.35 | 10.58 | 11.11 | 10.76 | 10.72 | 10.84 | 10.79 | 10.68 | 10.61 | 10.87 |
| Na2O | 1.61 | 2.16 | 2.31 | 1.98 | 2.33 | 2.31 | 2.12 | 2.25 | 2.37 | 1.96 |
| K2O | 0.62 | 0.93 | 0.96 | 0.72 | 0.89 | 0.94 | 0.82 | 0.76 | 0.83 | 0.65 |
| H2O | 1.92 | 1.78 | 1.86 | 1.81 | 1.81 | 1.87 | 1.88 | 1.84 | 1.87 | 1.84 |
| F | 0.25 | 0.49 | 0.36 | 0.39 | 0.39 | 0.32 | 0.28 | 0.41 | 0.34 | 0.39 |
| Cl | 0.01 | 0.03 | 0.01 | 0.03 | 0.03 | 0.01 | 0.01 | 0.01 | 0.02 | 0.02 |
| O=F | 0.11 | 0.21 | 0.15 | 0.16 | 0.16 | 0.13 | 0.12 | 0.17 | 0.14 | 0.16 |
| O=Cl | 0.00 | 0.01 | 0.00 | 0.01 | 0.01 | 0.00 | 0.00 | 0.00 | 0.00 | 0.00 |
| Total | 99.75 | 98.71 | 98.98 | 99.29 | 99.20 | 98.34 | 100.07 | 98.72 | 98.69 | 99.94 |
| #Si IV | 6.79 | 6.31 | 6.52 | 6.71 | 6.50 | 6.53 | 6.65 | 6.68 | 6.61 | 6.87 |
| #Al IV | 1.21 | 1.69 | 1.48 | 1.29 | 1.50 | 1.47 | 1.35 | 1.32 | 1.39 | 1.13 |
| #Fe +3 | - | - | - | - | - | - | - | - | - | - |
| #Ti IV | - | - | - | - | - | - | - | - | - | - |
| T site | 8.00 | 8.00 | 8.00 | 8.00 | 8.00 | 8.00 | 8.00 | 8.00 | 8.00 | 8.00 |
| #Al VI | 0.34 | 0.24 | 0.30 | 0.24 | 0.33 | 0.25 | 0.30 | 0.27 | 0.30 | 0.25 |
| #Fe +3 | 0.27 | 0.23 | 0.22 | 0.31 | 0.29 | 0.21 | 0.32 | 0.21 | 0.21 | 0.28 |
| #Ti | 0.10 | 0.18 | 0.16 | 0.12 | 0.13 | 0.15 | 0.13 | 0.15 | 0.14 | 0.09 |
| #Cr | 0.00 | 0.01 | 0.01 | 0.00 | 0.00 | 0.01 | - | 0.02 | 0.02 | 0.00 |
| #Mg | 2.87 | 3.37 | 3.20 | 2.67 | 2.75 | 3.40 | 2.54 | 3.29 | 3.35 | 2.87 |
| #Fe +2 | 1.42 | 0.97 | 1.11 | 1.66 | 1.49 | 0.98 | 1.71 | 1.05 | 0.99 | 1.50 |
| #Zn | - | - | - | - | - | - | - | - | - | - |
| #Mn | - | - | - | - | - | - | - | - | - | - |
| #Ca | - | - | - | - | - | - | - | - | - | - |
| M1,2,3 | 5.00 | 5.00 | 5.00 | 5.00 | 5.00 | 5.00 | 5.00 | 5.00 | 5.00 | 5.00 |
| #Mg | - | - | - | - | - | - | - | - | - | - |
| #Fe +2 | 0.08 | 0.32 | 0.12 | 0.12 | 0.13 | 0.19 | 0.09 | 0.15 | 0.18 | 0.10 |
| #Zn | - | - | - | - | - | - | - | - | - | - |
| #Mn | 0.04 | 0.02 | 0.02 | 0.04 | 0.03 | 0.02 | 0.05 | 0.03 | 0.02 | 0.04 |
| #Ca | 1.79 | 1.66 | 1.76 | 1.73 | 1.72 | 1.72 | 1.72 | 1.69 | 1.67 | 1.72 |
| #Na | 0.08 | - | 0.11 | 0.11 | 0.12 | 0.07 | 0.14 | 0.13 | 0.12 | 0.14 |
| M4 site | 2.00 | 2.00 | 2.00 | 2.00 | 2.00 | 2.00 | 2.00 | 2.00 | 2.00 | 2.00 |
| #Ca | - | 0.02 | - | - | - | - | - | - | - | - |
| #Na | 0.37 | 0.62 | 0.56 | 0.47 | 0.56 | 0.60 | 0.47 | 0.51 | 0.56 | 0.42 |
| #K | 0.12 | 0.18 | 0.18 | 0.14 | 0.17 | 0.18 | 0.16 | 0.14 | 0.16 | 0.12 |
| A site | 0.49 | 0.82 | 0.74 | 0.60 | 0.73 | 0.77 | 0.62 | 0.65 | 0.71 | 0.54 |
| #O | 22.00 | 22.00 | 22.00 | 22.00 | 22.00 | 22.00 | 22.00 | 22.00 | 22.00 | 22.00 |
| #OH | 1.88 | 1.76 | 1.83 | 1.81 | 1.81 | 1.85 | 1.87 | 1.81 | 1.84 | 1.81 |
| #F | 0.12 | 0.23 | 0.17 | 0.18 | 0.18 | 0.15 | 0.13 | 0.19 | 0.16 | 0.18 |
| #Cl | 0.00 | 0.01 | 0.00 | 0.01 | 0.01 | 0.00 | 0.00 | 0.00 | 0.00 | 0.00 |

| | 89006 | 90211 | 90211 | 90211 | 90211 | 90211 | 90211 | 90211 | 90211 | 90215 |
|---|---|---|---|---|---|---|---|---|---|---|
| SiO2 | 43.45 | 44.21 | 55.26 | 44.74 | 44.98 | 45.36 | 52.08 | 42.89 | 49.03 | 48.39 |
| TiO2 | 1.23 | 1.28 | 0.05 | 1.30 | 1.03 | 0.88 | 0.41 | 1.49 | 0.66 | 0.90 |
| Al2O3 | 10.95 | 10.23 | 0.27 | 10.25 | 8.81 | 10.19 | 3.20 | 11.04 | 5.05 | 7.26 |
| Cr2O3 | 0.15 | 0.07 | 0.02 | 0.06 | 0.04 | 0.06 | 0.04 | 0.05 | 0.03 | - |
| Fe2O3 | 2.37 | 1.86 | 2.20 | 1.96 | 2.84 | 2.26 | 2.13 | 2.16 | 2.64 | 2.06 |
| FeO | 12.08 | 9.47 | 11.22 | 9.97 | 14.47 | 11.51 | 10.87 | 11.02 | 13.46 | 12.39 |
| MnO | 0.23 | 0.21 | 0.52 | 0.25 | 0.33 | 0.22 | 0.38 | 0.24 | 0.34 | 0.29 |
| MgO | 12.43 | 15.18 | 15.59 | 14.13 | 11.53 | 13.75 | 15.08 | 13.71 | 13.25 | 13.93 |
| ZnO | - | - | - | - | - | - | - | - | - | - |
| CaO | 10.90 | 10.42 | 12.08 | 11.30 | 10.63 | 10.77 | 11.84 | 11.14 | 11.62 | 10.80 |
| Na2O | 2.34 | 2.44 | 0.20 | 2.09 | 1.95 | 2.07 | 0.63 | 2.27 | 1.67 | 1.48 |
| K2O | 1.00 | 0.82 | 0.02 | 1.18 | 0.79 | 0.56 | 0.27 | 1.08 | 0.45 | 0.04 |
| H2O | 1.75 | 1.93 | 2.01 | 1.87 | 1.86 | 1.93 | 1.97 | 1.83 | 1.94 | 2.04 |
| F | 0.55 | 0.20 | 0.15 | 0.34 | 0.29 | 0.25 | 0.18 | 0.37 | 0.22 | 0.02 |
| Cl | 0.02 | - | - | 0.02 | 0.02 | - | 0.02 | 0.03 | 0.01 | 0.01 |
| O=F | 0.23 | 0.08 | 0.06 | 0.14 | 0.12 | 0.11 | 0.08 | 0.16 | 0.09 | 0.01 |
| O=Cl | 0.00 | - | - | 0.00 | 0.00 | - | 0.00 | 0.01 | 0.00 | 0.00 |
| Total | 99.21 | 98.24 | 99.53 | 99.31 | 99.44 | 99.70 | 99.02 | 99.16 | 100.27 | 99.60 |
| #Si IV | 6.47 | 6.54 | 7.95 | 6.58 | 6.73 | 6.65 | 7.57 | 6.38 | 7.20 | 7.06 |
| #Al IV | 1.53 | 1.46 | 0.05 | 1.42 | 1.27 | 1.35 | 0.43 | 1.62 | 0.80 | 0.94 |
| #Fe +3 | - | - | 0.00 | - | - | - | - | - | - | - |
| #Ti IV | - | - | - | - | - | - | - | - | - | - |
| T site | 8.00 | 8.00 | 8.00 | 8.00 | 8.00 | 8.00 | 8.00 | 8.00 | 8.00 | 8.00 |
| #Al VI | 0.40 | 0.33 | - | 0.36 | 0.29 | 0.41 | 0.12 | 0.31 | 0.07 | 0.31 |
| #Fe +3 | 0.27 | 0.21 | 0.24 | 0.22 | 0.32 | 0.25 | 0.23 | 0.24 | 0.29 | 0.23 |
| #Ti | 0.14 | 0.14 | 0.01 | 0.14 | 0.12 | 0.10 | 0.04 | 0.17 | 0.07 | 0.10 |
| #Cr | 0.02 | 0.01 | 0.00 | 0.01 | 0.00 | 0.01 | 0.00 | 0.01 | 0.00 | - |
| #Mg | 2.76 | 3.35 | 3.35 | 3.10 | 2.57 | 3.00 | 3.27 | 3.04 | 2.90 | 3.03 |
| #Fe +2 | 1.42 | 0.96 | 1.35 | 1.17 | 1.70 | 1.23 | 1.32 | 1.24 | 1.65 | 1.34 |
| #Zn | - | - | - | - | - | - | - | - | - | - |
| #Mn | - | - | 0.06 | - | - | - | 0.01 | - | 0.01 | - |
| #Ca | - | - | - | - | - | - | - | - | - | - |
| M1,2,3 | 5.00 | 5.00 | 5.00 | 5.00 | 5.00 | 5.00 | 5.00 | 5.00 | 5.00 | 5.00 |
| #Mg | - | - | - | - | - | - | - | - | - | - |
| #Fe +2 | 0.08 | 0.21 | - | 0.05 | 0.11 | 0.18 | - | 0.13 | - | 0.17 |
| #Zn | - | - | - | - | - | - | - | - | - | - |
| #Mn | 0.03 | 0.03 | 0.00 | 0.03 | 0.04 | 0.03 | 0.04 | 0.03 | 0.04 | 0.04 |
| #Ca | 1.74 | 1.65 | 1.86 | 1.78 | 1.70 | 1.69 | 1.84 | 1.77 | 1.83 | 1.69 |
| #Na | 0.15 | 0.11 | 0.06 | 0.14 | 0.14 | 0.10 | 0.12 | 0.06 | 0.14 | 0.11 |
| M4 site | 2.00 | 2.00 | 1.92 | 2.00 | 2.00 | 2.00 | 2.00 | 2.00 | 2.00 | 2.00 |
| #Ca | - | - | - | - | - | - | - | - | - | - |
| #Na | 0.53 | 0.59 | - | 0.46 | 0.42 | 0.49 | 0.06 | 0.59 | 0.34 | 0.31 |
| #K | 0.19 | 0.15 | 0.00 | 0.22 | 0.15 | 0.10 | 0.05 | 0.20 | 0.08 | 0.01 |
| A site | 0.72 | 0.74 | 0.00 | 0.68 | 0.57 | 0.59 | 0.11 | 0.80 | 0.42 | 0.32 |
| #O | 22.00 | 22.00 | 22.00 | 22.00 | 22.00 | 22.00 | 22.00 | 22.00 | 22.00 | 22.00 |
| #OH | 1.74 | 1.91 | 1.93 | 1.84 | 1.86 | 1.88 | 1.91 | 1.82 | 1.90 | 1.99 |
| #F | 0.26 | 0.09 | 0.07 | 0.16 | 0.14 | 0.12 | 0.08 | 0.17 | 0.10 | 0.01 |
| #Cl | 0.01 | - | - | 0.00 | 0.01 | - | 0.00 | 0.01 | 0.00 | 0.00 |

| | 90215 | 90215 | 90215 | 90215 | 90215 | 90215 | 90215 | 90215 |
|---|---|---|---|---|---|---|---|---|
| SiO2 | 45.27 | 45.15 | 46.78 | 47.37 | 44.70 | 45.31 | 45.86 | 46.53 |
| TiO2 | 1.10 | 1.00 | 0.86 | 1.01 | 1.55 | 1.17 | 1.17 | 0.84 |
| Al2O3 | 9.54 | 10.65 | 7.81 | 7.85 | 10.44 | 10.46 | 9.60 | 8.25 |
| Cr2O3 | 0.05 | 0.32 | - | 0.03 | 0.18 | 0.24 | 0.05 | 0.02 |
| Fe2O3 | 1.87 | 1.58 | 2.18 | 2.07 | 1.37 | 1.35 | 1.57 | 2.18 |
| FeO | 11.24 | 9.52 | 13.10 | 12.48 | 8.24 | 8.14 | 9.43 | 13.13 |
| MnO | 0.17 | 0.12 | 0.38 | 0.30 | 0.04 | 0.18 | 0.22 | 0.30 |
| MgO | 13.91 | 15.17 | 13.10 | 13.37 | 16.33 | 15.93 | 15.15 | 13.45 |
| ZnO | - | - | - | - | - | - | - | - |
| CaO | 10.87 | 11.02 | 10.75 | 10.70 | 10.23 | 10.77 | 11.29 | 10.59 |
| Na2O | 2.28 | 2.15 | 1.86 | 1.65 | 2.46 | 2.15 | 1.81 | 1.95 |
| K2O | 0.65 | 0.80 | 0.52 | 0.57 | 1.00 | 1.47 | 0.86 | 0.53 |
| H2O | 1.99 | 1.95 | 1.97 | 1.90 | 2.02 | 1.83 | 1.99 | 1.91 |
| F | 0.09 | 0.22 | 0.11 | 0.28 | 0.06 | 0.48 | 0.13 | 0.26 |
| Cl | - | - | 0.01 | 0.05 | - | 0.02 | - | 0.01 |
| O=F | 0.04 | 0.09 | 0.05 | 0.12 | 0.03 | 0.20 | 0.05 | 0.11 |
| O=Cl | - | - | 0.00 | 0.01 | - | 0.00 | - | 0.00 |
| Total | 98.99 | 99.56 | 99.38 | 99.50 | 98.60 | 99.29 | 99.07 | 99.84 |
| #Si IV | 6.68 | 6.58 | 6.92 | 6.96 | 6.54 | 6.60 | 6.70 | 6.85 |
| #Al IV | 1.32 | 1.42 | 1.08 | 1.04 | 1.46 | 1.40 | 1.30 | 1.15 |
| #Fe +3 | - | - | - | - | - | - | - | - |
| #Ti IV | - | - | - | - | - | - | - | - |
| T site | 8.00 | 8.00 | 8.00 | 8.00 | 8.00 | 8.00 | 8.00 | 8.00 |
| #Al VI | 0.34 | 0.41 | 0.28 | 0.32 | 0.34 | 0.39 | 0.36 | 0.28 |
| #Fe +3 | 0.21 | 0.17 | 0.24 | 0.23 | 0.15 | 0.15 | 0.17 | 0.24 |
| #Ti | 0.12 | 0.11 | 0.10 | 0.11 | 0.17 | 0.13 | 0.13 | 0.09 |
| #Cr | 0.01 | 0.04 | - | 0.00 | 0.02 | 0.03 | 0.01 | 0.00 |
| #Mg | 3.06 | 3.29 | 2.89 | 2.93 | 3.56 | 3.46 | 3.30 | 2.95 |
| #Fe +2 | 1.26 | 0.98 | 1.50 | 1.41 | 0.76 | 0.85 | 1.03 | 1.43 |
| #Zn | - | - | - | - | - | - | - | - |
| #Mn | - | - | - | - | - | - | - | - |
| #Ca | - | - | - | - | - | - | - | - |
| M1,2,3 | 5.00 | 5.00 | 5.00 | 5.00 | 5.00 | 5.00 | 5.00 | 5.00 |
| #Mg | - | - | - | - | - | - | - | - |
| #Fe +2 | 0.13 | 0.18 | 0.12 | 0.12 | 0.25 | 0.15 | 0.12 | 0.18 |
| #Zn | - | - | - | - | - | - | - | - |
| #Mn | 0.02 | 0.01 | 0.05 | 0.04 | 0.00 | 0.02 | 0.03 | 0.04 |
| #Ca | 1.72 | 1.72 | 1.70 | 1.68 | 1.60 | 1.68 | 1.77 | 1.67 |
| #Na | 0.13 | 0.08 | 0.13 | 0.15 | 0.14 | 0.15 | 0.09 | 0.11 |
| M4 site | 2.00 | 2.00 | 2.00 | 2.00 | 2.00 | 2.00 | 2.00 | 2.00 |
| #Ca | - | - | - | - | - | - | - | - |
| #Na | 0.52 | 0.52 | 0.40 | 0.32 | 0.56 | 0.46 | 0.43 | 0.45 |
| #K | 0.12 | 0.15 | 0.10 | 0.11 | 0.19 | 0.27 | 0.16 | 0.10 |
| A site | 0.64 | 0.67 | 0.50 | 0.42 | 0.75 | 0.73 | 0.59 | 0.55 |
| #O | 22.00 | 22.00 | 22.00 | 22.00 | 22.00 | 22.00 | 22.00 | 22.00 |
| #OH | 1.96 | 1.90 | 1.95 | 1.86 | 1.97 | 1.77 | 1.94 | 1.88 |
| #F | 0.04 | 0.10 | 0.05 | 0.13 | 0.03 | 0.22 | 0.06 | 0.12 |
| #Cl | - | - | 0.00 | 0.01 | - | 0.00 | - | 0.00 |

| | 89037 | 89037 | 89037 | 89037 | 89037 | 89037 | 90192 | 90192 | 90192 | 90117 |
|---|---|---|---|---|---|---|---|---|---|---|
| SiC2 | 43.05 | 42.37 | 43.02 | 44.82 | 44.80 | 42.83 | 54.41 | 51.73 | 44.69 | 47.51 |
| TiO2 | 1.71 | 1.86 | 1.41 | 1.50 | 1.54 | 1.42 | 0.16 | 1.01 | 1.31 | 0.69 |
| Al2O3 | 12.00 | 12.70 | 11.67 | 11.36 | 9.88 | 12.26 | 3.10 | 3.91 | 10.24 | 7.63 |
| Cr2O3 | - | 0.08 | 0.07 | 0.02 | 0.03 | 0.05 | 0.12 | 0.03 | 0.07 | 0.13 |
| Fe2O3 | 3.81 | 2.62 | 3.47 | 2.67 | 2.34 | 3.47 | 1.52 | 2.54 | 2.44 | 2.47 |
| FeO | 13.71 | 9.43 | 12.49 | 9.62 | 8.43 | 12.48 | 5.46 | 9.14 | 8.78 | 8.90 |
| MnO | 0.26 | 0.14 | 0.28 | 0.19 | 0.17 | 0.24 | 0.17 | 0.39 | 0.12 | 0.14 |
| MgO | 10.62 | 13.72 | 11.61 | 13.44 | 15.62 | 11.05 | 19.20 | 16.63 | 15.17 | 15.59 |
| ZnO | - | - | - | - | - | - | - | - | - | - |
| CaO | 9.96 | 11.15 | 11.43 | 11.33 | 11.26 | 11.34 | 12.05 | 10.37 | 10.95 | 11.05 |
| Na2O | 2.28 | 2.22 | 1.72 | 1.86 | 1.87 | 1.88 | 1.80 | 2.04 | 2.28 | 2.24 |
| K2O | 0.46 | 1.42 | 1.17 | 0.70 | 1.05 | 0.77 | 0.21 | 0.60 | 1.25 | 0.79 |
| H2O | 1.93 | 1.93 | 1.93 | 2.00 | 1.89 | 1.94 | 1.98 | 1.76 | 1.73 | 1.92 |
| F | 0.17 | 0.23 | 0.19 | 0.12 | 0.34 | 0.15 | 0.34 | 0.71 | 0.66 | 0.29 |
| Cl | 0.02 | 0.01 | 0.02 | 0.01 | - | 0.02 | - | 0.01 | 0.01 | - |
| O=F | 0.07 | 0.10 | 0.08 | 0.05 | 0.14 | 0.06 | 0.14 | 0.30 | 0.28 | 0.12 |
| O=Cl | 0.00 | 0.00 | 0.00 | 0.00 | - | 0.00 | - | 0.00 | 0.00 | - |
| Total | 99.91 | 99.78 | 100.40 | 99.58 | 99.07 | 99.84 | 100.38 | 100.57 | 99.42 | 99.23 |
| #Si IV | 6.39 | 6.23 | 6.37 | 6.54 | 6.56 | 6.35 | 7.61 | 7.39 | 6.54 | 6.92 |
| #Al IV | 1.61 | 1.77 | 1.63 | 1.46 | 1.44 | 1.65 | 0.39 | 0.61 | 1.46 | 1.08 |
| #Fe +3 | - | - | - | - | - | - | - | - | - | - |
| #Ti IV | - | - | - | - | - | - | - | - | - | - |
| T site | 8.00 | 8.00 | 8.00 | 8.00 | 8.00 | 8.00 | 8.00 | 8.00 | 8.00 | 8.00 |
| #Al VI | 0.49 | 0.43 | 0.40 | 0.49 | 0.26 | 0.50 | 0.12 | 0.05 | 0.31 | 0.24 |
| #Fe +3 | 0.43 | 0.29 | 0.39 | 0.29 | 0.26 | 0.39 | 0.16 | 0.27 | 0.27 | 0.27 |
| #Ti | 0.19 | 0.21 | 0.16 | 0.16 | 0.17 | 0.16 | 0.02 | 0.11 | 0.14 | 0.08 |
| #Cr | - | 0.01 | 0.01 | 0.00 | 0.00 | 0.01 | 0.01 | 0.00 | 0.01 | 0.01 |
| #Mg | 2.35 | 3.01 | 2.56 | 2.92 | 3.41 | 2.44 | 4.00 | 3.54 | 3.31 | 3.39 |
| #Fe +2 | 1.54 | 1.06 | 1.49 | 1.12 | 0.90 | 1.51 | 0.64 | 1.03 | 0.96 | 1.02 |
| #Zn | - | - | - | - | - | - | - | - | - | - |
| #Mn | - | - | - | - | - | - | 0.02 | - | - | - |
| #Ca | - | - | - | - | - | - | 0.03 | - | - | - |
| M1,2,3 | 5.00 | 5.00 | 5.00 | 5.00 | 5.00 | 5.00 | 5.00 | 5.00 | 5.00 | 5.00 |
| #Mg | - | - | - | - | - | - | - | - | - | - |
| #Fe +2 | 0.16 | 0.10 | 0.06 | 0.05 | 0.14 | 0.04 | - | 0.06 | 0.12 | 0.07 |
| #Zn | - | - | - | - | - | - | - | - | - | - |
| #Mn | 0.03 | 0.02 | 0.04 | 0.02 | 0.02 | 0.03 | - | 0.05 | 0.01 | 0.02 |
| #Ca | 1.58 | 1.76 | 1.81 | 1.77 | 1.77 | 1.80 | 1.80 | 1.59 | 1.72 | 1.73 |
| #Na | 0.22 | 0.13 | 0.09 | 0.16 | 0.08 | 0.12 | 0.20 | 0.30 | 0.15 | 0.19 |
| M4 site | 2.00 | 2.00 | 2.00 | 2.00 | 2.00 | 2.00 | 2.00 | 2.00 | 2.00 | 2.00 |
| #Ca | - | - | - | - | - | - | -3E-02 | - | - | - |
| #Na | 0.44 | 0.50 | 0.40 | 0.37 | 0.46 | 0.42 | 0.29 | 0.26 | 0.50 | 0.44 |
| #K | 0.09 | 0.27 | 0.22 | 0.13 | 0.20 | 0.15 | 0.04 | 0.11 | 0.23 | 0.15 |
| A site | 0.52 | 0.77 | 0.62 | 0.50 | 0.65 | 0.56 | 0.30 | 0.37 | 0.73 | 0.59 |
| #O | 22.00 | 22.00 | 22.00 | 22.00 | 22.00 | 22.00 | 22.00 | 22.00 | 22.00 | 22.00 |
| #OH | 1.92 | 1.89 | 1.91 | 1.94 | 1.84 | 1.92 | 1.85 | 1.68 | 1.69 | 1.87 |
| #F | 0.08 | 0.11 | 0.09 | 0.06 | 0.16 | 0.07 | 0.15 | 0.32 | 0.31 | 0.13 |
| #Cl | 0.01 | 0.00 | 0.01 | 0.00 | - | 0.01 | - | 0.00 | 0.00 | - |

| | 90117 | 90117 | 90117 | 153-1 | 90185 | 90185 | 90185 | 90185 | 90185 | 90187 |
|---|---|---|---|---|---|---|---|---|---|---|
| SiO2 | 46.67 | 46.63 | 46.81 | 45.14 | 49.29 | 48.51 | 47.39 | 50.25 | 50.40 | 47.75 |
| TiO2 | 1.18 | 0.60 | 1.22 | 0.95 | 0.66 | 0.75 | 0.79 | 0.66 | 0.59 | 0.79 |
| Al2O3 | 7.33 | 8.81 | 7.45 | 8.66 | 5.37 | 5.90 | 6.59 | 5.14 | 5.14 | 6.35 |
| Cr2O3 | 0.05 | 0.09 | 0.09 | - | 0.04 | - | - | 0.01 | - | 0.02 |
| Fe2O3 | 2.52 | 2.51 | 2.76 | 3.52 | 2.54 | 2.66 | 2.76 | 2.48 | 2.54 | 2.76 |
| FeO | 9.07 | 9.02 | 9.95 | 12.66 | 12.96 | 13.58 | 14.09 | 12.66 | 12.94 | 14.09 |
| MnO | 0.23 | 0.19 | 0.22 | 0.26 | 0.43 | 0.42 | 0.38 | 0.35 | 0.33 | 0.40 |
| MgO | 15.42 | 15.55 | 15.43 | 10.95 | 13.44 | 12.99 | 12.58 | 13.82 | 13.78 | 12.72 |
| ZnO | - | - | - | - | - | - | - | - | - | - |
| CaO | 10.76 | 10.94 | 10.66 | 10.01 | 10.68 | 10.70 | 10.90 | 10.65 | 10.98 | 10.65 |
| Na2O | 2.54 | 2.02 | 2.03 | 3.11 | 1.86 | 1.95 | 2.07 | 1.62 | 1.65 | 2.04 |
| K2O | 0.60 | 0.67 | 0.68 | 0.72 | 0.74 | 0.70 | 0.83 | 0.58 | 0.63 | 0.84 |
| H2O | 1.78 | 1.89 | 1.86 | 1.99 | 1.68 | 1.84 | 1.66 | 1.63 | 1.78 | 1.59 |
| F | 0.53 | 0.34 | 0.39 | - | 0.77 | 0.42 | 0.78 | 0.90 | 0.62 | 0.94 |
| Cl | - | - | 0.01 | - | - | 0.01 | 0.01 | 0.02 | 0.01 | 0.01 |
| O=F | 0.22 | 0.14 | 0.16 | - | 0.32 | 0.18 | 0.33 | 0.38 | 0.26 | 0.40 |
| O=Cl | - | - | 0.00 | - | - | 0.00 | 0.00 | 0.00 | 0.00 | 0.00 |
| Total | 98.46 | 99.12 | 99.40 | 97.97 | 100.14 | 100.25 | 100.50 | 100.39 | 101.12 | 100.55 |
| #Si IV | 6.88 | 6.80 | 6.85 | 6.82 | 7.22 | 7.13 | 7.00 | 7.30 | 7.29 | 7.04 |
| #Al IV | 1.12 | 1.20 | 1.15 | 1.18 | 0.78 | 0.87 | 1.00 | 0.70 | 0.71 | 0.96 |
| #Fe +3 | - | - | - | - | - | - | - | - | - | - |
| #Ti IV | - | - | - | - | - | - | - | - | - | - |
| T site | 8.00 | 8.00 | 8.00 | 8.00 | 8.00 | 8.00 | 8.00 | 8.00 | 8.00 | 8.00 |
| #Al VI | 0.15 | 0.32 | 0.13 | 0.36 | 0.15 | 0.15 | 0.14 | 0.18 | 0.16 | 0.14 |
| #Fe +3 | 0.28 | 0.28 | 0.30 | 0.40 | 0.28 | 0.29 | 0.31 | 0.27 | 0.28 | 0.31 |
| #Ti | 0.13 | 0.07 | 0.13 | 0.11 | 0.07 | 0.08 | 0.09 | 0.07 | 0.06 | 0.09 |
| #Cr | 0.01 | 0.01 | 0.01 | - | 0.00 | - | - | 0.00 | - | 0.00 |
| #Mg | 3.39 | 3.38 | 3.37 | 2.46 | 2.94 | 2.85 | 2.77 | 2.99 | 2.97 | 2.79 |
| #Fe +2 | 1.05 | 0.95 | 1.05 | 1.60 | 1.55 | 1.62 | 1.70 | 1.48 | 1.52 | 1.67 |
| #Zn | - | - | - | - | - | - | - | - | - | - |
| #Mn | - | - | - | 0.03 | - | - | - | - | - | - |
| #Ca | - | - | - | 0.04 | - | - | - | - | - | - |
| M1,2,3 | 5.00 | 5.00 | 5.00 | 5.00 | 5.00 | 5.00 | 5.00 | 5.00 | 5.00 | 5.00 |
| #Mg | - | - | - | - | - | - | - | - | - | - |
| #Fe +2 | 0.07 | 0.15 | 0.17 | - | 0.03 | 0.05 | 0.04 | 0.06 | 0.04 | 0.07 |
| #Zn | - | - | - | - | - | - | - | - | - | - |
| #Mn | 0.03 | 0.02 | 0.03 | - | 0.05 | 0.05 | 0.05 | 0.04 | 0.04 | 0.05 |
| #Ca | 1.70 | 1.71 | 1.67 | 1.62 | 1.68 | 1.69 | 1.72 | 1.66 | 1.70 | 1.68 |
| #Na | 0.20 | 0.12 | 0.13 | 0.38 | 0.24 | 0.22 | 0.18 | 0.24 | 0.22 | 0.20 |
| M4 site | 2.00 | 2.00 | 2.00 | 2.00 | 2.00 | 2.00 | 2.00 | 2.00 | 2.00 | 2.00 |
| #Ca | - | - | - | -4E-02 | - | - | - | - | - | - |
| #Na | 0.52 | 0.46 | 0.44 | 0.53 | 0.29 | 0.34 | 0.41 | 0.22 | 0.24 | 0.38 |
| #K | 0.11 | 0.12 | 0.13 | 0.14 | 0.14 | 0.13 | 0.16 | 0.11 | 0.12 | 0.16 |
| A site | 0.63 | 0.58 | 0.57 | 0.63 | 0.43 | 0.47 | 0.56 | 0.33 | 0.36 | 0.54 |
| #O | 22.00 | 22.00 | 22.00 | 22.00 | 22.00 | 22.00 | 22.00 | 22.00 | 22.00 | 22.00 |
| #OH | 1.75 | 1.84 | 1.82 | 2.00 | 1.64 | 1.80 | 1.63 | 1.58 | 1.71 | 1.56 |
| #F | 0.25 | 0.16 | 0.18 | - | 0.36 | 0.20 | 0.36 | 0.41 | 0.28 | 0.44 |
| #Cl | - | - | 0.00 | - | - | 0.00 | 0.00 | 0.00 | 0.00 | 0.00 |

| | 90187 | 90187 | 90187 | 90038 | 90038 | 90038 | 90038 | 90038 | S11 | S12 |
|---|---|---|---|---|---|---|---|---|---|---|
| SiO2 | 47.46 | 48.30 | 48.51 | 40.36 | 43.21 | 42.06 | 40.86 | 41.15 | 39.98 | 48.20 |
| TiO2 | 0.78 | 0.72 | 0.65 | 1.52 | 1.32 | 1.60 | 1.86 | 1.72 | 5.73 | 0.73 |
| Al2O3 | 6.28 | 6.08 | 5.75 | 12.25 | 11.73 | 11.43 | 11.80 | 11.56 | 13.72 | 6.44 |
| Cr2O3 | 0.02 | 0.02 | 0.03 | - | 0.01 | 0.03 | 0.03 | - | - | - |
| Fe2O3 | 2.64 | 2.66 | 2.69 | 5.40 | 3.80 | 4.06 | 4.35 | 4.46 | 1.10 | 1.11 |
| FeO | 13.48 | 13.55 | 13.69 | 13.13 | 9.26 | 9.88 | 10.59 | 10.86 | 11.21 | 9.30 |
| MnO | 0.32 | 0.36 | 0.31 | 0.32 | 0.26 | 0.26 | 0.31 | 0.40 | 0.16 | 0.14 |
| MgO | 13.21 | 13.43 | 13.35 | 10.31 | 13.86 | 13.05 | 11.71 | 11.50 | 11.62 | 16.49 |
| ZnO | - | - | - | - | - | - | - | - | - | - |
| CaO | 10.37 | 10.66 | 10.55 | 11.21 | 11.66 | 11.26 | 11.33 | 11.23 | 9.80 | 11.63 |
| Na2O | 2.08 | 2.01 | 1.99 | 2.24 | 1.97 | 2.54 | 2.33 | 2.27 | 3.11 | 2.85 |
| K2O | 0.75 | 0.77 | 0.78 | 2.02 | 1.35 | 1.12 | 1.40 | 1.35 | 1.66 | 0.55 |
| H2O | 1.81 | 1.69 | 1.75 | 1.92 | 1.93 | 1.88 | 1.79 | 1.80 | 2.03 | 2.06 |
| F | 0.45 | 0.75 | 0.61 | 0.15 | 0.24 | 0.28 | 0.39 | 0.38 | - | - |
| Cl | 0.01 | 0.01 | - | 0.01 | 0.02 | 0.01 | 0.03 | 0.01 | - | - |
| O=F | 0.19 | 0.32 | 0.26 | 0.06 | 0.10 | 0.12 | 0.16 | 0.16 | - | - |
| O=Cl | 0.00 | 0.00 | - | 0.00 | 0.00 | 0.00 | 0.01 | 0.00 | - | - |
| Total | 99.46 | 100.69 | 100.41 | 100.77 | 100.52 | 99.34 | 98.61 | 98.53 | 100.12 | 99.50 |
| #Si IV | 7.04 | 7.08 | 7.13 | 6.07 | 6.32 | 6.26 | 6.18 | 6.23 | 5.91 | 7.01 |
| #Al IV | 0.96 | 0.92 | 0.87 | 1.93 | 1.68 | 1.74 | 1.82 | 1.77 | 2.09 | 0.99 |
| #Fe +3 | - | - | - | - | - | - | - | - | - | - |
| #Ti IV | - | - | - | - | - | - | - | - | - | - |
| T site | 8.00 | 8.00 | 8.00 | 8.00 | 8.00 | 8.00 | 8.00 | 8.00 | 8.00 | 8.00 |
| #Al VI | 0.14 | 0.13 | 0.12 | 0.25 | 0.34 | 0.27 | 0.28 | 0.29 | 0.31 | 0.11 |
| #Fe +3 | 0.29 | 0.29 | 0.30 | 0.61 | 0.42 | 0.45 | 0.49 | 0.51 | 0.12 | 0.12 |
| #Ti | 0.09 | 0.08 | 0.07 | 0.17 | 0.15 | 0.18 | 0.21 | 0.20 | 0.64 | 0.08 |
| #Cr | 0.00 | 0.00 | 0.00 | - | 0.00 | 0.00 | 0.00 | - | - | - |
| #Mg | 2.92 | 2.93 | 2.92 | 2.31 | 3.02 | 2.90 | 2.64 | 2.59 | 2.56 | 3.57 |
| #Fe +2 | 1.56 | 1.56 | 1.58 | 1.65 | 1.08 | 1.20 | 1.34 | 1.37 | 1.37 | 1.11 |
| #Zn | - | - | - | - | - | - | - | - | - | - |
| #Mn | - | - | - | 0.01 | - | - | 0.04 | 0.04 | - | - |
| #Ca | - | - | - | - | - | - | - | - | - | - |
| M1,2,3 | 5.00 | 5.00 | 5.00 | 5.00 | 5.00 | 5.00 | 5.00 | 5.00 | 5.00 | 5.00 |
| #Mg | - | - | - | - | - | - | - | - | - | - |
| #Fe +2 | 0.12 | 0.10 | 0.10 | - | 0.05 | 0.03 | - | - | 0.02 | 0.02 |
| #Zn | - | - | - | - | - | - | - | - | - | - |
| #Mn | 0.04 | 0.04 | 0.04 | 0.03 | 0.03 | 0.03 | 0.00 | 0.01 | 0.02 | 0.02 |
| #Ca | 1.65 | 1.67 | 1.66 | 1.81 | 1.83 | 1.80 | 1.83 | 1.82 | 1.55 | 1.81 |
| #Na | 0.20 | 0.19 | 0.20 | 0.16 | 0.09 | 0.14 | 0.16 | 0.17 | 0.41 | 0.15 |
| M4 site | 2.00 | 2.00 | 2.00 | 2.00 | 2.00 | 2.00 | 2.00 | 2.00 | 2.00 | 2.00 |
| #Ca | - | - | - | - | - | - | - | - | - | - |
| #Na | 0.40 | 0.38 | 0.36 | 0.50 | 0.47 | 0.59 | 0.52 | 0.50 | 0.48 | 0.65 |
| #K | 0.14 | 0.14 | 0.15 | 0.39 | 0.25 | 0,21 | 0.27 | 0.26 | 0.31 | 0.10 |
| A site | 0.54 | 0.53 | 0.51 | 0.88 | 0.72 | 0.80 | 0.79 | 0.76 | 0.79 | 0.75 |
| #O | 22.00 | 22.00 | 22.00 | 22.00 | 22.00 | 22.00 | 22.00 | 22.00 | 22.00 | 22.00 |
| #OH | 1.79 | 1.65 | 1.72 | 1.93 | 1.88 | 1.87 | 1.81 | 1.82 | 2.00 | 2.00 |
| #F | 0.21 | 0.35 | 0.28 | 0.07 | 0.11 | 0.13 | 0.19 | 0.18 | - | - |
| #Cl | 0.00 | 0.00 | - | 0.00 | 0.00 | 0.00 | 0.01 | 0.00 | - | - |

| | S13 | S14 |
|---|---|---|
| SiO2 | 42.98 | 51.32 |
| TiO2 | 1.87 | 0.39 |
| Al2O3 | 10.17 | 2.14 |
| Cr2O3 | - | - |
| Fe2O3 | 3.78 | 0.82 |
| FeO | 8.02 | 14.12 |
| MnO | 0.05 | 0.53 |
| MgO | 14.83 | 14.48 |
| ZnO | - | - |
| CaO | 11.31 | 7.23 |
| Na2O | 2.26 | 4.54 |
| K2O | 0.84 | 0.89 |
| H2O | 2.02 | 2.01 |
| F | - | - |
| Cl | - | - |
| O=F | - | - |
| O=Cl | - | - |
| Total | 98.13 | 98.47 |
| #Si IV | 6.39 | 7.64 |
| #Al IV | 1.61 | 0.36 |
| #Fe +3 | - | - |
| #Ti IV | - | - |
| T site | 8.00 | 8.00 |
| #Al VI | 0.17 | 0.02 |
| #Fe +3 | 0.42 | 0.09 |
| #Ti | 0.21 | 0.04 |
| #Cr | - | - |
| #Mg | 3.29 | 3.21 |
| #Fe +2 | 0.91 | 1.64 |
| #Zn | - | - |
| #Mn | - | - |
| #Ca | - | - |
| M1,2,3 | 5.00 | 5.00 |
| #Mg | - | - |
| #Fe +2 | 0.09 | 0.12 |
| #Zn | - | - |
| #Mn | 0.01 | 0.07 |
| #Ca | 1.80 | 1.15 |
| #Na | 0.11 | 0.66 |
| M4 site | 2.00 | 2.00 |
| #Ca | - | - |
| #Na | 0.55 | 0.65 |
| #K | 0.16 | 0.17 |
| A site | 0.70 | 0.82 |
| #O | 22.00 | 22.00 |
| #OH | 2.00 | 2.00 |
| #F | - | - |
| #Cl | - | - |

# Appendix B

## Current Research Paper

"Duality of magmatism along
the Kirkland Lake-Larder Lake fault zone, Ontario"

by Guy S. Levesque, Eion M. Cameron and
André E. Lalonde

in Current Research, Part C, Geological Survey of Canada,
Paper 91-1C, p. 17-24, 1991.

# Duality of magmatism along the Kirkland Lake-Larder Lake fault zone, Ontario

Guy S. Levesque[1], Eion M. Cameron, and André E. Lalonde[1]
Mineral Resources Division

*Levesque, G.S., Cameron, E.M., and Lalonde, A.E., Duality of magmatism along the Kirkland Lake-Larder Lake fault zone, Ontario; in Current Research, Part C, Geological Survey of Canada, Paper 91-1C, p. 17-24, 1991.*

*Abstract*

*Magmatism in the Kirkland Lake-Larder Lake fault zone (KLF) is characterized by compositional duality. Two suites, syenitic (quartz-free) and granitic (quartz-normative or quartz-bearing) rocks, are present within three magmatic domains. Domain 1, the fault zone, contains both suites. In Domain 2, immediately north of the KLF, only granitic rocks are observed. Domain 3, south of the KLF, contains both syenitic and granitic rocks. These occur either together as phases of composite intrusions or separately as discrete plutons. The Larder Lake fault (LLF), forming the south margin of the KLF, is the boundary between two levels of emplacement: rocks to the south are plutonic, whereas those to the north are hypabyssal or extrusive. This supports previous interpretations for relative upward movement of the crust south of the fault zone. The syenitic and granitic rocks in Domain 1, which host gold, share mineralogical and compositional similarities with the magmatic rocks in other domains.*

*Résumé*

*Le magmatisme à l'intérieur et près de la zone faillée de Kirkland Lake-Larder Lake (FKL) se caractérise par une dualité compositionnelle. Deux séries, une syénitique (sans quartz) et l'autre granitique (avec quartz modal ou normatif) se retrouvent dans trois domaines magmatiques. Dans le domaine 1, qu'est la zone faillée, on retrouve les deux séries. Le domaine 2, immédiatement au nord de la FKL, est composé seulement de roches granitiques. Enfin, le domaine 3 au sud de la FKL possède les deux séries. Dans ce dernier domaine, les deux séries se retrouvent sous forme d'intrusions composées ou distinctes. La faille de Larder Lake, bordure méridionale de la FKL, agit comme frontière démarquant deux niveaux d'emplacement distincts: au sud les roches sont plutoniques, alors qu'au nord elles sont hypabyssales ou effusives. Ceci vient appuyer les interprétations antérieures d'un soulèvement relatif de la croûte au sud de la zone faillée. Les roches syénitiques et granitiques de la zone faillée (domaine 1), qui renferment la minéralisation aurifère, partagent des traits minéralogiques et compositionnels communs avec les roches magmatiques des deux autres domaines.*

[1] Department of Geology, University of Ottawa, Ottawa, Canada K1N 6N5

## INTRODUCTION

The Kirkland Lake-Larder Lake fault zone (KLF), at the western termination of the major east-trending Cadillac-Larder Lake fault, is host to one of North America's major gold camps. Magmatism, which is closely associated with gold, shows a compositional duality, in that both syenitic (quartz-free) and granitic types are present. These are variably distributed between three domains. Domain 1 comprises the KLF; Domains 2 and 3 are, respectively, the country north and south of the KLF (Fig. 1).

Domain 1 is largely composed of sedimentary rocks of the Timiskaming Group (Fig. 1), which lie unconformably on metamorphosed greenstone basement. Alkaline volcanic units (trachytes) are interbedded with the Timiskaming sedimentary rocks. The Timiskaming is cut by elongate intrusions of alkali-feldspar syenite and lamprophyre and by similarly elongate quartz-monzonite (feldspar porphyry) bodies. Domain 3, south of the KLF, also contains both magmatic types, which occur as different phases of large plutons, such as the Otto and Murdock Creek stocks. Other plutons within this domain appear to be exclusively syenitic (Lebel) or exclusively granitic (McElroy). In Domain 2, north of the KLF, only quartz-bearing rocks occur, these as elongated plutons in and around McVittie Township.

Rocks from the two magmatic suites are exposed at different levels of emplacement along the KLF. Rocks within and immediately north of the KLF are almost exclusively hypabyssal or extrusive, while those to the south are distinctly plutonic. These different styles of emplacement are clearly distinguished on the map (Fig. 1): hypabyssal and extrusive units are thin and elongated, whereas plutonic rocks are usually elliptical.

The spatial relationship between gold mineralization and felsic/alkaline intrusions in the Superior Province has long been recognized (Hodgson and MacGeehan, 1982; Cherry, 1983; Colvine et al., 1988; Burrows and Spooner, 1989). Only recently have attempts been made to establish the temporal relationship between gold-bearing veins and magmatism. The results are controversial: some data show a small time gap between gold mineralization and intrusion (Marmont and Corfu, 1989; Claoué-Long et al., 1990), while others show the gold to be significantly younger. For example, Bell et al. (1989) assign a Proterozoic age to the mineralizing event.

At Kirkland Lake there is a distinct time difference between the syenitic intrusions that are the principal host to the gold and the mineralizing event. The elongate intrusions of Domain 1 were formed during an extensional phase of tectonism, while the gold was introduced during a subsequent phase of transpression (Cameron, 1990). Thus the ore-bearing fluids could not have been derived from the batch of magma that formed these intrusions. Archean gold has frequently been ascribed to fluids expelled during prograde regional metamorphism. However, as Jolly (1978) showed, regional metamorphism at Kirkland Lake was complete prior to the deposition of the Timiskaming Group and thus well before alkaline magmatism.

There remains an enigma of an apparently close spatial connection between magmatism and gold mineralization at Kirkland Lake, but not an exact temporal overlap between the two. This enigma is present in other Archean gold camps. It has prompted a series of studies on the nature of alkaline magmatism at Kirkland Lake (Levesque, 1989; S.M. Rowins, pers. comm., 1990; Rowins et al., in press). For the Murdock Creek stock (Fig. 1), Rowins et al. (in press) found that the magma was intrinsically oxidized, which matches the unusually oxidized nature of the gold-bearing fluids at Kirkland Lake (Cameron and Hattori, 1987). Rowins et al. (in press) proposed that the magma was derived from oxid-

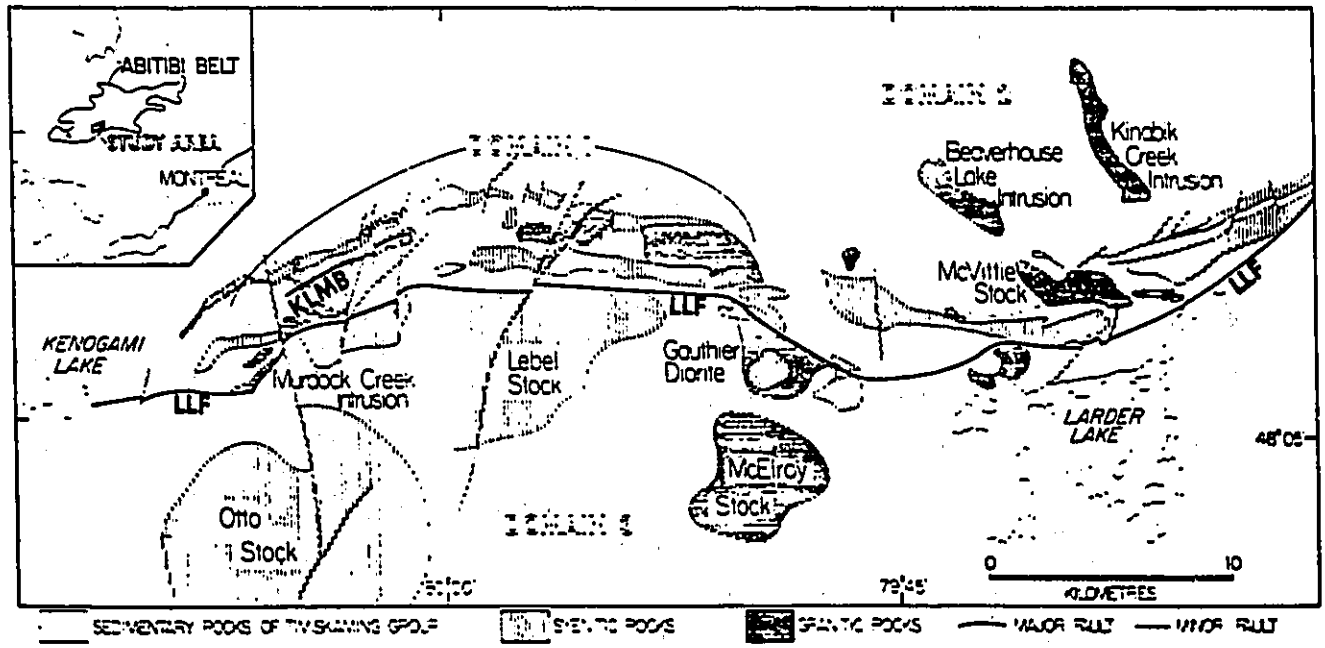


**Figure 1.** Geology and distribution of magmatic rocks along the Kirkland Lake-Larder Lake fault zone (KLF). The KLF is bounded to the south by the Larder Lake fault (LLF), and to the north by the basal Timiskaming unconformity (dashed line). (KLMB = Kirkland Lake Main Break).

ized and metasomatized upper mantle; they suggest a common genetic link between magma generation, $CO_2$ (represented by carbonatization), and gold-bearing fluids. The objective of the present study, which commenced in 1990, is to examine the relationship between the quartz-bearing and the alkaline igneous rocks. This paper presents some preliminary observations on this topic.

## DESCRIPTION AND PETROGRAPHY OF ROCK UNITS

All syenitic plutonic rocks described are classified according to the IUGS nomenclature (Streckeisen, 1976). Some of the granitic rocks cannot, at present, be similarly classified, given the difficuity in identifying the primary constituents of their microcrystalline groundmass. Petrographic examination was of least-altered specimens for each rock type.

### Units within the Kirkland Lake-Larder Lake fault zone (Domain 1)

Six igneous rock units occur within the KLF: alkali-feldspar melasyenite, alkali-feldspar syenite, trachyte, lamprophyre, feldspar porphyry, and quartz-feldspar porphyry. Several descriptive names have been used in past literature; a short review of these names, and a proposed classification is given.

#### *Alkali-feldspar melasyenite*

This is the largest unit of the intrusive syenitic complexes within the fault zone. Traditionally named augite syenite, several other terms have been used to describe this unit; these include basic syenite, mafic syenite, lamprophyre, and augite porphyrite. However, most primary pyroxene compositions (Levesque, 1989) fall in or above the diopside field of the IMA pyroxene nomenclature (Morimoto, 1989).

Least-altered alkali-feldspar melasyenite is dark olive-grey, medium grained, and hypidiomorphic to idiomorphic. This unit is texturally slightly heterogeneous, essentially composed of two phases: a porphyritic phase containing large pyroxene and biotite phenocrysts set in a fine grained groundmass of alkali feldspar (Fig. 2c), and an equigranular phase consisting of interlocking pyroxene, biotite, and alkali-feldspar crystals.

Alkali-feldspar melasyenite (Fig. 2d) (Colour Index(CI) = 40) is distinctive by the abundance (30 to 40 vol.%) of large (0.2 to 1.0 cm) euhedral pyroxenes that are commonly zoned. Other mafic minerals include biotite, magnetite, and apatite (total 10 vol.%). Subhedral perthitic feldspar, composed of roughly equal amounts of alkali feldspar and albite, constitutes 50 to 60 vol.% of this rock type.

#### *Alkali-feldspar syenite*

This is the least abundant intrusive rock type within the KLF. It has been called syenite, felsic syenite, acid syenite, massive syenite, and red syenite. It is the felsic equivalent of the alkali-feldspar melasyenite unit. Predominance of alkali feldspar over pyroxene imparts a pinkish-brown colour to hand specimens. Contact relationships between this rock type and the alkali-feldspar melasyenite are varied: in areas, alkali-feldspar syenite grades into alkali-feldspar melasyenite, while in others a sharp intrusive contact is observed. This indicates that the rock types are consanguinous and were emplaced penecontemporaneously. The alkali-feldspar syenite contains turbid, reddish microperthitic alkali feldspar (85 to 95 vol.%). Sparse pyroxene and biotite phenocrysts, along with fine grained magnetite, are common (less than 15 vol.%).

#### *Trachyte*

Trachyte, in the terminology of Cooke and Moorehouse (1969), constitute the volumetrically most important, and only extrusive member of the syenitic suite within the KLF. Unfortunately, these are the least well-preserved rocks within the fault zone. Nonetheless, three distinct trachytic phases can be identified on the basis of characteristic relict textures: felsic trachyte, mafic trachyte, and pseudoleucite-bearing trachyte.

Felsic trachyte is extensively altered, cataclastically deformed, and, for the most part, identifiable only by association to mafic and/or leucite-bearing trachytes. This rock type is typically fine grained due to complete recrystallization, displays mottled pink (hematite) and green (chlorite + carbonate) patches, and is schistose. A few outcrops display large, centimetre-sized fresh alkali feldspars in a fine grained reddish-orange groundmass composed of fine acicular alkali feldspar, chlorite, and carbonate.

Mafic trachyte (pyroxene trachyte) (Fig. 2a) is generally altered and cataclastically deformed. The mafic phenocryst is commonly weathered out, or completely altered to a yellowish-brown colour. Textures are somewhat better preserved in this unit, and primary mineral alignment, defined by altered pyroxenes, is often recognized (Fig. 2a). The recrystallized groundmass is composed of alkali feldspar and carbonate with minor iron oxides, epidote, and biotite. Relatively unaltered pyroxenes can be observed in a few locations (Fig. 2b), including an excellent exposure on the eastern shore of Bear Lake, in the western part of McVittie Township.

Pseudoleucite trachyte, which originally contained primary leucite (Cooke and Moorhouse, 1969), is characterized by equant, euhedral patches of fine grained orthoclase, carbonate, and minor sericite and iron oxide. These patches represent polygonal pseudoleucite crystals. The groundmass is usually composed of alkali feldspar, albite, carbonate, and iron oxide. Locally, this rock type contains pyroxene as both a phenocryst and groundmass phase; this rock was named leucite tephrite by Cooke and Moorhouse (1969). More rarely, the pseudoleucite crystals are completely altered to a fine interlocking mesh of sericite, carbonate, and alkali feldspar. This gives the rock a distinct green-spotted appearance, hence the name green-spotted trachyte (MacLean, 1956).

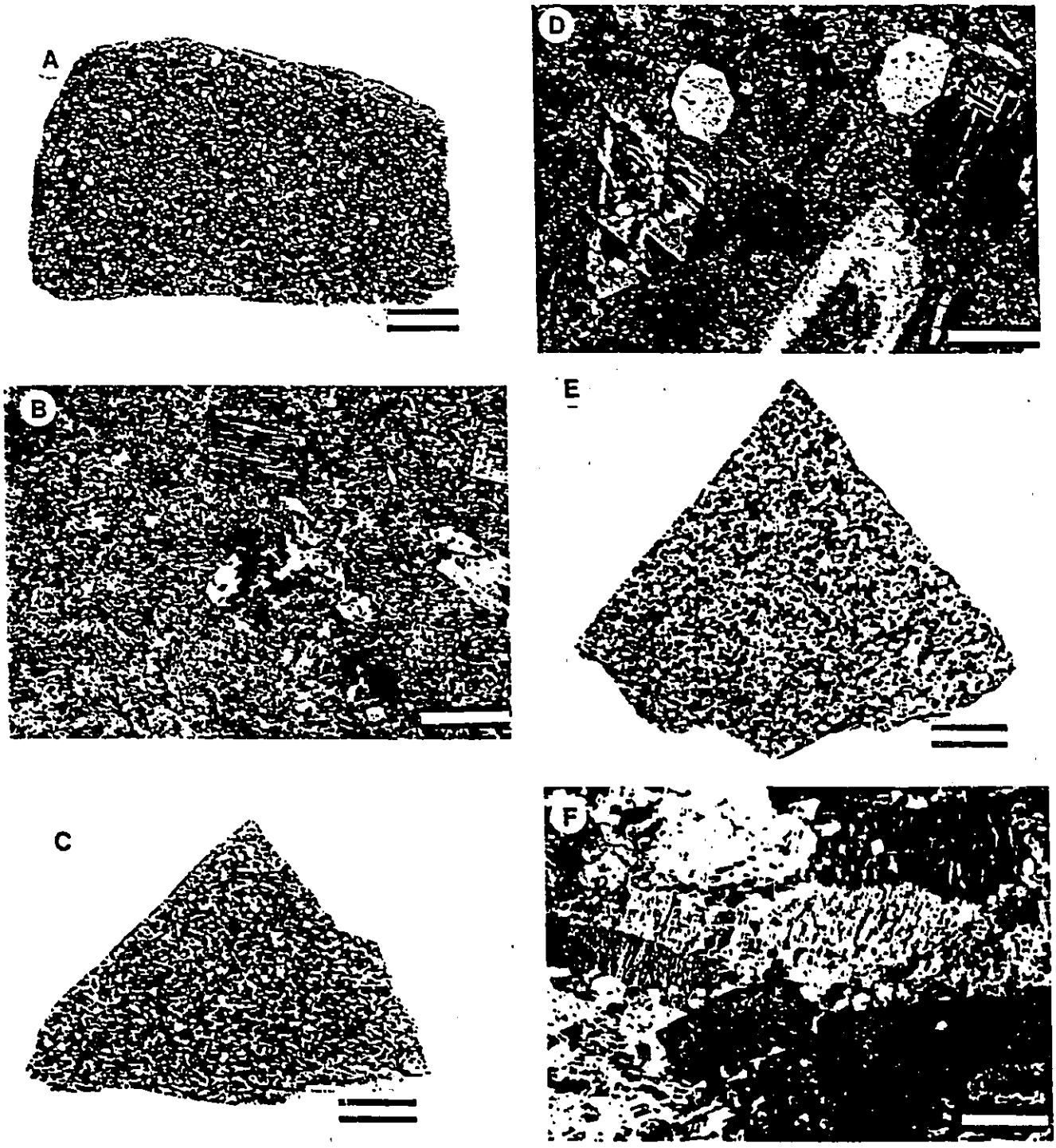


**Figure 2.** Spectrum of syenitic rocks observed along the KLF; scale bar for A, C, and E measures 2 cm; scale bar for B, D, and F is 2 mm.
A. extrusive mafic trachyte. Note primary pyroxene alignment; B. photomicrograph of mafic trachyte, showing subparallel feldspar and pyroxene phenocrysts; C. hypabyssal alkali-feldspar melasyenite; D. photomicrograph of alkali-feldspar melasyenite, displaying large euhedral pyroxenes: E. plutonic alkali-feldspar melasyenite (Otto stock); F. photomicrograph of Otto stock melasyenite displaying large perthitic alkali feldspar.

*Lamprophyre*

Two different types of calc-alkaline lamprophyre, following the IUGS nomenclature (Streckeisen, 1979), are observed within the fault zone: minette and vogesite. Minette dykes are most common; they contain large Mg-rich biotite phenocrysts set in a finer groundmass of alkali feldspar, plagioclase, and magnetite, with minor carbonate and chlorite. The second type of lamprophyre, vogesite, is characterized by the abundance of commonly zoned clinopyroxene phenocrysts enclosed in a groundmass of biotite, alkali feldspar, magnetite, chlorite, plagioclase, and carbonate.

*Feldspar porphyry*

Feldspar porphyry is the common name given to the most abundant hypabyssal granitic rock found within the KLF. It has also been called syenite porphyry (Thompson, 1950). A detailed description of this unit is given by Hicks and Hattori (1988), which is the basis for the description below.

Feldspar porphyry (Fig. 3a) is typically hypidiomorphic and dark olive-grey, containing abundant phenocrysts set in a fine groundmass composed of varying amounts of plagioclase and orthoclase, with minor quartz, magnetite, apatite, and titanite (Fig. 3b). Three phases can be distinguished based on phenocryst assemblages: plagioclase-biotite porphyry, plagioclase-orthoclase-biotite porphyry, and plagioclase-hornblende-biotite porphyry. As with the two alkali-feldspar syenite units, intrusive contacts vary from gradational to sharp, indicating the consanguinity of these three phases.

The name feldspar porphyry has been kept at present because of the difficulty in estimating modal percentages of primary alkali feldspar and plagioclase in the groundmass. However, these rocks have been classified as quartz monzonites and quartz monzodiorites by Hicks and Hattori (1988).

*Quartz-feldspar porphyry*

This forms a minor part of the granitic rocks within the KLF. It is practically indistinguishable from feldspar porphyry in hand specimen. Both units are mineralogically identical; the presence of large, rounded quartz phenocrysts distinguishes this unit. The subhedral nature, roughly hexagonal outlines, and embayed crystal edges of quartz phenocrysts are indicative of rapidly cooled magmatic rocks. This is commonly referred to as amoeba quartz. The strong similarities between feldspar porphyry and this unit indicate that both are genetically related; this unit would probably fall in or near the granodiorite field of the QAP diagram of Streckeisen (1976).

**Rock units north of the KLF (Domain 2)**

Three intrusive bodies lie immediately north of the KLF, in and adjacent to McVittie Township; they are the McVittie stock, which transects the northern limit of the fault zone, the Beaverhouse Lake intrusion, and the Kinabik Creek intrusion (Fig. 1). These rocks have many features in common with the granitic magmatic rocks found within the KLF; they occur as thin, elongated bodies and display porphyrytic textures.

The McVittie stock and the Beaverhouse Lake intrusion are composed of euhedral plagioclase, hornblende, and rare, large, subhedral alkali-feldspar phenocrysts set in a fine grained groundmass of plagioclase, alkali feldspar, and minor magnetite, apatite, titanite, and quartz. These two intrusions are identical to the feldspar porphyry bodies observed within the fault zone. The Kinabik Creek intrusion (Fig. 3c) differs from the other two intrusions only by the presence of large, subhedral, often embayed quartz phenocrysts, which occur along with the plagioclase, hornblende, and alkali-feldspar phenocrysts (Fig. 3d). Accordingly, the Kinabik Creek intrusion is a quartz-feldspar porphyry.

**Rock units south of the KLF (Domain 3)**

The large plutons located to the south of the KLF include the predominantly syenitic Otto, Murdock Creek, and Lebel stocks, the granitic McElroy stock, and a diorite intrusion in Gauthier Township. These plutons are usually rounded, although those in fault contact with the southern limit of the KLF are truncated and appear more elongate.

Recent investigations on the Murdock Creek intrusion (Rowins et al., 1989; Rowins et al., in press) and the Otto stock (Smith and Sutcliffe, 1988) have revealed that these largely syenitic plutons contain quartz-bearing phases. The Murdock Creek stock is composed of an extensive alkali-feldspar syenite and melasyenite core enclosed by a thin mafic margin composed of clinopyroxenite, meladiorite, melamonzonite, and hornblendite (Rowins et al., 1989). The Otto stock (Fig. 2e) is composed of five lithological units: syenite, quartz syenite, mafic syenite (Fig. 2f), porphyritic syenite, and hornblendite/diorite (Smith and Sutcliffe, 1988). Leucocratic monzonite also appears as a very minor unit.

The Lebel stock is composed of at least two transitional syenitic units: a foliated, marginal alkali-feldspar melasyenite (CI = 30), and alkali-feldspar syenite (CI = 20). Large perthitic alkali-feldspar laths define the foliation in the marginal unit. Clinopyroxene, which is commonly zoned, biotite, magnetite, minor apatite and titanite account for up to 35 vol.% of this phase. Traces of primary quartz and zircon are also present. In the alkali-feldspar syenite, hornblende replaces clinopyroxene as the main mafic mineral phase, and alkali feldspar is present as large, equant, sometimes porphyritic, subhedral crystals. Biotite, magnetite, titanite, apatite, and zircon are accessory phases.

The McElroy stock (Fig. 3e) is a large, homogeneous quartz monzonite (CI = 10) intrusion. This unit consists principally of microcline, albite, and quartz; hornblende, magnetite, pyroxene, titanite (up to 2 vol.%) and apatite are also present (Fig. 3f). Myrmekitic textures are commonly observed at alkali feldspar-plagioclase contacts.

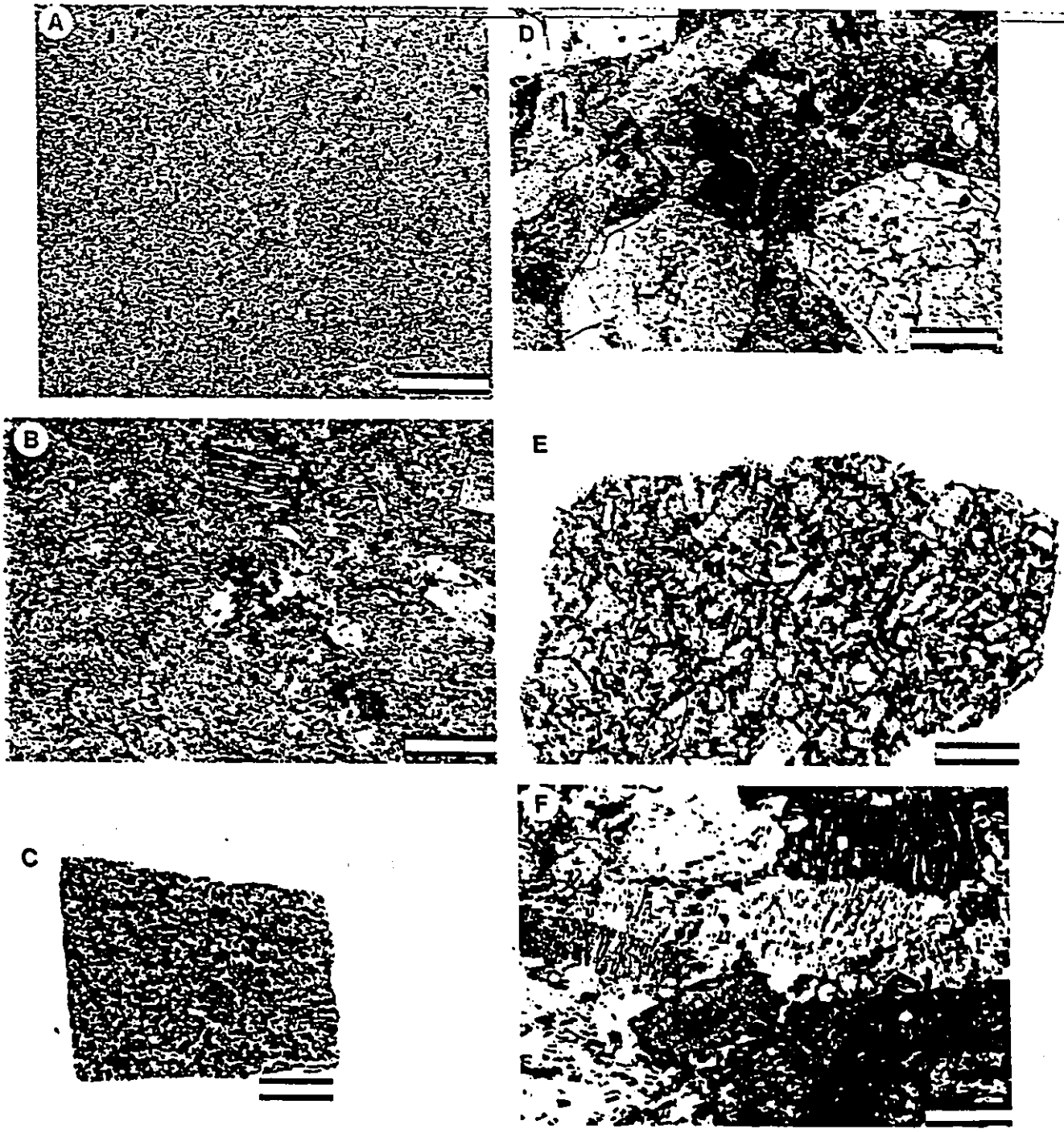


**Figure 3.** Spectrum of granitic rocks observed along the KLF; scale bar for A, C, and E measures 2 cm; scale bar for B, D, and F is 2 mm.
A. hypabyssal quartz monzonite (feldspar porphyry); B. photomicrograph of feldspar porphyry, showing large alkali-feldspar phenocrysts (lower right corner), and smaller abundant plagioclase phenocrysts; C. hypabyssal quartz-feldspar porphyry (Kinabik Creek intrusion); D. photomicrograph of quartz-feldspar porphyry. Note euhedral pseudohexagonal quartz phenocrysts; E. plutonic quartz monzonite (McElroy stock); F. photomicrograph of McElroy stock quartz monzonite, displaying subhedral amphibole.

A large dioritic intrusion, located north of the McElroy stock, is in fault contact with the southern limit of the KLF. Only a few occurrences of diorite have been noted south of the KLF. The rock is generally equigranular, hypidiomorphic, and medium grained. Common to rocks within the fault zone, diorite is also slightly heterogeneous; it ranges from leucodiorite to diorite to meladiorite. Leucodiorite (CI = 15) and diorite (CI = 40) are composed of plagioclase, hornblende, quartz, magnetite, and titanite. The elongate plagioclase laths commonly enclose hornblende and magnetite. The meladiorite contains large euhedral clinopyroxene crystals (up to 80 vol.%) with interstitial plagioclase and titanite. Hornblende alteration rims around pyroxene are commonly observed.

Rocks found to the south of the KLF are distinctive in the textures they display. Large, rounded plutons displaying medium- to coarse-grained hypidiomorphic, equigranular textures are not observed anywhere else along the fault zone. These rocks were emplaced at depth, and in most cases, contain both granitic and syenitic units. This indicates that the compositional duality of magmatism is not restricted to rocks within the KLF.

## DISCUSSION AND SUMMARY

Two suites of magmatic rocks are present within and near the Kirkland Lake-Larder Lake fault zone. Syenitic (quartz-free) rocks and granitic (quartz-bearing or quartz-normative) rocks occur in three well-defined magmatic domains (Fig. 4). Within the fault zone (Domain 1), both syenitic and granitic rocks outcrop as thin, elongated units. Magmatism immediately north of the KLF (Domain 2) is characterized by elongate granitic bodies. South of the KLF (Domain 3), three types of large, rounded intrusions are encountered. Predominantly syenitic composite intrusions with minor mafic margins (Otto, Murdock Creek, Lebel stocks) are most common. One homogeneous granitic pluton (McElroy stock) outcrops south of the fault zone, and a diorite intrusion borders the fault zone in Gauthier Township.

The Larder Lake fault (LLF), which marks the southern limit of the KLF, defines two zones of magmatic emplacement: rocks to the south are distinctly plutonic, while rocks north of the LLF are either hypabyssal or extrusive (Fig. 5). The rounded shape and textures of the intrusions lying south of the KLF are strong evidence for forceful emplacement by diapiric rise, while the porphyritic and elongated nature of the syenitic and granitic bodies within and north of the fault zone indicate high-level passive emplacement, or extrusion in the case of the trachytes.

The syenitic phases of the large intrusions south of the KLF (Domain 3) exhibit similarities to the syenitic bodies within the fault zone (Domain 1). Both fall in the alkali-feldspar syenite field of the QAP diagram (Streckeisen, 1976), with diopsidic clinopyroxene and Mg-rich biotite as the dominant mafic mineral phases. Compositionally, the clinopyroxenes from these two domains are identical (Levesque, 1989). Alkali feldspar in both domains is perthitic, containing roughly equal amounts of orthoclase and albite.

The granitic rocks (feldspar porphyry and quartz-feldspar porphyry) north of the fault zone are mineralogically and texturally identical to the granitic rocks found within the fault zone. They also share a common style of intrusion and level of emplacement, occurring as thin, elongated hypabyssal bodies. Furthermore, these rocks share common mineralogical characteristics with the diorite intrusion (hornblende and plagioclase assemblage in the leucodiorite and diorite) and the monzonitic phases (quartz-bearing) of the composite intrusions south of the KLF. The majority of granitic rocks within the

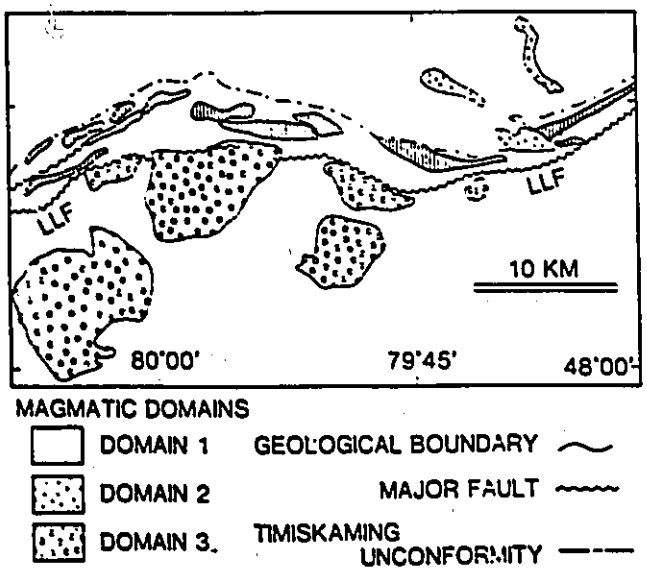


Figure 4. Magmatic domains along the KLF. The Larder Lake fault (LLF) separates Domain 3 from Domain 1, while the northern limit of the KLF (dashed line) marks the boundary between Domain 1 and Domain 2.

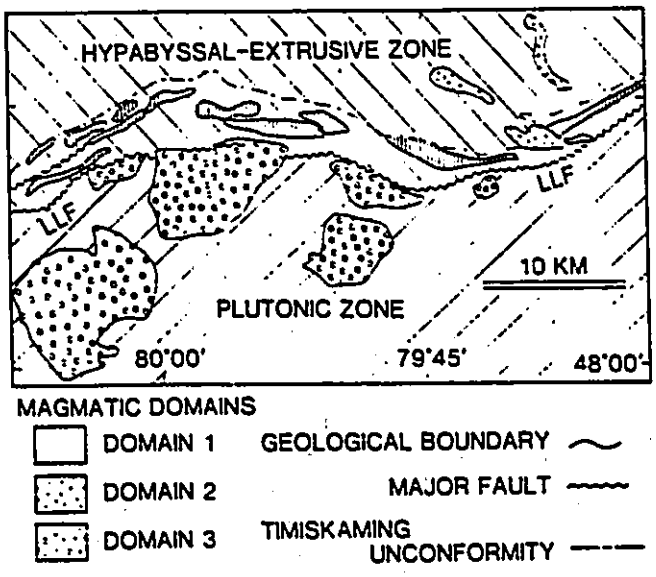


Figure 5. Emplacement levels of magmatic rocks along the KLF. The Larder Lake fault (LLF) defines the boundary between the plutonic zone and the hypabyssal-extrusive zone.

KLF are cataclastically deformed and intensely altered; those north of the fault zone are less altered and undeformed. These three intrusions (McVittie, Beaverhouse Lake, and Kinabik Creek) provide an opportunity to examine unaltered rocks from the granitic suite, which are a host to gold within the KLF.

Textural differences between the magmatic rocks occurring within and to the north of the KLF (Domains 1 and 2), and those found to the south (Domain 3) are striking (Fig. 5). Rocks to the south exhibit coarse grained, holocrystalline, hypidiomorphic, equigranular to inequigranular textures, indicative of emplacement at depth. Rocks found within and to the north of the KLF feature hiatal-porphyritic and trachytic textures, with idiomorphic phenocrysts (including amoeba quartz), and a microgranular groundmass. These textures are indicative of rapid cooling and high-level emplacement, or extrusion.

Movements along the Kirkland Lake and Larder Lake faults have been interpreted as south side up (Thompson, 1950). The textural evidence given above supports this; subsequent to intrusion, deeper levels to the south have been uplifted. Our working hypothesis is that the hypabyssal syenitic bodies of Domain 1 and the syenitic plutons of Domain 3 were generated from the same parental magma, differing only in their level of emplacement. This scenario may possibly be extended to the rocks of the granitic suite.

## ACKNOWLEDGMENTS

We would like to thank J.F. Tardif and G. Mrazek for the preparation of thin sections and the staff of the Ontario Geological Survey core library in Swastika. Invaluable assistance with drafting and photography was provided by Edward Hearn.

## REFERENCES

**Bell, K., Anglin, C.D., and Franklin, J.M.**
1989: Sm-Nd and Rb-Sr isotope systematics of scheelites: possible implications for the age and genesis of vein-hosted gold deposits; Geology, v. 17, p. 500-504.

**Burrows, D.R. and Spooner, E.T.C.**
1989: Relationships between Archean gold quartz vein-shear zone mineralization and igneous intrusions in the Val d'Or and Timmins areas, Abitibi Subprovince, Canada; Economic Geology, Monograph 6, p. 424-444.

**Cameron, E.M.**
1990: Alkaline magmatism at Kirkland Lake, Ontario: product of strike-slip orogenesis; in Current Research, Part C, Geological Survey of Canada, Paper 90-1C, p. 261-269.

**Cameron, E.M. and Hattori, K.**
1987: Archean gold mineralization and oxidized hydrothermal fluids; Economic Geology, v. 82, p. 1177-1191.

**Cherry, M.E.**
1983: The association of gold and felsic intrusions-examples from the Abitibi belt; in The Geology of Gold in Ontario, edited by A.C. Colvine, Ontario Geological Survey, Miscellaneous Paper 110, p. 48-55.

**Claoué-Long, J.C., King, R.W., and Kerrich, R.**
1990: Archaean hydrothermal zircon in the Abitibi greenstone belt: constraints on the timing of gold mineralisation; Earth and Planetary Science Letters, v. 98, p. 109-128.

**Colvine, A.C., Fyon, J.A., Heather, K.B., Marmont, S., Smith, P.M., and Troop, D.G.**
1988: Archean lode gold deposits in Ontario; Ontario Geological Survey, Miscellaneous Paper 139, 136 p.

**Cooke, D.L. and Moorhouse, W.W.**
1969: Timiskaming volcanism in the Kirkland Lake area, Ontario, Canada; Canadian Journal of Earth Sciences, v. 6, p. 117-132.

**Hicks, K.D. and Hattori, K.**
1988: Magmatic-hydrothermal and wall rock alteration petrology at the Lake Shore gold deposit, Kirkland Lake, Ontario; Ontario Geological Survey, Miscellaneous Paper 140, p. 192-204.

**Hodgson, C.J. and MacGeehan, P.J.**
1982: A review of the geological characteristics of 'gold-only' deposits in the Superior Province of the Canadian Shield; in The Geology of Canadian Gold Deposits, Canadian Institute of Mining and Metallurgy, Special Volume 24, p. 211-228.

**Jolly, W.T.**
1978: Metamorphic history of the Archean Abitibi belt; in Metamorphism in the Canadian Shield, edited by J.A. Fraser and W.W. Heywood, Geological Survey of Canada, Paper 78-10, 367 p.

**Levesque, G.S.**
1989: The Kirkland Lake intrusive complex: a petrographical and chemical approach; B.Sc. thesis, University of Ottawa, Ottawa, Ontario, 83 p.

**MacLean, A.**
1956: Geology of Lebel Township; Ontario Department of Mines, Bulletin 150, p. 1-63.

**Marmont, S. and Corfu, F.**
1989: Timing of gold introduction in the late Archean tectonic framework of the Canadian Shield: evidence from U-Pb zircon geochronology of the Abitibi subprovince; Economic Geology, Monograph 6, p. 101-111.

**Morimoto, N.**
1989: Nomenclature of pyroxenes; Canadian Mineralogist, v. 27, p. 143-156.

**Rowins, S.M., Lalonde, A.E., and Cameron, E.M.**
1989: Geology of the Archean Murdock Creek intrusion, Kirkland Lake, Ontario; in Current Research, Part C, Geological Survey of Canada, Paper 89-1C, p. 313-323.
in press: Magmatic oxidation in the syenitic Murdock Creek intrusion, Kirkland Lake, Ontario: evidence from the ferromagnesian silicates; Journal of Geology.

**Smith, A.R. and Sutcliffe, R.H.**
1988: Plutonic rocks of the Abitibi Subprovince: Project 88-08, Ontario Geological Survey, Miscellaneous Paper 141, p. 188-196.

**Streckeisen, A.**
1976: To each plutonic rock its proper name; Earth Science Reviews, v. 12, p. 1-33.
1979: Classification and nomenclature of volcanic rocks, lamprophyres, carbonatites, and melilitic rocks: recommendations and suggestions of the IUGS subcommission on the systematics of igneous rocks; Geology, v. 7, p. 331-335.

**Thompson, J.E.**
1950: Geology of Teck township and the Kenogami Lake area, Kirkland Lake gold belt; Ontario Department of Mines Annual Report for 1948, Part 5, v. 57, p. 1-53.